

Domestic Greywater Systems: A Potential Reservoir of Antibiotic Resistance Genes Transfer



Min-ghah Kariem

*A thesis submitted in partial fulfilment of the requirements for the degree of Magister
Scientiae in the Department of Biotechnology, University of the Western Cape*

March 2024

Supervisor: Dr Bronwyn Kirby-McCullough

Co-supervisor: Professor Marla Trindade

Keywords

Domestic Greywater Systems

Greywater

Western Cape Drought

Antibiotic Resistance Genes

Real-Time PCR

Horizontal Gene Transfer



UNIVERSITY *of the*
WESTERN CAPE

Abstract

Domestic Greywater Systems: A Potential Reservoir of Antibiotic Resistance Genes

M Kariem

MSc Thesis, Department of Biotechnology, University of the Western Cape

During the Western Cape drought from 2015 to 2018, the use of greywater to alleviate pressure on the limited potable water available in the province was encouraged. Greywater, however, has the potential to harbour residual antibiotics and pathogenic bacteria, thereby potentially supporting the growth and proliferation of antibiotic resistant bacteria. This study combined traditional microbiology tests with molecular biology to detect resistant microorganisms within domestic greywater systems and their associated biofilms, while Quantitative PCR (qPCR) was used to determine the levels of clinically relevant antibiotic resistance genes (ARGs) (*vanA*, *ampC* and *aadA*), as well as the *intI1* gene, which serves as a marker of horizontal gene transfer.

Phenotypic resistance was confirmed using the Kirby-Bauer disc diffusion method. Notably, high levels of resistance to ampicillin and kanamycin were found in greywater and biofilm samples, as well as resistance to vancomycin. Bacterial viability was assessed using flow cytometry using the LIVE/DEAD BacLight Bacterial Viability kit, and it was revealed that a large portion of the cell population within greywater was dead or injured. qPCR analysis confirmed the presence of clinically relevant ARGs *vanA* and *ampC*, in domestic greywater samples, with abundance fluctuating in response to seasonal change. Additionally, the *intI1* gene was detected in all greywater and biofilm samples, which suggests that genetic exchange occurs amongst bacteria in greywater and biofilm samples.

Our findings support the hypothesis that greywater systems are colonised by resistant bacteria, which can form stable communities within the water environment which allows for high levels of genetic exchange. These findings support the use of qPCR and flow cytometry, in combination with traditional microbiology tests for monitoring antibiotic resistance in environmental samples. While the use of greywater is a viable method to reduce the demand for potable water, this study highlights the fact that the improper use of greywater poses a risk to the environment and public health. As such, the public should be better educated on how to safely use these systems.



**UNIVERSITY of the
WESTERN CAPE**

University of the Western Cape

Private Bag X17, Bellville 7535, South Africa

Telephone: ++27-21- 959 2255/959 2762 Fax: ++27-21- 959 1268/2266

Email: bfielding@uwc.ac.za

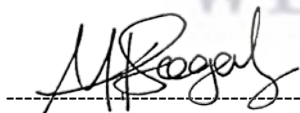
FACULTY OF NATURAL SCIENCE

PLAGIARISM DECLARATION

Name: MIN-GHAH KARIEM

Student number: 3363830

I declare that "*Domestic Greywater Systems: A Potential Reservoir of Antibiotic Resistance Genes*" is my own work, that it has not been submitted for any degree or examination in any other university, and that all the sources I have used or quoted have been indicated or acknowledged by complete references.



Signature

6th March 2024

Date

Acknowledgements

In the name of Allah, the Most Gracious, the Most Merciful

I would like to express my sincere gratitude to my supervisor Dr Bronwyn Kirby-McCullough, for her constant guidance, support, and encouragement throughout this journey. Thank you for allowing me the opportunity to grow as a female scientist under your guidance. I will forever be grateful for all you have taught me.

To Professor Marla Trindade, my co-supervisor, thank you for always sharing your vast knowledge and insight. The guidance, support and motivation were greatly appreciated. To Dr L van Zyl, thank you for all the laboratory and technical support throughout this process, for always taking the time to teach and guide all the members of IMBM. Additionally, the constant encouragement and support was appreciated.

To all the members of IMBM, past and present, thank you for creating a great working environment. Additionally, thank you to Ms Robin Karelse and Ms Carmen Cupido for the administrative and technical support.

I wish to extend my sincerest appreciation to the Water Research Commission (WRC) and National Research Foundation (NRF) for funding me, and the Institute of Microbial Biotechnology and Metagenomics (IMBM) for providing the equipment and support needed to complete my research.

To my dear friend Zaida Parsons, you have been a constant support and source of motivation throughout this journey, thank you.

To my husband, Yaseen Segals, I would like to thank you for your patience, resilience and always being by my side supporting, encouraging, and guiding me.

To my in-laws, thank you for all the support and love throughout my academic career.

To my parents and siblings, Imrah, Zuhaa and Iyaath, none of what I have done and achieved could have been possible without you, your constant belief, patience, and guidance has been a source of strength and motivation.

To my son, Uthmaan, I dedicate this manuscript to you.

Contents

Keywords	<i>i</i>
Abstract	<i>i</i>
PLAGIARISM DECLARATION	<i>ii</i>
Acknowledgements	<i>iii</i>
List of Figures	<i>viii</i>
List of Tables	<i>xi</i>
ACRONYMS & ABBREVIATIONS	<i>xiii</i>
Chapter 1: Literature Review	<i>1</i>
1. Introduction	<i>1</i>
1.1 Drought in South Africa	<i>1</i>
1.1.1 Drought in the Western Cape – Western Cape Water Crisis	<i>2</i>
1.2 Greywater	<i>4</i>
1.3 Antibiotic Resistance in the Environment	<i>5</i>
1.4 Antibiotic resistance genes	<i>8</i>
1.4.1 Antibiotic Resistance Genes of Interest	<i>8</i>
1.4.1.1 Resistance to Aminoglycosides	<i>9</i>
1.4.1.2 Resistance to Vancomycin	<i>10</i>
1.4.1.3 Resistance to β-lactams	<i>11</i>
1.4.2 Horizontal Gene Transfer of ARGs	<i>13</i>
1.5 Assessing Antibiotic Resistance Genes in the Environment	<i>13</i>
1.5.1 Molecular Techniques used for the detection and characterisation of environmental ARGs.	<i>14</i>
1.5.1.1 Gene-specific PCR (Conventional PCR)	<i>14</i>
1.5.1.2 Quantitative PCR – Real-Time PCR	<i>15</i>
1.5.1.3 Flow-cytometry and cell sorting	<i>16</i>
1.6 Aims & Objectives of the study.	<i>17</i>
Chapter 2: Phenotypic Resistance Analysis and Cell Viability Assessment of Greywater Samples	<i>18</i>
2.1 Introduction	<i>18</i>
2.1.1 Antimicrobial Susceptibility Testing	<i>18</i>
2.1.2 Kirby-Bauer Disc Diffusion Assay	<i>19</i>
2.1.3 The LIVE/DEAD BacLight Bacterial Viability Assay	<i>21</i>
2.1.4 Aim of Chapter 2	<i>21</i>
2.2 Materials and Methods	<i>22</i>
2.2.1 Site Identification	<i>22</i>
2.2.1 Sampling Equipment	<i>22</i>
2.2.2 Greywater and Biofilm Sample Collection	<i>22</i>
2.2.3 Kirby-Bauer Disc Diffusion Assay	<i>23</i>
2.2.3.1 Preparation of Antibiotic discs	<i>24</i>
2.2.3.2 Kirby-Bauer Disc Diffusion Assay of Greywater and Biofilm Samples	<i>24</i>

2.2.4 LIVE/DEAD BacLight Assay using Flow Cytometry	24
2.2.4.1 Bacterial Strains	24
2.2.4.2 Media and Chemicals.....	24
2.2.4.3 Preparation of LIVE and DEAD Bacterial Cultures.....	24
2.2.4.4 Preparation of Greywater samples for analysis	25
2.2.4.5 Staining of Samples.....	25
2.2.4.6 Flow Cytometric measurements	26
2.3 Results & Discussion	26
2.3.1 Kirby-Bauer Disc Diffusion Assay	26
2.3.2 LIVE/DEAD BacLight Bacterial Viability Assay of Greywater Samples.....	32
2.4 Conclusion of the Chapter	38
Chapter 3: Quantification of Antibiotic Resistance Genes in Greywater Systems using qPCR	39
3.1 Introduction	39
3.1.1 Antibiotic Resistance Genes	40
3.1.1.1 <i>aadA</i> Resistance Gene	40
3.1.1.2 <i>ampC</i> Resistance Gene	41
3.1.1.3 <i>vanA</i> Resistance Gene	41
3.1.2 Real-Time qPCR	42
3.1.2.1 Total RNA Extractions.....	43
3.1.2.2 RT-PCR Detection Chemistries.....	43
3.1.2.3 Absolute Quantification	45
3.1.3 Aim of Chapter 3.....	45
3.2 Materials and Methods.....	46
3.2.1 Sample Processing.....	46
3.2.2 Optimization of Total RNA Extractions from Greywater Samples.....	46
3.2.2.1 Commercial Kits and Reagents.....	46
3.2.2.2 Organic/Chemical RNA Extraction Methods.....	47
3.2.2.3 RNA Quality Analysis	49
3.2.2.4 16s rRNA gene Polymerase Chain Reaction for contaminating DNA in RNA samples.....	50
3.2.2.5 Ambion TURBO DNase-free Kit Treatment.....	51
3.2.3 cDNA synthesis	51
3.2.4 Selection of Primers and Bioinformatic Analysis.....	51
3.2.4.1 Growth conditions for bacterial strains.....	52
3.2.4.2 Genomic DNA Extraction using the Ammonium Acetate based Method.	52
3.2.4.3 Genomic DNA Extraction using the NucleoSpin Kit	53
3.2.4.4 Plasmid Miniprep	53
3.2.5 PCR Optimization of Reference Genes	53
3.2.6 PCR Optimization of Antibiotic Resistance Genes.....	54
3.2.6.1 PCR Optimisation of <i>vanA</i> gene PCR	54
3.2.6.2 PCR Optimisation of <i>ampC</i> gene PCR	54
3.2.6.3 PCR Optimisation of <i>aadA</i>	54
3.2.7 Construction of Plasmid standards for Real-time PCR.....	55
3.2.8 Real-Time PCR	56

3.2.8.1 Construction of the Standard Curve	56
3.2.8.2 Absolute Quantification of ARGs in greywater samples	57
3.3 Results & Discussion	58
3.3.1 Optimization of Total RNA Extractions from greywater samples.....	58
3.3.1.1 Organic Conventional Extraction Methods	58
3.3.1.2 Commercial Kits and Reagents	61
3.3.1.2 Optimization of the Hot Phenol SDS Method for greywater samples	64
3.3.1.3 RNA Quality Analysis	66
3.3.1.4 16S rRNA gene Polymerase Chain Reaction for contaminating DNA in RNA samples	67
3.3.1.5 Ambion TURBO-DNAse free Treatment	69
3.3.2 cDNA synthesis	71
3.3.3 PCR optimization of Reference Gene Primer sets	73
3.3.4 PCR Optimization of Antibiotic Resistance Genes Primer sets.....	75
3.3.5 Construction of plasmids for RT-PCR.....	77
3.3.6 Real-Time PCR	78
3.3.6.1 Copy Number Calculations of Target Genes.....	78
3.3.7.2. Standard curves and Melt Curve Analysis of Target Genes	78
3.3.7.2.1 Standard curves and Melt curve analysis of Reference Genes	79
3.3.7.2.2 Standard curves and Melt curve analysis of Antibiotic Resistance Genes	80
3.3.7.3 Absolute quantification of Antibiotic Resistance Genes in Greywater Samples	82
3.3.7.3.1. Comparison of ARG abundance and collection sites	83
3.3.7.3.2 Comparison of ARG abundance and Collection seasons	90
3.4 Conclusion of Chapter	94
Chapter 4: Detection and Quantification of Class 1 Integrons as Markers of Horizontal Gene Transfer in Domestic Greywater Systems	95
4.1.1 Introduction	95
4.1.2 Horizontal Gene Transfer and Antibiotic Resistance	96
4.1.2.1 Transformation	97
4.1.2.2 Transduction.....	97
4.1.2.3 Conjugation	98
4.1.3 Integrons	98
4.1.3.1 Classes of Integrons	99
4.1.4 <i>Int1</i> as a marker for Horizontal Gene Transfer.....	100
4.2 Materials and Methods.....	101
4.2.1 Metagenomic DNA Extraction from Greywater Samples	101
4.2.1.2 Phosphate, SDS, and Chloroform Bead-Beater Method	101
4.2.1.2 DNEasy PowerSoil® DNA Isolation kit	101
4.2.2 Metagenomic DNA Extraction from Biofilm Samples.....	101
4.2.3 16S rRNA Polymerase Chain Reaction	102
4.2.4 PCR Optimization of Target Genes	102
4.2.5 Construction of plasmid controls for Real-Time PCR.....	103

4.2.6 Real-Time PCR	104
4.2.6.1 Construction of Standard Curves.....	104
4.2.6.2 Absolute Quantification of the <i>int1</i> gene and 16S rRNA reference gene.....	104
4.2.6.3 Statistical Analysis.....	105
4.3 Results & Discussion	106
4.3.1 Comparison of Metagenomic DNA Extraction methods.....	106
4.3.2 Metagenomic DNA Extraction from Greywater and Biofilm Samples	110
4.3.3 PCR Optimization of Target Genes – <i>int1</i> gene and 16S rRNA gene	112
4.3.4 Construction of plasmid controls for RT-PCR.....	113
4.3.5 Real-time PCR.....	113
4.3.5.1 Generation of Standard Curves for the <i>Int1</i> and 16S rRNA gene for qPCR	113
4.3.5.2 Absolute Quantification of <i>int1</i> gene and 16S rRNA RT gene in greywater and biofilm mDNA samples.....	115
4.3.5.2.1 Melt Curve Analysis	115
4.3.5.2.1.1 Melt Curve Analysis of <i>Int1</i> gene in mDNA samples	115
4.3.5.2.1.2 Melt Curve Analysis of 16S rRNA gene in mDNA samples	116
4.3.5.3 Comparison of <i>Int1</i> abundance at different collection sites	117
4.3.5.4 Comparison of Seasons and <i>int1</i> gene Abundance	125
4.4 Conclusion of Chapter	129
Chapter 5: Conclusion and Future work.....	132
Reference List.....	134
Appendix A – Chapter 2	152
Appendix B – Chapter 3	153
DNA and RNA Quantification Tables	153
Gel Electrophoresis Figures – Total RNA Extractions	156
Standard Curves and Melt Curves analysis for qPCR Target Genes	159
Appendix C – Chapter 4.....	164
Gel Electrophoresis Figures – mDNA Extractions	164
Melt curve Analysis	166

List of Figures

Figure 1.1: A map representing the Western Cape Water Supply System.	3
Figure 1.2: Examples of domestic greywater collection and storage.	4
Figure 1.3: A overview of the possible sources of antibiotic resistance development.	8
Figure 2.1: A schematic overview of the Kirby-Bauer disc diffusion method.	20
Figure 2.2: Example of the Kirby-Bauer Disc Diffusion method of QC Strain <i>S. aureus</i> ATCC 29213 using in-house prepared antibiotic discs.	27
Figure 2.3: Example of the Kirby-Bauer Disc Diffusion method of greywater sample GWS4S5 using in-house prepared antibiotic discs.	28
Figure 2.4: Example of the Kirby-Bauer Disc Diffusion method of greywater sample GWS4S5 using commercial antibiotic discs supplied by Oxoid TM.	28
Figure 2.5: Analysis of <i>Escherichia coli</i> pure bacterial culture using the LIVE/DEAD BacLight Bacterial Viability and Counting Kit.	32
Figure 2.6: Analysis of <i>Staphylococcus aureus</i> pure bacterial culture using the LIVE/DEAD BacLight Bacterial and Counting Kit	33
Figure 2.7: Analysis of Greywater Site 1 Samples (GWS1S3A and GWS1S4 B) using the LIVE/DEAD BacLight Bacterial Viability and Counting Kit.	34
Figure 2.8: Analysis of Greywater Site 2 Samples (GWS2S2B, GWS2S3B and GWS12S4 A) using the LIVE/DEAD BacLight Bacterial Viability and Counting Kit.	34
Figure 2.9: Analysis of Greywater Site 3 Samples (GWS3S3A; GWS3S4A; GWS3S5A; GWS3S6A and GWS3S7A) using the LIVE/DEAD BacLight Bacterial Viability and Counting Kit.	35
Figure 2.10: Analysis of Greywater Site 4 Samples (GWS4S2A; GWS4S3A; GWS4S4B; GWS4S5A; GWS4S6A and GWS4S7 A) using the LIVE/DEAD BacLight Bacterial Viability and Counting Kit.	36
Figure 3.1: Potential pathways and threats associated with antibiotic resistant bacteria and antibiotic resistance genes to human health and the environment.	40
Figure 3.2: Mechanism of action of SYBR Green 1 Dye.	44
Figure 3.3: Schematic overview of the optimized Hot Acid Phenol RNA Isolation Method used for the extraction of total RNA from greywater samples.	48
Figure 3.4: Schematic diagram of optimization for removal of contaminating DNA.	50
Figure 3.5: Equation used to calculate number of copies.	56
Figure 3.6: Total RNA extracted from trial greywater samples using the CTAB RNA Extraction method.	59
Figure 3.7: RNA extracted from greywater samples using the Hot-Acid Phenol RNA extraction method.	60
Figure 3.8: 1.2% TBE Agarose gel depicting RNA samples extracted from greywater using the Hot Phenol SDS method.	61
Figure 3.9: A 1.2% TBE Agarose gel depicting RNA samples extracted using TRIzol reagent from greywater samples.	63
Figure 3.10: The pellet collected after the sequential centrifugation of 4 L of greywater.	64
Figure 3.11: 1.2% TBE Agarose gel containing RNA extracted using the Hot Acid Phenol Method.	64
Figure 3.12: A 1.2% Agarose gel depicting RNA samples extracted from greywater samples using the Hot Phenol SDS Method.	65
Figure 3.13: 1% Agarose gel depicting the 16S rRNA PCR for DNA contamination after 1X DNase I treated RNA samples.	68

Figure 3.14: 1% TAE Agarose gel of 16S rRNA PCR for DNA contamination after 3X DNase 1 treated RNA samples.	69
Figure 3.15A & 3.15B: RNA extracted from GWS4S5 and GWS3S4 respectively, using the Hot Phenol SDS Method.	70
Figure 3.16 Gel A: Optimised amplification conditions for the 16S rRNA primer set. Gel B: Optimised amplification conditions for the <i>gapA</i> gene primer set. Gel C: Optimised amplification conditions for the <i>mdh</i> gene primer set.	74
Figure 3.17 Gel A: Optimised amplification conditions for the <i>vanA</i> gene primer set. Gel B: Optimised amplification conditions for the <i>ampC</i> gene primer set. Gel C: Optimised amplification conditions for the <i>aadA</i> gene primer set.	76
Figure 3.18: A 1% TAE agarose gel depicting the PCR confirmation of inserts using the pJET Sequencing Primers and the confirmation of insert using gene-specific primers for each target gene.	77
Figure 3.19: Standard curve generated using the <i>gapA</i> reference gene primers.	80
Figure 3.20: Standard curve generated using the <i>vanA</i> gene primers.	81
Figure 3.21: Melt Curve of <i>vanA</i> gene amplicons generated using a dilution series of control plasmids.	82
Figure 3.22: Standard curve for <i>vanA</i> gene primer set, with greywater samples collected at all four sites.	83
Figure 3.23: Standard curve for <i>ampC</i> gene primer set, with greywater samples collected from all four sites.	84
Figure 3.24: Standard curve for <i>aadA</i> gene primer set, with samples from all four collection sites.	85
Figure 3.25: Mean Copy number of ARGs detected in greywater samples collected from all four sites.	85
Figure 3.26: Relative abundance of ARGs in Greywater samples.	89
Figure 3.27: A graphical representation of the greywater sample collection seasons and the <i>vanA</i> gene absolute abundance using qPCR.	92
Figure 3.28: A graphical representation of the greywater sample collection seasons and the <i>ampC</i> gene absolute abundance using qPCR.	93
Figure 4.1: Diagram showing the main mechanisms involved in Horizontal Gene transfer.	96
Figure 4.2: Schematic diagram of the basic Integron structure and function.	99
Figure 4.3: A 1% TAE agarose gel depicting the extraction of metagenomic DNA using the Phosphate, SDS, Chloroform and Bead-beater Method and the corresponding 16S rRNA gene PCR of the metagenomic DNA samples.	107
Figure 4.4: 1% TAE agarose gels confirming the quality and integrity of the metagenomic DNA extracted using the DNEasy PowerSoil DNA Isolation Kit (Gel A) and the corresponding 16S rRNA PCR products of the metagenomic DNA samples extracted.	109
Figure 4.5. A 2% TAE gel depicting the amplicons from the optimised <i>intI1</i> and 16S rRNA gene PCR, respectively.	112
Figure 4.6: A 1% TAE agarose gel depicting the PCR confirmation of the inserts for <i>intI1</i> and 16S rRNA RT genes using gene-specific primers.	113
Figure 4.7. Melt Curve of <i>intI1</i> gene amplicons generated using a dilution series of control plasmids.	114
Figure 4.8. Standard curve for the <i>intI1</i> primers of the log molecules/ μ l versus the Cp value.	114

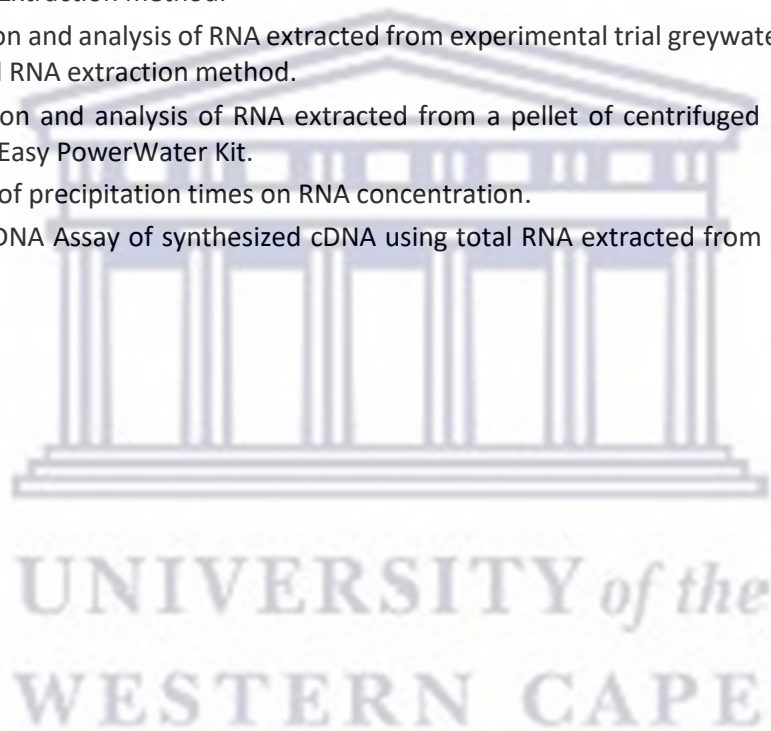
Figure 4.9. Melt Curve of 16S rRNA gene amplicons generated using a dilution series of control plasmids.	115
Figure 4.10. Standard curve for the 16S rRNA gene primers of the Log molecules/ μ l versus the Cp value.	115
Figure 4.11: Melting Peaks for <i>intl1</i> primers in Group 1 mDNA samples.	116
Figure 4.12: Melting peaks for 16S rRNA primers in Group 1 mDNA samples.	117
Figure 4.13: Standard curve of the <i>intl1</i> primer set with greywater samples present on the graph.	118
Figure 4.14: Standard curve of the <i>intl1</i> primer set with biofilm samples present on the graph.	121
Figure 4.15: Standard curve of the 16S rRNA primer set with greywater samples present on the graph.	122
Figure 4.16: Standard curve of the 16S rRNA RT primer set with biofilm samples present on the graph.	122
Figure 4.17: Mean copy number (a) and relative abundance (b) of <i>intl1</i> gene in greywater samples collected from all four collection sites.	123
Figure 4.18: Mean copy number (a) and relative abundance (b) of <i>intl1</i> gene in biofilm samples collected from all four collection sites.	124
Figure 4.19: Greywater Sample Collection Seasons and the correlating <i>intl1</i> gene copy numbers.	127
Figure 4.20: Biofilm Sample Collection Seasons and the correlating <i>intl1</i> gene copy numbers.	128
Figure B1: RNA extracted from filtered greywater samples using the RNeasy PowerWater Kit.	156
Figure B2: A comparison of the DNA and RNA extracted from filtered greywater samples using the commercial kits.	157
Figure B3: 1% TAE Agarose gel illustrating the 16S rRNA PCR of cDNA synthesized using the QuantiNova Reverse Transcription Kit.	158
Figure B4: Melt Curve analysis of <i>gapA</i> gene amplicons generated using a dilution series of control plasmids.	159
Figure B5: Standard curve generated using the 16S rRNA RT reference gene primers.	160
Figure B6: Melt Curve of 16S rRNA RT gene amplicons generated using a dilution series of control plasmids.	160
Figure B7: Standard curve generated using the <i>mdh</i> reference gene primers.	161
Figure B8: Melt Curve of <i>mdh</i> gene amplicons generated using a dilution series of control plasmids.	161
Figure B9: Standard curve generated using the <i>ampC</i> reference gene primers.	162
Figure B10: Melt Curve of <i>ampC</i> gene amplicons generated using a dilution series of control plasmids.	162
Figure B11: Standard curve generated using the <i>aadA</i> reference gene primers.	163
Figure B12: Melt Curve of <i>aadA</i> gene amplicons generated using a dilution series of control plasmids.	163
Figure C1. A 1% TAE gel representing metagenomic DNA extracted from greywater and biofilm samples using the DNEasy PowerSoil Pro Kit.	164
Figure C2: A 1% TAE gel representing environmental DNA extracted from greywater samples using the DNEasy PowerSoil Pro Kit.	164
Figure C3: A 1% TAE gel representing Metagenomic DNA extracted from biofilm samples using the DNEasy PowerSoil Pro Kit.	165

Figure C4: A 1% TAE gel depicting a 16S rRNA PCR of environmental DNA extracted from biofilm samples.	165
Figure C5: 1% TAE gel depicting a 16S rRNA PCR of environmental DNA extracted from greywater samples.	165
Figure C6: Melting peaks for <i>int11</i> primers in Group 2 mDNA samples.	166
Figure C7: Melting peaks for <i>int11</i> primers in Group 3 mDNA samples.	166
Figure C8: Melting peaks for <i>int11</i> primers in Group 4 mDNA samples.	167
Figure C9: Melting peaks for <i>int11</i> primers in Group 5 mDNA samples.	167
Figure C10: Melting peaks for <i>int11</i> primers in Group 6 mDNA samples.	168
Figure C11: Melting peaks for 16S rRNA primers in Group 2 mDNA samples.	169
Figure C12: Melting curves for 16S rRNA primers in Group 3 mDNA samples.	169
Figure C13: Melting peaks for 16S rRNA primers in Group 4 mDNA samples.	170
Figure C14: Melting peaks for 16S rRNA primers in Group 5 mDNA samples.	170
Figure C15: Melting peaks for 16S rRNA primers in Group 6 mDNA samples.	171

List of Tables

Table 1.1: Aminoglycoside Resistance Genes found in Aquatic Environments.	10
Table 1.2: Vancomycin resistance genes in Aquatic environments.	11
Table 1.3: β -lactam and penicillin resistance genes in Aquatic environments.	13
Table 2.1: Sample Collection Season specifications according to weather patterns in the Western Cape.	23
Table 2.2: Greywater and Biofilm Sample Collection Schedule for 2018 to 2021.	23
Table 2.3: Kirby-Bauer Disc Diffusion method to determine the zone of inhibition (mm) in Greywater samples.	30
Table 2.4: Kirby-Bauer Disc Diffusion Assay of Biofilm Samples.	31
Table 3.1: The primer set, and amplification conditions used for the RNA-DNA contamination assessment.	51
Table 3.2: List of primers used in this study.	52
Table 3.3: Reference genes Primer sets Optimised Amplification conditions.	54
Table 3.4: Antibiotic Resistance Genes for RT-PCR Optimised Amplification Conditions.	55
Table 3.5: qPCR Cycling Parameters for Reference Genes and ARGs.	57
Table 3.6: Quantitation and analysis of total RNA extracted from greywater samples using the Hot Phenol SDS Method.	60
Table 3.7: Quantitation and analysis of RNA extracted from centrifuged greywater samples using TRIzol reagent.	63
Table 3.8: NanoDrop results of RNA extracted from Greywater samples using the Hot Phenol SDS Method.	67
Table 3.9: Comparison of RNA Yield using Nanodrop ND-1000 when using the TURBO DNase-free kit.	70
Table 3.10: Overview of Total RNA Extractions and cDNA synthesis of WRC K3/2803 Greywater Samples.	72
Table 3.11: Copy number of Target Plasmid Standards for reference and antibiotic resistance genes.	78
Table 3.12: Mean Ct values and Gene Copy Number for Antibiotic Resistance Gene qPCR Assay.	87

Table 3.13: Mean Ct values and Gene Copy Number for Antibiotic Resistance Gene qPCR Assay.	88
Table 4.1: 16S rRNA PCR Primer Set and PCR Cycling Conditions for bacterial identification.	102
Table 4.2. Primer sets used in for integron RT-PCR.	102
Table 4.3: PCR Cycling conditions used for the int1 and 16S RNA gene primers.	103
Table 4.4: Nanodrop results for Metagenomic DNA extracted using the PSC-B Method.	106
Table 4.5: Nanodrop results for Metagenomic DNA extracted using the PSC-B Method.	109
Table 4.6: Samples collected and analysed for the IntI1 qPCR Assay.	110
Table 4.7: Qubit HS DNA Assay concentrations for Metagenomic DNA samples.	111
Table 4.8: Mean Ct values and Copy Numbers for the Integron qPCR Assay – Greywater Samples.	119
Table 4.9: Mean Ct values and Copy Numbers for the Integron qPCR Assay – Biofilm Samples.	120
Table A: Zone of Inhibition Criteria used to evaluate greywater and biofilm samples.	152
Table B1: Quantitation and analysis of RNA extracted from experimental trial greywater samples using the CTAB RNA Extraction method.	153
Table B2: Quantitation and analysis of RNA extracted from experimental trial greywater samples using the Hot Phenol RNA extraction method.	153
Table B3: Quantitation and analysis of RNA extracted from a pellet of centrifuged greywater sample using the RNEasy PowerWater Kit.	154
Table B4: The effect of precipitation times on RNA concentration.	154
Table B5: Qubit HS DNA Assay of synthesized cDNA using total RNA extracted from greywater samples.	155



ACRONYMS & ABBREVIATIONS

AMP10	Ampicillin 10µg
ARB	Antibiotic Resistant Bacteria
ARDRA	Amplified ribosomal DNA restriction analysis
ARG	Antibiotic Resistance Genes
BF	Biofilm
BLAST	Basic Local Alignment Search Tool
cDNA	complementary DNA
CM25	Chloramphenicol 25µg
CPD10	Cefpodoxime 10µg
CTAB	Cetyltrimethylammonium bromide
DEPC	Diethyl pyro carbonate
DNA	Deoxyribonucleic acid
DNase	Deoxyribonuclease
dNTPs	Deoxynucleotide triphosphates
EDTA	Ethylenediaminetetraacetic acid
ESBL	Extended spectrum β-lactamase
GW	Greywater
HCL	Hydrochloric Acid
HGT	Horizontal Gene Transfer
HOA	Home-Owners Association
KAN30	Kanamycin 30µg
KF30	Cephalothin 30µg
LB	Luria-Bertani
LiCl2	Lithium Chloride
mDNA	Metagenomic DNA
MDR	Multi-drug resistant
MH	Muller-Hinton
NEB	New England Biolabs
PCR	Polymerase Chain Reaction
PSC-B	Phosphate, Sodium dodecyl sulphate, Chloroform Bead-Beater
qPCR	Quantitative polymerase chain reaction
RNA	Ribonucleic Acid
RNAse	Ribonucleases
RT	Room Temperature
S10	Streptomycin 10µg
SDS	Sodium Dodecyl Sulphate
TAE	Tris, Acetic acid and Ethylenediaminetetraacetic acid
TBE	Tris, Borate and Ethylenediaminetetraacetic acid
TE	Tris Ethylenediaminetetraacetic acid
TEC30	Teicoplanin 30µg
T-RFLP	Terminal-Restriction fragment length polymorphism
UV	Ultra-violet
VAN30	Vancomycin 30µg

VBNC
VRE
WC
WHO

Viable but non-culturable
Vancomycin-Resistant Enterococcus
Western Cape
World Health Organization



UNIVERSITY *of the*
WESTERN CAPE

Chapter 1: Literature Review

1. Introduction

The availability of potable water remains a concern throughout Southern Africa. Specifically, in the Western Cape Province which experienced its most severe drought between 2015 and 2018 (Dube *et al.*, 2022). The introduction of level 6B water restrictions and increased tariff rates encouraged residents to develop innovative approaches for the sustainable use of the available water, such as greywater reuse.

Domestic greywater is a sustainable and effective approach to conserving ground water. Greywater is defined as untreated household or commercial building wastewater generated from non-toilet uses (Maimon *et al.*, 2010). Despite the immediate benefits of greywater usage, there is concern over its safety especially when used improperly. Particularly the potential for these systems to harbour residual antibiotics and bacteria which can support the proliferation of resistant organisms.

Resistance genes can alter the fitness of bacterial pathogens and delay the administration of an appropriate microbial therapy required to treat an infection (Winward *et al.*, 2008). As the number of antibiotic resistant infections increase globally it should be acknowledged that greywater systems and their associated biofilms could be acting as a potential environmental reservoir of antibiotic resistant bacteria (ARB) and antibiotic resistance genes (ARGs). Moreover, recent studies into ARGs prevalence and proliferation in water sources have mainly focused on commercial and agricultural wastewater streams, with limited information available regarding its prevalence in domestic greywater.

1.1 Drought in South Africa

South Africa is a water-scarce and drought prone country. In recent years, the country has faced severe pressure with respect to water security mainly due to an increase in water demand as the population increases, coupled with poor management of water resources and the recurrence of droughts over the past four decades (Mahlalela *et al.*, 2020; Meza *et al.*, 2021). Periods of decreased precipitation over the years, coupled with Southern Africa experiencing extreme El Niño events has led to the Western Cape and Eastern Cape Province specifically, experiencing severe droughts (Meissner and Jacobs-Mata, 2017; Calverley and Walther, 2022).

Drought is a recurrent event in all climates and is generally defined as a period of abnormally low precipitation, when compared to the long-term average climate of a particular region, which severely impacts hydrological resources (IPCC, 2014; Meza *et al.*, 2021). In semi-arid regions such as South Africa, water scarcity is a major issue (Calverley and Walther, 2022). A recent study by the South

African Weather Service in 2021, found that the annual temperature in 2020 was 0.5 °C higher than the average experienced between 1981- 2010.

1.1.1 Drought in the Western Cape – Western Cape Water Crisis

The Western Cape Province of South Africa has a Mediterranean climate with winter rainfall and hot, dry summers (Sorensen, 2017). The province experienced one of the most severe droughts in recent history between 2015 and 2018. The drought was particularly rare as it manifested across four drought classes: meteorological, agricultural, hydrological, and socio-economic. This water crisis was one of global significance, particularly as it was the first recent example of a developed city dealing with the threat of completely empty dams and no potable water (Botai *et al.*, 2017; Odoulami *et al.*, 2021).

The Western Cape Water Supply System (WCWSS) as shown in Figure 1.1 is composed of an elaborate interconnected system of dams, rivers and pipes of which is almost entirely dependent on rainfall. Significant dams which feed the Cape Town Metropolis and its approximately 3.7 million inhabitants include the Streenbras Dam in the Hottentots Holland Mountains, the Voelvlei Dam near Gouda, the Wemmershoek Dam in the Drakenstein Mountains and the Theewaterskloof Dam near Villersdorp, of which Theewaterskloof is the largest in terms of capacity (Sorensen, 2017; Rawlins, 2019). The Cape Town Metropolitan Area sources approximately 95% of its water from the WCWSS, of which an estimated 64% is used for drinking water, 29% for agriculture and 7% for other municipal purpose. A useful feature of the WCWSS system is that it allows for the transfer of water between dams and catchment systems, allowing for instances of excess water to be stored in one of the dams for the dry seasons (Calverley and Walther, 2022). According to Bruhl *et al.*, 2020, Cape Town has the highest number of households with direct access to piped water in South Africa, of which water consumption is metered for formal properties in the City. The average domestic consumption in 2018 was 660 L per day for households and 460 L per day for complexes and flats.

In 2017, the Western Cape experienced its lowest annual rainfall since 1933, which saw the overall dam levels drop from 92.5% capacity to 23% after a steady decrease in annual rainfall for a decade before (Calverly and Walther, 2022). The “Day Zero” notice was released by the city in January 2018, gaining global attention. Day Zero was the point at which the dam levels that supply the city with water would reach 13.5% and city-wide water rationing would be implemented. This peak of modern-day water rationing would see the taps being shut off and water being distributed through communal standpipes, limited to 25 L per person (Calverley and Walther, 2022).

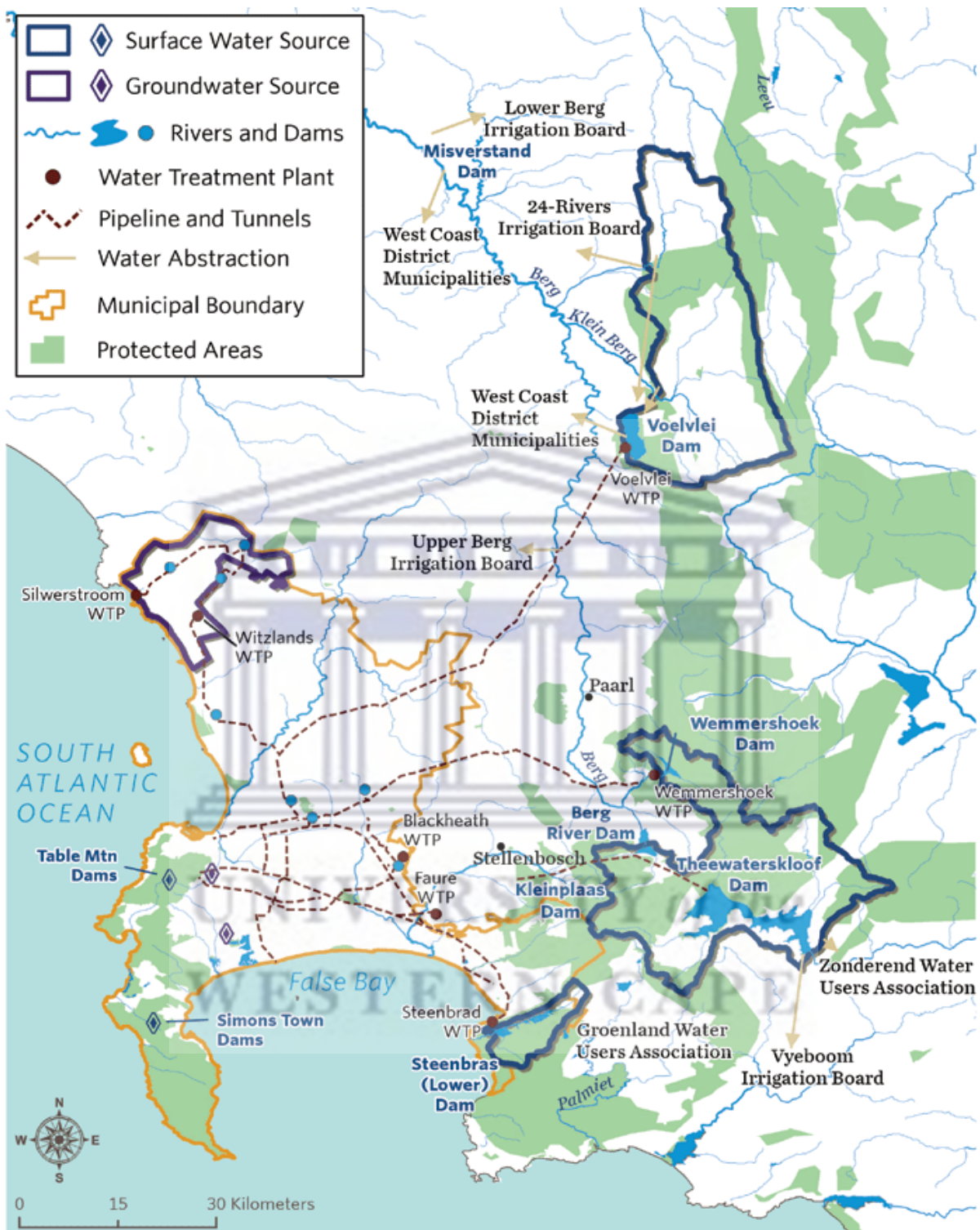


Figure 1.1: A map representing the Western Cape Water Supply System. Contributors and users including the Cape Town metropolitan area, the agricultural sector, smaller municipalities, and communities are indicated. (Adapted from Stafford *et al.*, 2019).

The Western Cape drought was a result of three consecutive dry winters (2015 to 2017) resulting in a major rainfall deficit and was one of the worst water crises to be experienced in a metropolitan area (Pascale *et al.*, 2020). In May 2018, water levels in the Western Cape Water Supply System responsible

for supplying water to the Cape Town Metropolitan area dropped to 20%. This triggered strict water usage restrictions to delay the dam levels reaching the dangerously low levels of 13.5% - the stage at which large majorities of the city's municipal water supply would have been disconnected. These restrictions encouraged innovative approaches to water conservation and sustainable use, with many individuals exploring alternative water sources such as natural spring water, groundwater, and greywater reuse.

1.2 Greywater

Greywater is defined as domestic wastewater generated from non-toilet activities such as water from baths, hand-basins, showers and washing machines (Ghaitidak and Yadav, 2015; Troiano *et al.*, 2018). Greywater often constitutes 50-80% of a household's wastewater and its storage and reuse can reduce a single household's potable water usage by up to 50% (Troiano *et al.*, 2018). At a domestic level, greywater is often used in a sustainable manner, for example toilet-flushing, garden irrigation and landscaping. Recent technologies have allowed for on-site greywater treatment, which is maintained by homeowners, often lowering the risk of exposure to harmful contaminants (Henderson *et al.*, 2022).

The collection and reuse of greywater was an ideal approach for the residents of the Western Cape, as systems varied from bucket collection of washing machine water to intricate greywater systems attached to homes as shown in Figure 1.2. The reuse of greywater effectively addressed the problems of water scarcity whilst conserving freshwater sources (Henderson *et al.*, 2022).



Figure 1.2: Examples of domestic greywater collection and storage. A: represents simple hand-bucket collection of shower water or washing machine run-off. B: Represents an intricate greywater collection and storage system attached to a home.

Generally public perception of greywater is that it is harmless and safe for reuse. However, as greywater is mainly sourced from laundry, showers, baths, and hand basins, its composition will vary and it is possible that it can allow for the growth and proliferation of antibiotic resistant bacteria.

Recent studies have suggested that water bodies such as reclaimed or greywater plays a pivotal role in the transport and transfer of ARGs (Lupo *et al.*, 2012). Additionally, greywater systems provide the perfect conditions for biofilms to form. Biofilms are defined as an aggregation of microorganisms embedded in a self-produced extracellular polymeric substance. Biofilms are a site of immense bacterial interactions due to its high bacterial density and nutritional richness (Madsen *et al.*, 2012). Recent studies have identified that horizontal gene transfer (HGT) and biofilm formation in water bodies are interconnected (Madsen *et al.*, 2012). Biofilm formation and HGT interactions have been investigated in wastewater treatment plants (Schwartz *et al.*, 2003). Many of the conditions present in wastewater treatment plant biofilms are likely to be mimicked in domestic greywater tanks, such as periods of stagnation and high bacterial loads (Aminov, 2011), thus, serving as a platform for biofilm formation. Ultimately greywater systems and their associate biofilms have the potential to act as an environmental reservoir for the proliferation and spread of ARGs. As the number of antibiotic resistant infections increases globally, it should be acknowledged that greywater systems (particularly their biofilms) could be acting as potential environmental reservoir of ARB and ARGs.

The quality of domestic greywater is directly dependant on the health, habits, and socio-economic status of the household occupants. Previous studies have identified various pathogens such as pathogenic *Escherichia coli*, *Staphylococcus aureus*, *Pseudomonas aeruginosa* and enteric viruses in recycled water (O'Toole *et al.*, 2012; Maimon *et al.*, 2014). Pathways of exposure to pathogens in greywater would likely be through handling with broken skin, as well as ingestion from greywater irrigated vegetables and herbs (Leonard *et al.*, 2016). Greywater provides the ideal environment for proliferation of ARBs, and the emergence and exchange of ARGs as the exposure of microbes to antibiotics and additional external pressure caused by micropollutants such as biocides (Henderson *et al.*, 2022). Antibiotics are considered to be an environmental pollutant of emerging concern which represents a real health risk. As such, the detection and removal of ARB and ARGs needs advanced analytical techniques (Noman *et al.*, 2022).

1.3 Antibiotic Resistance in the Environment

Antibiotic overuse has greatly contributed to the current antimicrobial resistance crisis and the increased presence of ARBs in the environment (Noman *et al.*, 2022). The introduction of antibiotics in the 1950s has revolutionized medicine, veterinary health and agriculture (Davies and Davies, 2010). It is an impossible task to quantify the impact antibiotics have had on modern medicine and human

health. However, with minimal regulation and widespread overuse and misuse in both clinical therapy and animal husbandry (Tennstedt *et al.*, 2003; Ventola, 2015), antibiotics have become a source of a whole new problem. Globally, an estimated 70 billion doses of antibiotics are used in the clinical sector per annum (Woolhouse *et al.*, 2016), with a further 63 151 tons being consumed in the livestock sector as part of animal feed (van Boeckel *et al.*, 2014).

Antibiotic resistance is defined as the ability of a microorganism to resist the effects of an antibiotic it was once susceptible to. Exposure to antibiotics serves as one of the main drivers for the development and spread of ARGs which can be transmitted to humans via direct and indirect contact (van Boeckel *et al.*, 2014). There has been a recent surge in the development of resistance to common antimicrobial therapies detected in important bacterial pathogens. This coupled with the emergence of multi-drug resistant (MDR) bacteria has become one of the most concerning problems faced by the modern-day health care industry (Lupo *et al.*, 2012). Globally, the number of antibiotic resistant infections is increasing. An estimated 23 000 annual deaths are attributed to resistant infections in the USA. In developing countries, such as South Africa, resistant infections are increasing pressure on an already overburdened public health system. In South Africa the burden of infectious disease is particularly high with approximately 7.97 million people living with human immunodeficiency virus (HIV) in combination with having the fourth largest population infected with tuberculosis (Chetty, 2021).

Antibiotics are widely used globally, with a complex inter-relationship developing between antibiotic usage by humans, animals, and the environment. Antibiotics are often excreted into the environment unchanged and are known to contaminate water sources (Zhang *et al.*, 2009). These off-spills into the environment serve as a driving force for the selection and proliferation of antibiotic resistant organisms. There is increasing evidence that environmental antibiotic contamination is widespread. In fact, antibiotics are so ubiquitous that researchers have even been able to detect antibiotics in groundwater at a depth of over 10 m (Batt *et al.*, 2006). Recent studies have shown that other than so called "pristine" mountainous sites, most surface water sources that encounter either urban or agricultural areas are contaminated with antibiotics (Yang and Carlson, 2003). Given the prevalence of antibiotics in nature, researchers have started to recognise the importance of screening for ARG in environmental microbial communities (including non-pathogenic organisms) and not limiting their studies to hospitals and clinics. When focusing specifically on water systems, most investigations focus on sewage treatment or wastewater emanating from commercial food production (meat processing, aquaculture, and agriculture), with sporadic studies investigating the natural environment. From published studies it is evident that ARGs associated with clinically relevant antibiotics can be detected in wastewater treatment plants, surface water, ground water, rivers and estuaries (Auerbach *et al.*, 2007; Czekalski *et al.*, 2012; Fahrenfield *et al.*, 2013).

Numerous studies have shown that ARGs can enter the environment either by direct discharge of untreated wastewater or as sludge/effluents emanating from sewage treatment plants (Auerbach *et al.*, 2007) as shown in Figure 1.3. ARGs can also enter soil from animal manure or bio-sludge, where they can leach into groundwater or contaminate shallow water. The resistance genes present in contaminated drinking water can be further disseminated as the water passes through drinking water treatment facilities and re-enters the water distribution system (Schwartz *et al.*, 2003).

Genes associated with tetracycline resistance (*tet* genes) appear to be the most frequently detected ARGs in environmental samples and have been detected in wastewaters worldwide (Agersø and Sandvang, 2005; Agersø and Peterson, 2007). Mackie and co-workers (2006) were able to show that the same *tetM*, *O*, *Q* and *W* genes present in swine lagoons could also be detected in groundwater downstream of these lagoons. However, ARGs in wastewater are not limited to tetracycline resistance. Chloramphenicol resistance genes (*catII*, *IV* and *B3*) (Jacobs and Chenia, 2007) and sulphonamide resistance genes (*sull*, *II*, *III* and *A*) (Agersø and Peterson, 2007) have been detected in aquaculture systems. Schwartz *et al.* (2003) reported the presence of methicillin resistant (*mecA*) *Staphylococcus* strains in hospital wastewater biofilms. Alarming ARGs are also present in slightly or non-polluted natural waters (Rahman *et al.*, 2008). The *vanA* gene has been detected in drinking water biofilms, even in the absence of enterococci, possibly indicating that gene transfer to autochthonous drinking water bacteria has occurred. Similarly, the enterobacterial *ampC* resistance gene has been detected via PCR in wastewater, surface water and drinking water biofilms (Schwartz *et al.*, 2003). β -lactamase genes were detected in nearly 80% of the ampicillin resistant *Enterobacteriaceae* and 10% of the resistant *Aeromonas* isolated from the Ria de Aveiro estuary (Henriques *et al.*, 2006). Multiple-antibiotic resistant *E. coli* carrying ARGs to aminoglycosides, β -lactams, tetracyclines, and trimethoprim-sulfamethoxazoles were detected from drinking water in the Rize region, Turkey (Alpay-Karaoglu *et al.*, 2007).

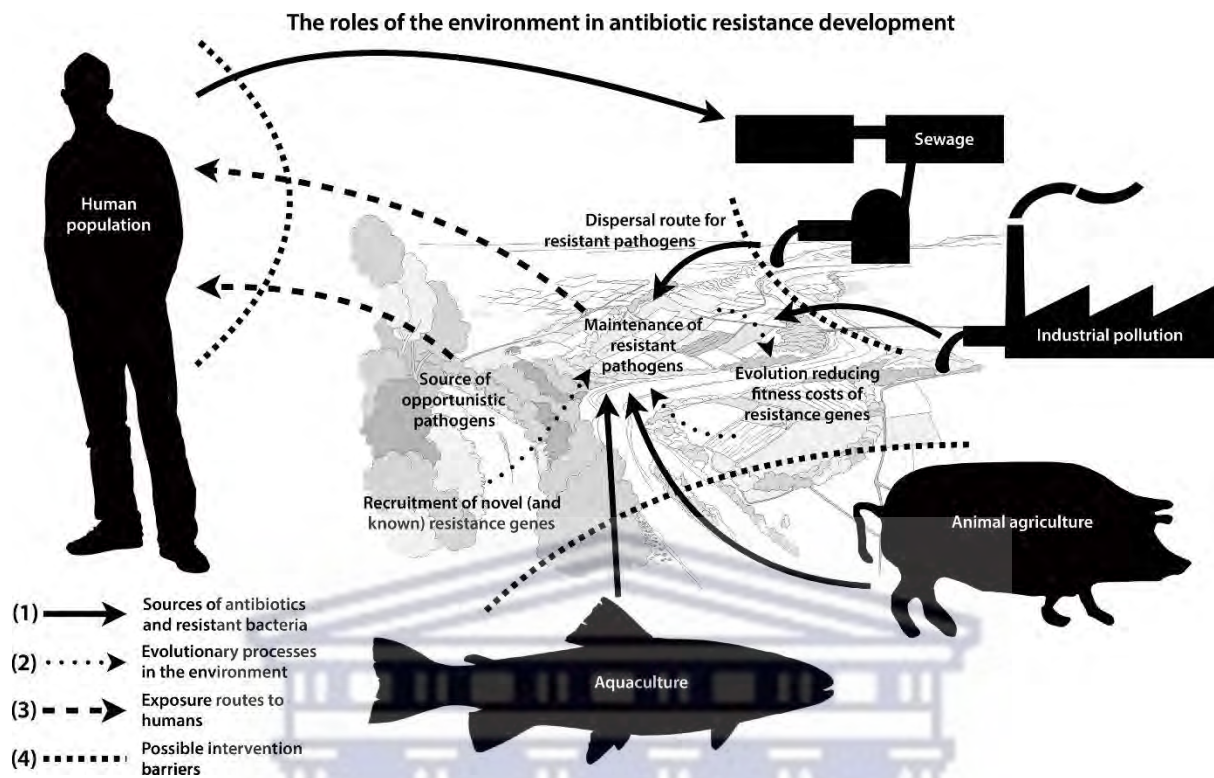


Figure 1.3: A overview of the possible sources of antibiotic resistance development. The illustration provides insight into the environmental processes and activities influencing the development and spread of antibiotic resistance. (Adapted from Larson *et al.*, 2018).

1.4 Antibiotic resistance genes

Resistant microorganisms are more difficult to treat, requiring alternative medications or higher doses of antimicrobials. These approaches are often more expensive, require more toxic drugs or both. Bacteria which are resistant to multiple antimicrobials are termed “multi-drug resistant” (MDR). Antibiotic resistance arises through one of three mechanisms: 1) natural resistance in certain types of bacteria (particularly in antibiotic producing strains); 2) genetic mutation; 3) acquisition of resistance genes from other microorganisms (horizontal gene transfer) (Davies and Davies, 2010). While there are several mechanisms by which microbes resist antibiotics, resistance mechanisms can be broadly subdivided into four categories – 1) target bypass; 2) efflux pumps; 3) antibiotic inactivation; 4) target modification. Overcoming resistance is further compounded by the fact that resistance to an antibiotic may not be limited to a single resistance mechanism.

1.4.1 Antibiotic Resistance Genes of Interest

Based on either their clinical or environmental relevance in South Africa, three antibiotic resistance genes (*vanA*, *ampC* and *aadA*) were targeted in this study. One selection criterion was the presence of drug resistant nosocomial infections associated with particular antibiotics used to treat ESKAPE

pathogens (*Enterococcus faecium*, *Staphylococcus aureus*, *Klebsiella pneumoniae*, *Acinetobacter baumannii*, *Pseudomonas aeruginosa* and *Enterobacter* species). The resistance genes, associated resistance mechanism and the prevalence of these genes in the environment, particularly aquatic environments, will be discussed briefly in the following sections.

1.4.1.1 Resistance to Aminoglycosides

Aminoglycosides are a group of therapeutic agents which contain an amino-modified glycoside sugar. Streptomycin, originally derived from *Streptomyces griseus*, was the first in-class aminoglycoside released in 1944 and was the earliest modern agent effective against *Mycobacterium tuberculosis*. Following on from the success of streptomycin, a series of other milestone compounds were released, namely kanamycin, gentamicin, tobramycin and neomycin. Aminoglycoside antibiotics display concentration-dependent bactericidal activity against Gram-negative aerobes and some anaerobic bacilli. Currently they are used for the treatment of *Acinetobacter baumannii*, *Enterobacteriaceae* species, *Escherichia coli*, *Klebsiella pneumoniae* and *Pseudomonas aeruginosa* (Garneau-Tsodikova and Labby, 2016). Aminoglycosides' primary mode of action is the inhibition of protein synthesis, and as such is most effective against rapidly multiplying susceptible bacteria. As aminoglycosides are poorly absorbed via the gut, they are typically administered intravenously or intramuscularly. Due to their limited antimicrobial spectrum and toxicity, they were not widely used. However, with the emergence of resistance to other mainline drugs, there is renewed interest in this class of compounds.

Aminoglycoside resistance is conferred via direct deactivation of the antibiotic by enzymatic modification. There are over 50 enzymes involved in resistance which are classified, based on their biochemical action on the aminoglycoside substrate, into three groups: namely acetyltransferase (*aac* genes), phosphotransferases (*aph*) and nucleotidyltransferases (*ant*). Studies have shown that the *aac*, *aph* and *ant* genes are widely distributed in various genera isolated from polluted and natural aquatic environments including *Aeromonas*, *Escherichia*, *Vibrio*, *Salmonella* and *Listeria* species (Lee *et al.*, 1998; Heuer *et al.*, 2002; Titilawo and Okoh, 2015) (Table 1.1).

Table 1.1: Aminoglycoside Resistance Genes found in Aquatic Environments

Gene	Biological source	Environmental source*	Function	Reference
<i>aacA4</i>	Plasmid pTB11	NW	Aminoglycoside-6'-N-acetyltransferase	Mukherjee and Chakraborty 2006
<i>aacC1</i>	Microbial communities	NW	Aminoglycoside-3'-N-acetyltransferase	Lee <i>et al.</i> , 1998
<i>aadA1</i>	<i>Aeromonas</i> , <i>Citrobacter</i> and <i>Shigella</i> ; Plasmid pTB11	NW	Aminoglycoside-3-9-adenylyltransferase	Henriques <i>et al.</i> , 2006a; Mukherjee and Chakraborty 2006
<i>aadA2</i>	<i>Aeromonas</i> , <i>Escherichia</i> and <i>Vibrio</i>	NW, SD	Aminoglycoside-3'-adenylyltransferase	Dalsgaard <i>et al.</i> , 200; Taviani <i>et al.</i> , 2008
<i>aadA5</i>	<i>Escherichia</i> and <i>Vibrio</i>	NW	Aminoglycoside-3''-9-adenylyltransferase	Park <i>et al.</i> , 2003; Mohapatra <i>et al.</i> , 2008
<i>aphA1</i>	<i>Salmonella</i>	DW, NW	Aminoglycoside-3'-phosphoryltransferase	Cernat <i>et al.</i> , 2007; Poppe <i>et al.</i> , 2006
<i>aphA2</i>	<i>Escherichia</i>	DW	Class B acid phosphatase	Cernat <i>et al.</i> , 2007
<i>nptII</i>	Microbial communities	NW	Neomycin phosphotransferase	Zhu 2007
<i>strA</i>	<i>Listeria</i> , <i>Salmonella</i> and <i>Vibrio</i> ; Plasmid pB10	NW	Streptothricin phosphoryltransferase	Jacobs and Chenia, 2007; Mohapatra <i>et al.</i> , 2008

*The antibiotic resistance genes were detected in the following water environments: EW effluent water; NW natural water; SD sediments; and DW drinking water.

1.4.1.2 Resistance to Vancomycin

The glycopeptide antibiotic vancomycin was initially isolated from the bacterium *Amycolatopsis orientalis* by a missionary in the jungles of Borneo (Rubinstein and Keynan, 2014). Due to its apparent potency, it was called vancomycin, derived from the Latin word for “to vanquish”. Vancomycin is a “last resort drug” and its use is limited to the treatment of serious, life-threatening infections caused by Gram-positive bacteria which are unresponsive to other antibiotics. The recent emergence of vancomycin-resistant enterococci is of great concern and has resulted in the Centre for Disease Control (CDC) and WHO developing guidelines which restricts the use of vancomycin to a limited number of indications. Currently it is only recommended for the treatment of complicated skin

infections, bloodstream infections, endocarditis, bone and joint infections, and meningitis caused by methicillin-resistant *Staphylococcus aureus*. It is also used for the treatment of severe *Clostridium difficile* colitis (Kang and Park, 2015).

It is believed that vancomycin resistance initially emerged in hospitals, firstly in enterococci before spreading to other species, including *S. aureus*. There are six types of vancomycin resistance genes with *vanA* and *vanB* most frequently detected in water environments (Messi *et al.*, 2006) (Table 1.2). The *vanA* gene has been detected in environmental water bodies such as wastewater and surface water biofilms (Schwartz *et al.*, 2003). Vancomycin resistance is manifested by the expression of the *van* gene clusters which encode proteins that alter and prevent the action of the antibiotic. The *vanA* gene encodes for an alteration in the peptidoglycan biosynthesis pathway and results in the production of modified peptidoglycan precursors to which glycopeptides exhibit low affinities (van Hoek *et al.*, 2011). The *vanA* gene is the most widespread of all the *van* gene clusters and has been detected in six Gram-positive bacterial genera namely *Enterococcus*, *Erysipelothrix*, *Lactobacillus*, *Pediococcus* and *Staphylococcus* (van Hoek *et al.*, 2011). Many environmental *Enterococcus* species harbouring the *vanA* gene are resistant to both vancomycin and teicoplanin.

Table 1.2. Vancomycin resistance genes in Aquatic environments

Gene	Biological source	Environmental source *	Function	Reference
<i>vanA</i>	<i>Enterococcus</i> and <i>Staphylococci</i>	DW, EW, NW	Vancomycin resistance protein	Schwartz <i>et al.</i> , 2003; Messi <i>et al.</i> , 2006
<i>vanB</i>	<i>Enterococcus</i>	EW, NW, UW	Vancomycin B-type resistance protein	Caplin <i>et al.</i> , 2008

*The antibiotic resistance genes were detected in the following water environments: EW effluent water; NW natural water; SD sediments; and DW drinking water.

1.4.1.3 Resistance to β -lactams

β -lactam antibiotics, particularly penicillin, are of historical importance in medicine. Penicillin (derived from *Penicillium* fungi) was discovered by Alexander Fleming in 1928. The process for its large-scale production was driven by World War II and it was first used to treat infections in 1942. β -lactam antibiotics are a class of broad-spectrum antibiotics which contain a beta-lactam ring in their molecular structure; this includes penicillin derivatives (penams), cephalosporins (cephems), monobactams and carbapenems. Due to their broad activity spectrum and low toxicity, β -lactams are the most widely used group of antibiotics worldwide, and until 2003 accounted for half of all commercially used antibiotics. While first generation β -lactams were only active against Gram positive

bacteria, chemical modification has extended their range and broad spectrum β -lactams effective against both Gram positive and Gram negative organisms are now available. β -lactams are bacteriocidal and their mode of action is blocking of cell wall synthesis via the inhibition of peptidoglycan synthesis - the peptidoglycan layer is the outermost and primary component of the bacterial cell wall, particularly of Gram-positive organisms, and as such plays a critical role in maintaining cellular structural integrity.

Bacteria develop resistance to β -lactam antibiotics by producing β -lactamases which cleave the β -lactam ring. To overcome this resistance, β -lactam antibiotics are often given in conjunction with a β -lactamase inhibitor such as clavulanic acid. Resistance to this class of compounds is particularly concerning as many developing countries, with limited access to other antibiotics, rely on β -lactams for the treatment of a host of bacterial infections. While there are several mechanisms of resistance the direct deactivation of antibiotics by β -lactamases is the most common, especially in Gram negative organisms. There are many different types of β -lactamases which have been detected in water/sediment from aquaculture, dairy farms, sewage treatment plants, and surface water (Table 1.3). This review, however, focuses on AmpC β -lactamases which have been detected in microbes colonizing wastewater, surface water and drinking water (Schwartz *et al.*, 2003). The Ambler classification scheme states that AmpC β -lactamases are class C enzymes, as they contain serine residues in their active site for catalysis. AmpC β -lactamase resistance is divided into three categories: (1) inducible resistance via chromosomally encoded *ampC* genes, which has been detected in *Enterobacter cloacae*, (2) plasmid-mediated resistance, present in *Klebsiella pneumoniae* and (3) non-inducible chromosomal resistance due to promoter mutations such as the *Escherichia coli* and *Acinetobacter baumannii* (Tamma *et al.*, 2019).

Tamma *et al.*, (2019) states that exposure to β -lactams can trigger a cascade of events leading to significant AmpC production and β -lactam resistance, consequently complicating treatment decisions in an already complex multi-drug resistant climate. This is of particular concern in an environmental context as chromosomally encoded *ampC* genes can be induced in favourable environmental conditions leading to hyperexpression in pathogens such as *E. cloacae*, *Klebsiella aerogenes* and *P. aeruginosa* (Coertze and Bezuidenhout, 2019). In clinical settings, chromosomal and plasmid-mediated *ampC* genes have been well documented, however in an environmental context, more specifically water sources, knowledge is lacking on the distribution, dissemination, and impact *ampC* genes may have on the environment, especially as water systems play a crucial role in the integrated dissemination cycle of ARGs (Coertze and Bezuidenhout, 2019).

Table 1.3: β -lactam and penicillin resistance genes in Aquatic environments

Gene	Biological source	Environmental source *	Function	Reference
<i>ampC</i>	<i>Enterobacter</i> , <i>Salmonella</i>	DW, NW	<i>AmpC</i> type β - lactamase	Schwartz <i>et al.</i> , 2003; Poppe <i>et al.</i> , 2006
<i>bla</i> _{PSE-1}	<i>Aeromonas</i> , <i>Salmonella</i> and <i>Vibrio</i>	EW, SD	PSE-1 β -lactamase	Dalsgaard <i>et al.</i> , 2000; Jacobs and Chenai 2007; Taviani <i>et al.</i> , 2008
<i>bla</i> _{TEM-1}	<i>Escherichia</i>	DW	TEM-type β - lactamase	Alpay-Karaoglu <i>et al.</i> , 2007; Cernat <i>et al.</i> , 2007
<i>bla</i> _{OXA-2}	<i>Aeromonas</i> , Plasmids pB8, pB10 and pTB11	AS, EW	OXA-2 β -lactamase	Schulter <i>et al.</i> , 2005; Tennstedt <i>et al.</i> , 2003
<i>bla</i> _{OXA-}	Plasmid pTB11	AS	OXA-10 β -lactamase	Tennstedt <i>et al.</i> , 2003
³⁰ <i>mecA</i>	<i>Staphylococcus</i>	DW, NW	Penicillin-binding protein	Schwartz <i>et al.</i> , 2003

*: The antibiotic resistance genes were detected in the following water environments: EW effluent water; NW natural water; SD sediments; and DW drinking water.

1.4.2 Horizontal Gene Transfer of ARGs

Environmental bacteria are known to house antibiotic resistance genes and serve as a potential source of novel resistance determinants in clinical pathogens (Li *et al.*, 2012). A study by Aminov (2011) reviewed the role of HGT mechanisms (transformation, transduction and conjugation) in environmental microbiota. The study identified that HGT events are responsible for the acquisition of heterologous resistance mechanisms amongst bacterial species. HGT between bacterial strains is facilitated by mobile genetic elements such as integrons, plasmids, transposons, bacteriophages, insertion elements and genomic islands (Li *et al.*, 2012). Integrons are non-mobile bacterial genetic elements that are able to promote the acquisition of genes embedded within a gene cassette. Gene transfer via the exchange of integrons (and their constituent gene cassettes) is a common pathway for the acquisition of ARGs (Domingues *et al.*, 2012).

1.5 Assessing Antibiotic Resistance Genes in the Environment

The global issue of AMR has directly encouraged the use of innovative methods to monitor the occurrence of antibiotic resistance in the clinical setting and more recently in environmental monitoring (Rocha *et al.*, 2019). Whilst the implementation of monitoring campaigns is effective, there is a need for the standardization of methods used for the monitoring of AR, especially in environmental samples to generate comparable data and improve management practices.

Phenotypic antibiotic resistance using culture-dependent methods is still often used to assess antibiotic resistance in clinical pathogens, however in environmental samples there is a limited value due to many non-culturable bacteria often being present in environmental samples, thereby giving a restricted view of the total resistance present in microbial communities (Rocha *et al.*, 2019). Thus, there has been an increase in the use of methods that directly analyse environmental DNA to assess and quantify the presence and diversity of ARGs in environmental samples.

1.5.1 Molecular Techniques used for the detection and characterisation of environmental ARGs.

Annually microbiologists analyse thousands of environmental water samples to assess both the numbers and types of microorganisms present. Traditionally, culture-based assays were used, however, due to the widespread nature of ARGs in the environment there is a need for the development of molecular methods to investigate the presence, occurrence and distribution of environmental ARGs. Polymerase chain reaction (PCR) assays (conventional, multiplex or quantitative) have been extensively used for the detection of specific ARGs in pure and mixed environmental samples. A limited number of studies have employed DNA hybridisation-based techniques such as microarray and fluorescence *in-situ* hybridization (FISH) to study resistance, however due to the high cost, these methods are often limited to hospital settings. Most recently, metagenomics combined with next generation sequencing (NGS) has been used to detect ARGs in water samples.

1.5.1.1 Gene-specific PCR (Conventional PCR)

Environmental DNA (eDNA) is a DNA molecule derived from organisms present in water or soil samples which is typically only present in low concentrations. Due to its sensitivity and reliability PCR is ideally suited for the analysis of eDNA (Tsuji *et al.*, 2018). Traditional two primer, end point PCR has been extensively used for the analysis of environmental samples, as it allows for the amplification of a specific fragment of DNA present in a complex pool of DNA (Garibyan and Avashia, 2013; Fernando *et al.*, 2016). Gene-specific PCR has been used for the detection and characterization of ARGs from a range of environmental aquatic sources. Although the occurrence of false positives has been documented, the use of simple PCR assays for ARG detection remains one of the most sensitive approaches for environmental water sample analysis (Jansson and Leser, 1996). The main limitation of gene-specific PCR is that prior knowledge of the target DNA sequence is required in order to design primers, and as such, novel resistance genes will not be detected. An important consideration when employing any PCR-based technique is the intrinsic bias which may be introduced. This bias may be due to differences in primer binding to template DNA, as well as the quality and concentration of the template DNA itself. Similarly, it can be costly to individually detect multiple genes using gene-specific PCR. Therefore, researchers are increasingly using multiplex PCR for the analysis of eDNA as it

overcomes some of the limitations of conventional PCR. Additional problems of using PCR for the detection of genes in eDNA is that the extracted DNA may contain compounds which inhibit the polymerase and that low DNA concentrations obtained from samples may be below the detection limit of the assay.

1.5.1.2 Quantitative PCR – Real-Time PCR

Quantitative PCR (qPCR) - also known as real-time qPCR (RT-qPCR)-, allows for the accumulation of DNA after each amplification cycle to be visualised in real time (Arya *et al.*, 2015). Reactions are performed on a specialised thermocycler which detects the increased fluorescence of a reporter molecule as the amount of PCR product increases after each amplification cycle (Ponchel *et al.*, 2003). The inclusion of the fluorescent reporter in the reaction vessel allows for the simultaneous amplification and detection of nucleic acids to detect amplification products (Bustin *et al.*, 2005). qPCR can be used to quantify either the absolute copy number of a gene or the concentration relative to a normalised gene. The three main types of reporter molecule systems used in qPCR are Taqman[®], Molecular Beacons and SYBR-Green. These reporter molecules are either fluorescent dyes which intercalate with double stranded DNA (ds-DNA) or are modified DNA oligonucleotide probes which fluoresce when hybridized to complementary DNA. Unlike other PCR based methods which provide a simple presence/absence result, qPCR allows for the direct quantification of the abundance of specific genes (Fierer *et al.*, 2005). qPCR has become an essential tool in molecular biology due to its specificity, reproducibility, high- sensitivity and simplicity (Gomes *et al.*, 2018).

qPCR is currently the most widely used tool for the quantitation of resistance mediating genes (Volkman *et al.*, 2004). The advantages of qPCR over conventional PCR for eDNA analysis include its speed, reproducibility and the ability to provide direct information regarding the abundance of the target ARG in an environmental sample (Luby *et al.*, 2016). However, the main advantage of qPCR is undoubtedly its exceptionally low detection level. Shannon *et al.* (2007) used qPCR to detect pathogens in wastewater and found that qPCR could detect DNA at concentrations as low as 100 fg (22 gene copies). qPCR using SYBR Green has been used to quantify ARGs such as *vanA*, *blaTEM-1*, *tetA* and *aacC1* in drinking water treatment plants and river water (Zhang *et al.*, 2016; Zhang *et al.*, 2009). Additionally, the methodology has been used to quantify sulphonamide resistance genes *sul(I)*, *sul(II)*, *tet(W)* and *tet(O)* in river sediment samples (Pei *et al.*, 2006). Genes such as *sul1* (Aminov *et al.*, 2001), *tet(O)* and *mecA* (McKinney and Pruden, 2012) have been quantified using qPCR in reclaimed water (Fahrenfield *et al.*, 2013). TaqMan assays have been developed for the quantifiable detection of *vanA* of enterococci, *ampC* of *Enterobacteriaceae*, and *mecA* of staphylococci in different municipal wastewater samples (Volkman *et al.*, 2004). Using the assay *vanA* was detected in 21% of the samples analysed, and *ampC* in 78%. The *mecA* gene was not found in any municipal wastewater

tested, but in two clinical wastewater samples. The main disadvantages of this approach highlighted by authors is that a bias may be introduced due to difficulty in isolating pure genomic DNA from environmental samples (Smits *et al.*, 2004; Shannon *et al.*, 2007).

1.5.1.3 Flow-cytometry and cell sorting

Flow Cytometry (FCM) and Fluorescence-activated cell sorting (FACS) are methods of direct optical detection which allows cells to be evaluated and sorted based on a combination of fluorescence and light scatter - where light scatter is influenced by cell size (Marutescu., 2023). One of the major advantages of FCM over PCR-based assays is that the resulting data is not limited to presence/absence. As FCM assays can test for the ability to reproduce, membrane integrity and metabolic activity, it allows researchers to study viability and physiological conditions. Another major advantage is that FACS allows for the recovery of a defined population (based on cellular properties) for further analyses.

In clinical microbiology, FCM has become a promising tool for the detection of bacteria with a sensitive, resistant, or intermediate resistance phenotype (Marutescu, 2023). Clinically, there have been several FCM-based antibiotic susceptibility testing (AST) methods which have been developed for the detection of AMR in pathogens. Many make use of fluorescent dyes to assess cell viability after exposure to specific antibiotics (Mulrone *et al.*, 2022). For example, Kallai and co-workers (2021), developed a simple FCM-based AST method called MICy, which was able to produce susceptibility profiles in clinical settings faster than conventional microdilution and phenotypic AST methods. Ultimately, these assays have the potential to accelerate decision making in a clinical setting (Mulrone *et al.*, 2022).

FCM has been used to assess water quality, whether it be to conduct absolute cell counting or to identify the relative size, complexity and nucleic acid content of microbial communities present in water samples (Safford and Bischel, 2019). In environmental microbiology, FCM has been used to investigate growth of pathogens in waters and lakes, as well as assist in the study of organisms that were likely present in viable but not-cultivable (VBNC) states in the environment (Tanaka *et al.*, 2000). Microbial communities in water samples have been characterized with the help of FCM, which mainly assists in sorting target cells for subsequent analysis by employing various staining and sorting techniques (Safford and Bischel, 2019).

Employing FCM in ecology studies of mixed cell populations, however, can be challenging. Firstly, as cytometry requires cells to be in suspension when studying soil communities, bacteria trapped in biofilms or closely associated with inert solid support will be missed. However, studies have shown that density gradient centrifugation using media such as Nycodenz can purify soil bacteria into liquid

suspension, and the community analysis results for samples prepared in this manner are comparable to the original communities. A second challenge one must take into consideration is the variability of the source material and the potential of non-specific binding to other biological material such as proteins. Thirdly, there may be high background autofluorescence due to photosynthetic pigments produced by algae/cyanobacteria or minerals present in water samples. Endogenous DNA components such as flavin nucleotides and pyridine can also lead to autofluorescence.

1.6 Aims & Objectives of the Study.

Greywater is highly variable and often contains significant microbial contamination, which may include pathogenic and resistant organisms (Winward *et al.*, 2008). The environmental and health risks associated with this is wide ranging, as greywater could be a potential source of bacterial contamination of groundwater. In addition, antibiotic resistant organisms can proliferate and spread resistant genes to environmental strains (Birks and Hills, 2007; Maimon *et al.*, 2014; Busgang *et al.*, 2018).

Therefore, based on its high organic content and growth conditions, greywater is able to support microbial growth and biofilm production. These microbial populations may include resistant and susceptible bacteria. Thus, it is hypothesized that greywater use, collection and storage may act as a platform for ARGs proliferation and exchange, acting as a hotspot for horizontal gene transfer.

The aim of this thesis was to determine whether domestic greywater is a source of antibiotic resistance genes (ARGs) and pathogenic organisms and to identify if domestic greywater serves as a potential hotspot for horizontal gene transfer (HGT).

The objectives are therefore:

1. To identify the phenotypic resistance profiles present in domestic greywater samples using culture-based antimicrobial susceptibility testing. Additionally, the cell viability of the microbial populations present in domestic greywater samples was verified using the LIVE/DEAD BacLight flow cytometry assay.
2. To quantify the levels of three ARGs (*vanA*, *ampC* and *aadA* genes) linked to domestic greywater and biofilms using qPCR.
3. To identify the presence of integrons in domestic greywater and biofilms and determine whether the *int11* gene is a marker of HGT using qPCR.

Chapter 2: Phenotypic Resistance Analysis and Cell Viability Assessment of Greywater Samples

2.1 Introduction

The environmental surveillance of antimicrobial resistance has become a priority in many countries around the world. The surge in interest has greatly shifted the focus into developing a standardized effective strategy or methodology for the monitoring of AMR in agricultural and water environments (Luby *et al.*, 2016).

Current research methodologies utilize classical phenotypic culture-based methods which target known or culturable bacteria in combination with molecular methods which target DNA, RNA or proteins. This approach has allowed for a rapid expansion in the tools available for effective AMR monitoring (Luby *et al.*, 2016; McLain *et al.*, 2016).

High-throughput molecular methods have a major benefit especially with regards to environmental water samples, in that the methods avoid culture bias (Luby *et al.*, 2016). However, they often do not confirm functionality within in the specific environment, which is easily achieved using phenotypic assays.

2.1.1 Antimicrobial Susceptibility Testing

Antimicrobial susceptibility testing (AST) remains an invaluable method for selecting the appropriate antimicrobial agents, especially to treat infectious diseases (Salam *et al.*, 2023). The core purposes of AST is aimed at assisting physicians with choosing the correct or most suitable antibiotic according to the specific needs of the patients, in a clinical setting for example. Additionally, AST provides insight into the microbial resistance within the community and areas whilst also allowing the development of prevention strategies (Salam *et al.*, 2023). The misuse of antimicrobials has led to an increase in multi-drug resistant infections at an alarming rate. Microorganisms possess the inherent or acquired ability to constantly change their susceptibility patterns to antibiotics. Therefore, to identify a pathogen's susceptibility profile is of vital importance.

According to Salam *et al.*, (2023) phenotypic susceptibility testing refers to a set of observable characteristics or traits which a microbe displays against a panel of preselected antimicrobial agents. These characteristics are either the inhibition of growth in the presence of bacteriostatic agents or death when in the presence of bactericidal agents. Phenotypic AST methods such as agar disc diffusion, broth dilution, gradient diffusion and commercially available automated and semi-automated systems remain widely used in many diagnostic and microbial testing laboratories.

Microbial classification for antibiotic resistance in both clinical and environmental settings is defined as either “susceptible”, “resistant” or “intermediate” of which each is defined based on the growth of the bacterium in the presence of defined *in-vitro* antibiotic concentrations. Clinical breakpoints specifically are defined based on the minimum-inhibitory concentrations (MIC). McLain *et al.*, (2016) defines MICs as the lowest concentration of an antimicrobial agent that will inhibit visible growth of a microorganism after an overnight incubation. A susceptible isolate would therefore be inhibited by the MIC at the site of infection, whereas a resistant isolate would not be affected by the MIC of an antibiotic. The intermediate category refers to isolates which display a relative resistance to a certain concentration of an antibiotic but are susceptible to antibiotic concentrations above the MIC (McLain *et al.*, 2016). Certain culture-based methods exploit this characteristic, such as the Kirby-Bauer method.

2.1.2 Kirby-Bauer Disc Diffusion Assay

A conventional method of phenotypic AST widely used in many clinical and research microbiology laboratories is the Kirby-Bauer disc diffusion method. This method is based on exposing the sample or pathogen to various antibiotics and measuring the bacterial growth/inhibition. Although time consuming and labour-intensive the visual evaluation of growth is highly effective in measuring efficacy.

The Kirby-Bauer disc diffusion method was proposed as a standardized method by Bauer *et al.* in 1966 and has been widely used to characterize antibiotic resistance for environmental isolates since (Khan *et al.*, 2019). The simple and reproducible culture-based method requires that the bacteria or environmental sample be spread across the surface of an agar plate, followed by the placement of discs impregnated with a standardized concentration of antibiotics on top of the sample shown in Figure 2.1. As the antibiotics diffuse from the impregnated discs into the agar, it establishes a concentration gradient, in which a higher concentration of the target antibiotic is closer to the disc whilst a diluted concentration is present further away from the disc. The targeted bacteria will therefore only grow to the point at which the antibiotic is at a concentration that will impede growth and proliferation. It should be noted that the size of the inhibitory zone is influenced by factors such as the diffusion rate of the antibiotics (McLain *et al.*, 2016).

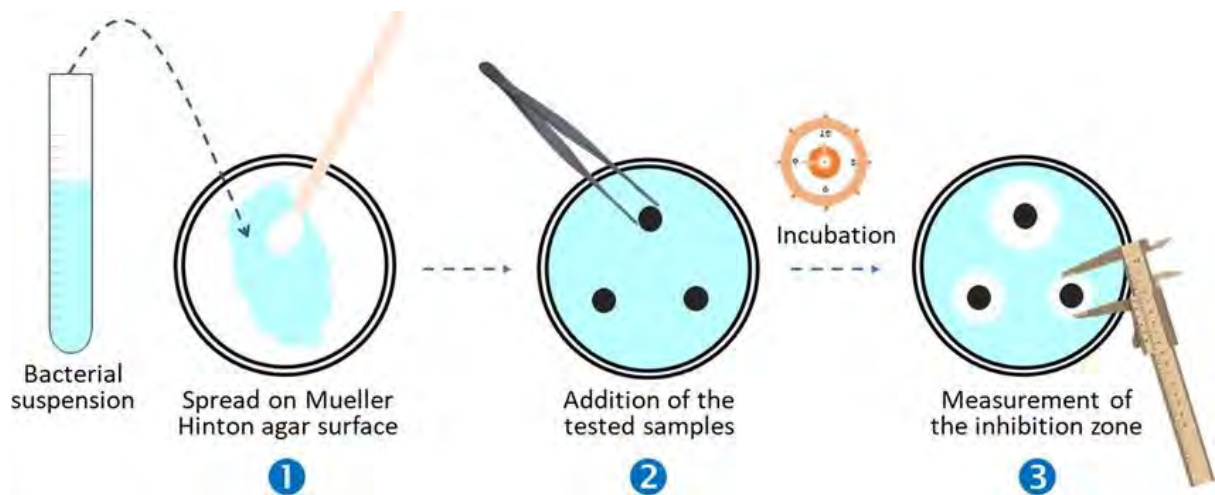


Figure 2.1: A schematic overview of the Kirby-Bauer disc diffusion method. Adapted from Guerraf *et al.*, (2022).

This method is used in many clinical laboratories and is a cost-effective methodology especially when monitoring environmental samples as it allows for the detection of multiple targets (Khan *et al.*, 2019).

The main disadvantage of the Kirby-Bauer method is that it is a relatively slow method, taking 16 to 24 hours and requiring the use of a selection of target antibiotic groups and target bacteria relevant to the environmental or clinical setting (Webber *et al.*, 2022). Additionally, culturing of target microorganisms from environmental water is often challenging given that samples may contain 10^6 to 10^{10} microorganisms per gram (Davis *et al.*, 2005).

Culture-based methods only provide information regarding viable cells and despite the vast amount of high-throughput methods available a standardized rapid AST methodology has not been proposed. Ideally, a rapid AST method should be faster and more informative than conventional AST methods and provide guidance on the selection of an effective antibiotic treatment in the clinical sector, for example (Robertson *et al.*, 2019). The desire for a faster and more rapid response to antibiotic resistance, especially in the clinical sector has resulted in the development of high-throughput, rapid diagnostics tests using advanced technology such as mass spectrometry, fluorescence imaging and fluorescent activated cell sorting. However, compared to culture-based AST, molecular-based high-throughput solutions are still in its infancy, and no ideal standardized methodology has been implemented yet.

The assessment of AST using fluorescent dyes provides a real-time alternative to culture-based methods as the use of dyes allow for rapid real-time quantification of bacterial viability. There are a variety of fluorescent viability dyes available which report on different cell processes such as

membrane potential (cellular energy); metabolism and membrane integrity (intact cell membrane/viability) which is often used to investigate AST (Robertson *et al.*, 2019).

An evaluation of literature revealed that rapid AST in recent years has focused on the assessment of cell viability using fluorescent dyes. One such methodology is the use of the LIVE/DEAD BacLight™ Bacterial Viability kit on clinical and environmental samples.

2.1.3 The LIVE/DEAD BacLight Bacterial Viability Assay

The LIVE/DEAD BacLight Bacterial Viability kit utilizes two fluorescent dyes, SYTO9 and propidium iodide (PI). These dyes are coupled to distinguishing between live and dead cells based on their membrane integrity. SYTO9 is membrane permeable and can therefore enter all cells and results in green fluorescence. Conversely, propidium iodide is membrane impermeable and can only enter cells which have a compromised membrane or cell wall, regarded as “dead cells” in microbiology. PI results in red fluorescence.

The LIVE/DEAD BacLight methodology has been used to investigate and rapidly determine the proportion of live cells in a population, in both the clinical setting and environmental monitoring. Unlike PCR-based methods which cannot differentiate between DNA derived from viable, dead and viable but non-culturable (VBNC) bacteria, the BacLight assay allows the researcher to differentiate between these populations (Robertson *et al.*, 2021).

In a mixed environmental population cell viability can greatly influence the transfer of ARGs within the environment as the presence of extracellular ARGs and nonviable cells that contain ARGs in the environment increases the risk of potentially harmful ARGs being incorporated into competent host genomes by transformation. Insight into the relative proportion of ARGs that are present in viable and nonviable cells allows for further understanding of the different mechanisms of ARG proliferation, especially in environmental settings (Eramo *et al.*, 2019).

2.1.4 Aim of Chapter 2

The aim of this chapter was to identify the phenotypic resistome of the domestic greywater and biofilm samples collected using the Kirby-Bauer method. Furthermore, flow cytometry was used to identify the cell viability of the bacterial population present in the domestic greywater samples.

2.2 Materials and Methods

2.2.1 Site Identification

Samples were collected from four residential properties in Pinehurst, a suburb in Durbanville, Western Cape (GPS -33.839,18.665). The suburb is predominantly middle class and as a Garden Cities Development belongs to their Homeowners Association (HOA). Entry level/mid-range greywater collection systems with minimal treatment were selected for study as this is the most popular system installed. All four systems were similar entry level systems, with 120 L capacity and minimal treatment in order to 'normalise' the operational parameters such as treatment, retention time etc. However, it should be noted that the household sizes, occupants, and demographics did vary.

2.2.1 Sampling Equipment

Sampling equipment was prepared according to the *Handbook for Water-Resource Investigations* (Wilde, 2004). The 10 L High Density Polyethylene No. 2 Nalgene bottles (HDPE, #2) and lids were washed using commercial dishwashing liquid, followed by two thorough rinses with tap water. The interior and exterior surfaces were washed with 5% hydrochloric acid (HCl) solution. The bottles were left in the fume hood to allow the remaining HCl solution to evaporate. An additional rinse of the bottles was conducted using dH₂O for both the interior and exterior surfaces. The bottles were then washed with HPLC Grade Methanol. Finally, the bottles were rinsed using UV-treated Millipore water and deemed ready for sample collection. Sealed sterile bottles were stored in plastic bags until sample collection.

2.2.2 Greywater and Biofilm Sample Collection

A 10 L sample of greywater was collected from each respective site using the acid-washed 10 L Nalgene bottles, in compliance with risk assessment requirements over a period of 12 months. Greywater was collected by partially immersing the acid-washed 10 L Nalgene collection bottle directly in the collection tank until approximately 10 L of greywater was collected. Biofilm samples were collected from each site, using a sterile buccal swab (Puritan Sterile Polyester Tipped Applicators), by scraping the inside of the greywater collection tanks (~5 cm² area) about 5 cm below the waterline with considerable pressure. As a control, 50 ml of the household potable, municipal tap water was sampled at the beginning of the study. This served as a baseline and to ensure no microbes or sources of potentially ARGs were introduced by the input water itself.

All samples were processed within 48 hours of collection. All samples will be stored at 4 °C at the Institute of Microbial Biotechnology and Metagenomics (IMBM), UWC. A complete list of samples collected for the duration of the study is provided in Table 2.1.

Table 2.1: Sample Collection Season specifications according to weather patterns in the Western Cape.

Seasons	Dates/ Period
Summer	1 December - 28/29 February
Autumn	1 March - 31 May
Winter	1 June -19 September
Spring	20 September - 30 November

Table 2.2: Greywater and Biofilm Sample Collection Schedule for 2018 to 2021

Site	Sample	Greywater Sample	Biofilm Sample	Collection Season
1	1	GWS1S1	BFS1S1	Spring
	2	GWS1S2	BFS1S2	Winter
	3	GWS1S3	BFS1S3	Summer
	4	GWS1S4	BFS1S4	Autumn
2	1	GWS2S1	BFS2S1	Spring
	2	GWS2S2		Spring
	3	GWS2S3	BFS2S3	Summer
	4	GWS2S4	BFS2S4	Autumn
3	1	GWS3S1	BFS3S1	Spring
	2	GWS3S2	BFS3S2	Summer
	3	GWS3S3	BFS3S3	Spring
	4	GWS3S4		Summer
	5	GWS3S5	BFS3S5	Winter
	6	GWS3S6	BFS3S6	Spring
	7	GWS3S7	BFS3S7	Autumn
4	1	GWS4S1	BFS4S1	Summer
	2	GWS4S2	BFS4S2	Autumn
	3	GWS4S3	BFS4S3	Autumn
	4	GWS4S4	BFS4S4	Spring
	5	GWS4S5	BFS4S5	Summer
	6	GWS4S6	BFS4S6	Winter
	7	GWS4S7	BFS4S7	Spring

2.2.3 Kirby-Bauer Disc Diffusion Assay

To identify the phenotypic resistance patterns of the greywater and biofilm samples, the Kirby-Bauer disc diffusion method was used. Muller-Hinton agar (Merck) was prepared according to the manufacturers' specifications.

For the antibiotics cefpodoxime (30 µg); cephalothin (30 µg) and teicoplanin (10 µg), a 90 mm antimicrobial susceptibility disc dispenser (Oxoid TM, South Africa) was used to dispense the antibiotic discs on the various sample plates.

For the antibiotics: ampicillin (10 µg), streptomycin (10 µg), gentamicin (10 µg), kanamycin (30 µg), vancomycin (30 µg), and chloramphenicol (25 µg), antibiotic discs were prepared using an in-house method as described by Vineetha *et al.*, in 2015.

2.2.3.1 Preparation of Antibiotic discs

Antibiotic powders were prepared according to the manufacturers' specifications. Stock solutions were then diluted at the time of analysis to obtain the desired working solutions. The sterile Whatmann circle discs of 6 mm in diameter were placed in sterile petri dishes, respectively, for impregnation. The discs were impregnated with 20 µl of antibiotic solution to obtain the desired antibiotic concentration. The discs were then allowed to dry prior to plating.

2.2.3.2 Kirby-Bauer Disc Diffusion Assay of Greywater and Biofilm Samples

To ensure efficacy, the test organisms *E. coli* ATCC 25922, *S. aureus* ATCC 25923 and *E. faecalis* ATCC 29212 were used as QC standards. In order to test the greywater samples a sterile swab was placed into the greywater and streaked on the agar surface using aseptic techniques, in order to form a bacterial lawn. The entire plate was streaked in one direction followed by rotating the plate 90° and then streaking the plate again in the same direction. This rotation was repeated three times to obtain uniform growth over the entire plate. For biofilm samples, the collection swab was streaked directly on the agar in the same manner. The MH agar plate was left to dry. The prepared antibiotic discs were placed on the inoculated MH agar plates and incubated at 37 °C overnight. The zone of inhibition for each antibiotic was measured and compared to the CLSI guidelines (Clinical and Laboratory Standards Institute, USA, 2023) to determine the incidence of susceptibility to each antibiotic.

2.2.4 LIVE/DEAD BacLight Assay using Flow Cytometry

2.2.4.1 Bacterial Strains

The following strains were used in this study for control purposes: *E. coli* ATCC 25922 as a Gram negative and *S. aureus* ATCC 33591 as a Gram positive, respectively as per manufacturer's guidelines. Bacterial cultures were grown at 37 °C for 16 hours in Luria Bertani Broth, shaking at 180 rpm.

2.2.4.2 Media and Chemicals

Cell biology reagents were purchased from Sigma Aldrich. HPLC-grade 2-Propanol (99.9%) was used to prepare 70% Isopropyl alcohol.

2.2.4.3 Preparation of LIVE and DEAD Bacterial Cultures

Live-cell (untreated) and dead-cell (alcohol-treated) *E. coli* and *S. aureus* cultures were prepared according to the manufacturer's instructions provided with the BacLight Kit (Invitrogen, 2004). These

cultures were used to adjust the flow cytometer according to the instructions provided by the manufacturer.

For the Live-cell suspension: 2 ml of each bacterial culture was centrifuged at 5 000 xg for 3 minutes to pellet the cells. The supernatant was removed, and the pellet was resuspended in 1 ml of 0.85% NaCl/saline solution. The suspension was then incubated at room temperature for 60 minutes, mixing the suspension every 15 minutes. Post-incubation, the bacterial cultures were centrifuged at 10 000 xg for 2 minutes and washed with 1 ml of 0.85% NaCl solution, after which the suspensions were re-centrifuged at 10 000 xg for 2 minutes and the resulting pellet was resuspended in 1 ml of 0.85% NaCl solution.

For Dead-cell suspensions: 2 ml of each bacterial culture was centrifuged at 5 000 xg for 3 minutes to pellet the cells. The supernatant was removed, and the pellet was resuspended in 1 ml of 70% isopropyl alcohol. The dead-cell suspension was incubated at room temperature for 60 minutes, mixing every 15 minutes. Post-incubation, the bacterial cultures were centrifuged at 10 000 xg for 2 minutes and washed with 1 ml of 0.85% NaCl solution, after which the suspensions were re-centrifuged at 10 000 xg for 2 minutes and the resulting pellet was resuspended in 1 ml of 0.85% NaCl solution.

2.2.4.4 Preparation of Greywater samples for analysis

For greywater samples, 1 ml of concentrated greywater sample was centrifuged at 10 000 xg for 2 minutes. The resulting pellet was washed with 1 ml of 0.85% NaCl solution and vortexed for 1 minute. After which the samples were re-centrifuged at 10 000 xg for 2 minutes, and the resulting pellet was re-suspended in 1 ml of 0.85% NaCl solution and incubated for 15 minutes prior to flow cytometry analysis.

Greywater was processed and concentrated as follows: 8 L of greywater was sequentially centrifuged, 500 ml at a time in metal-screw capped bottles (Nalgene) at 5 000 rpm for 20 minutes using the Sorvall Lynx 6000 centrifuge (Thermo Fischer Scientific, MA, USA). The resulting pellet was resuspended in 100 ml sterile diethyl pyrocarbonate (DEPC)-water.

2.2.4.5 Staining of Samples

Two fluorescent dyes were used, either alone or in combination: SYTO 9 nucleic acid stain (Invitrogen) and Propidium Iodide (PI) (Invitrogen). SYTO 9 and PI were used from the LIVE/DEAD BaLight Kit (Invitrogen) as per the manufacturer's instructions. Aliquots of 987 μ l of 0.85% NaCl solution were prepared in flow cytometry analysis tubes. Individual samples (standard and experimental) were prepared by adding 1.5 μ l of 3.34 mM SYTO 9 nucleic acid stain and 1.5 μ l of 30 mM Propidium Iodide to the tubes, followed by the addition of 10 μ l of bacterial suspension or prepared greywater sample.

The flow cytometry tube containing the staining solution and sample was vortexed for 5 minutes. The samples were incubated for 15 minutes at room temperature, protected from light prior to analysis.

2.2.4.6 Flow Cytometric measurements

Flow cytometric measurements were performed using the BD FACS Aria III Flow Cytometer and Cell Sorter (BD Life Sciences, San Jose, USA, 2016), which is capable of sorting four populations simultaneously. The flow cytometer has a digital platform cytometer with integrated software called FACSDiVA. It is fitted with three lasers: (1):488 nm Blue laser which detects 5 parameters as well as forward scatter and side-scatter; (2): a 633 nm red laser which detects two parameters and (3); a 405 nm violet laser capable of detecting two parameters. For the analysis a Nylon assay nozzle of 100 μ M (BD Biosciences) was used and the Neutral density filter 1 was used. Flow cytometry data was analysed and cytograms were produced using the FlowJo (v.10.8) software.

2.3 Results & Discussion

2.3.1 Kirby-Bauer Disc Diffusion Assay

The increased interest in greywater collection, storage and use as a manner of water management has prompted concerns regarding its safety and potential long-term health implications (Maimon *et al.*, 2010). Thus, in the present study to determine the antibiotic susceptibility pattern of greywater samples and their associated biofilms the Kirby-Bauer method was used to test for resistance against clinically relevant antibiotics.

Parallel culture-based microbiology testing was conducted as part of the larger study. The unpublished data revealed that the average bacterial load per site for the greywater samples ranged between 7.9×10^6 CFU/ml to 3.4×10^7 CFU/ml. Additionally, culturing revealed low diversity with four to six species present per site identified using amplified ribosomal DNA restriction analysis (ARDRA). It should be noted these preliminary studies revealed that *Enterobacter* sp. were present in all four greywater systems (R. Sunday; unpublished data). In addition, in a subsequent study ~60% of the strains isolated from the greywater and biofilms showed resistance to at least one antibiotic (B. Kota; unpublished data).

In the present study the Kirby-Bauer disc diffusion method was conducted to determine the resistance of microorganisms present in complex greywater and biofilm samples. Studies utilizing the Kirby-Bauer method in microbial ecology have shown that there is an abundance of resistant microorganisms present in water samples such as reclaimed water and wastewater treatment plants.

It should be noted that the Kirby-Bauer disc diffusion assay was used as a breakpoint assay (McLain *et al.*, 2016) as we did not evaluate specific antibiotic MICs but was rather utilized it to identify whether resistant microorganisms were present in domestic greywater and biofilm samples. The diameter of the zone of inhibition was measured in millimetres manually and compared to the standardized Clinical and Laboratory Standards Institute (CLSI) (CLSI, USA, 2023) interpretive criteria used to designate an isolate as sensitive or resistant to the antibiotic. A summarised version of the criteria based on the bacterial controls assessed in described in Table A (Appendix – Chapter 2). Figure 2.2 provides an example of the zones of inhibition present for a pure culture of *S. aureus* and also serves as the bacterial control for the assay.

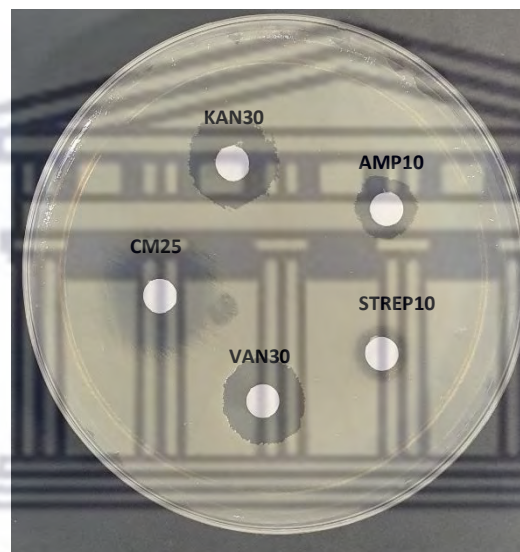


Figure 2.2: Example of the Kirby-Bauer Disc Diffusion method of QC Strain *S. aureus* ATCC 29213 using in-house prepared antibiotic discs.

Figure 2.3 and 2.4 provide examples for the type of growth and zones of inhibition observed when assessing the greywater samples. Table 2.3 and 2.4 represents the zone of inhibition per sample per antibiotic for the greywater and biofilm samples, respectively. The results indicate that 82% of the greywater samples analysed contained bacteria that were resistant to ampicillin, 94.4% resistant to kanamycin, 10.52% resistant to streptomycin, 5.26% resistant to gentamicin, 10.53% resistant to chloramphenicol and most concerning 94.4% and 87.5% of the greywater samples exhibited resistance to vancomycin and teicoplanin, respectively. The associated biofilms were also assessed per site, with similar resistance patterns being identified. For domestic biofilm samples 76.4% of the samples contained bacteria that were resistant to ampicillin, 93.3% to kanamycin, 17.64% to streptomycin and 68.75% to vancomycin. It should be noted that all biofilm samples exhibited resistance to teicoplanin. George *et al.* (2014) demonstrated similar findings when assessing drinking and surface water samples collected in Mafikeng, South Africa. The results obtained also reiterate those by Bartholin *et al.* in

2023, in which high levels of resistance was identified for β -lactam antibiotics such as ampicillin and cephalosporins. This result is not unsurprising as natural resistance to these antibiotics is often found in environmental and agricultural bacterial populations (Jaja *et al.*, 2020).

In terms of per site resistance patterns, similar resistance was experienced between the greywater samples and their corresponding biofilm sample. However, for some samples such as S3S5 and S4S6 intermediate zones were detected for greywater samples, whereas susceptible zones of inhibition were identified in the biofilm samples. This suggests the biofilm samples may have a more complex microbial community present differing to that of the greywater.

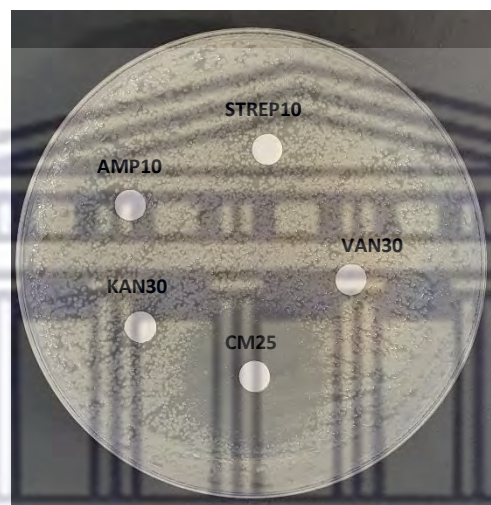
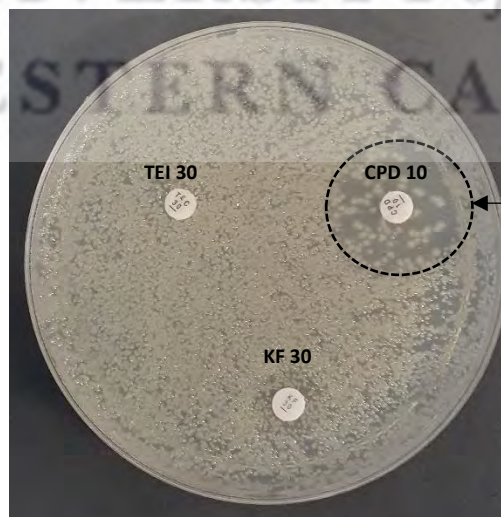


Figure 2.3: Example of the Kirby-Bauer Disc Diffusion method of greywater sample GWS4S5 using in-house prepared antibiotic discs.



Zone indicating resistant bacteria present in the greywater sample.

Figure 2.4: Example of the Kirby-Bauer Disc Diffusion method of greywater sample GWS4S5 using commercial antibiotic discs supplied by Oxoid TM.

AST methodologies rely greatly on selecting the correct target groups for bacteria and antibiotics (McLain *et al.*, 2016). Preliminary microbial analysis assisted in guiding the selection of the antibiotics assessed, as well as availability. Additionally, the relevance of antibiotics in both clinical and agricultural/environmental settings were taken into consideration when selecting the range of antibiotics used. McLain *et al.* (2016) stated the importance of targeting antibiotic classes used for the treatment of ESKAPE pathogens, especially *E. coli*, *K. pneumoniae*, *Enterococcus* and *Staphylococcus* which are widely distributed in the environment and have been proposed to play an evolutionary role in the development and spread of resistance.



Table 2.3: Kirby-Bauer Disc Diffusion method to determine the zone of inhibition (mm) in Greywater samples

SAMPLE	AMP 10	KAN 30	STREP 10	GEN 10	VAN 10	CM 25	TEC30	KF30
GWS1S2	-	14 BS [I]	20 [S]	18 [S]	no zone [R]	35 [S]	no zone [R]	no zone
GWS1S3	No zone [R]	no zone [R]	15 BS [S]	8 + 20 BS [R]	no zone [R]	11 + 30 BS [R]	no zone [R]	20 BS [I]
GWS1S4	no zone [R]	no zone [R]	18 BS [S]	18 [S]	no zone [R]	12 + 35 BS [R]	no zone [R]	11 BS
GWS2S2	25 BS [S]	no zone [R]	25 BS [S]	22 [S]	no zone [R]	25 + 33 BS [S]	no zone [R]	no zone [R]
GWS2S3	no zone [R]	11 [R]	15 BS [S]	20 [S]	no zone [R]	30 [S]	no zone [R]	25 BS [S]
GWS2S4	no zone [R]	no zone [R]	17 BS [S]	20 [S]	no zone [R]	30 BS [S]	-	-
GWS3S2	no zone [R]	no zone [R]	8 + 24 BS [R]	18 + 23 BS [S]	18 BS [R]	25 [S]	20 BS [S]	9 BS [R]
GWS3S3	no zone [R]	no zone [R]	18 [S]	23 [S]	no zone [R]	23 [S]	no zone [R]	no zone [R]
GWS3S4	no zone [R]	11 [R]	23 [S]	12 + 22 BS [S]	no zone [R]	20 BS [S]	-	17 [R]
GWS3S5	14 BS [I]	12 BS [R]	14 BS [I]	17 + 22 BS [S]	7mm [R]	25 + 35 BS [S]	-	-
GWS3S6	8 BS [R]	20 BS	14 [I]	20 [S]	no zone [R]	30 BS [S]	no zone [R]	no zone [R]
GWS3S7	no zone [R]	no zone [R]	17 BS [S]	18 + 23 BS [S]	no zone [R]	24 BS + 35 [S]	no zone [R]	14 BS [R]
GWS4S1	no zone [R]	no zone [R]	11 + 22 BS [R]	18 + 25 BS [S]	12mm BS [R]	28 [S]	no zone [R]	12 BS [R]
GWS4S2	-	no zone [R]	17 [S]	14 + 22 BS [I]	no zone [R]	30 [S]	no zone [R]	no zone [R]
GWS4S3	25 [S]	no zone [R]	25 [S]	22 [S]	no zone [R]	29 [S]	no zone [R]	no zone [R]
GWS4S4	no zone [R]	no zone [R]	17 + 24 BS [S]	22 + 24 BS [S]	25 BS	27 [S]	24 BS [S]	12 BS [R]
GWS4S5	no zone [R]	12 BS [R]	25 BS [S]	29 [S]	25 BS	34 BS [S]	no zone [R]	15 BS [R]
GWS4S6	no zone [R]	no zone [R]	12 [I]	18 + 25 BS [S]	no zone [R]	35 [S]	no zone [R]	no zone [R]
GWS4S7	no zone [R]	no zone [R]	13 BS [I]	20 + 25 BS [S]	no zone [R]	25 BS [S]	no zone [R]	no zone [R]

For this study the following terms are defined: [R] – Resistant bacteria present in sample; [I] – Intermediate bacteria present in sample; [S] – Susceptible bacteria present in sample. BS represents a “bacteriostatic zone” whereby resistant bacteria may be present in the sample.

Table 2.4: Kirby-Bauer Disc Diffusion Assay of Biofilm Samples

Sample	AMP 10	KAN 30	STREP 10	GEN 10	VAN 10	CM 25	TEC 30	KF 30
BFS1S1	25 [S]	-	20 [S]	-	no zone [R]	-	no zone [R]	23 [S]
BFS1S2	16 BS [I]	-	20 [S]	-	no zone [R]	-	no zone [R]	no zone [R]
BFS1S3	8 BS [R]	10 BS [R]	9 BS [R]	20 BS [S]	9 BS [R]	33 BS [S]	-	-
BFS1S4	no zone [R]	no zone [R]	14 BS [I]	22 BS [S]	no zone [R]	33 BS [S]	-	-
BFS2S3	no zone [R]	no zone [R]	no zone [R]	25 BS [S]	no zone [R]	13 BS [I]	-	-
BFS2S4	no zone [R]	no zone [R]	no zone [R]	28 BS [S]	no zone [R]	9 BS [R]	-	-
BFS3S2	15 [I]	13 [R]	20 [S]	30 [S]	30 BS [S]	15 [I]	no zone [R]	22 [S]
BFS3S3	no zone [R]	no zone [R]	20 BS [S]	27 [S]	30 BS [S]	28 BS [S]	-	-
BFS3S5	no zone [R]	no zone [R]	16 [S]	-	no zone [R]	30 BS [S]	no zone [R]	no zone [R]
BFS3S6	no zone [R]	no zone [R]	20 BS [S]	26 BS [S]	-	11 + 28 [R]	no zone [R]	no zone [R]
BFS3S7	no zone [R]	15 BS [I]	20 BS [S]	25 BS [S]	no zone [R]	38 BS [S]	-	-
BFS4S1	15 [I]	no zone [R]	17 [S]	28 [S]	36 BS	30 BS [S]	no zone [R]	22 [S]
BFS4S2	no zone [R]	9 [R]	17 [S]	24 BS [S]	no zone [R]	37 BS [S]	no zone [R]	no zone [R]
BFS4S3	no zone [R]	12 BS [R]	27 [S]	30 [S]	35 BS*	35 BS* [S]	no zone [R]	no zone [R]
BFS4S4	no zone [R]	12 [R]	24 [S]	27 [S]	2 [S]	27 [S]	-	-
BFS4S6	no zone [R]	8 [R]	15 [S]	24 [S]	no zone [R]	18 + 25 BS [S]	no zone [R]	20 BS [I]
BFS4S7	no zone [R]	no zone [R]	18 BS [S]	25 BS [S]	no zone [R]	35 BS [S]	no zone [R]	20 BS [I]

For this study the following terms are defined: [R] – Resistant bacteria present in sample; [I] – Intermediate bacteria present in sample; [S] – Susceptible bacteria present in sample. BS represents a “bacteriostatic zone” whereby resistant bacteria may be present in the sample.

WESTERN CAPE

2.3.2 LIVE/DEAD BacLight Bacterial Viability Assay of Greywater Samples

Antimicrobial resistance is increasingly creating a significant health burden, especially on the already strained healthcare system in South Africa. Therefore, the need for rapid and reliable diagnostics is critical to addressing the issues associated with AMR and the treatment of multi-drug resistant infections (Robertson *et al.*, 2019). Culture-based methods such as the Kirby-Bauer Method described in Section 2.3.1, only allow for the assessment of culturable and viable cells. These methods also have slow lead times, ranging from 3 to 5 days.

Flow cytometry is increasingly considered to be an essential technology for the study of microbial communities in environmental samples (Cichocki *et al.*, 2020). The LIVE/DEAD BacLight Bacterial Viability kit is popular amongst researchers in microbiology and molecular biology, especially as it allows for the visualization of intermediate states, which is when cell-injury has occurred (Berney *et al.*, 2007).

This study evaluated the cell viability of thirteen greywater samples using the LIVE/DEAD BacLight Bacterial Viability kit as a high-throughput alternative to traditional culture-based AST. The cell viability assay was performed as per manufacturer's instructions.

Bacterial suspensions of *S. aureus* and *E. coli* was prepared and assessed as bacterial controls for a Gram-positive and Gram-negative bacterial sample, respectively. Figure 2.5 and 2.6 represents the cytograms of live and dead bacterial suspensions for *E. coli* and *S. aureus* respectively, displayed as red fluorescence (PE-Texas Red-A) versus green fluorescence (Alexa Fluor 488-A).

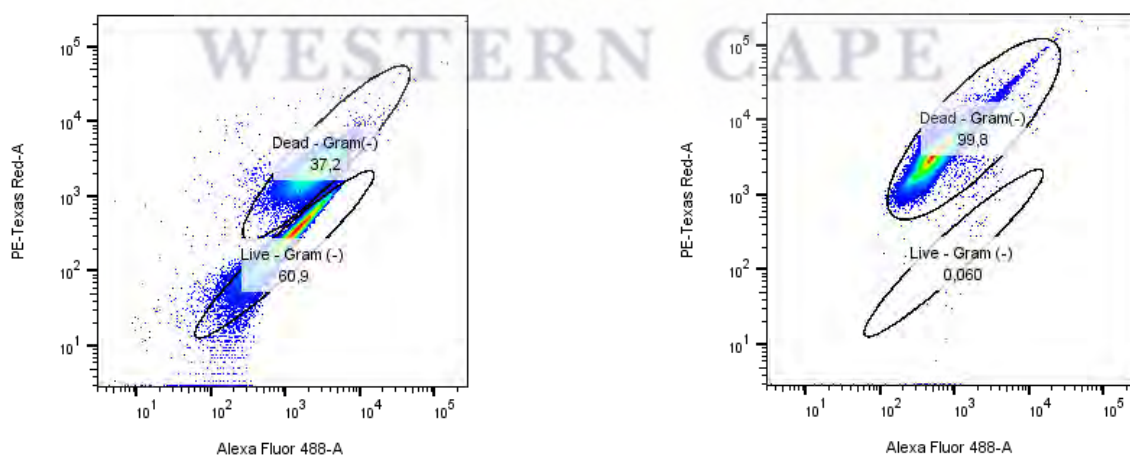


Figure 2.5: Analysis of *Escherichia coli* pure bacterial culture using the LIVE/DEAD BacLight Bacterial Viability and Counting Kit. Bacterial suspensions of live (untreated) and dead (alcohol-treated) cells were stained and analysed using flow cytometry. The above cytogram displays red fluorescence (PE-Texas Red-A) versus green fluorescence (Alexa Fluor 488-A).

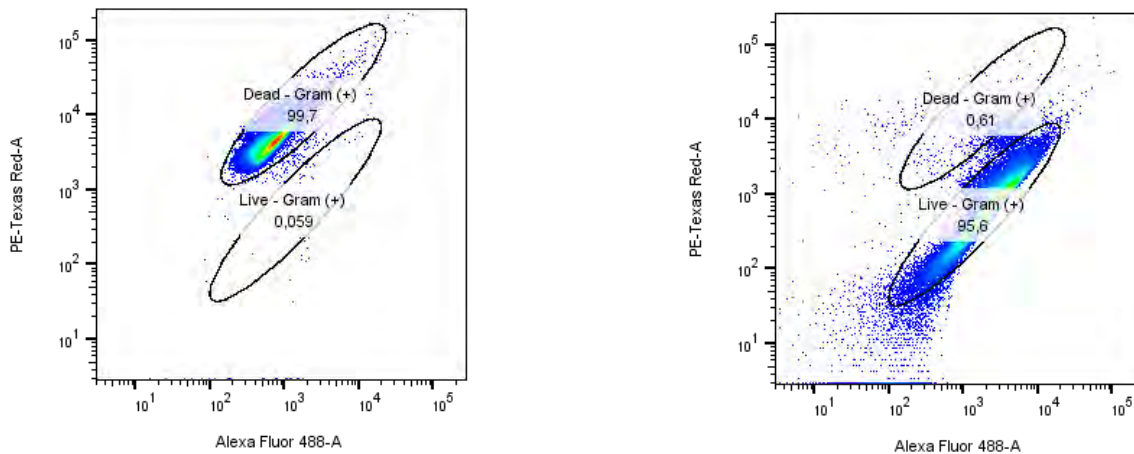


Figure 2.6: Analysis of *Staphylococcus aureus* pure bacterial culture using the LIVE/DEAD BacLight Bacterial and Counting Kit. Bacterial suspensions of live (untreated) and dead (alcohol-treated) cells were stained and analysed using flow cytometry. The above cytogram displays red fluorescence (PE-Texas Red-A) versus green fluorescence (Alexa Fluor 488-A).

Within these cytograms the live and dead populations were gated or selected based on their interactions with the dyes used. These gating strategies were based on the manufacturers' instructions and furthermore supported by a study by Berney *et al.* (2007), in which the community of freshwater bacteria in river water samples were analysed using the viability assay.

The greywater samples were stained using SYTO9 and PI and assessed using the FACS AriaIII (BD Biosciences). Trial greywater samples were evaluated using the *E. coli* and *S. aureus* gating strategies shown above, respectively. Based on the trial samples results (not shown) it was identified that the greywater samples had similar staining patterns to the Gram-negative *E. coli* bacterial suspension. This supports findings by Berney *et al.* (2007), in which the freshwater samples analysed exhibited similar staining patterns to that of *E. coli*. Furthermore, in various countries, such as South Africa and more specifically Cape Town, tap water or drinking water is produced from freshwater which then undergoes various treatment stages. Findings by Vaz-Moreira *et al.* in 2017 highlighted that drinking water microbiota is known to be complex and affected by treatment and distribution systems, this directly affects the quality of microbial community present in greywater as in our study, where tap water from residential properties served as the source water sample. Gram negative *Proteobacteria* are known to be present in tap water samples, thereby supporting the gating strategy proposed (Vaz-Moreira *et al.*, 2017).

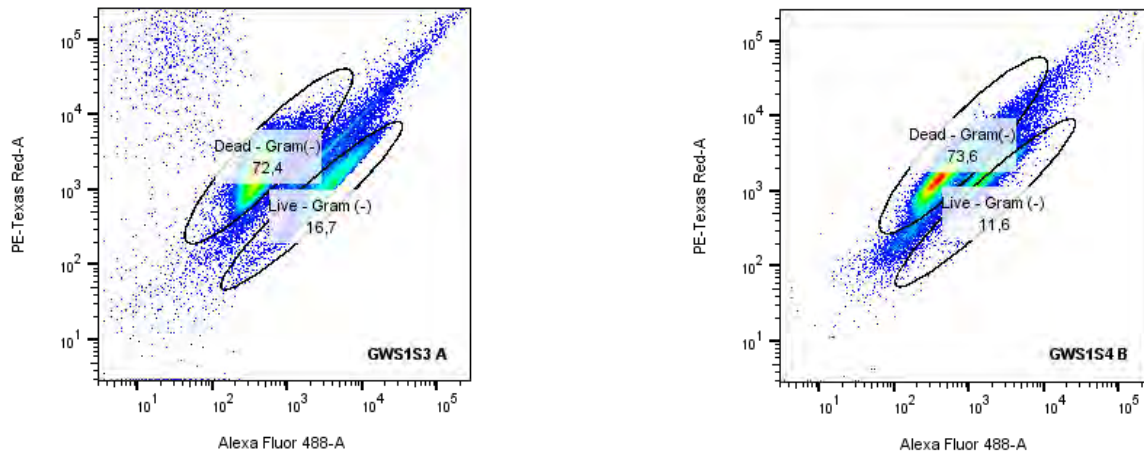


Figure 2.7: Analysis of Greywater Site 1 Samples (GWS1S3A and GWS1S4 B) using the LIVE/DEAD BacLight Bacterial Viability and Counting Kit. The above cytogram displays red fluorescence (PE-Texas Red-A) versus green fluorescence (Alexa Fluor 488-A) using the gating strategy applied to the Gram-negative *E. coli* bacterial control.

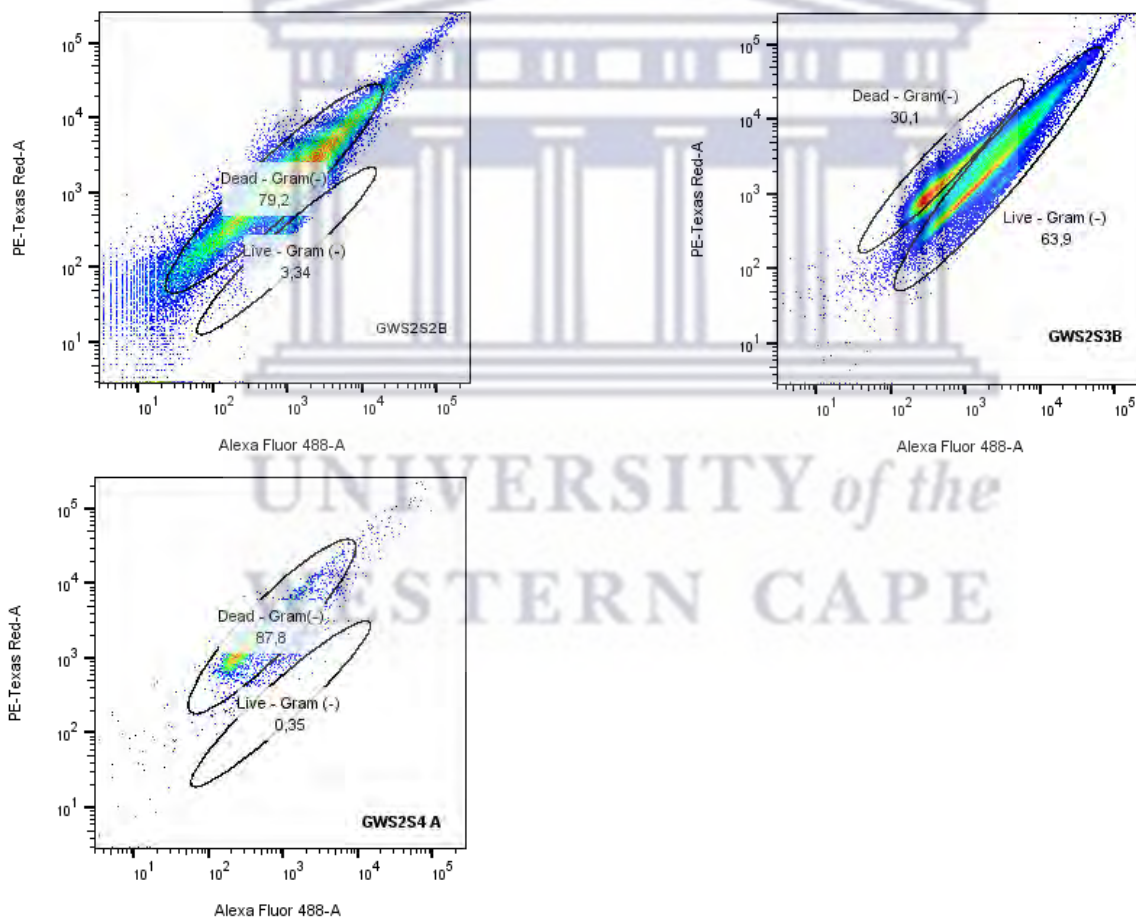


Figure 2.8: Analysis of Greywater Site 2 Samples (GWS2S2B, GWS2S3B and GWS12S4 A) using the LIVE/DEAD BacLight Bacterial Viability and Counting Kit. The above cytogram displays red fluorescence (PE-Texas Red-A) versus green fluorescence (Alexa Fluor 488-A) using the gating strategy applied to the Gram-negative *E. coli* bacterial control.

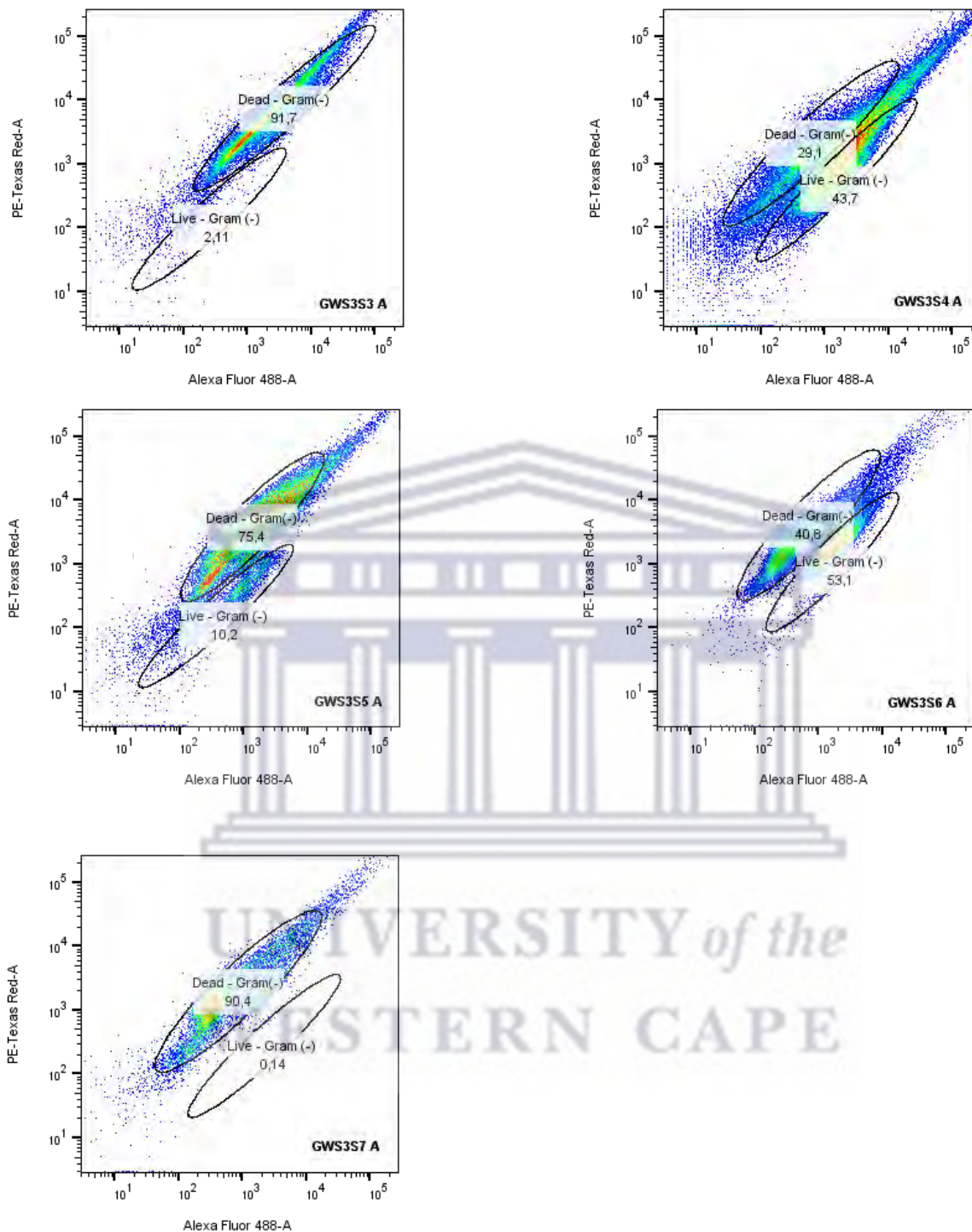


Figure 2.9: Analysis of Greywater Site 3 Samples (GWS3S3A; GWS3S4A; GWS3S5A; GWS3S6A and GWS3S7A) using the LIVE/DEAD BacLight Bacterial Viability and Counting Kit. The above cytogram displays red fluorescence (PE-Texas Red-A) versus green fluorescence (Alexa Fluor 488-A) using the gating strategy applied to the Gram-negative *E. coli* bacterial control.

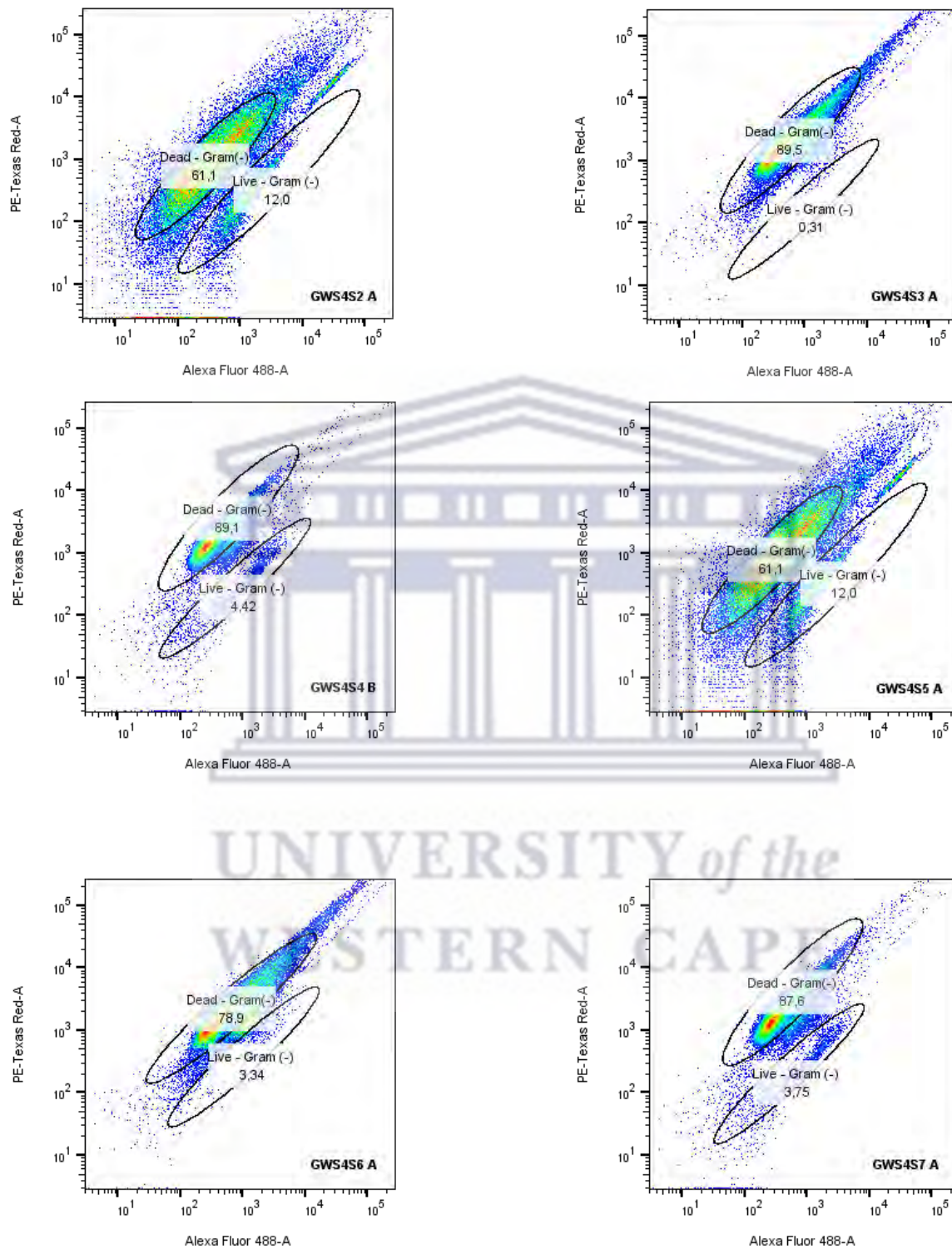


Figure 2.10: Analysis of Greywater Site 4 Samples (GWS4S2A; GWS4S3A; GWS4S4B; GWS4S5A; GWS4S6A and GWS4S7 A) using the LIVE/DEAD BaLight Bacterial Viability and Counting Kit. The above cytogram displays red fluorescence (PE-Texas Red-A) versus green fluorescence (Alexa Fluor 488-A) using the gating strategy applied to the Gram-negative *E. coli* bacterial control.

Bacterial cell viability of greywater samples using flow cytometry is represented in Figures 2.7; 2.8; 2.9 and 2.10 for the greywater sites 1, 2,3 and 4, respectively. As shown in the cytograms many of the greywater samples had a higher proportion of dead cell populations present. This may be since many of the samples were not evaluated immediately after collection. Instead, samples were stored at 4 °C until analysis. Samples were analysed within 6 months of collection; this was mainly due to LIVE/DEAD BacLight kit availability. These storage conditions may have affected certain populations of microorganisms present, thereby shifting the number of viable cells and microbes present in the sample. These results build on existing evidence by Liu and Muller, (2019) which states that bacterial communities rapidly change their structure due to the short generation times of their members. However, it should be considered that given the conditions inside the greywater tanks, especially the high levels of detergents present, it is probably not unsurprising that such a high proportion of non-viable cells were detected, especially in greywater samples. This can be attributed to the presence of detergents and disinfectants that may have been used in the households, which are known to have varying bactericidal effects and are known to reduce microbial numbers.

Future work should ensure that the bacterial viability assay is conducted within 24-48 hours of collection to ensure a more accurate snapshot of the population present in the sample collected. In addition, a time course experiment should be conducted analysing samples stored in the fridge every 24 hours for several days to determine how the populations shift over time. It should be noted that for samples GWS2S3 and GWS3S4 a higher proportion of live cells were present in the sample at the time of analysis. This may indicate a variation in the microbial community present, which is able to withstand physiological changes such as temperature change.

Unfortunately, the microsphere beads provided in the kit were not included in the analysis of the greywater samples. Therefore, a statistical ratio of live to dead cells could not be calculated. It is recommended that any future analysis incorporates the beads to allow for the quantification of the proportion of live to dead cells present in the greywater samples. Robertson *et al.* (2019) suggests that a variety of dye concentrations, incubation times and bacterial stains be evaluated, especially when analysing complex environmental samples. For environmental water samples the use of the dye-combination SYBR Green – PI has been proposed (Berney *et al.*, 2007) to ensure more homogenous clusters and better visualisation of intermediate states.

2.4 Conclusion of the Chapter

This Chapter aimed to identify the phenotypic antibiotic resistance pattern of the greywater and biofilm samples collected using the Kirby-Bauer method and to identify the bacterial viability present in greywater samples using flow cytometry. Incorporating a combination approach of culture-based analysis with high-throughput molecular assays as a form of effective AST.

Based on the results it can be concluded that resistant microorganisms are present in greywater samples and their associated biofilms. Resistance to ampicillin and kanamycin was the most abundant amongst the samples analysed, however the presence of bacteria resistant to vancomycin and teicoplanin is the most concerning. The use of the Kirby-Bauer method served as an effective starting point for our study, as it provided a phenotypic answer to whether resistance may or may not be present in the greywater systems. Furthermore, supporting the selection of target antibiotics to be assessed using molecular methods.

The LIVE/DEAD BacLight Bacterial Viability assay revealed that for many of the samples had a larger proportion of dead cells. The use of flow cytometry for mixed or environmental samples is complex, mainly as different organisms have different staining patterns, which shifts as the microbial communities fluctuate. As such, one cannot have a single “baseline” profile which can be extrapolated to all samples within a study cohort. Furthermore, careful consideration needs to be taken when selecting the stains used and the staining procedure, as literature has revealed interactions between SYTO9 and PI can differ based on the cell wall permeability (Robertson et al., 2019). Future work with regards to cell viability should also take into consideration time of analysis as well as storage as these factors are known to shift microbial communities. In addition, intact biofilms could be analysed using *in situ* staining and fluorescent microscopy to determine the viability of cells within the biofilm.

However, despite these limitations bacterial viability assays are now frequently used to perform microbiological quality monitoring of water and environmental samples, with the main aim of evaluating antimicrobial properties and to assess unculturable environmental species.

Chapter 3: Quantification of Antibiotic Resistance Genes in Greywater Systems using qPCR

3.1 Introduction

Human population growth in combination with rapid urbanization has greatly accelerated the migration and spread of antibiotic resistant bacteria (ARB) and antibiotic resistant genes (ARGs) in the environment (Zhang *et al.*, 2022). Antibiotic resistance has been recognized as a modern-day health threat due to its direct association with the increasing failure of life-saving and therapeutic drugs (Rocha *et al.*, 2019). In recent years ARGs have been viewed as the new environmental pollutant posing as a threat to human and environmental health (Zhang *et al.*, 2022).

Aquatic environments have been identified as a key reservoir of ARBs and ARGs (Singh *et al.*, 2022). Whilst various studies have focused on the presence and persistence of ARB and/or ARGs in wastewater treatment plants, agricultural operations, and hospitals (Scott *et al.*, 2020), there is very little information regarding the proliferation of ARBs and ARGs in aquatic environments such as greywater and reclaimed water. Current domestic greywater systems are not designed to remove emerging pollutants such as microplastics, ARBs and ARGs (Itzhari and Ronen, 2023). For example, the occurrence of ARGs has been reported in small-scale greywater reuse systems (Porob *et al.*, 2020; Troiano *et al.*, 2018). The direct reuse of greywater is often conducted by homeowners and may potentially release residual antibiotic, ARBs and ARGs into the environment (Henderson *et al.*, 2022). Figure 3.1 depicts possible transmission routes between ARGs and the environment, indicating the potential of greywater as a reservoir of microbial communities and horizontal gene transfer. From this figure it is evident that the detection and quantification of ARBs and ARGs serve as an important proxy for identifying the resistome of domestic greywater and the potential of any risks associated with its collection and reuse within households.

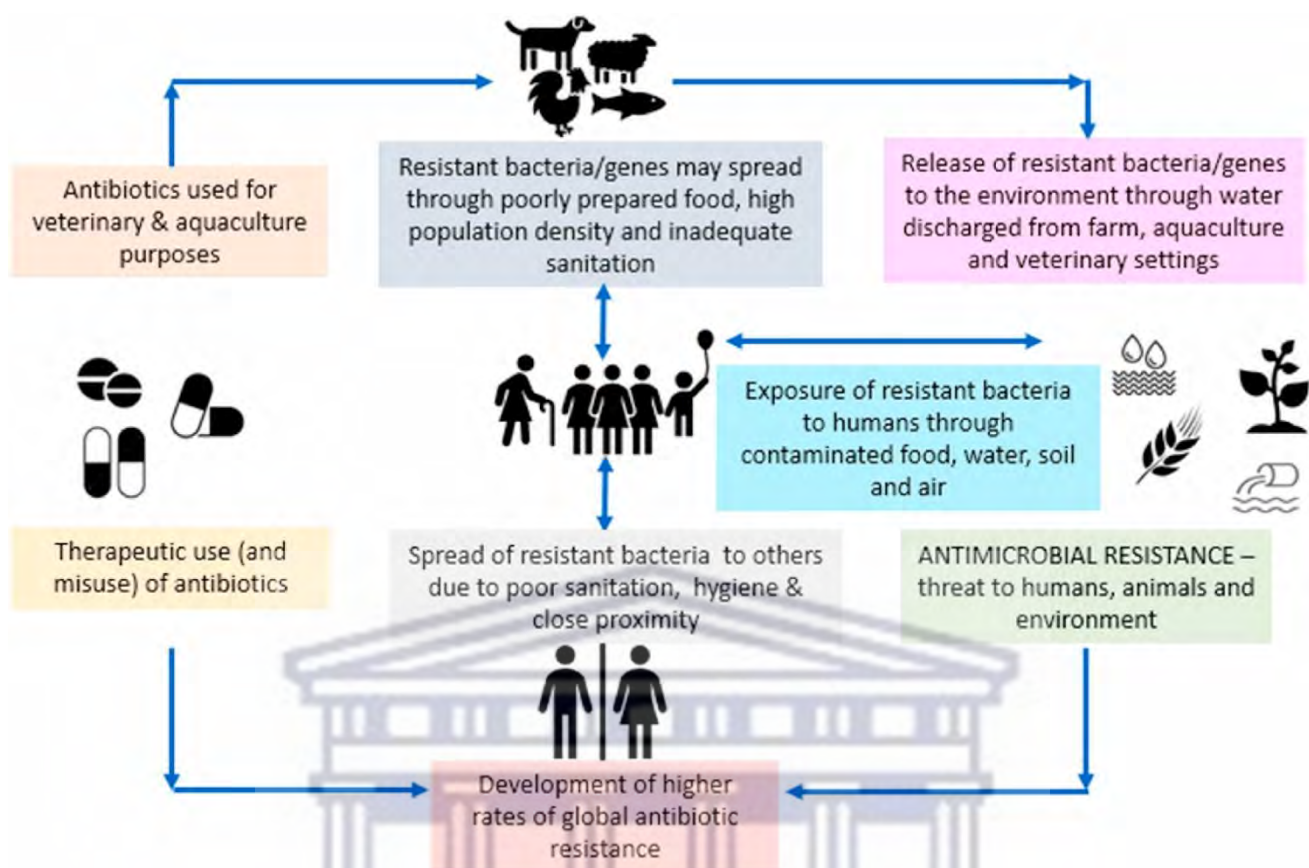


Figure 3.1: Potential pathways and threats associated with antibiotic resistant bacteria and antibiotic resistance genes to human health and the environment. (Taken from Hazra *et al.*, 2022).

3.1.1 Antibiotic Resistance Genes

Antibiotic resistance genes provide adaptive changes to bacteria whether in the presence or absence of antibiotics (Nappier *et al.*, 2020). A study by Zhang *et al.*, (2022) identified that the dissemination of ARGs across various environments and the transfer of ARGs via HGT between pathogenic and non-pathogenic microorganisms is closely related to anthropogenic activities. Aquatic environments near human activity are known to be enriched with mobile genetic elements such as transposons, integrons and conjugative plasmids, which are highly effective carriers of ARGs (Cacace *et al.*, 2019).

The target antibiotic resistance genes (*aadA*, *ampC* and *vanA*) in this study were selected based on either their clinical relevance (particularly the occurrence of ESKAPE pathogens (acronym for *Enterococcus faecium*, *Staphylococcus aureus*, *Klebsiella pneumoniae*, *Acinetobacter baumannii*, *Pseudomonas aeruginosa* and *Enterobacter* species) or elevated levels in aquatic environments (Santajit and Indrawattana, 2016).

3.1.1.1 *aadA* Resistance Gene

Aminoglycoside resistance in aquatic environments has been widely reported (Shin *et al.*, 2023) due to the use of aminoglycosides in clinical settings, as well as widespread use in livestock and animal

husbandry (including the use of streptomycin as growth promoters in cattle, duck, chicken and pig feeds, along with antibiotics such as penicillins and tetracyclines (Koch *et al.*, 2021)), and also in agriculture. Locally, streptomycin is used in the first line and second line treatment regimens for tuberculosis (TB) (Mtetwa *et al.*, 2021). Therefore, selecting the *aadA* gene was of clinical and environmental relevance. The *aadA* resistance gene encodes resistance to streptomycin and spectinomycin via an aminoglycoside adenyltransferase enzyme. The gene is prevalent in class 1 and class 2 integrons (Sunde and Norstorm, 2005). The presence of the *aadA* gene cassettes located within multi-resistance integrons have been reported in Gram negative bacteria as well as multi-drug resistant *Staphylococcus aureus* (Cohen *et al.*, 2020). The *aadA* gene has been detected in wastewater and environmental samples in Sweden (Khan and Jass, 2019), and in South Africa, particularly river water and wastewater using PCR (Ekwanzala *et al.*, 2016).

3.1.1.2 *ampC* Resistance Gene

β -lactam antibiotics are one of the most widely used classes of antibiotics mainly due to their potency in combination with the ease of delivery, low toxicity and low cost (King *et al.*, 2016). Commonly used for the treatment of humans and animal infections (Fernando *et al.*, 2016) it is no surprise that β -lactamases of clinical importance have been detected in environmental niches (Coertze and Bezuidenhout, 2020). β -lactamases belonging to the Class C (*ampC*) confer resistance to broad-spectrum β -lactams (penicillin, monobactam, and cephalosporins) (Coertze and Bezuidenhout, 2020). *ampC* encoded β -lactamases are clinically important and have been detected in wastewater and drinking water samples. For example, it has been detected in two tap water samples in the First Nations community in Canada using RT-PCR (Fernando *et al.*, 2016). Furthermore, it has been detected in farm and environmental settings in South Africa (Ekwanzala *et al.*, 2018).

3.1.1.3 *vanA* Resistance Gene

The detection of resistance to several last resort antibiotics have been reported in South Africa (Sekyere, 2016). Particularly, there have been several major outbreaks of antibiotic resistant infections as reported by the National Institute of Communicable Diseases, including a vancomycin-resistant *Enterococci* outbreak in 2012. Vancomycin is a WHO reserved-use antibiotic and the presence of vancomycin resistance genes and more specifically Vancomycin resistant *Enterococci* (VRE) and Vancomycin resistant *Staphylococcus aureus* is a serious issue, especially in South Africa, where a large portion of the population are immunocompromised and battling HIV/AIDS, tuberculosis and diabetes (Foka *et al.*, 2018). The unregulated antibiotic usage in agricultural practices coupled with the misuse of antibiotics in hospitals and animal rearing facilities has led to the emergence of VRE reservoirs in the environment, allowing for the subsequent transmission of resistance genes to susceptible pathogens (Foka *et al.*, 2018). The *vanA* resistance gene is noted as a standard qPCR target in

environmental antibiotic resistance gene monitoring, especially in water environments. The *vanA*, *B* and *C1* genes were detected in clinical samples in the Western Cape in 2013 (Lochan *et al.*, 2016), in addition to farm, environmental and clinical settings (Ekwazala *et al.*, 2018). The *vanA* resistance gene can be transferred from VRE by mobile transposons or a plasmid to the chromosome cassette of other microorganisms, particularly VRSA, which is often co-isolated with VRE.

3.1.2 Real-Time qPCR

Real-time quantitative PCR (qPCR) is often used in microbial ecology as it can measure the number of copies of a gene in an environmental sample (Brankatschk *et al.*, 2012). It is based on the real-time monitoring of amplicon formation by a reporter molecule such as SYBR Green 1. The amount of synthesized amplicon is proportional to the fluorescence measured after each temperature cycle (Brankatschk *et al.*, 2012). Quantification may either be relative or absolute and can be performed using either gene-specific fluorescent probes or non-specific intercalating dyes (Boutler *et al.*, 2016).

For accurate quantification of gene expression using RT-qPCR, there are a series of experimental parameters which must be carefully followed: (1) determining the correct number of biological replicates; (2): strict quality control in the steps of RNA extraction and reverse transcription, and (3): the suitable selection and validation of reference genes that will be used as the controls necessary to normalize the data in relative quantification analysis (Rocha *et al.*, 2015). The accuracy of quantification of relative mRNA levels by RT-PCR relies on the normalization of data against internal reference genes (McMillan and Pereg, 2014).

Normalization of functional biological data is a key component in a workflow for performing and analysing raw data to ensure the accurate and consistent interpretation of results. The MIQE Guidelines for qPCR by Bustin *et al.*, in 2009 states, "Normalization is an essential component of a reliable qPCR assay because this process controls for variations in extraction yield, reverse-transcription yield, and efficiency of amplification, thus enabling comparisons of mRNA concentrations across different samples". The most accepted approach to minimize any variation in analysis is to perform a relative normalization, in which the expression level of a target gene is normalized relative to the expression of an endogenous, stably expressed gene, also known as a reference gene or internal control (Gomes *et al.*, 2018). Thus, choosing the appropriate reference gene is crucial for relative gene expression analysis, since the accuracy of the normalised expression data relies on the stable expression of the reference gene.

3.1.2.1 Total RNA Extractions

The extraction of high-quality biomolecules (such as RNA, DNA and proteins) from biological material has become the cornerstone of molecular ecology (El-Ashram *et al.*, 2016). In recent years there has been a need for simple and efficient novel methods of extracting both DNA and RNA, from both prokaryotic and eukaryotic organisms, especially with the rapid development of molecular techniques.

Total RNA is widely used in several molecular assays, notably gene-expression analysis using RT-PCR. As discussed earlier, accurate and reliable gene expression data relies on the proper extraction of purified, high-quality RNA (Toni *et al.*, 2018). However, the 2' hydroxyl group attached to the pentose sugar ring of RNA makes the backbone intrinsically more sensitive to breakage than DNA. Hence, extracting intact RNA for downstream applications is challenging and requires extensive optimisation (compared to DNA extraction which is relatively easy) (Nilsen, 2013).

Nucleic acid isolation can be broadly divided into organic and inorganic extraction methods, as well as solid-phase extraction methods. However, there are four integral steps required for successful RNA isolation and purification which is common to all methods: (1) Effective cell lysis, (2) RNA separation and protein denaturation, (3) RNA precipitation and (4) an effective final RNA wash and solubilization step. For microbial ecology studies each of these steps may need to be optimized. Environmental samples contain a wide range of components that may interfere with molecular analysis techniques, especially when large volumes of water are concentrated into small volumes needed for effective molecular detection. In addition, microbes are typically present in water at low concentrations, which makes it difficult to optimize extraction methods to achieve both high nucleic acid recovery and purity (Hill *et al.*, 2015).

Numerous studies have shown that due to inherent biases and differences in efficiencies, the DNA extraction method employed can ultimately affect which microbes are detected in environmental sample, specifically in water distribution systems (Hwang *et al.*, 2012). The co-extraction of PCR-inhibitors, incomplete cell lysis, cell damage or degradation of DNA often occurs resulting in unsuccessful DNA isolation, which can subsequently influence all downstream analyses. For this reason, in the present study different RNA extraction protocols were tested to compare the quality and quantity of RNA extracted from greywater and biofilm samples.

3.1.2.2 RT-PCR Detection Chemistries

The main components of a functional RT-PCR instrument are a thermal cycler with an integrated excitation light source, a fluorescence detection system and software which displays the recorded fluorescence data (Navarro *et al.*, 2015). Fluorescence is either provided in the form of a double stranded DNA (dsDNA) intercalating dye, or a fluorophore labelled probe added to the reaction.

Fluorophore-labelled probes are fluorophores attached to oligonucleotides and therefore only detect specific PCR products. This method of detection ensures accuracy and high specificity. Taqman for example, is a popular dual-labelled probe and has been used for the quantification of ARGs in environmental samples. However, this probe-based method requires the synthesis of different probes for different target sequences and therefore may become expensive and time consuming in environmental studies (Navarro *et al.*, 2015).

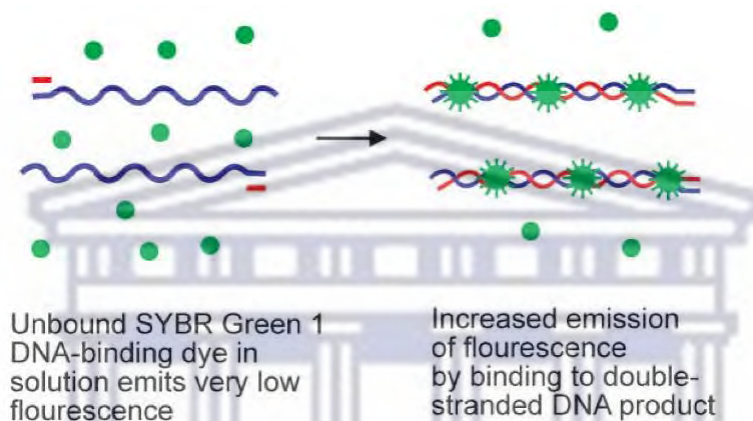


Figure 3.2: Mechanism of action of SYBR Green 1 Dye. The SYBR Green 1 dye when free in solution exhibits very little fluorescence. However, during primer elongation and subsequent polymerization, the SYBR Green 1 molecules are incorporated into the resulting double-stranded amplicons causing an increase in emitted fluorescence. Taken from Artika *et al.*, 2022.

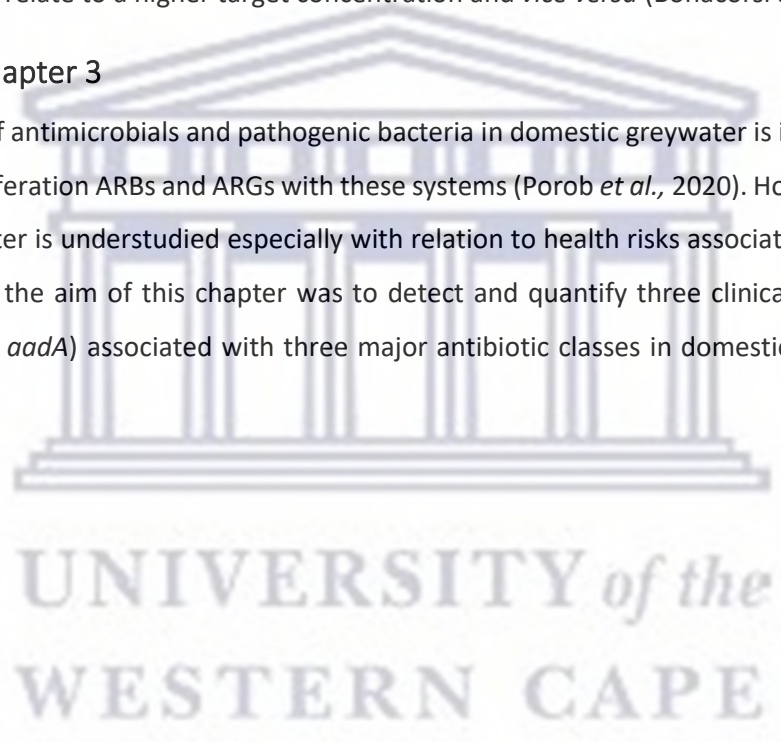
Double-stranded DNA intercalating agents such as SYBR Green I and EvaGreen are widely used in environmental monitoring using qPCR (Hatt and Löffler, 2012). These intercalating dye bind to the minor groove of the amplified dsDNA PCR amplicons, irrespective of the DNA sequence, and leads to fluorescence emission which is measured in the extension phase of the qPCR reaction (Artika *et al.*, 2022) (Figure 3.2). In principle the strength of the fluorescence signal is ultimately dictated by amount of dsDNA present in the reaction (Navarro *et al.*, 2015; Artika *et al.*, 2022). The use of SYBR Green I requires a melt curve analysis to ensure the specificity of the reaction, as the dye will bind to any dsDNA present even non-specific products or primer-dimers. The use of DNA intercalating dyes is favourable for environmental studies mainly due to its cost effectiveness and ability to conduct multiplex assays (Navarro *et al.*, 2015).

3.1.2.3 Absolute Quantification

Absolute quantification using qPCR allows for the precise quantification of a target gene (Hou *et al.*, 2020) and is often used to determine the absolute number of microbial pathogens in a sample (Beinhauerova *et al.*, 2020). Absolute quantification requires a standard curve or calibration curve in order to quantify the exact gene copy number present. A standard curve is constructed using a serially diluted quantification standard (such as plasmid DNA) which contains a known number of copies of the targeted gene (Beinhauerova *et al.*, 2020). The Threshold Cycle (Ct) value in qPCR represents the number of amplification cycles required for the fluorescent signal to exceed the basal threshold level. These values are inversely related to the number of copies of the target gene within a sample, thus a lower Ct value correlate to a higher target concentration and *vice versa* (Bonacorsi *et al.*, 2021).

3.1.3 Aim of Chapter 3

The occurrence of antimicrobials and pathogenic bacteria in domestic greywater is identified as a key factor in the proliferation ARBs and ARGs with these systems (Porob *et al.*, 2020). However, untreated domestic greywater is understudied especially with relation to health risks associated with ARBs and ARGs. Therefore, the aim of this chapter was to detect and quantify three clinically relevant ARGs (*vanA*, *ampC* and *aadA*) associated with three major antibiotic classes in domestic greywater using qPCR.



3.2 Materials and Methods

3.2.1 Sample Processing

For nucleic acid extraction all greywater samples collected over the study period were subjected to the following sample processing. The 8 L of greywater collected per site, was sequentially centrifuged 500 ml at a time in metal-screw capped bottles (Nalgene) at 5 000 rpm for 20 minutes using the Sorvall Lynx 6000 centrifuge (Thermo Fischer Scientific, MA, USA). The resulting pellet was resuspended in 100 ml sterile diethyl pyrocarbonate (DEPC)-water.

Sample processing of biofilm samples was conducted by submerging the buccal swab in 250 µl of 1X Phosphate Buffer Saline (PBS) and vortexing for 5 minutes at maximum speed to dislodge bacteria. Cells were harvested by centrifugation at 13 500 rpm for 10 minutes and the pellet was resuspended in 500 µl of 1X TE (10mM Tris, 1mM EDTA, pH 8.0), of which 250 µl of the resulting suspension was used for nucleic acid extraction.

3.2.2 Optimization of Total RNA Extractions from Greywater Samples

For accurate and reliable gene expression analysis ARGs in greywater, high quality, intact RNA was required. The extraction method had to be reproducible and adaptable in terms of sample size and type. For this reason, four different extraction methodologies were initially tested.

Prior to RNA extraction, all solutions and glassware were rendered RNase-free by treatment with DEPC, and only certified RNase-and DNase-free plasticware was used.

3.2.2.1 Commercial Kits and Reagents

3.2.2.1.1 RNeasy PowerWater Kit

RNA was extracted using the RNeasy PowerWater Kit (Qiagen) according to the manufacturer's instructions, with minor modifications. RNA was extracted by adding 250 µl of the pre-processed cellular material (Section 3.2.1) to the PowerBead tubes. Greywater samples were filtered to remove cellular debris prior to RNA extraction. The vacuum pump was set up with the filter funnel attached to a 500 ml glass bottle. Sequential filtering of the greywater sample was performed using 20 µm Nylon Net Filters (Merck Millipore Ltd, Tullagreen), 10 µm Nylon Net Filters, and lastly a 0.45 µm MCE Membrane filters. The 0.45 µm filters were inserted directly into the Power-Bead Tubes and the RNA was extracted according to the manufacturer's instructions.

3.2.2.1.2 TRIzol™ Reagent

For RNA extractions using TRIzol reagent (Invitrogen), 2 L of greywater was sequentially centrifuged. The resulting pellet was resuspended in sterile DEPC water. Prior to extraction, the resuspended pellet was re-centrifuged at 5 000 rpm for 15 minutes. RNA was extracted using the commercial reagent

TRIzol, as per the manufacturer's instructions for cells grown in suspension. Five hundred microlitres (500 µl) of greywater sample was used per reaction. Precipitation and solubilization was conducted as per the manufacturer's instructions.

3.2.2.2 Organic/Chemical RNA Extraction Methods

3.2.2.2.1 CTAB RNA extraction

A modified CTAB method (Simister *et al.*, 2011) was followed. The pellet obtained following centrifugation of 250 ml greywater was resuspended in DEPC-water. Two hundred and fifty microlitres (250 µl) of sample were transferred to a clean Eppendorf tube and 1.5 ml of Extraction buffer (10% CTAB (w/v); 0.7M NaCl, 240mM Potassium Phosphate Buffer, pH 8.0) was immediately added. The samples were vortexed for 30 seconds followed by incubation at 65 °C for 30 minutes. Samples were centrifuged for 10 minutes at 16 000 *xg* at RT and 950 µl of the supernatant was transferred to a new tube. One volume (950 µl) of chloroform:*iso*-amyl alcohol (24:1; v/v) solution was added and vortexed for 30 seconds. The samples were centrifuged for 10 minutes at 16 000 *xg* at 4 °C and the supernatant was transferred to a new tube. One volume (~950 µl) of chloroform:*iso*-amyl alcohol (24:1; v/v) solution was added and the samples were vortexed for 30 seconds. Samples were centrifuged for 10 minutes at 16 000 *xg* at 4 °C and the supernatant was transferred to a new tube. Lithium Chloride (LiCl) was added to a final concentration of 2M, and the samples were incubated overnight at 4 °C to precipitate the RNA. The precipitated samples were centrifuged (pre-chilled) for 1 hour at 4 °C at 16 000 *xg*. The supernatant was discarded, and the pellet was washed with 70% (v/v) ethanol. The ethanol was removed with a pipette and the tubes were centrifuged for 20 minutes at 16 000 *xg* at 4 °C to remove any residual ethanol. The tubes were left to dry on ice for 10 minutes followed by resuspension of the pellet in 60 µl of DEPC water.

3.2.2.2 Optimized Sample Processing for RNA Extractions using the Hot-Phenol SDS Method

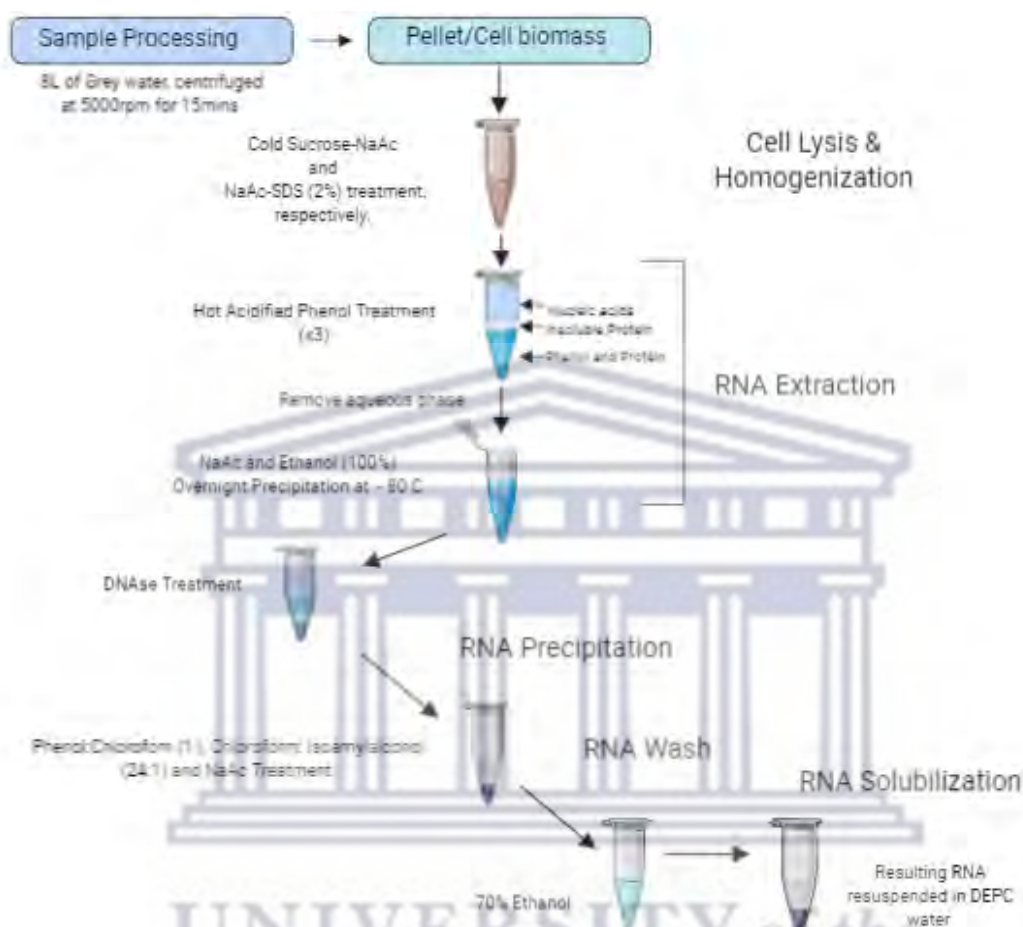


Figure 3.3: Schematic overview of the optimized Hot Acid Phenol RNA Isolation Method used for the extraction of total RNA from greywater samples.

Figure 3.3 represents a schematic overview of the Hot Phenol SDS RNA isolation method optimized for greywater samples. Key elements such as solubilization and precipitation times were optimized to ensure the efficient and effective extraction of total RNA from metagenomic greywater samples. Following sequential centrifugation, the resulting pellet was resuspended in 50 ml sterile DEPC-water and stored at 4 °C. Prior to extraction, the resuspended pellet was re-centrifuged at 5 000 rpm for 15 minutes and the subsequent resulting pellet was used for RNA extraction.

3.2.2.2.3 Hot Phenol RNA extraction

RNA was extracted using a modified hot phenol method as described by Ares *et al.*, (2012). Following centrifugation, the resulting pellet was resuspended in ice cold sucrose (0.3 M) and sodium acetate (0.01M) (pH 4.5). The sample was split into two 2 ml Eppendorf tubes and 500 µl of sodium acetate

(0.01M)-SDS (2% v/v) solution was added to each. The reaction was heated in a waterbath at 65 °C for 90 seconds. An equal volume of heated (65 °C) acidified phenol:chloroform:IAA (125:24:1; v/v/v) pH 4.5 (Ambion) was added. The samples were vortexed and incubated for three minutes at 65 °C. Samples were then chilled rapidly on ice for 30 seconds, followed by centrifugation at room temperature for 10 minutes at maximum speed. The aqueous phase was transferred to a clean tube and re-extracted twice, as outlined above. RNA was precipitated using 1/10 volume sodium acetate (3M) (pH 5.2) and three volumes of 96% (v/v) ethanol (AR Grade), overnight at -80 °C. Post-precipitation, the samples were centrifuged at 4 °C for 30 minutes at maximum speed. The samples were then treated with DNase 1 (NEB), according to the manufacturer's instruction, however omitting the heat inactivation step. Equal volumes of phenol:chloroform (1:1; v/v) was added to the sample followed by centrifugation at room temperature (22±2 °C) for two minutes at maximum speed. The aqueous layer was transferred to a clean tube, and an equal volume of chloroform: *iso*-amyl alcohol (24:1; v/v) was added. The sample was vortexed and centrifuged at RT for two minutes at maximum speed. The aqueous layer was transferred, and the RNA re-precipitated by the addition of 1/10 volume sodium acetate (3M) (pH 5.2) and three volumes of 96% ethanol (AR Grade) at -80 °C for one hour. The samples were centrifuged at 4 °C for 15 minutes at maximum speed and washed with 70% (v/v) ethanol, after which the sample was centrifuged again at 4 °C for 15 minutes at 10 000 *xg*. The resulting RNA pellet was resuspended in 40 µl of sterile DEPC-water.

3.2.2.3 RNA Quality Analysis

Total RNA was quantified using micro-spectrophotometry (Nano-Drop Technologies, Inc), and the quality of the isolated RNA was assessed by observing the absorbance at 260 and 280 nm. The A260/280 ratio was calculated to determine the purity of the RNA sample.

Additionally, all RNA samples were analysed by gel electrophoresis. RNA integrity was evaluated by the presence and intensity of the 23S and 16S rRNA bands on a 1.2% (w/v) agarose gel using Fermentas RNA loading dye (95% Formamide, 1% SDS, 0.25% Bromophenol blue, 0.026M Xylene Cyanol, 10 mg/ml Ethidium bromide and 0.5M EDTA). As per recommendations, equal volume of RNA sample and 2X loading dye was mixed and heated at 70 °C for 10 minutes. The samples were then chilled on ice for two minutes and loaded on the gel. All gels contained 10 µg/ml ethidium bromide and were electrophoresed in 1X TBE buffer at 80 Volts for 90 minutes.

Prior to cDNA synthesis, each RNA sample was evaluated using the Qubit BR RNA Assay kit (Invitrogen) as per the manufacturer's instructions.

3.2.2.4 16s rRNA gene Polymerase Chain Reaction for contaminating DNA in RNA samples

To ensure no contaminating genomic DNA was present in RNA samples prior to cDNA synthesis, the necessary checks, depicted in Figure 3.4 were conducted. A 16S rRNA gene PCR was carried out in 25 µl reaction volumes. Each reaction contained 0.5U KAPA 2G Robust DNA Polymerase, 0.2mM dNTP mix, 1X KAPA Enhancer, 1X KAPA 2G Buffer B, 0.5µM forward and reverse primer, and 10 ng of RNA, made to a final volume using PCR-grade water. The primers and amplification conditions are provided in Table 3.1. Amplicons were electrophoresed on 1% agarose gels which contained 10 µg/ml ethidium bromide and were electrophoresed in 1X TAE buffer at 90V for 1 hour.

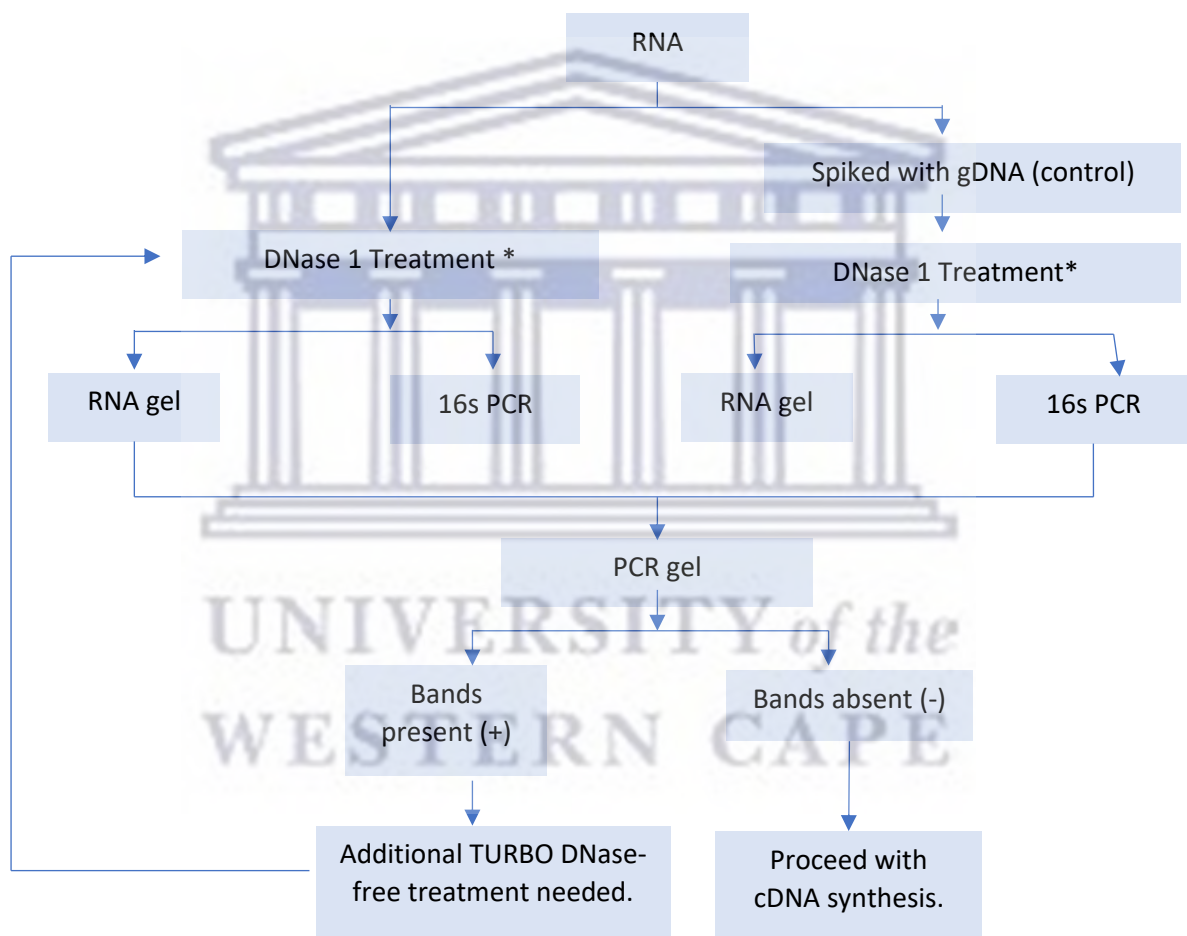


Figure 3.4: Schematic diagram of optimization for removal of contaminating DNA.

Table 3.1: The primer set, and amplification conditions used for the RNA-DNA contamination assessment.

Primer	Sequence (5'-3')	Amplification conditions	Reference
Forward (F1)	AGAGTTTGATCITGGTCAG	95 °C for 3 minutes 30 cycles at 95 °C for 15 seconds,	Meyers, 2003.
Reverse (R5)	GTATTACCGCGGCTGCTGGCAC	56 °C for 15 seconds 72 °C for 15 seconds 1 minute at 72 °C	

3.2.2.5 Ambion TURBO DNase-free Kit Treatment

As per flowchart (Figure 3.4) any samples where a 16S rRNA gene amplicon was detected, the RNA sample was treated with TURBO DNase 1 using the TURBO DNase-free kit (Ambion, Life Technologies, USA) in 50 µl reactions as per the manufacturer's instructions prior to cDNA synthesis.

3.2.3 cDNA synthesis

Once DNA-free RNA was obtained, cDNA synthesis was performed using the QuantiNova Reverse Transcription kit according to the manufacturer's instructions (Qiagen). Each reaction contained 100 ng of RNA in 15 µl of RNase-free water, 4 µl of Quanti-Nova Reverse Transcription mix and 1 µl of Quanti-Nova Reverse Transcription enzyme. The reaction conditions were 25 °C for 3min, 45 °C for 10 min and 85 °C for 5 min. The cDNA was then diluted and stored at -20 °C.

A final 16S rRNA gene PCR was conducted on the cDNA sample using the KAPA 2G Robust PCR Kit (KAPA Biosystems, South Africa), as described above. The integrity of the cDNA was determined by agarose gel electrophoresis on a 1% agarose gel.

3.2.4 Selection of Primers and Bioinformatic Analysis

A comprehensive list of target genes and the relevant primers was compiled. Selection criteria for primers were as follows: a) primer set must amplify amplicons within the optimal size range (50-200 bp), b) primers should target a wide range of bacterial genera, c) be specific for the target gene. Selected primers were analysed via primer-BLAST to confirm their specificity and identify their species range. Selected primers are listed in Table 3.2.

Table 3.2: List of primers used in this study.

Gene	Encoded protein and function	Size (bp)	Bacterial control strain	Reference
16S rRNA	Ribosomal RNA Translation of mRNA	194	<i>Enterobacter cloacae</i> subsp. <i>cloacae</i> derived from ATCC BAA-1143	Parnanen <i>et al.</i> , 2019
gapA	Glyceraldehyde-3-phosphate dehydrogenase A Energy production – involved in glycolysis	185	<i>Escherichia coli</i> derived from NCTC 13846	Parnanen <i>et al.</i> , 2019
mdh	Malate dehydrogenase Catalyzes the interconversion between malate and oxaloacetate	197	<i>Escherichia coli</i> ATCC 25922	Parnanen <i>et al.</i> , 2019
vanA	Dehydrogenase (VanH) Reduces pyruvate to d-Lac, thereby inhibiting cell wall synthesis	65	<i>Enterococcus faecium</i> ATCC 700221	Volkman <i>et al.</i> , 2004
ampC	Beta-lactamase Hydrolysis of the β -lactam ring	67	<i>Enterobacter cloacae</i> subsp. <i>cloacae</i> derived from ATCC BAA-1143	Volkman <i>et al.</i> , 2004
aadA	Aminoglycoside-3-N acetyltransferase Chemical modification of target	295	<i>Escherichia coli</i> derived from NCTC 13846	Wang <i>et al.</i> , 2018

3.2.4.1 Growth conditions for bacterial strains

E. coli ATCC 25922 was grown at 37 °C shaking at 180 rpm for 16 hours in Luria-Bertani broth (LB). *E. coli* derived from NCTC 13846 and *Enterobacter cloacae* subsp. *cloacae* ATCC BAA-1143 was grown at 37 °C shaking at 180 rpm for 16 hours in Tryptic Soy Broth. *Enterococcus faecium* ATCC 700221 was grown in Brain Heart Infusion broth, supplemented with 50 μ g/ml vancomycin hydrochloride, at 37 °C shaking at 180 rpm for 16 hours.

3.2.4.2 Genomic DNA Extraction using the Ammonium Acetate based Method.

Genomic DNA was extracted according to the method of Crouse *et al.*, 1987. Bacterial cells were harvested from a 5 ml overnight culture by centrifugation at 5 000 rpm for 5 minutes and washed with sterile 1X TE (10mM Tris, 1mM EDTA, pH 8.0). Cells were resuspended in 1 ml SET buffer (25% sucrose, 2mM EDTA, 50mM Tris, pH 8.0) and lysozyme (1 mg/ml) was added. The samples were incubated for 30 minutes at 37 °C, after which proteinase K was added to a concentration of 1 mg/ml and the samplers were incubated for 30 minutes at 37 °C. Post-incubation 500 μ l of 1X TE was added in addition to 50 μ l of 10% SDS to lyse the cells. The bacterial suspensions were incubated overnight at

50 °C to allow the proteinase K to degrade cellular proteins. Five hundred microlitres (500 µl) of 7.5M ammonium acetate was then added and the samples were incubated at room temperature for 1 hour. Samples were centrifuged at 13 000 rpm for 15 minutes at room temperature and 500 µl of the resulting supernatant was then transferred to a new tube and 2 volumes of 99.9% absolute ethanol was added. Samples were placed on ice for 5 minutes and then centrifuged at room temperature for 30 minutes at 13 000 rpm. The resulting pellet was washed with 70% ethanol. Samples were then centrifuged for 5 minutes at 13 000 rpm, and the resulting DNA pellet was resuspended in 1X TE containing RNase A (Thermo) to a final concentration of 100 ng/ml and incubated at 37 °C for 30 minutes. Prior to quantification using the NanoDrop ND-1000 spectrophotometer (Thermo Fischer Scientific, MA, USA) genomic DNA samples were centrifuged at 13 000 rpm for 15 seconds.

3.2.4.3 Genomic DNA Extraction using the NucleoSpin Kit

Genomic DNA was extracted from *E. faecium* ATCC 700221 and *E. coli* derived from NCTC 13846 using the NucleoSpin[®] Microbial DNA Extraction Kit (MACHEREY-NAGEL), according to the manufacturers' instructions from a 5 ml of overnight culture. Genomic DNA was quantified using the Qubit dsDNA HS Assay kit (Invitrogen).

3.2.4.4 Plasmid Miniprep

Plasmid DNA was extracted from *E. faecium* ATCC 700221 and *E. coli* derived from NCTC 13846, using the QIAprep Spin Miniprep Kit (Qiagen) according to the manufacturer's instructions from 5 ml of overnight bacterial culture. Plasmid Minipreps were quantified using the Qubit dsDNA HS assay.

3.2.5 PCR Optimization of Reference Genes

For the purpose of this study, previously published reference genes with universal primer sequences were evaluated for use in the antibiotic resistance genes expression analysis.

Prior to conducting experiments using cDNA, PCR conditions were optimised using genomic DNA. Each 50 µl reaction contained 1.25U DreamTaq Polymerase (Thermo Fischer Scientific), 0.2mM dNTP mix, 1X DreamTaq Reaction buffer, 0.2µM forward and reverse primer, and made to a final volume using PCR grade water and 500 ng of respective genomic DNA. The *gapA* PCR reactions contained additional magnesium chloride, to a final concentration of 2.5mM. The primers and amplification conditions are provided in Table 3.3. PCR products were electrophoresed on 2% (w/v) agarose gels. All gels contained 10 µg/ml ethidium bromide and were electrophoresed in 1X TAE at 90 V for 1 hour.

Table 3.3: Reference genes Primer sets Optimised Amplification conditions.

Gene	Primers	Sequence (5'-3')	Amplification Conditions
16S rRNA	16S rRNA FP:	CCTACGGGAGGCAGCAG	95 °C for 3 minutes 40 cycles at 95 °C for 30 seconds, 59 °C for 30 seconds, 72 °C for 1 minute 5 minutes at 72 °C.
	16S rRNA RP:	ATTACCGCGGCTGCTGGC	
gapA	gapA FP:	CCGTTGAAGTGAAAGACGGTC	95 °C for 3 minutes 40 cycles at 95 °C for 30 seconds, 60 °C for 30 seconds, 72 °C for 1 minute 5 minutes at 72 °C.
	gapA RP:	AACCACTTTCTTCGCACCAGC	
mdh	Mdh FP:	AAGAAACGGGCGTACTGACC	95 °C for 3 minutes 40 cycles at 95 °C for 30 seconds, 57 °C for 30 seconds, 72 °C for 1 minute 5 minutes at 72 °C.
	Mdh RP:	GTGGCTGATCTGACCAAACG	

3.2.6 PCR Optimization of Antibiotic Resistance Genes

3.2.6.1 PCR Optimisation of *vanA* gene PCR

PCR optimisation was carried out in 50 µl reaction volumes. Each reaction contained 1.25U DreamTaq Polymerase, 0.4mM dNTP mix, 1X DreamTaq Reaction buffer, 3mM magnesium chloride, 1µM forward and reverse primer, and made to a final volume using PCR grade water and 1 ng of *E. faecium* ATCC 700221 plasmid DNA. The primers and amplification conditions are listed in Table 3.6. Amplicons were electrophoresed on 2% agarose gels. All gels contained 10 µg/ml ethidium bromide and were electrophoresed in 1X TAE at 90V for 1 hour.

3.2.6.2 PCR Optimisation of *ampC* gene PCR

PCR optimisation was carried out in 50 µl reaction volumes. Each reaction contained 1.25U DreamTaq Polymerase, 0.4mM dNTP mix, 1X DreamTaq Reaction buffer, 2.5mM magnesium chloride, 0.4µM forward and reverse primer, and made to a final volume using PCR grade water and 1 µg of *E. cloacae* subsp. *cloacae* ATCC BAA-1143 genomic DNA. The primers and amplification conditions are provided in Table 3.6. Amplicons were electrophoresed on 2% agarose gels. All gels contained 10 µg/ml ethidium bromide and were electrophoresed in 1X TAE at 90V for 1 hour.

3.2.6.3 PCR Optimisation of *aadA*

PCR optimisation was carried out in 50 µl reaction volumes. Each reaction contained 1.25U DreamTaq Polymerase, 0.2mM dNTP mix, 1X DreamTaq Reaction buffer, 0.2µM forward and reverse primer, and made to a final volume using PCR grade water and 500 ng of *E. coli* NCTC 13846 genomic DNA. The primers and amplification conditions are provided in Table 3.4. Amplicons were electrophoresed on

2% agarose gels. All gels contained 10 µg/ml ethidium bromide and were electrophoresed in 1X TAE at 90V for 1 hour.

Table 3.4: Antibiotic Resistance Genes for RT-PCR Optimised Amplification Conditions

Gene	Primers	Sequence (5'-3')	Amplification Conditions
<i>vanA</i>	<i>vanA</i> -FP:	CTGTGAGGTCGGTTGTGCG	95 °C for 3 minutes
	<i>vanA</i> -RP:	TTTGGTCCACCTCGCCA	40 cycles at 95 °C for 1 minute, 60 °C for 45 seconds, 72 °C for 1 minute 5 minutes at 72 °C
<i>ampC</i>	<i>ampC</i> -FP:	GGGAATGCTGGATGCACAA	95 °C for 3 minutes
	<i>ampC</i> -RP:	CATGACCCAGTTCGCCATATC	40 cycles at 95 °C for 1 minute, 60 °C for 45 seconds, 72 °C for 1 minute 5 minutes at 72 °C.
<i>aadA</i>	<i>aadA</i> -FP:	CAGCGCAATGACATTCTTGC	95 °C for 3 minutes
	<i>aadA</i> -RP:	GTCGGCAGCGACAYCCTTCG	40 cycles at 95°C for 30 seconds, 60 °C for 30 seconds, 72 °C for 1 minute 5 minutes at 72 °C.

3.2.7 Construction of Plasmid standards for Real-time PCR

Separate plasmids containing the ARGs (*vanA*, *ampC* and *aadA*), as well as the housekeeping genes (*gapA*, 16S *rRNA* and *mdH*) were constructed to be used as a control for the qPCR assay.

Amplicons for each of the genes were generated by conventional PCR using the optimised conditions. The four PCR reactions for each primer set were pooled and purified using the NucleoSpin Gel and PCR Clean Up Kit (Macherey- Nagel) according to the manufacturer's instructions, eluting in 30 µl of elution buffer. The PCR products were cloned into the pJET1.2 cloning vector using the ThermoScientific Clone-Jet PCR Cloning Kit according to the manufacturer's instructions. The recombinant vectors were transformed into electro-competent *E. coli* DH5α cells via electroporation and 50 µl of transformed culture was spread onto LB plates containing 100 µg/ml ampicillin. Transformed colonies were picked and colony PCR was conducted to confirm positive transformants. Plasmid DNA was extracted from confirmed positive clones using the QIAprep Spin Miniprep Kit according to the manufacturer's instructions. Plasmid DNA was quantified using the Qubit HS DNA assay and quality was assessed by conducting gel electrophoresis and gene-specific PCR to confirm the presence of the insert. The constructs were designated *pJET_gapA*; *pJET_mdh*; *pJET_16SrRNA* for the reference genes, and *pJET_ampC*; *pJET_vanA* and *pJET_aadA* for the ARGs being investigated.

3.2.8 Real-Time PCR

Real-Time PCR was performed on an LightCycler 480 II (Roche Diagnostics, IN, USA). qPCR reactions were set up in white 96-well PCR plates (Roche).

3.2.8.1 Construction of the Standard Curve

The control plasmids generated for each primer set were quantified using the Qubit dsDNA HS assay (Invitrogen) and the number of molecules/ μl was determined using the formula below (Lee *et al.*, 2006). A serial dilution was prepared over a range of 10^8 to 10^2 for each construct.

$$\text{Number of copies} = \frac{\text{Amount (ng)} \times 6.022 \times 10^{23}}{\text{Length (bp)} \times 1 \times 10^9 \times \text{Mass of DNA bp}}$$

Figure 3.5: Equation used to calculate number of copies

For the reference genes, 16S rRNA and *gapA*, qPCR was performed using the Quantinova SYBR Green I Kit (QIAGEN,) in 10 μl reaction volumes, containing 9 μl of master mix and 1 μl of template DNA. For the generation of a standard curve, serially diluted plasmid DNA (pJET_ *gapA* and pJET_16SrRNA) served as the input DNA. qPCR cycling conditions were as follows: initial activation step at 95 $^{\circ}\text{C}$ for 2 minutes, followed by 40 cycles of denaturation at 95 $^{\circ}\text{C}$ for 10 s, followed by a combined annealing/extension at 60 $^{\circ}\text{C}$ for 30 s. Melt curve analysis was performed from 60 $^{\circ}\text{C}$ with a gradual increase in temperature to 97 $^{\circ}\text{C}$, during which time changes in fluorescence were monitored.

For the *mdh* reference gene, qPCR was performed using the LightCycler 480 SYBR Green I Mastermix (Roche) in 10 μl reaction volumes, containing 9 μl of mastermix and 1 μl plasmid DNA (pJET_ *mdh*). For the generation of a standard curve, serially diluted purified PCR amplicons served as the input DNA. qPCR cycling conditions were as follows: initial activation step at 95 $^{\circ}\text{C}$ for 5 minutes, followed by 45 cycles of 95 $^{\circ}\text{C}$ for 10s followed by a combined annealing/extension at 57 $^{\circ}\text{C}$ for 15 s. Melt curve analysis was performed from 56 $^{\circ}\text{C}$ with a gradual increase in temperature to 97 $^{\circ}\text{C}$, during which time changes in fluorescence were monitored.

For the ARGs (*vanA*, *ampC* and *aadA*), qPCR was performed in 10 μl reaction volumes, using the Quantinova SYBR Green I Kit (QIAGEN,) in 10 μl reaction volumes, containing 9 μl of master mix and 1 μl of template DNA. For the generation of a standard curve, serially diluted plasmid DNA served as the input DNA. qPCR cycling conditions were as follows: initial activation step at 95 $^{\circ}\text{C}$ for 2 minutes, followed by 40 cycles of denaturation at 95 $^{\circ}\text{C}$ for 10 s, followed by a combined annealing/extension at 60 $^{\circ}\text{C}$ for 30 s. Melt curve analysis was performed from 60 $^{\circ}\text{C}$ with a gradual increase in temperature

to 97 °C, during which time changes in fluorescence were monitored. Quantification for all primer sets was performed using the LC480 software and Microsoft excel.

3.2.8.2 Absolute Quantification of ARGs in greywater samples

For the quantification of the *gapA* gene, each reaction contained 1X KAPA SYBR Master Mix, 0.4µM of each primer and adjusted to a final volume of 8 µl using Molecular Grade water. Two microlitres (2 µl) of template DNA was added for each reaction, for the standard curve the input DNA was the control plasmid pJET_gapA and for the environmental samples ~1 ng of metagenomic cDNA was added. qPCR cycling conditions were as follows: initial activation step at 95 °C for 20 s, followed by 40 cycles of denaturation at 95 °C for 10 seconds and a combined 20 second annealing/extension at 60 °C. Melt curve analysis was performed from 59 to 97 °C.

All target reference and ARGs were quantified as described above. Variations in cycling parameters are presented in table 3.5.

Table 3.5: qPCR Cycling Parameters for Reference Genes and ARGs

Reference Genes	Initial activation	Denaturation	Annealing and Extension	Melt Curve Analysis
<i>gapA</i>	95 °C for 20 s	40 cycles of denaturation at 95 °C for 10 s	60 °C for 20 s	59 to 97 °C
<i>16S rRNA</i>	95 °C for 20 s	40 cycles of denaturation at 95 °C for 10 s	59 °C for 20 s	58 to 97 °C
<i>mdH</i>	95 °C for 20 s	40 cycles of denaturation at 95 °C for 10 s	57 °C for 20 s	55 to 97 °C
ARGs				
<i>vanA</i>	95 °C for 20 s	40 cycles of denaturation at 95 °C for 10 s	60 °C for 20 s	59 to 97 °C
<i>ampC</i>	95 °C for 20 s	40 cycles of denaturation at 95 °C for 10 s	60 °C for 20 s	59 to 97 °C
<i>aadA</i>	95 °C for 20 s	40 cycles of denaturation at 95 °C for 10 s	60 °C for 20 s	59 to 97 °C

All reactions were performed in triplicate for each sample, including the no template control (NTC). The average of each triplicate set was used for quantitative analysis. Quantification was performed using the LC480 software and Excel. Gene copy number of each ARG were normalized to the reference gene copy number and the relative abundance per sample was determined and expressed in gene copy numbers per litre.

3.3 Results & Discussion

3.3.1 Optimization of Total RNA Extractions from greywater samples

The accurate analysis of gene expression is strongly influenced by the quality and quantity of the RNA template (Fleige & Pfaffl, 2006). Therefore, obtaining high quality RNA in sufficient amounts is the most important preliminary step for any investigation in molecular biology (Ma *et al.*, 2015). However, the extraction of total RNA from greywater - which is rich in inhibitors such as detergents, debris and various dissolved inorganic and organic compounds - is a time-consuming and tedious task. These inhibitory substances can interfere with the RNA isolation procedures. This problem is further compounded by the variability of water samples. Therefore, in this project considerable effort was taken to develop an efficient method for the extraction of RNA from greywater.

The extraction method used may affect RNA quality, and therefore careful consideration must be taken when choosing isolation procedures. Ideally, a method should be reproducible and able to effectively lyse the source of the RNA, which in this case is microbes present in greywater. A reliable isolation technique must yield intact high-quality RNA that is free of RNases, proteins and genomic DNA. The extraction and purification procedures should also be free of PCR and real-time PCR inhibitors (Jahn *et al.*, 2008). An additional requirement of an effective RNA isolation technique for this study, was that it was able to isolate RNA from both Gram-negative and Gram-positive bacteria present in the greywater.

For this study, various RNA extraction methods, both commercial kits and the conventional chemical protocols were evaluated to identify which would be most effective in extracting RNA from greywater and biofilm samples.

3.3.1.1 Organic Conventional Extraction Methods

The cetyltrimethylammonium bromide (CTAB) protocol is rapid and inexpensive compared to other expensive and time-consuming methods (Gambino *et al.*, 2008). This method utilizes β -mercaptoethanol and PVP as reducing agents in the extraction buffer to increase the overall yield and quality of RNA extracted. CTAB is used as a non-ionic detergent, which has the ability to precipitate acidic polysaccharides and nucleic acids from various low ionic strength solutions (Tan and Yiap, 2009). For this reason, it may be better for biofilm samples. An added benefit of this method is that it avoids toxic chemicals such as guanidium isothiocyanate, phenol or guanidium hydrochloride (Chang *et al.*, 1993). The extraction method was attempted on trial greywater samples collected at site 1 and 2 (described in Chapter 2). As shown in Figure 3.6, the method was initially only successful for one

greywater sample (GWS 2B) and the two control *E. coli* cultures, which served as positive controls for the extraction method, based on the presence of faint 23S and 16S ribosomal RNA bands. The RNA gel also shows the presence of genomic DNA for lanes 4, 5, 6 and 9, indicating a DNase treatment would need to be included for future experiments. As the initial RNA yields from this method were relatively low, the CTAB extraction was repeated on the greywater sample 1 (GW1A) and several RNA extractions were pooled in the final resuspension step. The results obtained for the pooled sample had brighter 23S and 16S ribosomal RNA bands as shown in lane 3 of Figure 3.6 (gel B). Additionally, the concentration of the pooled sample was 123.2 ng/μl, which is significantly higher than the concentration range of the first extraction which ranged from 4.0 to 31 ng/μl. (Table B1 – Appendix B)

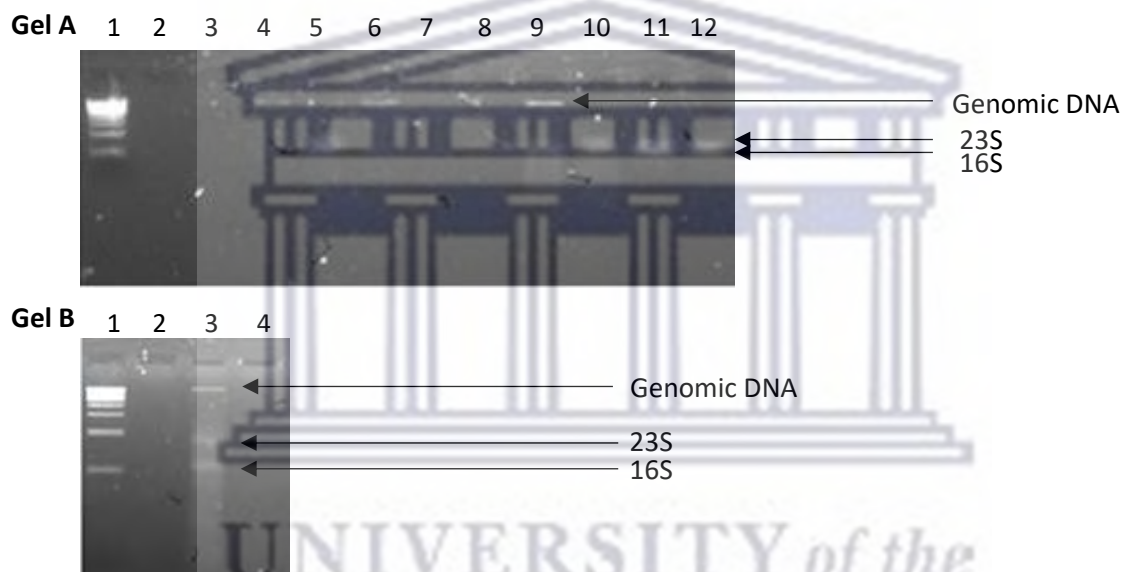


Figure 3.6: Total RNA extracted from trial greywater samples using the CTAB RNA Extraction method.

Gel A – Lane 1: 1kb NEB marker; Lane 2: GWS1SA; Lane 3: GWS1S1B; Lane 4: GWS2S1A; Lane 5: GWS2S1B; Lane 6: BFS1S1; Lane 7: BFS2S1; Lane 8: Blank; Lane 9: Tap water control 1; Lane 10: Tap water control 2; Lane 11: *E. coli* (+) control 1; Lane 12: *E. coli* (+) control 2. Gel B – Lane 1: 1kb NEB marker; Lane 2: Blank; Lane 3: Pooled samples (3X of Greywater 1A into one tube).

For comparison purposes, an additional organic- or chemical-based method was evaluated on the trial samples. A conventional acidified-phenol-based method was used. The hot acid phenol method was tested on the experimental trial samples collected from site 1 and site 2. Initial results shown in Figure 3.7, indicates the extraction method was successful only for the positive control (*E. coli*). No RNA was detectable for the experimental samples. Despite the fact that no RNA was detected on a gel NanoDrop readings indicated low concentrations of RNA (Table B2, Appendix B), whereby the concentration ranged between 3.5 and 30 ng/ul for the greywater experimental samples, which is likely below the detection level on a gel. This implied that the amount of starting material may not

have been sufficient to obtain good RNA yield. Despite the low yields, the extracted RNA appeared relatively pure, based on A260/A280 ratios for most samples being ~2.1. However, A260/A230 ratios indicated high protein contamination for the greywater samples.

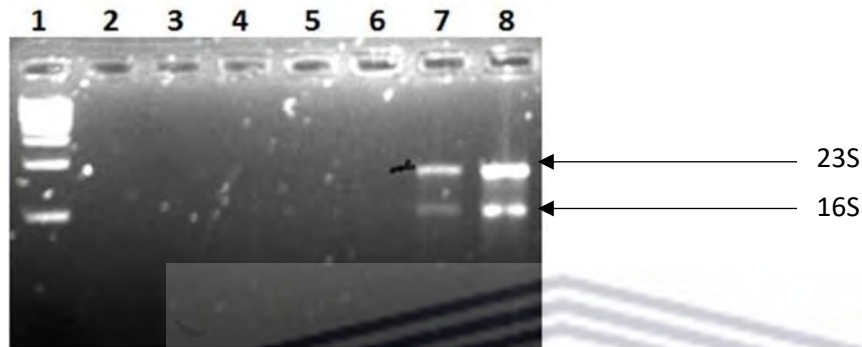


Figure 3.7: RNA extracted from greywater samples using the Hot-Acid Phenol RNA extraction method.

Lane 1: 1kb NEB marker, Lane 2: Blank, Lane 3: GW1A, Lane 4: GW1B, Lane 5: GW 2A, Lane 6: GW 2B, Lane 7: *E. coli* 1 (+) control, and Lane 8: *E. coli* 2 (+) control.

Based on the success of the isolation method on the positive control (*E. coli*), the method was repeated. However, the amount of greywater processed via centrifugation was increased to identify whether a lack of starting material was the reason for the failed extraction. As shown in Figure 3.8, the isolation method successfully extracted total RNA from 4 L of greywater samples, with concentrations ranging from 279.0 ng/ul for GWS4S2 to 532.5 for GWS4S1 (Table 3.6).

Table 3.6: Quantitation and analysis of total RNA extracted from greywater samples using the Hot Phenol SDS Method.

Samples	Concentration (ng/ul)	A260/280	A260/230
GWS3S2	399.0	1.82	1.01
GWS3S2	493.8	1.94	1.15
GWS4S1	366.9	1.97	1.68
GWS4S1	532.5	2.08	2.14
GWS4S2	446.1	1.96	1.15
GWS4S2	279.0	1.87	1.01

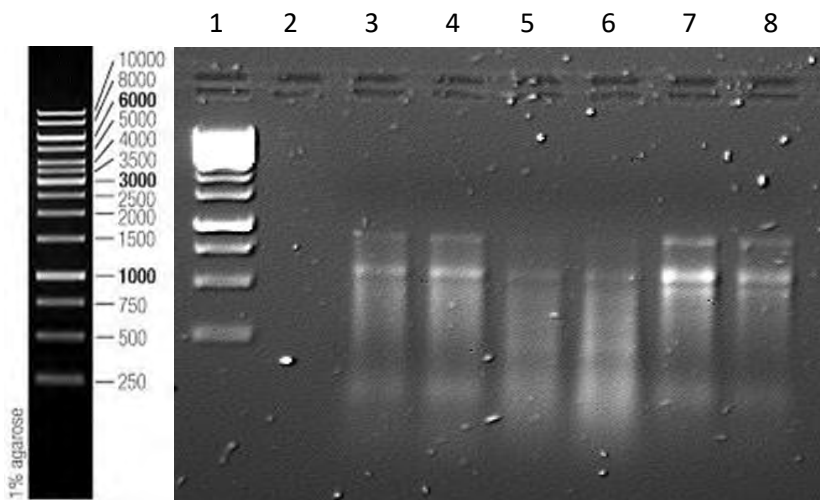


Figure 3.8: 1.2% TBE Agarose gel depicting RNA samples extracted from greywater using the Hot Phenol SDS method.

Lane 1: 1Kb Marker; Lane 2: Blank; Lane 3: GWS3S2; Lane 4: GWS3S2; Lane 5: GWS4S1; Lane 6: GWS4S1 ; Lane 7: GWS4S2; Lane 8: GWS4S2

3.3.1.2 Commercial Kits and Reagents

Commercial kits have been developed to improve the yield, quality, and efficiency of extracting nucleic acids, especially RNA. These kits however vary in the amount and quality of nucleic acids extracted, which may affect the results of various downstream applications. The yield and quality of RNA obtained using kits are often dependent on the sample type. Water samples always require a concentration step of the sample prior to any extraction procedure, which may be achieved through filtration, centrifugation, or a combination of methods (Felczykowska *et al.*, 2015).

For the testing of commercial kits and reagents, the RNEasy PowerWater kit and TRIzol reagent was assessed on experimental greywater samples. The RNEasy PowerWater Kit is a widely used kit and has been used for RT-PCR and NGS studies of wastewater, notably for the monitoring of the SARS-CoV-2 RNA virus (Alygizakis *et al.*, 2020). The kit allows for rapid isolation (within 40 minutes) and has been designed with the ability to extract total RNA from Gram positive and Gram negative microorganisms present in environmental samples. TRIzol reagent (ThermoFisher Inc) is a widely used commercial reagent and has been used for a variety of sample types, including wastewater samples. The popularity of the reagent is mainly due to affordability, as it is generally cheaper than column-based kits (Trujillo *et al.*, 2021) and allows for the extraction of total RNA from various sample types.

For the effective assessment of the RNEasy PowerWater kit on our greywater samples, two methods of sample concentration were evaluated, filtration or centrifugation prior to extraction. The pellet obtained from centrifuging 250 ml greywater sample was used for the extraction of RNA

depicted in Figure B1 (Appendix – Chapter 3). Lanes 3 and 4 indicate faint 23S and 16S bands, however the samples were degraded. The presence of smearing on the agarose gel may be due to secondary structures or other RNA transcripts such as mRNA. The concentration of RNA extracted from the duplicate samples was 39.6 ng/ul and 65.2 ng/ul respectively, and the A260/280 ratios ranged from 1.9 to 2.2 (Table B3, Appendix, Chapter 3). For comparative purposes greywater was also sequentially filtered using the filter sizes 20 µm, 10 µm and 0.45 µm, which allowed an increased volume (430 ml) of greywater to be filtered. Based on the integrity of the RNA extracted from the filtered samples (Figure B2, gel B – Appendix, Chapter 3) a faint intact 23S and 16S bands was present in lane 5. A DNA extraction using the DNEasy PowerSoil DNA Isolation kit as shown in Figure B2, gel A (Appendix- Chapter 3), using the same filters was also conducted to identify the efficiency of the sequential filtering to capture bacteria.

TRIzol reagent (Invitrogen) is a ready-to-use commercially available reagent widely used to isolate nucleic acids and denature proteins from multiple sources including human, animal, bacteria, and yeast (Rio *et al.*, 2010). The commercialized reagent is a monophasic solution of phenol and guanidinium isothiocyanate. The basis of the RNA extraction methodology is that post-solubilization using TRIzol reagent, the addition of chloroform results in a phase separation whereby proteins present reside in the organic phase, DNA resolves at the interface and RNA is found in the aqueous phase after homogenization. RNA is then precipitated from the aqueous phase using isopropanol (Chomczynski, 1993).

In this study, RNA was extracted from 250 ml of processed greywater which was concentrated using centrifugation. As shown in Figure 3.9, total RNA was extracted from three greywater samples in duplicate. RNA integrity analysis using gel electrophoresis however indicates the denaturing of the RNA as seen in lanes 6 and 7 of Figure 3.9. Faint 23S and 16S bands were present for samples GWS2S2 and GWS4S2, however the corresponding NanoDrop results ranged from 643.5 ng/ul and 900.6 ng/ul, see Table 3.9, which can likely be attributed to excess phenol present in the extracted RNA. A commercialized reagent such as TRIzol has been optimized for use on pure cultures of eukaryotic and prokaryotic cells, the introduction of environmental factors such as debris may have negatively impacted the effectiveness of the reagent. Additionally, low amounts of cells being present in the sample may have affected the yield.

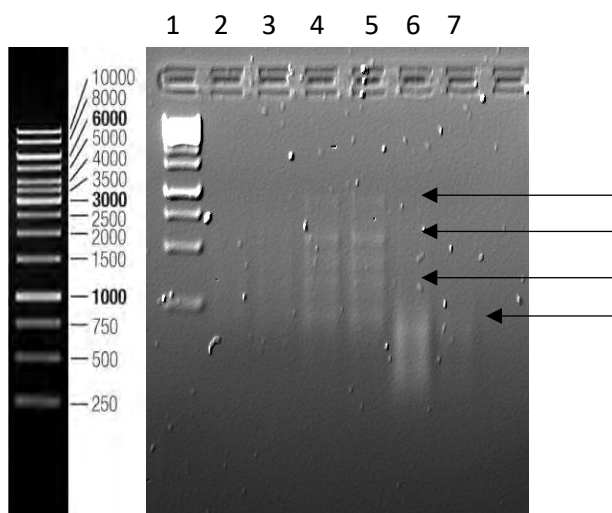


Figure 3.9: A 1.2% TBE Agarose gel depicting RNA samples extracted using TRIzol reagent from greywater samples.

Lane 1: 1kb O'Gene Ruler; Lane 2: GWS2S2; Lane 3: GWS2S2; Lane 4: GWS4S2; Lane 5: GWS4S2; Lane 6: GWS4S3; Lane 7: GWS4S3; Lane 8: Blank.

Table 3.7: Quantitation and analysis of RNA extracted from centrifuged greywater samples using TRIzol reagent

Sample	Concentration (ng/ul)	A260/A280	A260/230
GWS2S2 A	760	1,81	0,54
GWS2S2 B	767,4	1,82	0,58
GWS4S2 A	900,6	1,89	0,71
GWS4S2 B	643,5	1,82	0,53
GWS4S3 A	1366,1	2,03	1,12
GWS4S3 B	1169	1,9	0,99

Thus, from the results obtained when comparing RNA extraction methods, both commercial and organic/chemical, it was concluded that although the RNEasy PowerWater kit was effective, it gave low yields and reproducibility was a problem, as the amount of sample being processed per filter often differed between samples. Due to the nature of the greywater, the filters would reach capacity quickly which impacted on sample processing. Ultimately, the hot phenol SDS RNA extraction method was the most successful in extracting RNA from the greywater samples. The success of the organic or chemical based methodology was mainly due to the reproducibility and adaptability in terms of sample size and the efficiency in which the method was able to cope with inhibitors present in the greywater samples. Therefore, it was decided to optimize the hot phenol SDS method to increase the yield of total RNA extracted from greywater samples. It should be noted that due to low cell mass, total RNA was not extracted from biofilm samples.

3.3.1.2 Optimization of the Hot Phenol SDS Method for greywater samples

Initially, low-to-no RNA was extracted when tested on small sample volumes (< 1 L) Therefore, it was decided to increase the sample volume which was processed by sequential centrifugation. Figure 3.10 shows the increased cell mass which resulted from processing 4 L of greywater.



Figure 3.10: The pellet collected after the sequential centrifugation of 4 L of greywater.

When the Hot-Phenol SDS extraction method was tested on these larger samples there was an increase in yield and a significant increase in RNA (Figure 3.11). These findings were supported in a study done by Jahn *et al.*, (2008), which found that a modified version of a hot-SDS phenol method proposed had significantly higher yields than that of the RNEasy Kit (Qiagen) and even TRIzol reagent (Invitrogen), when extracting RNA from *D. dadantii*, a phytopathogenic member of the *Enterobacteriaceae* family.

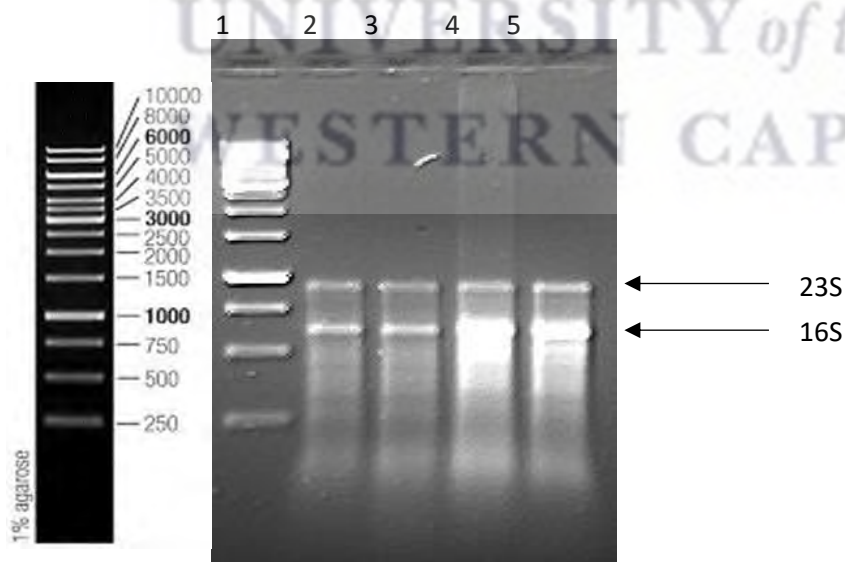


Figure 3.11: 1.2% TBE Agarose gel containing RNA extracted using the Hot Acid Phenol Method.

Lane 1: 1kb O'Gene Ladder; Lane 2: GWS1S2; Lane 3: GWS2S2; Lane 4: GWS3S2 and Lane 5: GWS4S2.

Based on these findings it was decided that all experimental samples would be processed using the hot phenol SDS method using 8 L of greywater.

A vital step in any purification techniques is solubilization of the material from which RNA is to be extracted. The basic goal is to minimize nuclease activity while simultaneously optimizing recovery. It is advisable to inactivate nucleases as efficiently and effectively as possible. This can be achieved by solubilizing biological material in a chaotropic salt, such as guanidine isothiocyanate or a denaturing detergent such as SDS, which is used as a solubilizing agent in the method proposed above (Nilsen, 2013). Careful consideration should be taken when choosing a precipitating salt, as SDS and potassium salts for instance are not compatible. This combination forms an insoluble potassium dodecyl sulphate precipitate (Rio *et al.*, 2010a). RNA is inherently hydrophilic and therefore dissolves readily in water. However, its hydrophobicity can be reduced by the presence of salt at acidic pH and furthermore by the addition of ethanol (Rio *et al.*, 2010b). Therefore, the precipitation method used in the modified hot-phenol SDS method is highly effective, especially when recovering RNA from aqueous solutions. However, it should be noted that ethanol precipitation is concentration dependent and careful consideration should be taken when precipitating samples which are likely to have either very high or very low amount of RNA present. As shown in Figure 3.12, ethanol precipitation incubation times were compared to identify the effect it may have on yield. Based on the results gel electrophoresis and NanoDrop results shown in Table B4, Appendix – Chapter 3) it was identified that an overnight incubation at -80 °C for the initial precipitation step in the protocol increased the yield and quality of total RNA extracted.

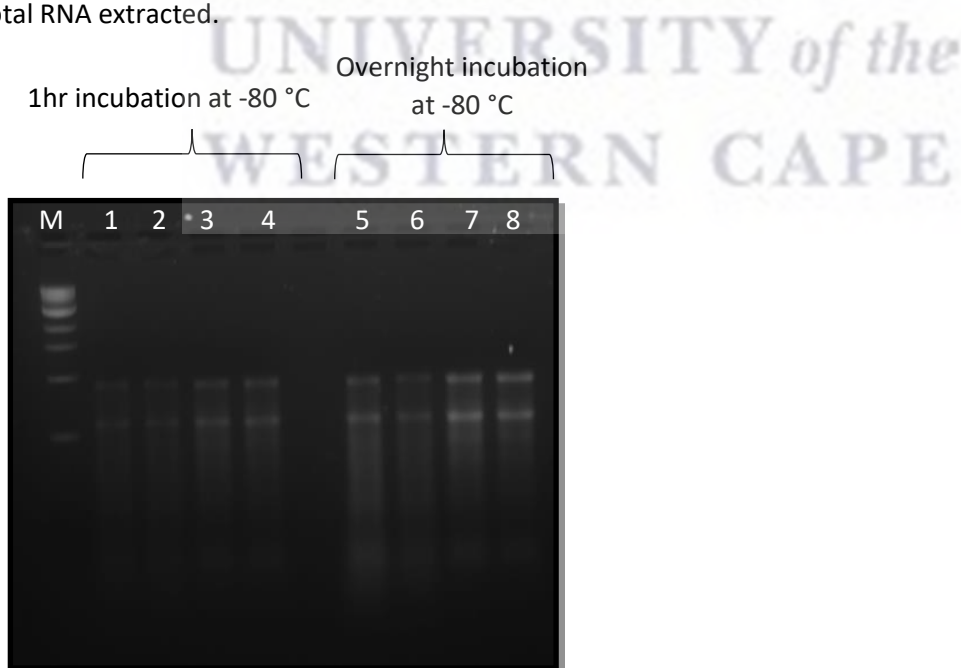


Figure 3.12: A 1.2% Agarose gel depicting RNA samples extracted from grey water samples using the Hot Phenol SDS Method. Lane M: 1kb NEB marker; Lane 1: GWS4S1; Lane 2: GWS4S1; Lane 3: GWS2S2; Lane 4: GWS2S2; Lane 5: GWS4S1; Lane 6: GWS4S1; Lane 7: GWS2S2; Lane 8: GWS2S2.

3.3.1.3 RNA Quality Analysis

The purity and integrity of RNA are critical elements for the overall success of RNA-based analysis, as low-quality RNA may compromise the results of downstream applications. The assessment of RNA integrity is especially crucial when aiming to obtain meaningful gene expression data (Fleige and Pfaffl, 2006). The most popular RNA quantification methods use a spectrophotometer/nano-spectrophotometer to measure the absorbance at 260 nm (A260). This is because the nucleotides present in RNA absorb ultraviolet (UV) light in the 250 to 265 nm range, thus this property can be used to quantitatively measure the concentration of an RNA solution by using the average absorbance for the four nucleotide bases (Rio *et al.*, 2010c). Spectrophotometric methods can also be used to determine the purity of the sample, by looking at ratios of the absorbances at 230, 260, and 280 nm. For purified RNA, the A260/280 ratio should be greater than 1.8, as the unpaired bases in RNA absorb more UV light than the base-paired bases in DNA (Rio *et al.*, 2010c; Fleige & Pfaffl, 2006). Additionally, the A260/230 ratio is also considered an indicator for nucleic acid purity, with ratios between 2.0 and 2.2 considered to indicate that the sample is pure.

In this study the A260/280 ratio for many samples extracted using the hot-phenol SDS method were within the range of 1.8 – 2.0, which is considered relatively pure. In addition, the A260/230 ratios for many samples were between 2.0 and 2.2. Although analysing quality based on the A260/280 ratio is generally reliable, this method can be hindered if the samples are contaminated with DNA, protein, or phenol, all of which absorb UV light at 260 nm. An indicator of protein contamination is absorbance at 280 nm, and phenol is absorbed at 270 nm (Rio *et al.*, 2010c). If the A260/280 ratio exceeds 2.0 as seen for greywater samples, protein contamination is probable and re-extraction with phenol is recommended. DNA contamination is harder to detect using a spectrophotometer, as RNA and DNA essentially have identical absorbance spectra. Therefore, if abnormal A260 and A260/280 ratios are present and phenol and protein contamination has been ruled out, the RNA sample is most likely contaminated with DNA (Rio *et al.*, 2010c). The presence of genomic DNA can compromise absorbance leading to an over-estimation of the actual amount of RNA present (Fleige and Pfaffl, 2006).

Table 3.8: NanoDrop results of RNA extracted from Greywater samples using the Hot Phenol SDS Method

Sample Name	Collection Date	HPM Extraction	RNA NanoDrop results		
			Replicate 1	Replicate 2	Average RNA (ng/ul)
GWS1S2	25/06/2019	✓	614,9	427,4	521,15
GWS1S3	05/02/2021	✓	152	216,3	184,15
GWS1S4	10/03/2021	✓	42,8	66	54,4
GWS2S2	22/02/2019	✓	274,9	330,9	302,9
GWS2S3	28/01/2021	✓	39,2	39	39,1
GWS2S4	8/03/2021	✓	192,2	132	162,1
GWS3S2	28/02/2019	✓	399	493,8	446,4
GWS3S4	28/01/2020	✓	403,3	237,3	320,3
GWS3S5	14/08/2020	✓	256,8	122,6	189,7
GWS3S6	15/10/2020	✓	214,6	178,5	196,55
GWS3S7	17/03/2021	✓	217,2	325,1	271,15
GWS4S1	29/01/2019	✓	366,9	532,5	449,7
GWS4S2	24/05/2019	✓	97,6	251,7	174,65
GWS4S3	30/05/2019	✓	286,2	626,2	456,2
GWS4S5	17/02/2020	✓	347,9	389,2	368,55
GWS4S6	07/09/2020	✓	514,4	27,5	270,95
GWS4S7	07/10/2020	✓	438,7	63,8	251,25

*RNA NanoDrop results prior to any additional DNase treatments

Additionally, all RNA extractions were analysed by agarose gel electrophoresis to assess RNA integrity. While there are several methods of assessing RNA integrity, agarose gels remain very popular as it is cost-effective, scalable and uses limited amounts of chemicals. However, it should be noted large quantities of RNA is required when running an RNA agarose gel, which may be prohibitive for many microbial ecology applications. As shown in Figure 3.12 total RNA extracted using the hot phenol SDS isolation method had bright bands at 3000 bp and 1500 bp. These bands correspond to the 23S and 16S ribosomal RNA, respectively, which are an indication that the RNA is intact. However, it should be noted that the smear present in sample GWS3S2 in addition to the representative ribosomal RNA bands is indicative of potential genomic DNA contamination.

3.3.1.4 16S rRNA gene Polymerase Chain Reaction for contaminating DNA in RNA samples

DNA contamination remains a problem with many RNA extraction methods, especially from prokaryotic organisms. Its removal often requires rigorous DNase treatments, which may affect the amount and purity of extracted RNA.

To confirm the complete digestion of gDNA in RNA samples, the presence of the 16S rRNA gene was assessed using RNA as a template. Figure 3.13 illustrates the presence of a 1.5 kb band in RNA samples extracted using the hot-phenol SDS method which would indicate the presence of contaminating DNA. Based on the flow diagram depicted in Figure 3.1, these samples required an additional DNase I treatment. Additionally, the presence of residual gDNA alongside samples with no amplifiable gDNA highlights the importance of checking all samples for the presence of contaminating gDNA (Lim *et al.*, 2016). Lim *et al.* stated that a large proportion of publications fail to demonstrate that their RNA extracts are DNA-free. Hence, it is strongly recommended including methods that can detect even trace amounts of gDNA in your workflow to avoid the overestimation of active microbial communities in greywater due to the presence of contaminating genomic DNA (Lim *et al.*, 2016).

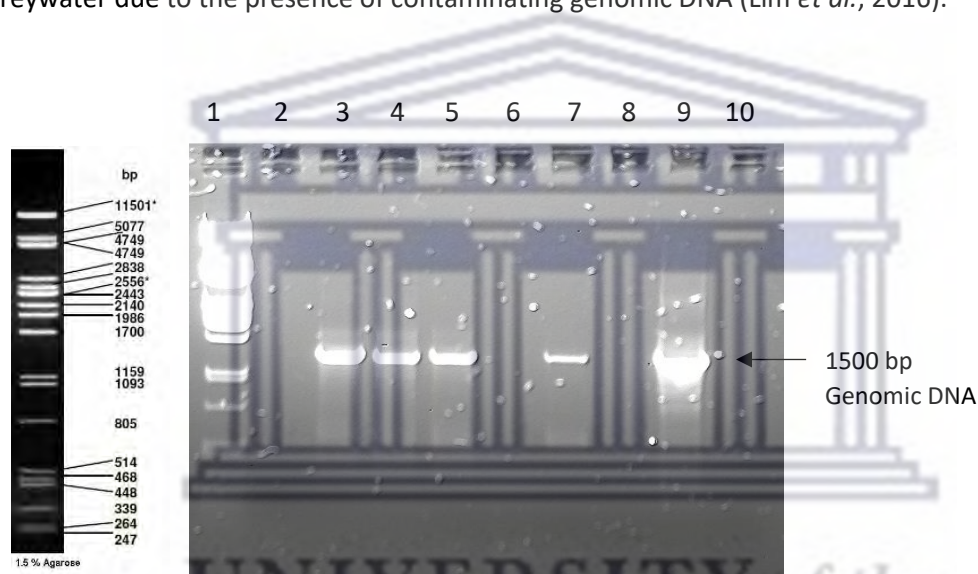


Figure 3.13: 1% Agarose gel depicting the 16S rRNA PCR for DNA contamination after 1X DNase I treated RNA samples.

Lane: 1: Lambda PST1; 2: GWS1S2A; 3: GWS1S2B; 4: GWS2S2A; 5: GWS2S2B; 6: GWS4S3B; 7: GWS3S2; 8: gDNA treated with DNase; 9: gDNA (+) control; 10: NTC.

After conducting extensive optimisation, it was found that when using the hot-phenol SDS method, two rigorous DNase treatments were required to render the samples genomic DNA free, as shown in Figure 3.14. It should be noted that a study by Jahn *et al.* (2008), identified that RNA isolated using a phenol-SDS approach required fewer DNase treatments compared to commercial proprietary reagents.



Figure 3.14: 1% TAE Agarose gel of 16S rRNA PCR for DNA contamination after 3X DNase 1 treated RNA samples.

Lane 1: Lambda PST, Lane 2: GWS2S2; Lane 3: GWS2S2; Lane 4: GWS2S2; Lane 5: GWS2S2; Lane 6: *E. coli* RNA; Lane 7: *E. coli* gDNA, Lane 8: NTC.

3.3.1.5 Ambion TURBO-DNase free Treatment

The Ambion TURBO DNase-free kit (Ambion, Life Technologies, USA) is renowned for having a markedly higher affinity for DNA than conventional DNase 1 and is therefore more effective in removing trace quantities of DNA contamination. Based on these properties, we evaluated the efficiency of the TURBO DNase-free kit on greywater samples, which are inherently complex and highly contaminated RNA samples. The rigorous protocol was conducted on 50 μ l RNA preparation. It should be noted that this treatment was conducted after a DNase treatment using ThermoScientific DNase 1, which is present in the Hot Phenol SDS method.

As seen in Figure 3.15 the contaminating gDNA present in gel A was removed after two rigorous treatments of TURBO DNase 1 (gel B). Importantly, the RNA remained intact after treatment, which is indicated by the presence of well-defined 23S and 16S bands in gel B. As seen in Table 3.9, RNA yield did not decrease as much as what was experienced using other DNase treatments.

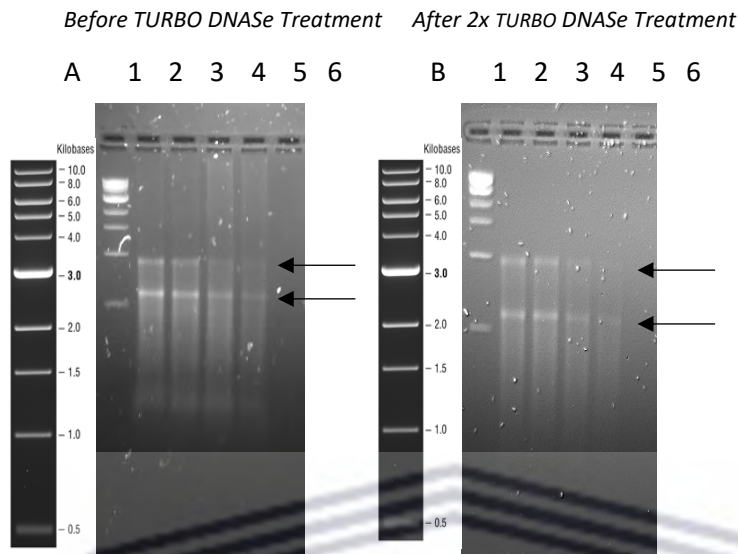


Figure 3.15A & 3.15B: RNA extracted from GWS4S5 and GWS3S4 respectively, using the Hot Phenol SDS Method.

Lane 1: 1Kb NEB Ladder, Lane 2: GWS4S5A, Lane 3: GWS4S5 B; Lane 4: GWS3S4A; Lane 5: GWS3S4B.

Table 3.9: Comparison of RNA Yield using Nanodrop ND-1000 when using the TURBO DNase-free kit

Sample	Before TURBO DNase-free Kit Treatment Concentration (ng/μl)	1X TURBO DNase-free kit Treatment Concentration (ng/μl)	2X TURBO DNase-free kit Treatment Concentration (ng/μl)
GWS4S5 A	557.5	435.0	347.9
GWS4S4 B	560.8	507.6	389.2
GWS3S4 A	587.9	527.6	403.3
GWS3S4 B	323.8	309.6	237.3

Methods for isolating intact total RNA from bacterial cells can be challenging technically (Jahn *et al.*, 2008). These tedious methods often make use of toxic and expensive chemicals to inhibit RNAses. In addition, while commercial kits may save the researcher time, in reality they often introduce bias and lead to unreproducible results.

With regards to the extraction of total RNA from greywater samples, it is proposed that we have found and optimized the methodology to ensure the reproducible extraction of high-quality RNA for downstream applications. Although laborious, the Hot-Phenol SDS RNA Isolation method is cost-effective and efficient when working with metagenomic samples.

3.3.2 cDNA synthesis

cDNA, also known as complementary DNA, is generated from a single strand RNA template by reverse transcription using the enzyme reverse transcriptase. The generation of cDNA is often required for gene expression analysis using qPCR, as it indicates which genes are being actively transcribed under a particular set of conditions. In the proposed workflow, RNA samples are only converted to cDNA once all the necessary checks have been conducted. This takes into consideration the presence of contaminating genomic DNA as well as the presence of any PCR inhibitors introduced during the workflow. Figure B3 (Appendix – Chapter 3) represents RNA samples which were converted to cDNA after two additional DNase digestion treatments. Prior to cDNA conversion, RNA samples were quantified using the Qubit BR RNA Assay kit as per the manufacturer's instructions as shown in Table B5 (Appendix – Chapter 3). After synthesis the cDNA was used as the template DNA in a 16S rRNA gene PCR to check for the presence of any contaminating DNA. For this experiment the absence of bands is the desired result. This optimised protocol consistently produced cDNA without contaminating gDNA, and as such, the cDNA was deemed suitable for gene quantification using qPCR. As shown in Table 3.10, total RNA was extracted from 19 samples of greywater over the period of the study. However, due to the rigorous steps taken to eliminate contaminating genomic DNA, as well as variations in yield, the amount of RNA was not always adequate for the synthesis of cDNA. In total, cDNA was successfully synthesized from 16 greywater samples for downstream analysis.

Table 3.10: Overview of Total RNA Extractions and cDNA synthesis of WRC K3/2803 Greywater Samples

Greywater Samples	RNA	Extraction Method	16S rRNA PCR for gDNA contamination	TURBO DNase-Free Kit Treatment	Qubit BR RNA Assay of RNA (ng/ μ l)	cDNA conversion	Qubit HS DNA Assay of cDNA (ng/ μ l)	
Site 1	GWS1S1							
	GWS1S2	✓	HPM	✓	✓	23,9	✓	0,524
	GWS1S3	✓	HPM	✓	✓	16,65	✓	7,122
	GWS1S4	✓	HPM	✓	✓	27,4	✓	2,88
Site 2	GWS2S1							
	GWS2S2	✓	HPM	✓	✓	40,8	✓	5,64
	GWS2S3	✓	HPM	✓				
	GWS2S4	✓	HPM	✓	✓	11,1	✓	1,536
Site 3	GWS3S1							
	GWS3S2	✓	HPM	✓	✓	19,3	✓	3,04
	GWS3S3		HPM					
	GWS3S4	✓	HPM	✓	✓	16,2	✓	4,52
	GWS3S5	✓	HPM	✓	✓	10,65	✓	1,938
	GWS3S6	✓	HPM	✓	✓	11	✓	6,16
	GWS3S7	✓	HPM	✓	✓	9,38	✓	2,62
Site 4	GWS4S1	✓	HPM	✓	✓	30,3	✓	4,88
	GWS4S2	✓	HPM	✓	✓	32	✓	1,036
	GWS4S3	✓	HPM	✓	✓	43,7	✓	7,94
	GWS4S4		HPM					
	GWS4S5	✓	HPM	✓	✓	19	✓	1,868
	GWS4S6	✓	HPM	✓	✓	4,835	✓	13,46
	GWS4S7	✓	HPM	✓	✓	6,35	✓	13,7

3.3.3 PCR optimization of Reference Gene Primer sets

According to MIQE guidelines, the most accurate experimental design requires between three and five good reference genes, thus it is recommended to test the stability of approximately 3-10 candidate reference genes in each of the experimental conditions evaluated (Rocha *et al.*, 2015). Reference genes are generally housekeeping genes selected from different parts of the genome to minimize the chance of transcriptional coupling affecting results. Additionally, genes are also selected to encode proteins involved in different metabolic activity, except for the ribosomal genes, to minimize the chances of co-regulation (Takle *et al.*, 2007).

To obtain consistent, reproducible and biologically relevant qPCR measurements researchers are encouraged to complete several technical steps, all of which influence the accuracy and precision of their qPCR results (Die *et al.*, 2016). Thus, prior to qPCR analysis conventional PCR was employed to optimise the cycling conditions of the target qPCR primer sets. The optimisation of each primer set was based on identifying the optimal cycling conditions, the ideal bacterial strain which gave consistent amplification, as well as the concentration of pivotal PCR components such as primers, dNTPs and magnesium chloride.

Figure 3.16 Gel A illustrates positive amplification for the 16S rRNA gene primer set, with an amplicon of 194 bp. Consistent amplification was achieved when using genomic DNA extracted from *E. cloacae* subsp. *cloacae* ATCC BAA-1143. For the *gapA* primer set, the 185 bp amplicon was successfully amplified from *E. coli* NCTC 13846 (Figure 3.16 Gel B). Additionally, for the *mdh* gene primer set the desired 197 bp amplicon was generated for genomic DNA extracted from *E. coli* ATCC 25922 (Figure 3.16 Gel C).

As a single fragment of the correct size was generated for the three reference gene primer sets, the resulting amplicons could be used as a template to construct control plasmids required for qPCR analysis. The optimized annealing temperature for each primer set was used as the initial conditions for qPCR experiments.

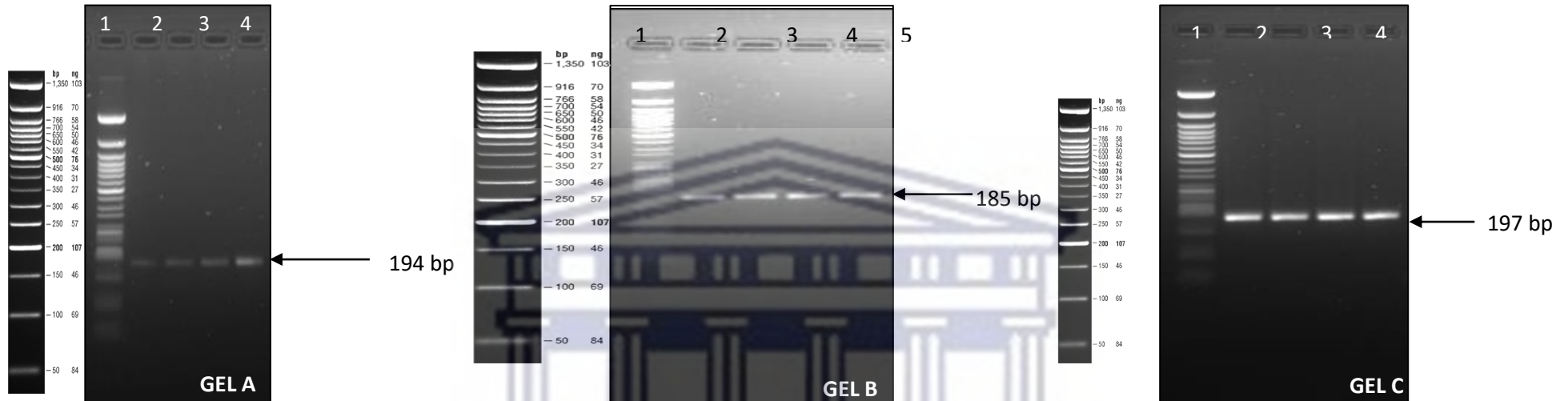


Figure 3.16 Gel A: Optimised amplification conditions for the 16S rRNA primer set. The amplicons represented above were purified and used to generate a standard curve for each target gene. Lane 1: 50 bp NEB Quick Load Ladder Lane 2-5: 16S rRNA gene amplicons generated using *Enterobacter cloacae* subsp. *cloacae* ATCC BAA-1143 genomic DNA. **Gel B: Optimised amplification conditions for the *gapA* gene primer set.** The amplicons represented above were purified and used to generate a standard curve for each target gene. Lane 1: 50 bp NEB Quick Load Ladder Lane 2-5: *gapA* gene amplicon generated from *Escherichia coli* derived from NCTC 13846 genomic DNA. **Gel C: Optimised amplification conditions for the *MdH* gene primer set.** The amplicons represented above were purified and used to generate a standard curve for each target gene. Lane 1: 50 bp NEB Quick Load Ladder Lane 2-5: *MdH* gene amplicons generated from *Escherichia coli* ATCC 25922 genomic DNA.

UNIVERSITY of the
WESTERN CAPE

3.3.4 PCR Optimization of Antibiotic Resistance Genes Primer sets

As shown in Figure 3.17 (Gel A), amplification of the *vanA* 65 bp amplicon was achieved using the DreamTaq polymerase. The targeted *vanA* gene, which encodes vancomycin resistance is plasmid-borne and therefore plasmid DNA extracted from *E. faecium* ATCC 700221 was used as a template for the PCR optimisation (McKenney *et al.*, 2016).

Figure 3.17 (Gel B) and 3.17 (Gel C) illustrates the amplification of the *ampC* and *aadA* gene primer sets, respectively. Each PCR optimization achieved the desired amplicon size of 67 bp and 295 bp. Positive amplification for the *ampC* primer set was achieved using genomic DNA extracted from *E. cloacae* subsp. *cloacae* ATCC BAA-1143; whereas for the *aadA* primer set genomic DNA derived from *E. coli* NCTC 13846 was the most successful in terms of amplification and consistency.



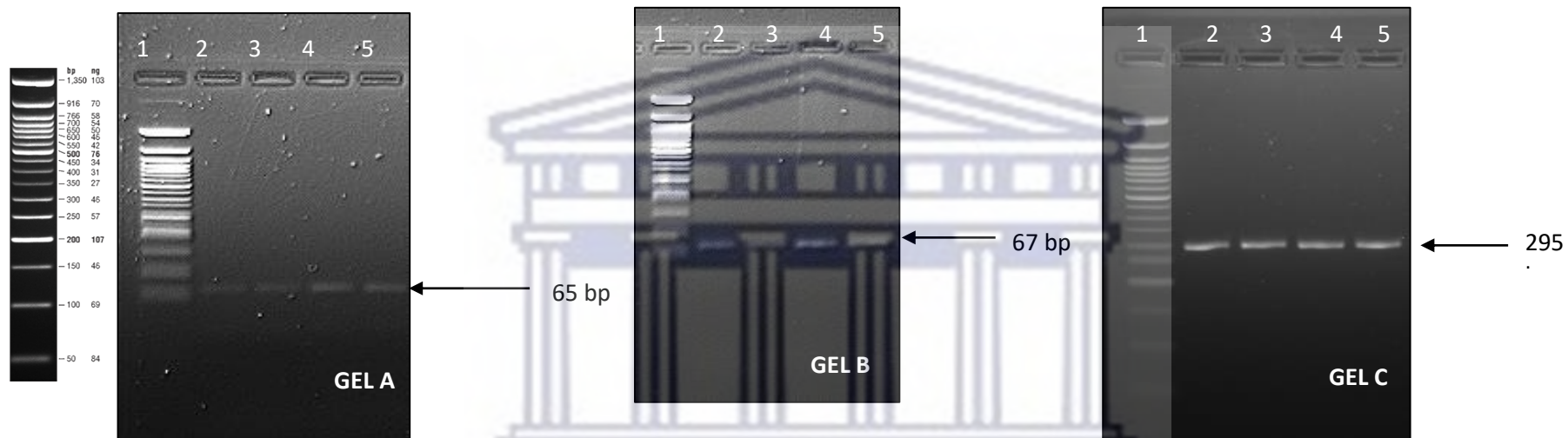


Figure 3.17 Gel A: Optimised amplification conditions for the *vanA* gene primer set. The amplicons represented above were purified and used for the cloning of single copy plasmids. Lane 1: 50 bp NEB Quick Load Ladder Lane 2-5: *vanA* gene amplicons generated using *Enterococcus faecium* ATCC 700221 plasmid DNA. **Gel B: Optimised amplification conditions for the *ampC* gene primer set.** The amplicons represented above were purified and used for the cloning of single copy plasmids. Lane 1: 50 bp NEB Quick Load Ladder Lane 2-5: *ampC* gene amplicons generated using *Enterobacter cloacae subsp. cloacae* ATCC BAA-1143 genomic DNA. **Gel C: Optimised amplification conditions for the *aadA* gene primer set.** The amplicons represented above were purified and used for the cloning of single copy plasmids. Lane 1: 50 bp NEB Quick Load Ladder Lane 2-5: *aadA* gene amplicons generated using *Escherichia coli* derived from NCTC 13846 genomic DNA.

3.3.5 Construction of plasmids for RT-PCR

For the purpose of this study absolute quantification was performed, which measures the target template of DNA or cDNA relative to a set of standards which are used to construct a standard curve (Svec *et al.*, 2015). Genomic DNA, plasmids or purified PCR products can be used as standards. While PCR amplicons are the easiest to produce, they often introduce side reactions due to their length which can greatly impact the efficiency of the qPCR assay (Svec *et al.*, 2015). Therefore, in the present study plasmids containing the gene of interest were constructed for calibration purposes. The amplicons of the optimised PCR reactions were used as the template for the plasmid controls. PCR products of the correct size were excised from the gel, gel purified and ultimately cloned into a pJET vector. PCR was then performed using the pJET sequencing primers and gene-specific primers to confirm the correct amplicon has been cloned. The inserts of interest are indicated by the arrows present on the gel Figure 3.18. Based on these results, the constructed plasmids were used for the generation of standard curves for each target gene to ensure qPCR efficiency and accuracy (Svec *et al.*, 2015).

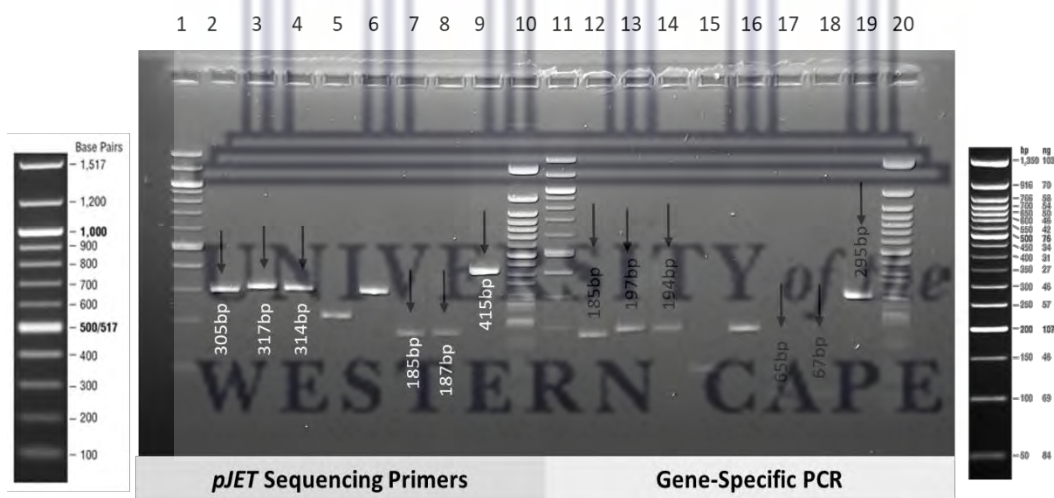


Figure 3.18: A 1% TAE agarose gel depicting the PCR confirmation of inserts using the pJET Sequencing Primers and the confirmation of insert using gene-specific primers for each target gene.

Lane 1: 100 bp NEB ladder; Lane 2: *gapA*; Lane 3: *mdh*; Lane 4: 16S rRNA RT; Lane 5: *int1*; Lane 6: 16S rRNA Int; Lane 7: *vanA*; Lane 8: *ampC*; Lane 9: *aadA*; Lane 10: 50 bp NEB Ladder; Lane 11: 100 bp NEB ladder; Lane 12: *gapA*; Lane 13: *mdh*; Lane 14: 16S rRNA RT; Lane 15: *int1*; Lane 16: 16S rRNA Int; Lane 17: *vanA*;

3.3.6 Real-Time PCR

The use and applications of quantitative PCR (qPCR) has greatly increased over the last two decades. The ability to effectively quantify minute amounts of nucleic acids in a sensitive and robust manner has revolutionised its applications in molecular biology and biotechnology (Svec *et al.*, 2015). qPCR is a technique that allows the simultaneous amplification and quantification of a target amplicon by measuring the fluorescence increment in each PCR cycle (Pinto *et al.*, 2012). There are two main categories of quantification, relative and absolute. For the purpose of this study, absolute quantification was performed. This method of quantification measures the target template relative to a set of standards used to construct a standard curve.

3.3.6.1 Copy Number Calculations of Target Genes

Table 3.11: Copy number of Target Plasmid Standards for reference and antibiotic resistance genes

Target Genes	Amplicon size (bp)	Concentration (ng/ μ l)	Copy Number (molecules/ μ l)
Reference Genes			
<i>gapA</i>	185	88.8	4.3196×10^{11}
<i>mdh</i>	197	110	5.1735×10^{11}
16S rRNA	194	82.6	3.8848×10^{11}
Antibiotic Resistance Genes			
<i>vanA</i>	65	76.8	1.077×10^{12}
<i>ampC</i>	67	100	1.36×10^{12}
<i>aadA</i>	295	84.6	2.616×10^{11}

As seen in Table 3.11 above, the concentration of the standards ranged from 76.8 ng/ μ l to 110 ng/ μ l. These concentrations corresponded to copy numbers of 1.36×10^{12} molecules/ μ l for the *ampC* gene, to 2.616×10^{11} molecules/ μ l for the *aadA* gene. All plasmid standards were stored at 4 °C for short term use and aliquots were prepared and stored in screwed cap tubes at -20 °C for long-term storage. It has been widely documented that isolation, quantification and storage of standards such as plasmid DNA is often a complex process which may introduce variation in the quantification of the nucleic acid. Variations in concentration estimation may introduce heterogeneity of quantitative results especially when conducting absolute quantification using qPCR.

3.3.7.2. Standard curves and Melt Curve Analysis of Target Genes

The accuracy and efficiency of a qPCR assay is governed by the standard curve of the target gene. A standard curve analysis is dual-functional, as it assesses the performance of a qPCR assay by estimating the efficiency (E) whilst simultaneously identifying the dynamic range, limit of detection and limit of quantification (Svec *et al.*, 2015). To estimate the efficiency of a qPCR assay by means of a standard

curve requires one to create a series of samples which have controlled relative amounts of target template, known as standards. The standards are prepared by serially diluting a concentrated stock of target template, mainly using 10-fold dilution steps.

A qPCR standard curve is a plot of the Threshold cycle (Ct) versus the logarithm of the amount of target template, with the Ct value plotted on the y-axis and the template concentrations on the x-axis. Features such as the slope, y-intercept and correlation coefficient (R²) values are used to extrapolate information regarding the performance of a reaction. The correlation coefficient reflects the linearity of the standard curve and serves as a measure of how effectively the data fits the standard curve produced. The slope of the log-linear phase of the amplification reaction is a measure of the reaction efficiency. For accurate and reproducible results, and slope of the curve generated from the dilution series should equate to -3.33 with an efficiency or correlation coefficient of 100%. Efficiency is calculated using the following formulae:

$$\text{Efficiency} = 10^{(-1/\text{slope})} - 1.$$

Therefore, standard curves were generated for each of the target reference and antibiotic resistance genes. Additionally, melting curve analysis (MCA) was conducted for each primer set.

A melting curve, also known as a dissociation curve, charts the change in fluorescence emitted when double-stranded DNA (dsDNA) coupled with dye molecules melts or dissociates into single-stranded DNA as the temperature of the reaction increases. Melting curve analysis capitalizes on the behaviour of non-specific DNA binding dyes (Zhang *et al.*, 2020), and is often used post-qPCR to distinguish genuine PCR products from potential reaction artefacts. The decreasing fluorescence is plotted against the increasing temperature to produce a melt curve, which is characteristic for a particular amplicon (Winder *et al.*, 2011). These first derivative curves can be converted into melt peak charts by plotting the negative derivative of fluorescence vs. temperature. The predicted and observed melt curve profiles are often compared to corroborate the amplification of the intended product (Winder *et al.*, 2011). This form of analysis serves as a robust and useful tool for detecting PCR products and has been used to determine the specificity of an amplicon to allow for genotyping and to detect single-nucleotide polymorphisms (SNPs) via high-resolution MCA (Zhang *et al.*, 2020).

3.3.7.2.1 Standard curves and Melt curve analysis of Reference Genes

The standard curves were generated for each primer set as per MIQE guidelines, with each consisting of at least five dilutions. For the *gapA* primer set, a standard curve generated using the *gapA* plasmid control (Figure 3.19) had a slope of -3.14 and a correlation coefficient (R²) value of 0.9979, thus falling within the desired range of 90 – 100%. From the melt curve analysis (Figure B4, Appendix – Chapter

3) it can be observed that the melting temperature is ~85 °C and a single specific size amplicon was generated.

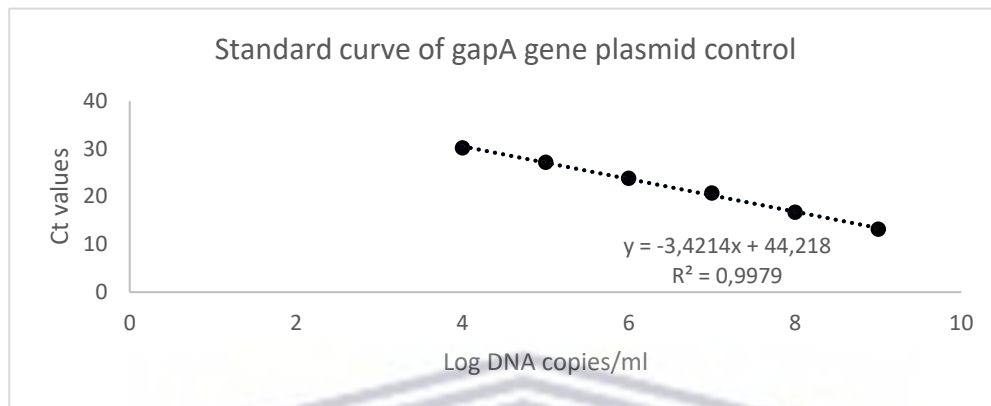


Figure 3.19: Standard curve generated using the *gapA* reference gene primers.

Similar results were generated for the 16S rRNA RT and *mdh* primer sets, respectively. For the 16S rRNA RT primer set the generated standard curve had a slope of -3.36 and a R^2 value of 0.998 as seen in Figure B5 (Appendix – Chapter 3), thereby falling within the desired PCR efficiency range. The melt curve analysis shown in Figure B6 (Appendix – Chapter 3), revealed that the primer set was specific and generated a single amplicon with an approximate melting temperature of 86 °C.

Similarly, the *mdh* primer set a standard curve had an efficiency of 99% (Figure B7 – Appendix, Chapter 3). The slope produced equated to -3.51 with a corresponding R^2 value of 0.9904. As shown in Figure B8 (Appendix – Chapter 3), specific amplification occurred as a single peak was produced for the dilution series at approximately 87 °C. The efficiency of the PCR assays for the reference genes described above was of vital importance for the progression of the study as it insured that subsequent quantification would be accurate and reproducible.

3.3.7.2.2 Standard curves and Melt curve analysis of Antibiotic Resistance Genes

For this study, it was important to ensure that the previously published primers used for the three targeted antibiotic resistance genes were accurately quantified in the control plasmids produced. Therefore, in order to determine the efficiency of the qPCR assays, a standard curve was produced for each primer set in conjunction with a melt curve analysis to ensure that a single amplicon was amplified.

The first resistance gene analysed was *vanA*. As seen in Figure 3.20, the standard curve had a slope of -3.3257 with a R^2 value of 0.9929. The melt curve analysis (Figure 3.21) revealed a single highly specific

amplicon at approximately 84 °C, indicating no non-specific amplification or artefact amplification had occurred.

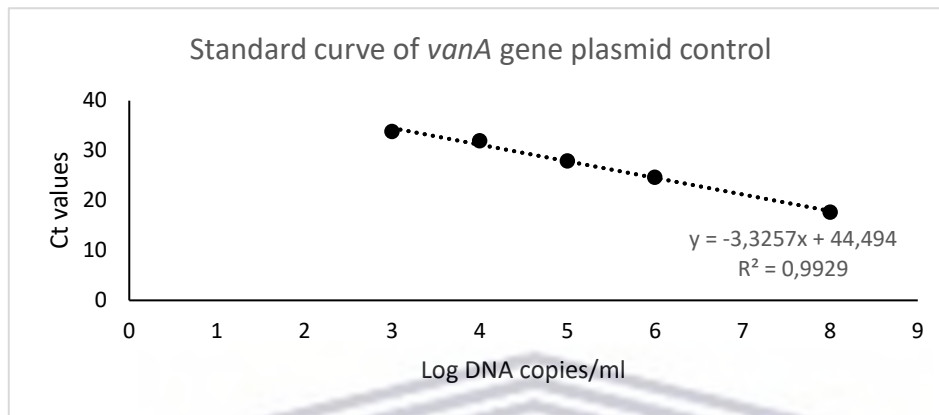


Figure 3.20: Standard curve generated using the *vanA* gene primers.

Figure B9 (Appendix B, Chapter 3) illustrates the standard curve for the *ampC* gene primer set. The slope generated was -3.1029 with a corresponding correlation coefficient value of 0.9959. The PCR efficiency is further corroborated by the presence of a single sized amplicon present in Figure B10 (Appendix B, Chapter 3), with a single melt peak at approximately 83 °C.

Finally, for the *aadA* gene primer set the standard curve illustrated in Figure B11 (Appendix B, Chapter 3), provided valuable information regarding the efficiency of the reaction. The primer set produced a slope of -3.3049 and a R^2 value of 0.9982 thus falling within the 90-100% efficiency range. The melt curve analysis revealed a specific single sized amplicon (Figure B12- Appendix B, Chapter 3) which is indicative of the efficiency of the assay and primer set.

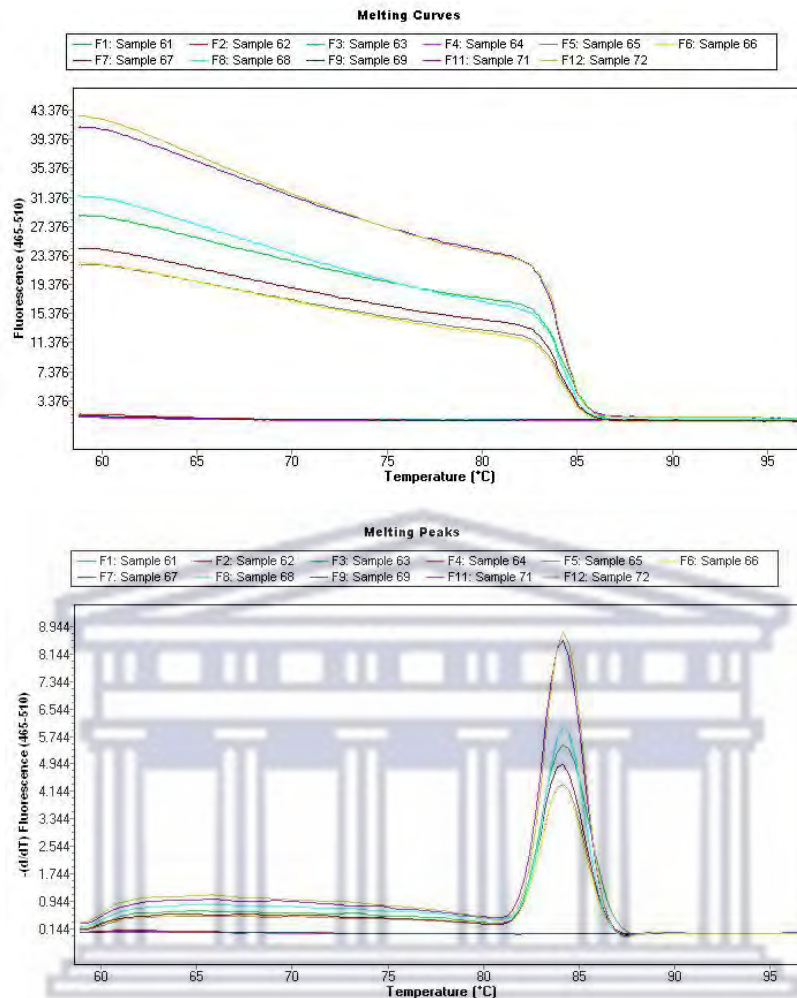


Figure 3.21: Melt Curve of *vanA* gene amplicons generated using a dilution series of control plasmids. Cp values for these amplicons were used to construct the standard curve used for subsequent absolute quantification experiments.

3.3.7.3 Absolute quantification of Antibiotic Resistance Genes in Greywater Samples

The establishment of ARG reservoirs in aquatic environments with human activities is not uncommon (Scott *et al.*, 2020). In recent years there has been a surge of interest in the environmental surveillance of antibiotic levels, ARBs and ARGs, particularly in wastewater treatment plants and other aquatic settings (Rocha *et al.*, 2015). With the modern lifestyle requiring large amounts of potable water and generating copious amounts of wastewater, the introduction of greywater usage and storage was an easy to implement and cost-effective approach, especially during the Western Cape water crisis. However, there is limited knowledge about greywater being a potential reservoir of ARGs and how this may impact usage and potential health risks. Therefore, the current study represents an investigation into whether greywater may harbour ARGs, as well as identifies the effectiveness of real-time qPCR as a molecular technique to monitor potential ARGs in greywater.

3.3.7.3.1. Comparison of ARG abundance and collection sites

For this study absolute quantification was performed using the Second derivate method, as the LightCycler 480 II software allows one to include internal controls when using the algorithm. Each sample was assessed in triplicate and the mean Ct value and copy number was derived from the standard curve. Based on previous studies a threshold cycle (Ct/Cp) of 32 was considered the limit of detection and only samples with all three replicates amplifying were considered as positive and used for further analysis (Zheng *et al.*, 2020). As stated earlier a total of 16 greywater cDNA samples were analysed.

Due to issues with optimization, limited sample availability and time, of the three reference genes intended to be assessed (*gapA*; 16S rRNA and *mdh*), a complete data set could only be obtained for the the *gapA* reference gene. Thus, the absolute quantification of the targeted ARGs for the purpose of this study will be relative to the abundance of the *gapA* reference gene.

Quantitative analysis revealed that the *vanA* gene was detected in 14 of the 16 greywater samples assessed, as shown in Table 3.11, which represents the mean Ct values and their corresponding mean copy numbers per sample per site collected. Samples GWS1S2 and GWS1S3 had mean Ct values which were beyond the limit of detection, this was supported by the results shown in Figure 3.20, which represents the standard curve for the *vanA* gene, with the greywater samples per site plotted. Copy numbers ranged between 1.29E+04 (GWS3S6, Spring sample) to 3.15E+05 (GWS3S7, Autumn sample). Figure 3.22 illustrates that most of the samples fall within the linear range of the standard curve for the *vanA* primer set, with the outlier's present being from Greywater Site 1. Given the low copy numbers detected in future studies one could use a standard curve with a broader concentration range.

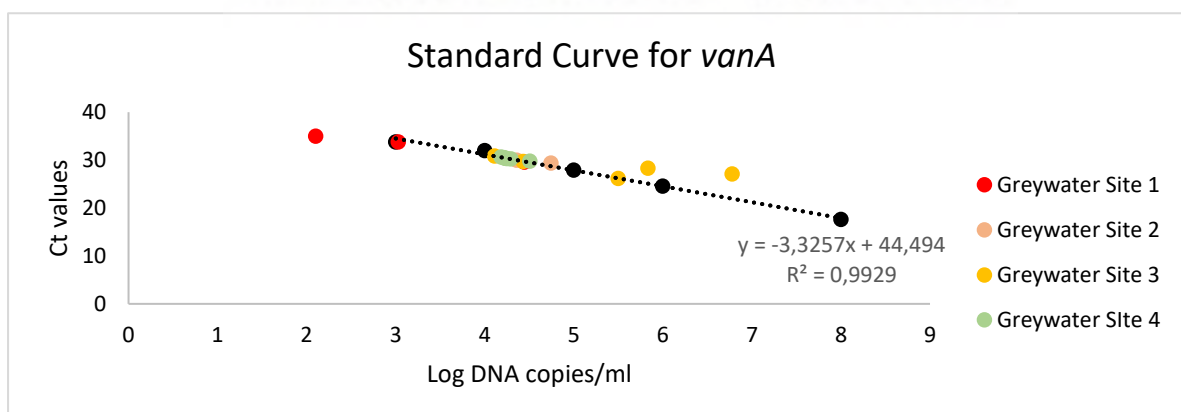


Figure 3.22: Standard curve for *vanA* gene primer set, with greywater samples collected at all four sites.

Based on the criteria for the quantification of ARGs in this study, the *ampC* resistance gene was detected in 12 of the 16 greywater samples assessed, as shown in Table 3.22 below. Figure 3.23 illustrates the standard curve of the *ampC* primer set and indicates that samples from site 4 (GWS4S2; GWS4S5; GWS4S6 and GWS4S7) were not within the linear range of the standard curve. The mean copy numbers for the *ampC* gene as shown in Table 3.11 ranged from 3.55E+01 (GWS4S6, Winter sample) to 4.25E+04 (GWS1S3, Summer Sample).

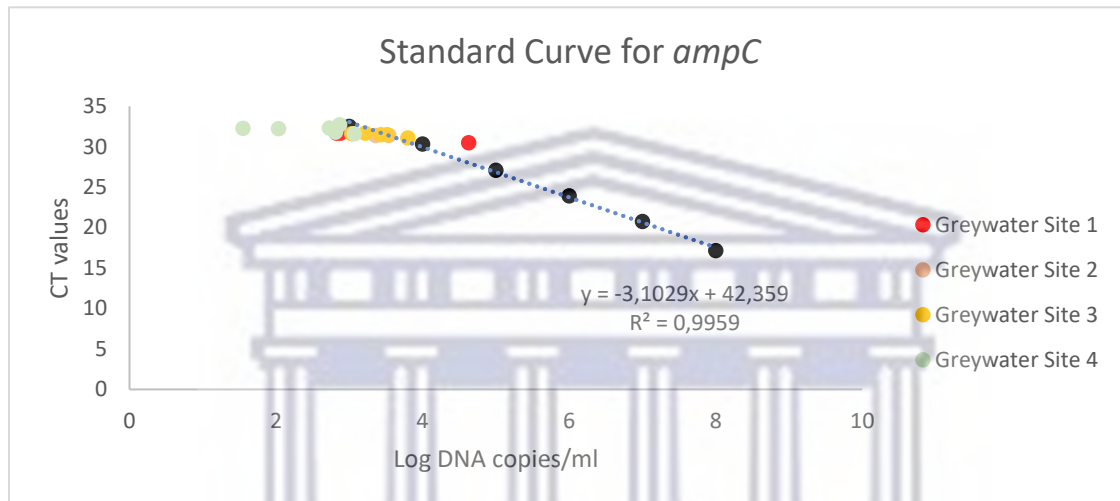


Figure 3.23: Standard curve for *ampC* gene primer set, with greywater samples collected from all four sites.

Based on quantitative analysis criteria for the ARGs assays used in this study, the *aadA* gene was not detected in any of the greywater samples analysed, as their Ct values exceeded 32 (Table 3.11). Higher Ct values ranging between 30 and 35 indicate that more cycles of amplification were required to detect the fluorescence which directly correlates to low levels of mRNA being present. The mean copy numbers generated ranged from 8.27E+01 (GWS3S5, Winter sample) to 6.45E+02 (GWS1S3, Summer Sample). As shown in Figure 3.24, which represents the standard curve for the *aadA* gene primer set, all the samples assessed were not within the linear range of the primer set. The data suggest that the aminoglycoside resistance genes are either not present or if present are being expressed at very low levels. Previous studies in China reported *aadA* gene abundances ranging between 10^3 to 10^5 copies/ml in river water samples (Wang *et al.*, 2018).

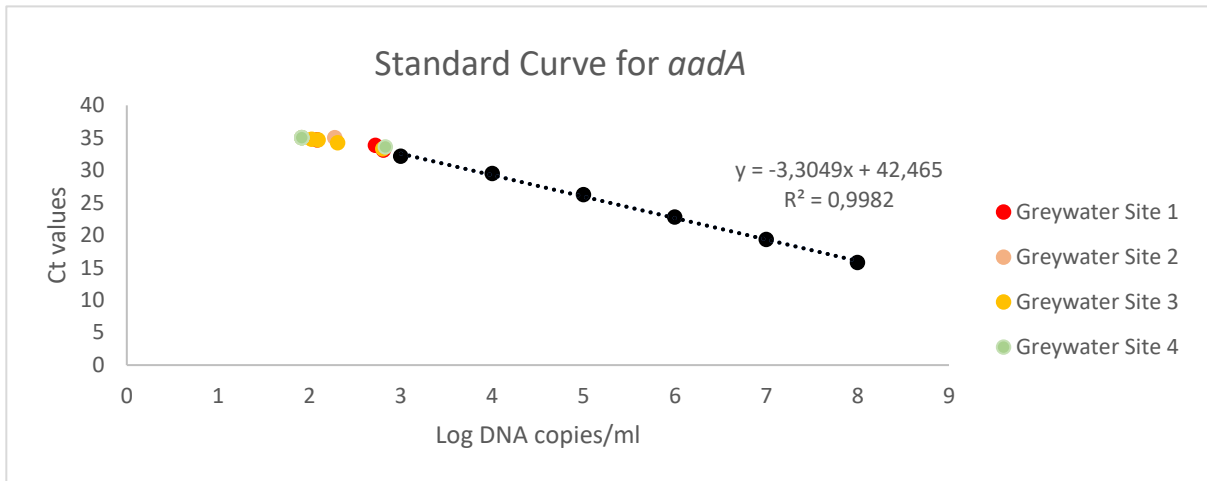


Figure 3.24: Standard curve for *aadA* gene primer set, with samples from all four collection sites.

Additionally, the occurrence of high Ct values as seen in Table 3.12 for the *aadA* gene may also be due to the issues with sample collection, processing, extraction, poor quality RNA or DNA or potential inhibitors that may reduce the sensitivity of the assay. Additional sources of high ct values such as the degradation of the probe-based fluorophore or by non-specific amplification of background sample/nucleic acid may attribute to the problem (Caraguel *et al.*, 2011). In future the occurrence of high Ct values may be corrected by investigating potential points of contamination, using more total RNA or a higher concentration of template. The motivation to include resistance to streptomycin in the present study was due to the fact that streptomycin use is limited to a few specific applications, including the last resort treatment of drug-resistant tuberculosis and complicated UTIs (where it is administered intravenously). As such the level of resistance was expected to be low. Based on the quantitative analysis of the *gapA* reference gene, it was concluded that the gene of interest was detected in all 16 greywater samples analysed. The mean Ct values per site ranged between 24.31 (GWS4S3) to 31.49 (GWS1S3) as shown in Table 3.12. The mean copy number was calculated as described above and ranged between 6.87E+01 (GWS1S2) to 7.11E+03 (GWS3S6).

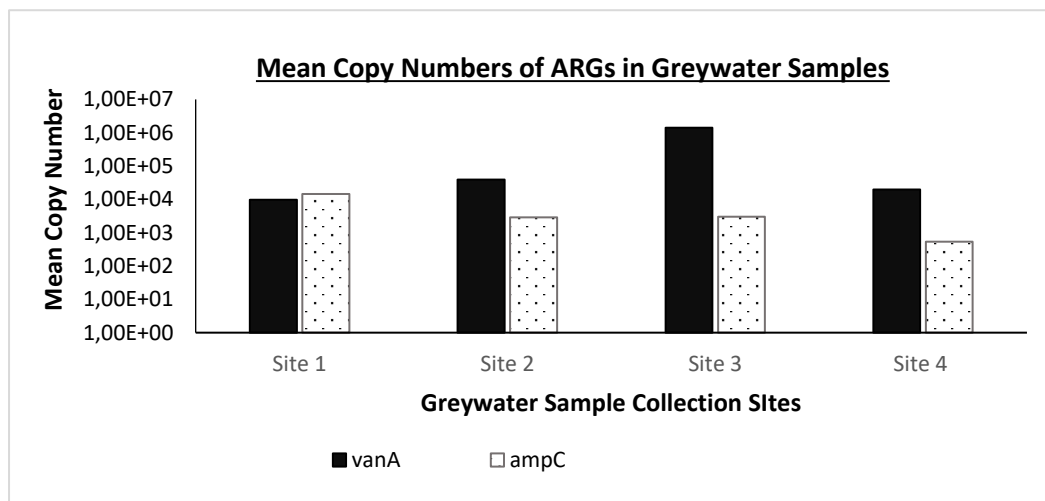


Figure 3.25: Mean Copy number of ARGs detected in greywater samples collected from all four sites.

Figure 3.25 serves as a graphical overview of the mean copy number of the ARGs *vanA* and *ampC* per site. As shown in the Figure 3.23, site 3 had the highest mean copy number for the *vanA* gene of $1.41\text{E}+06$, whereas site 1 had the highest mean copy number for the *ampC* gene of $1.46\text{E}+04$. It should be noted that the sites were not sampled proportionately. Site 1 and Site 2 were sampled on four separate occasions, respectively, of which three samples were successfully processed and converted to cDNA for site 1 and two samples for Site 2. Site 3 and 4 however, were sampled more frequent over the period of the study, each site was sampled 7 times, of which 5 samples were successfully processed and converted to cDNA for site 3 and 6 samples for site 4. The disproportionate sampling was mainly due to occupant availability as all greywater storage tanks were installed on private property. Overall, a variation in ARG levels in different samples and sites was expected as different households make use of different antibiotics at different times (Cheng *et al.*, 2021).



Table 3.12: Mean Ct values and Gene Copy Number for Antibiotic Resistance Gene qPCR Assay

Sample Name	Collection Season	Antibiotic Resistance Genes						Housekeeping Gene	
		<i>vanA</i>		<i>ampC</i>		<i>aadA</i>		<i>gapA</i>	
		Mean Ct value	Mean Copy Number	Mean Ct value	Mean Copy Number	Mean Ct value	Mean Copy Number	Mean Ct value	Mean Copy Number
GWS1S2	Winter	33,78	1,07E+03	31,66	7,51E+02	34,66	1,22E+02	31,44	6,87E-01
GWS1S3	Summer	35	1,26E+02	30,48	4,25E+04	33,09	6,45E+02	31,49	1,61E+03
GWS1S4	Autumn	29,58	2,79E+04	31,68	6,68E+02	33,82	5,29E+02	31,26	2,32E+02
Mean Copy Number for Site 1			9,70E+03		1,46E+04		4,32E+02		
GWS2S2	Summer	29,98	2,29E+04	31,41	3,49E+03		0,00E+00	30,69	1,03E+03
GWS2S4	Autumn	29,41	5,56E+04	31,41	2,27E+03	35	1,90E+02	30,72	6,34E+02
Mean Copy Number for Site 2			3,93E+04		2,88E+03		9,50E+01		
GWS3S2	Summer	29,76	2,69E+04	31,48	3,26E+03	34,2	2,03E+02	30,45	1,32E+03
GWS3S4	Summer	27,1	6,03E+06	31,47	2,70E+03	34,77	1,06E+02	30,18	1,60E+03
GWS3S5	Winter	28,32	6,81E+05	31,66	1,65E+03	35	8,27E+01	30,03	2,05E+03
GWS3S6	Spring	30,86	1,29E+04	31,08	6,27E+03	34,68	1,25E+02	28,37	7,11E+03
GWS3S7	Autumn	26,18	3,15E+05	31,59	1,08E+03	33,3	6,35E+02	29,34	3,26E+03
Mean Copy Number for Site 3			1,41E+06		2,99E+03		2,30E+02		
GWS4S1	Summer	30,42	1,69E+04	31,6	1,17E+03	35	8,27E+01	30,41	1,08E+03
GWS4S2	Autumn	30,55	1,65E+04	32,23	1,08E+02	35	8,27E+01	29,42	3,01E+03
GWS4S3	Autumn	30,34	1,78E+04	31,79	6,47E+02	35	8,27E+01	24,31	1,20E+05
GWS4S5	Summer	29,77	3,22E+04	32,71	7,42E+02	35	8,27E+01	30,64	6,41E+02
GWS4S6	Winter	30,7	1,53E+04	32,27	3,55E+01	33,56	6,80E+02	30,35	1,31E+03
GWS4S7	Spring	30,26	1,97E+04	32,31	5,37E+02	35	8,27E+01	30,04	1,95E+03
Mean Copy Number for Site 4			1,97E+04		5,40E+02		1,82E+02		

Table 3.13: Mean Ct values and Gene Copy Number for Antibiotic Resistance Gene qPCR Assay

Sample Name	Collection Season	Housekeeping Gene		Relative Abundance of ARGs	
		<i>gapA</i>		<i>vanA/gapA</i>	<i>ampC/gapA</i>
		Mean Ct value	Mean Copy Number	Normalized Gene Copy Number	Normalized Gene Copy Number
GWS1S2	Winter	31,44	6,87E-01	1,56E+03	1,09E+03
GWS1S3	Summer	31,49	1,61E+03	7,83E-02	2,64E+01
GWS1S4	Autumn	31,26	2,32E+02	1,20E+02	2,88E+00
Mean Copy Number for Site 1			6,14E+02	5,59E+02	3,74E+02
GWS2S2	Summer	30,69	1,03E+03	2,22E+01	3,39E+00
GWS2S4	Autumn	30,72	6,34E+02	8,77E+01	3,58E+00
Mean Copy Number for Site 2			8,32E+02	5,50E+01	3,48E+00
GWS3S2	Summer	30,45	1,32E+03	2,04E+01	2,47E+00
GWS3S4	Summer	30,18	1,60E+03	3,77E+03	1,69E+00
GWS3S5	Winter	30,03	2,05E+03	3,32E+02	8,05E-01
GWS3S6	Spring	28,37	7,11E+03	1,81E+00	8,82E-01
GWS3S7	Autumn	29,34	3,26E+03	9,66E+01	3,31E-01
Mean Copy Number for Site 3			3,07E+03	8,44E+02	1,24E+00
GWS4S1	Summer	30,41	1,08E+03	1,56E+01	1,08E+00
GWS4S2	Autumn	29,42	3,01E+03	5,48E+00	3,59E-02
GWS4S3	Autumn	24,31	1,20E+05	1,48E-01	5,39E-03
GWS4S5	Summer	30,64	6,41E+02	5,02E+01	1,16E+00
GWS4S6	Winter	30,35	1,31E+03	1,17E+01	2,71E-02
GWS4S7	Spring	30,04	1,95E+03	1,01E+01	2,75E-01
Mean Copy Number for Site 4			2,13E+04	1,55E+01	4,31E-01

To assess the relative abundance of the targeted ARGs present in greywater samples in this study, the copy numbers derived from the standard curves were normalized to that of the reference gene *gapA*. Normalization was achieved by dividing the mean copy number per ARG per site by the mean copy number of the *gapA* gene as shown in Table 3.12. It is assumed that only one gene copy of *gapA* is present per bacterium.

As shown in Table 3.13, the relative abundance of the *vanA* and *ampC* gene ranged between 7.83E-02 (GWS1S3) and 3.77E+03 (GWS3S4) for *vanA* gene and 5.39E-03 (GWS4S3) and 1.09E+03 (GWS1S2) for the *ampC* gene, respectively. Similar results were obtained in a study by Zielinski *et al.*, (2020) who detected the *vanA* gene at 9.73×10^1 gene copies per ml river water on average compared to the more concentrated untreated wastewater samples which had 8.28×10^5 gene copies per ml.

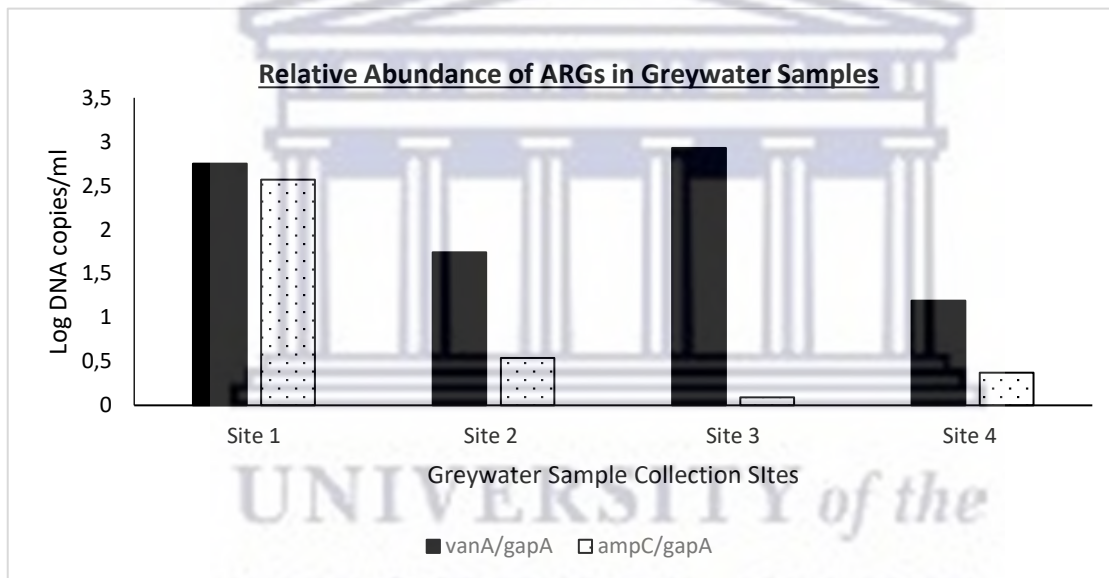


Figure 3.26: Relative abundance of ARGs in Greywater samples

Figure 3.26 is a graphical representation of the relative abundance of ARGs present in the greywater samples analysed. For the *vanA* gene, site 3 had the greatest relative abundance of 2.93 log DNA copies per ml of greywater compared to the *ampC* gene, of which site 1 had the greatest relative abundance of 2.57 log DNA copies per ml of greywater. Although sampled most frequently over various seasons, Site 4 had the lowest mean relative abundance of all the sites, with only 1.19 log DNA copies/ml of *vanA* and 0.37 log DNA copies of *ampC*. The results support findings by Volkman *et al.*, (2004) who detected the *vanA* gene in 21% and *ampC* gene in 78% of municipal wastewater samples analysed using RT-PCR.

These results indicate that ARGs (*vanA* and *ampC*) were detectable in greywater samples using qPCR and supports findings by Scott *et al.*, in 2020, which reiterated that ARGs are detectable in a multitude of environments. In addition, our data supports the findings of Shuai *et al.*, in 2023, who identified that there is a distinct correlation between conditions at individual households and their associated ARGs compositions, even when sharing the same municipal water supply. Greywater systems are similar to wastewater treatment plants in that the system is exposed to various residual antibiotics and co-selection factors such as surfactants and metals from daily activities (Lee *et al.*, 2017), therefore the positive identification of ARGs is not surprising.

Vancomycin resistance genes (*van*) have been detected in various water bodies (Zhang *et al.*, 2009). Notably in 2014, the vancomycin resistance genes *vanA*, *B* and *C1,2* and *3* were detected in domestic wastewater effluents in the Eastern Cape (Iweriebor *et al.*, 2015; Ekwazala *et al.*, 2016). Furthermore, the *ampC* gene was detected by Adefisoye and Okoh (2016) in environmental wastewater in the Eastern Cape using PCR. Similarly, the plasmid-mediated *ampC* gene has also been detected in the Crocodile West River in South Africa using ddPCR (digital droplet PCR), with key findings correlating the levels of *ampC* gene copies to population density (Coertze and Bezuidenhout, 2020).

Future analysis should include a more proportional sampling schedule with consideration taken to the number of samples collected per season. This may give a better understanding of the microbial load present in the greywater storage tanks, as well as the microbial community.

3.3.7.3.2 Comparison of ARG abundance and Collection seasons

Temperature is a vital factor when assessing water quality, as it directly influences key physical, chemical and biological processes such as microbial growth and competition (Preciado *et al.*, 2021). A study by Jiang *et al.* (2023) identified temperature as an important driving force in the variation of ARG profiles in environmental water samples. Thus, the relationship between collection season and the absolute abundance of the target ARGs was investigated to identify the effect seasonal changes may have on the microbial population within the greywater collection tanks.

It was hypothesized that seasonal variation would affect the microbial community present in the greywater samples, and thus the presence and abundance of potential ARGs. In this study collection season was based on the average weather conditions experienced each month in Cape Town and samples were grouped accordingly. Based on the results it was identified that the microbial population harbouring the *vanA* gene appear to be larger in the summer and autumn months compared to the winter and spring months. This can be seen when comparing the absolute abundance of the *vanA* gene and the sample collection season as shown in Figure 3.27. Similarly, the microbial population harbouring the *ampC* gene appear to be higher in the spring and summer months, compared to the

winter and autumn samples as shown in Figure 3.28. The data supports findings by Jiang *et al.* (2023) who found that higher absolute abundances of ARGs and MGE were present in warmer seasons as the higher temperatures and nutrient availability are conducive to faster microbial growth and proliferation. In line with the hypothesis these findings suggest a greater microbial load and more diverse microbial community in the warmer months. Although sampling was not proportional, the data illustrates a correlation between ARG profiles and seasonal variations. Providing pivotal information for future work which may take into consideration a multitude of variables (occupants, health, antibiotic usage) in conjunction with seasonal variation.



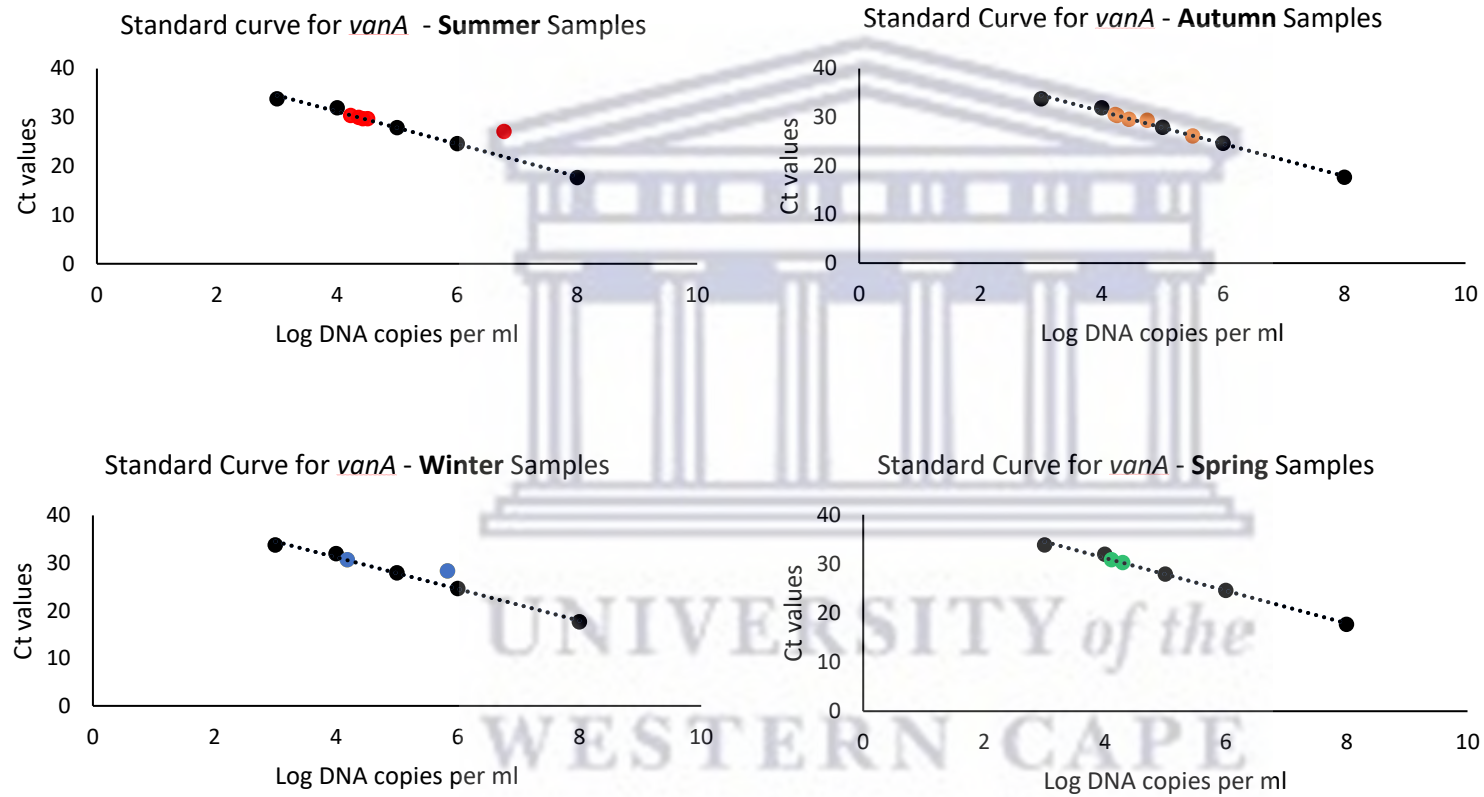


Figure 3.27: A graphical representation of the greywater sample collection seasons and the *vanA* gene absolute abundance using qPCR.

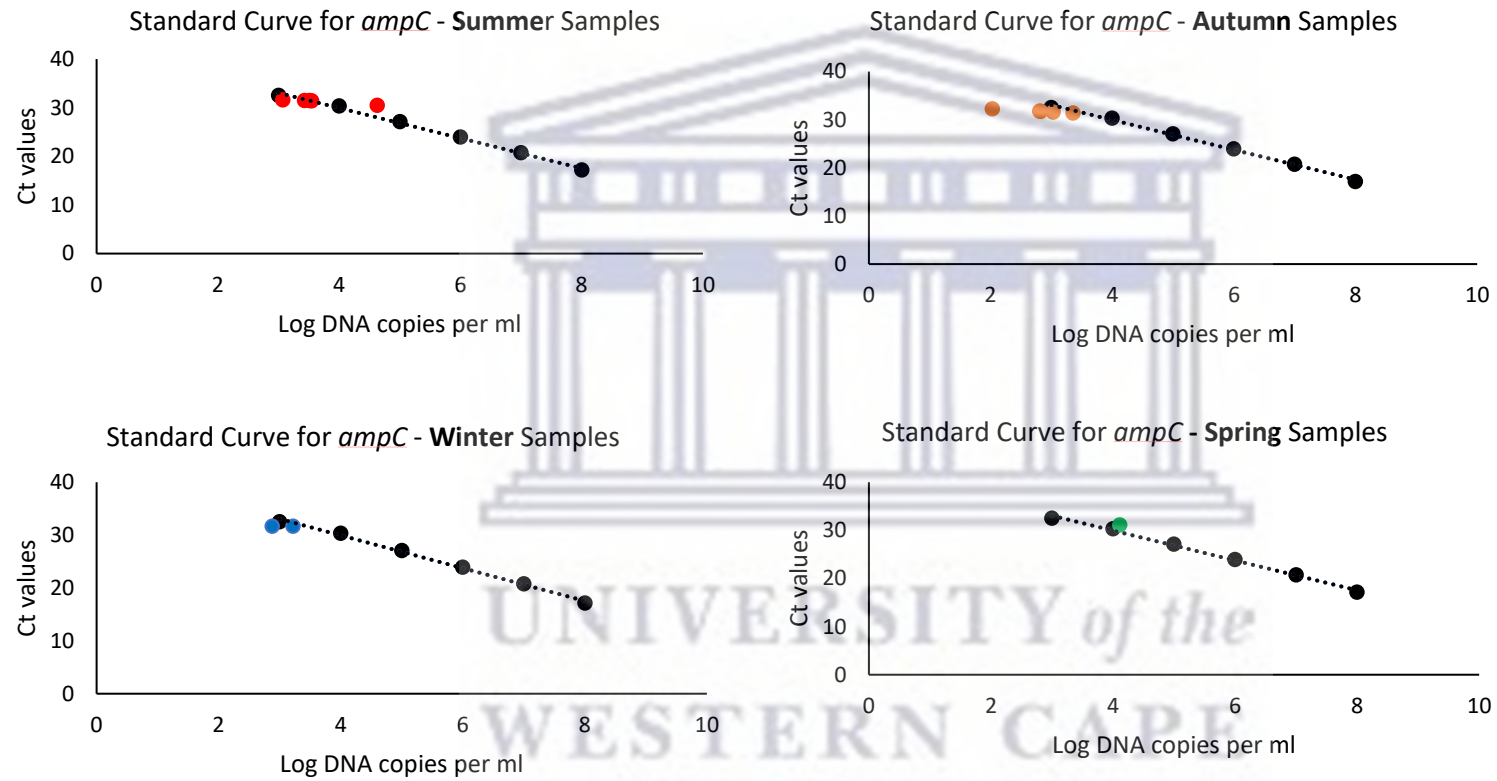


Figure 3.28: A graphical representation of the greywater sample collection seasons and the *ampC* gene absolute abundance using qPCR.

3.4 Conclusion of Chapter

This research study aimed to identify and enumerate the presence of ARGs in domestic greywater using qPCR. Based on quantitative analysis, it can be concluded the two clinically relevant ARGs, *vanA* and *ampC*, were detected in the greywater samples. Furthermore, the findings support previous data confirming that greywater is highly variable from different households (Leonard *et al.*,2016). This highlights the effectiveness of the research methodology proposed to detect and quantify ARGs in domestic greywater.

The primary aim of the study was to utilize qPCR to detect and quantify ARGs, which required intact high quality total RNA. Therefore, the use of an effective and reproducible RNA extraction method was important. It is proposed that we have found and optimized the Hot Acid Phenol SDS method by Ares *et al.*, (2018) to extract total RNA successfully and effectively from greywater samples for downstream applications. The methodology utilized acidified phenol which is cost-effective and malleable with regards to sample size compared to commercial kits available for RNA extractions from environmental samples.

A major limitation associated with the study of greywater using RT-PCR was the need for high-quality RNA, which required sufficient cell mass. Unfortunately, due to low cell mass we were unable to monitor the presence of ARGs within biofilm samples retrieved from the collection tanks. This hindered the ability to identify the relationship between ARGs and ARBs present in greywater and their associated biofilms. Additionally, there was limited information regarding the physiological parameters of the greywater collection tanks collected. Finally, our study had a small sample size within one area as it served as a pilot study to identify the effectiveness of the methodology proposed for ARGs monitoring of greywater. Therefore, the results presented only represent a fraction of a community using and storing greywater. Thus, future work may include the monitoring of a larger area with different socio and economic backgrounds to identify the influence of occupant health and environmental health on greywater. Furthermore, it is proposed that future work incorporate the use of next generation sequencing to identify the microbial community structure present within greywater and biofilm samples. Our study highlights that greywater collection storage and reuse is a reservoir of ARGs and furthermore encourages the proliferation of ARBs. The need for effective wastewater management guidelines especially for greywater use for food irrigation at a domestic level is vital to minimize the health risks associated with ARGs.

Chapter 4: Detection and Quantification of Class 1 Integrons as Markers of Horizontal Gene Transfer in Domestic Greywater Systems

4.1.1 Introduction

The prevalence and proliferation of ARGs have become a global public health challenge, ultimately threatening human and animal health, as well as food and environmental safety (Zheng *et al.*, 2020). HGT is the transfer of genetic material between bacteria of the same generation (Domingues *et al.*, 2012) which strategically plays an important role in evolution and remains one of the crucial reasons for the current bacterial antibiotic resistance crisis (Zheng *et al.*, 2020). As stated by Aminov (2011), HGT-mediated rapid evolution is especially noticeable among bacteria, which demonstrates adaptability in the face of environmental challenges. These challenges include the excessive use of antibiotics, industrial contamination, intensive agriculture, and the discharge of waste into waterways, which can all potentially change the indigenous microbial communities by exposing the bacteria to sub-lethal doses of antimicrobial/toxic compounds (Aminov, 2011; Paiva *et al.*, 2015).

Aquatic environments are known to harbour different antibiotic-resistance-associated mobile genes (Paiva *et al.*, 2015). The HGT-facilitated movement of genetic information has been implicated in the emergence of new bacterial phenotypes, especially in response to strong selective pressure, as seen in the rapid emergence of multi-drug resistant bacterial pathogens.

Mobile Genetic Elements, also referred to as MGEs are widely dispersed in bacterial communities. These elements include plasmids, bacteriophages, integrative and conjugative elements (ICEs), genome islands (GIs), transposons (Tns), insertion sequences and integrons (Domingues *et al.*, 2012). Integrons are bacterial genetic elements that can capture and express exogenous genetic material such as gene cassettes (Hall and Collins, 1995). These gene cassettes often carry genes which provide microorganisms with an adaptive advantage (Recchia and Hall, 1995). Integrons are extremely diverse and are classified into hundreds of classes, which together with their broad taxonomic distribution, suggests that they are ancient elements. Classes 1, 2 and 3 are well-studied and implicated in the dissemination of antibiotic resistance (Ploy *et al.*, 2000). Class 1 integrons specifically are known to confer resistance to a broad range of antibiotic classes, as well as biocides and heavy metals. Therefore, as stated by Lucassen *et al.* (2019), the relative prevalence of class 1 integrons can be seen as a proxy for antimicrobial resistance and anthropogenic pollution.

4.1.2 Horizontal Gene Transfer and Antibiotic Resistance

Bacteria can acquire novel DNA through HGT, a remarkable process that enables a microorganism to rapidly adapt to changing environmental conditions, thereby providing a competitive edge for survival (Brito, 2021). The acquisition of new genetic material via HGT allows for microbes to sample and share genetic material, which may encode traits which are specifically useful in their environments (Lerminiaux and Cameron, 2018). For instance, when bacterial organisms are faced with selective pressures such as the presence of antimicrobials, the horizontal acquisition of ARGs allows for the diversification of the genome, as well as creates a potential for increased fitness (Lerminiaux and Cameron, 2018; Brito, 2021). HGT has thereby been identified as a contributor to infections and outbreaks, as well as being linked to the adaptive ability of some microorganisms to form biofilms (Hiller *et al.*, 2010).

There are three primary mechanisms of HGT within prokaryotic organisms: transformation, transduction, and conjugation (Lerminiaux and Cameron, 2018; Lopez *et al.*, 2019), as shown in Figure 4.1 below.

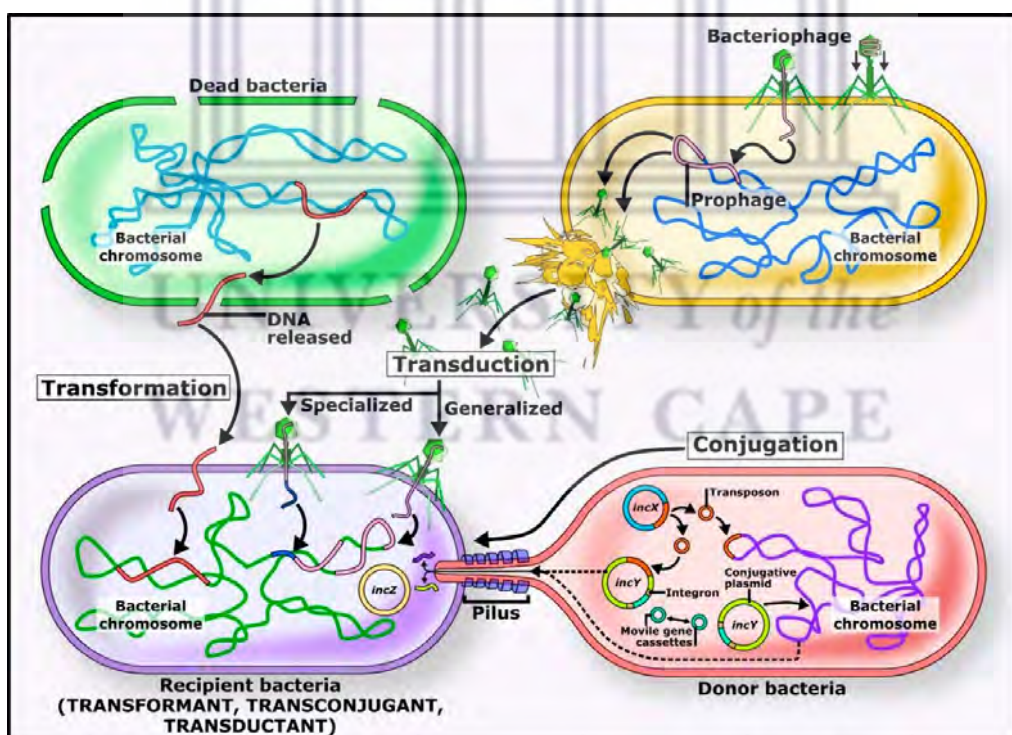


Figure 4.1: Diagram showing the main mechanisms involved in Horizontal Gene transfer. Transformation, transduction, and conjugation are mechanisms by which bacterial species can mobilize and share genetic material via mobile gene elements, between related and non-related species adapted from (Adapted from Lopez *et al.*, 2019).

4.1.2.1 Transformation

Genetic alteration in a cell due to bacterial transformation is a result of the direct absorption, incorporation, and expression of exogenous DNA between closely related bacteria, which is mediated chromosomally by proteins (Lopez *et al.*, 2019). The naked DNA is taken up by a competent cell in the environment (Brito, 2021). The competent state is often due to lack of nutrients or an elevated cell density. For bacterial transformation to be successful the exogenous DNA must be transferred from the surface of the cell to the cytoplasmic membrane, and then cross the cytoplasmic membrane through a highly conserved membrane channel (Lopez *et al.*, 2019). Antibiotics are known to increase transformation rates in laboratory settings, thereby suggesting the presence of antibiotics in the environment may facilitate HGT and the dissemination of resistant genes (Lopez *et al.*, 2019). There have been several clinically relevant antibiotic resistant pathogens reported that are capable of DNA uptake and natural transformation. These include *Acinetobacter*, *Neisseria*, *Haemophilus*, *Pseudomonas*, *Staphylococcus* and *Streptococcus* species. The genera *Escherichia*, *Klebsiella* and *Enterobacteriaceae* have also been predicted to be naturally competent, this is of particular concern as these genera are the leading causes of community-acquired and hospital-acquired antibiotic resistant infections, thereby raising the possibility that natural transformation directly contributes to the spread of ARGs in pathogenic organisms (Lerminiaux and Cameron, 2018).

4.1.2.2 Transduction

Transduction occurs when genetic material is introduced from a bacteriophage into bacterial genomes (Brito, 2021). Bacteriophages are bacterial viruses that can package segments of DNA into their capsid and inject it into a new host when environmental conditions trigger cell lysis (Lopez *et al.*, 2019). Transduction is completed when the bacterial DNA is recombined into the genome of the recipient cell. Transduction is identified as a potential contributor to the spread of ARGs, especially amongst members of the same species (Lerminiaux and Cameron, 2018). Phage particles are ideal for mediating DNA transfer due to their broad host ranges, resistance to environmental degradation as well as their compact size (Berglund, 2015). Transduction has been identified to be common in aquatic environments, such as the identification of the *mecA* gene (which is associated with methicillin resistant *S. aureus* (MRSA)), in bacteriophage DNA from wastewater treatment plants (WWTP) (Berglund, 2015). As stated by Lerminiaux and Cameron (2018), transduction has been a significant contributor to the emergence and persistence of AR in the clinical setting such as the transduction of multiple ARGs in Gram-negative bacteria. For example, the spread of ESBL genes from *Pseudomonas* hospital isolates to other *Pseudomonas* strains, as well as β -lactamase genes which have been transduced between *Acinetobacter* strains. Based on findings, it has been identified that both

chromosomal and plasmid borne ARGs can be transferred via transduction, with the presence of antibiotics likely increasing the rate of transfer (Berglund, 2015).

4.1.2.3 Conjugation

Bacterial conjugation relies on physical contact between the donor and recipient cells. During conjugation DNA transfer is conducted through a conjugative pili (Brito, 2021). Conjugation has been recognized as the main facilitator for the transfer of ARGs between bacteria. Conjugation has been identified in many different environments including soil, seawater, marine sediment, activated sludge and sewage wastewater (Berglund, 2015). Conjugative plasmids have become one of the most studied mobile genetic elements (Lopez *et al.*, 2019). Plasmids are defined as extrachromosomal genetic elements that can replicate independently of chromosomes. Their persistence has been known to improve when they carry genes, such as ARGs, that are particularly useful to the host cell (Lerminiaux and Cameron, 2018). For example, β -lactamase resistance genes located on plasmids have been known to disseminate via inter and intra-species conjugation in *Pseudomonas*, *Enterobacteriaceae* and *Acinetobacter* (Weingarten *et al.*, 2018; Lerminiaux and Cameron, 2018).

4.1.3 Integrons

Integrons are intricate genetic assembly platforms able to capture, integrate and express gene cassettes with minimal disturbance to the existing microbial genome (Domingues *et al.*, 2012). These multi-component systems are thus capable of natural cloning and expression, thereby effectively promoting the dissemination of antibiotic resistance genes within the bacterial world (Ploy *et al.*, 2000).

Integrons are composed of three key elements: (1) a gene encoding a site-specific integron- integrase (*intI1*), which is a member of the tyrosine recombinase family and is responsible for catalysing recombination between the incoming gene cassette and (2) the associated recombination site known as the *attI* which serves as the second key element. Once the gene cassette is recombined it is expressed by a third key element known as (3) an integron-associated promoter (P_c), which drives transcription and the expression of genes located in the cassettes inserted at *attI* (Mazel, 2004; Gillings, 2014). Integrons are incapable of self-transposition and are therefore often found to be associated with transposons and conjugative plasmids which ultimately serve as vehicles for their transmission (Ploy *et al.*, 2000). Integrons can incorporate one or more gene cassettes. It has been noted that generally in clinical settings integrons carry less than five gene cassettes, however other studies indicate that integrons with up to nine antibiotic resistance genes have been identified (Domingues *et al.*, 2012). Gene cassettes are simple structures, that generally consists of a single open reading frame (ORF) bounded by a cassette associated recombination site known as the *attC* (Gillings,

2014). The circular cassettes are integrated via site-specific recombination between the *attI* and *attC* recombination sites, which is mediated by the integron-integrase enzyme. The process is a reversible one, and gene cassettes may be excised as free circular DNA elements (Gillings, 2014) as shown in Figure 4.2.

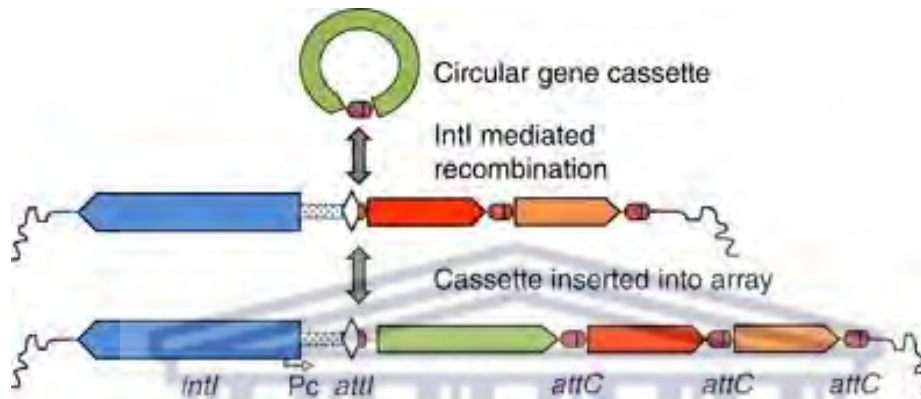


Figure 4.2: Schematic diagram of the basic Integron structure and function. Integrons consist of an integron-integrase gene (*intI*) which catalyses recombination between the *attI* recombination site and the *attC* recombination site of a circular gene cassette. Resulting in the sequential insertion of multiple gene cassettes which may form an array of hundreds of different genes. Inserted genes are expressed by an Integron-encoded promoter. Adapted from (Gillings *et al.*, 2014).

4.1.3.1 Classes of Integrons

The structure of an integron is generally defined by the presence of an integrase gene, however the amino acid sequence of the *intI* integrases has been used as the basis for dividing integrons into classes. There are four general classes of integrons termed class 1 to 4 integrons. Classes 1-3 are known as multi-resistant integrons, capable of acquiring the same-gene cassettes through their similar recombination platforms (Jones-Dias *et al.*, 2016). These classes are also of clinical relevance based on their on-going association with the accumulation of ARGs.

In terms of differentiation, class 2 and 3 are distinguished from class 1 by their divergent integron-integrase sequences (Malek *et al.*, 2015). Additionally, class 1 integrons are directly linked to Tn402-like transposons and often associated with Tn3 transposon family (Tn21 or Tn1696). These associated transposons serve as vehicles for the transmission of genetic material (Deng *et al.*, 2015). Whereas class 2 integrons are associated with transposon-7 (Tn7) (Jones-Dias *et al.*, 2016). Class 1 integrons also possess a 3'-conserved segment (3'-CS), which possesses the genes *qacEA1* and *sul1* downstream of the gene cassettes. These genes encode resistance to quaternary ammonium salts and sulfonamide, respectively (Deng *et al.*, 2015).

4.1.4 *Int11* as a marker for Horizontal Gene Transfer

Class 1 integrons were the first type of integrons to be described and remain the most intensely studied group to date (Hardwick *et al.*, 2008). According to Malek *et al.* (2015), class 1 integrons have been identified as the primary source of antimicrobial resistance genes and are suspected to serve as reservoirs and exchange platforms of resistant genes in a variety of Gram-negative bacteria.

Several studies have investigated the abundance of *int11* genes in non-clinical environments such as rivers (Luo *et al.*, 2010), coastal waters (Koenig *et al.*, 2008), wastewater plants, aquatic biofilms (Gillings *et al.*, 2009) and even Antarctic soils (Ghaly *et al.*, 2020). Hardwick and co-workers screened for the presence of *int11* gene in creek sediments and the levels of the gene were found to correlate with the prevailing ecological conditions, implying that the integron provides selective advantages relevant to environmental pressures other than the use of antibiotics (Hardwick *et al.*, 2008). Early studies only looked at the presence of the integrons in culturable bacteria, and as such were only able to detect a fraction of the genes present in any environment. Later studies used molecular biology techniques, mainly PCR-based such as terminal restriction fragment length polymorphism analysis (T-RFLP) or qPCR, which have much greater sensitivity. Using these culture-independent methods researchers were able to detect significantly more integrons in environmental samples. A recent study investigated the diversity of integrons (both mobile and sedentary) in soil using NGS and detected between 4,000 and 18,000 unique cassettes per 0.3 grams of soil (Ghaly *et al.*, 2020). This finding would imply that previous culture-based studies likely under-estimated the abundance of integrons in the environment.

Lucassen *et al.* (2019), stated that the prevalence of the class 1 integron-integrase gene (*int11*) per 16S rRNA gene copy could be used as a proxy for anthropogenic impact and has already been used as a marker for antimicrobial resistance gene dissemination. Studies have shown there is a strong association between the presences of integrons and multiple antibiotic resistance (MAR) phenotypes in bacteria (Leverstein-van-Hall *et al.* 2002). Integrons carrying four to five ARGs have been found in agricultural wastewater (Jacobs and Chenia 2007), urban wastewaters (Da Silva *et al.* 2007), and most concerning, water not recently exposed to antibiotics (Park *et al.* 2003). As integrons allow bacteria to adapt and evolve rapidly their potential to spread ARGs in the natural environment is of increasing concern.

However, whether the *int11* gene can be used a potential marker for horizontal gene transfer in greywater systems and furthermore as a potential indicator of ARGs remains unknown. Therefore, this chapter investigates the use of the *int11* gene as a marker of horizontal gene transfer in domestic greywater using qPCR.

4.2 Materials and Methods

4.2.1 Metagenomic DNA Extraction from Greywater Samples

4.2.1.2 Phosphate, SDS, and Chloroform Bead-Beater Method

DNA was extracted from greywater samples using a modified version of Miller *et al.* (1999). Bead-beater vials were made using 15 ml Greiner tubes filled with 0.5 g of 0.5 mm and 0.3 mm silica-zirconium beads, respectively. An aliquot of greywater (500 µl) was mixed with 300 µl of phosphate buffer and centrifuged. After centrifugation, 800 µl of the resuspension and 300 µl of SDS lysis buffer was added to the bead-beater vials and vortexed to thoroughly mix the sample. Then 300 µl of chloroform:*iso*-amyl alcohol (24:1; v/v) was added to the sample and vortexed at maximum speed for 2 minutes. To pellet the cellular debris the samples were centrifuged in a microfuge at 15 000 *xg* for 5 minutes. The supernatant (~650 µl) was transferred to a new tube and 7M NH₄OAc was added to a final concentration of 2.5M. The samples were shaken by hand, and then centrifuged at 13000 rpm for 5 minutes. The clear supernatant (~580 µl) was transferred to a clean tube followed by the addition of 315 µl of cold isopropanol. Samples were incubated at room temperature (~22±2 °C) for 5 minutes. The supernatant was carefully removed, and the pellet was washed with 1 ml of 70% ethanol. The samples were centrifuged at 12 000 *xg* for 5 minutes. The supernatant was removed, and the pellet was allowed to dry for 15 to 45 minutes. The resulting DNA pellet was resuspended in 100 µl of sterile water or 1M Tris buffer (pH 7.0) and stored at -20 °C for short term storage.

4.2.1.2 DNEasy PowerSoil® DNA Isolation kit

DNA was also extracted using the DNEasy PowerSoil® DNA Isolation kit (MoBio Laboratories, Carlsbad) according to the manufacturer's instructions. DNA was extracted by adding 250 µl of the centrifuged greywater sample (as per sample processing in Chapter 3, Section 3.2.1) to the DNEasy PowerBead Tube.

4.2.2 Metagenomic DNA Extraction from Biofilm Samples

Sample processing of biofilm samples was conducted by submerging the buccal swab in 250 µl of 1X Phosphate Buffer Saline (PBS) and vortexed for 5 minutes at maximum speed to dislodge bacteria present. Cells were harvested by centrifugation at 13 500 rpm for 10 minutes and the pellet was resuspended in 500 µl of 1X TE (10mM Tris-HCl; 1mM EDTA-Na₂, pH 8.0), of which 250 µl of the resulting suspension was then used. DNA was extracted using the DNEasy PowerSoil® DNA Isolation kit (MoBio Laboratories, Carlsbad) according to the manufacturer's instructions.

The concentration of each metagenomic DNA sample was determined by assessing 2 µl of DNA using the Qubit HS dsDNA Assay kit (Thermo Fisher Scientific) as per manufacturer's instructions, and diluted appropriately in sterile, filtered distilled water.

4.2.3 16S rRNA gene Polymerase Chain Reaction

PCR was carried out in 25 µl reaction volumes. Each reaction contained 0.5U KAPA 2G Robust DNA Polymerase, 0.2mM dNTP mix, 1X KAPA Enhancer and 1X KAPA 2G Buffer B, 0.5µM forward primer (F1), 0.5µM reverse primer (R5) and made to a final volume using PCR-grade water and approximately 1 ng of DNA. The PCR primers and amplification conditions are provided in Table 4.1. PCR amplicons were electrophoresed on 1% w/v agarose gels. All gels contained 10 µg/ml ethidium bromide and were electrophoresed in 1X TAE buffer at 90 V for 1 hour.

Table 4.1: 16S rRNA PCR Primer Set and PCR Cycling Conditions for bacterial identification

Primer	Sequence (5'-3')	Amplification conditions
Forward (F1)	AGAGTTTGATCITGGTCAG	95 °C for 3 minutes
Reverse (R5)	GTATTACCGCGGCTGCTGGCAC	30 cycles at 95 °C for 15 seconds,
		56 °C for 15 seconds
		72 °C for 15 seconds
		1 minute at 72 °C

4.2.4 PCR Optimization of Target Genes

Conventional PCR was conducted to identify the optimal conditions for the qPCR primers (Table 4.2). PCR optimization entailed identifying the optimal annealing temperature using gradient PCR, as well as the optimal primer concentrations and genomic DNA for amplification.

Table 4.2. Primer sets used in for integron RT-PCR

Gene	Gene Description	Purpose	Primers	Size (bp)	Reference
<i>IntI1</i>	<i>Class 1 Integrase</i> Involved in DNA Integration and DNA Recombination	Target Gene	qINT_3_MK qINT_4_MK	109	Paiva <i>et al.</i> , 2015
16S rRNA	16S ribosomal RNA	Reference/ Housekeeping Gene	16S_MK01F 16S_MK01R	194	Pärnänen <i>et al.</i> , 2019

Primers were tested against the following test strains: *E. coli* NCTC 13846, *E. cloacae* subsp. *cloacae* ATCC BAA-1143, *Klebsiella pneumoniae* subsp. *pneumoniae* ATCC 700603, *S. aureus* ATCC 29212 and *Streptomyces polyantibioticus* strain SPR^T. All bacterial strains, except for the *S. polyantibioticus*, were cultured in LB at 37 °C, and the genomic DNA was extracted using the ammonium acetate method. *S. polyantibioticus* genomic DNA was kindly donated by Prof Marilize Le Roes-Hill (CPUT).

The above real-time PCR primer sets were first optimised using conventional PCR. Each reaction contained 0.5U DreamTaq Polymerase (Thermo Scientific), 0.2mM dNTP mix, 1X DreamTaq Buffer, 0.5µM forward and reverse primer, and adjusted to a final volume of 25 µl using PCR-grade water. Primers were tested using 10, 50 and 100 ng genomic DNA. The amplification conditions are provided in the Table 4.3 below. PCR amplicons were electrophoresed on 2% agarose gels. All gels contained 10 µg/ml ethidium bromide and were electrophoresed in 1X TAE buffer at 90 V for 1 hour.

Table 4.3: PCR Cycling conditions used for the *int11* and 16S RNA gene primers.

Gene	Primer	Sequence (5'-3')	Amplification conditions
<i>int11</i>	Forward (qINT3)	TGCCGTGATCGAAATCCAGATCCT	95 °C for 3 minutes 40 cycles at 95 °C for 1 minute, 60 °C for 45 seconds,
	Reverse (qINT4)	TTTCTGGAAGGCGAGCATCGTTTG	72 °C for 1 minute 5 minutes at 72 °C
16S rRNA	Forward (16S_MK01F)	CCTACGGGAGGCAGCAG	95 °C for 3 minutes 40 cycles at 95 °C for 30 seconds,
	Reverse (16S_MK01R)	ATTACCGCGGCTGCTGGC	59 °C for 30 seconds, 72 °C for 1 minute 5 minutes at 72 °C

4.2.5 Construction of plasmid controls for Real-Time PCR

Separate plasmids containing the *int11* gene and 16S rRNA PCR products respectively, were constructed for use as a control for the qPCR assay. Conventional PCR was used to amplify the *int11* gene from *K. pneumoniae* subsp. *pneumoniae* ATCC 700603 DNA and the 16S rRNA from *Enterobacter cloacae* subsp. *cloacae* ATCC BAA-1143, several reactions were set up per primer set.

The amplicons for each primer set were pooled and purified using the NucleoSpin Gel and PCR Clean Up kit (Macherey- Nagel) according to the manufacturer's instructions, eluting in 30 µl of elution buffer. The PCR products were cloned into the pJET1.2 Cloning vector using the ThermoScientific Clone-Jet PCR Cloning kit according to the manufacturer's instructions. The recombinant vectors were transformed into electro-competent *E. coli* DH5α cells via electroporation and 50 µl of the transformed cells were spread onto LB plates containing 100 µg/ml ampicillin. Transformed colonies were picked and colony PCR was conducted to confirm positive transformants. Plasmid DNA was extracted from confirmed positive clones using the Qiaprep Spin Miniprep kit according to the manufacturer's instructions. Plasmid DNA was quantified using the Qubit HS DNA assay and quality was assessed by conducting gel electrophoresis and gene-specific PCR for *int11* and 16S rRNA genes to confirm the presence of the insert. The plasmids were designated *pJET_Int11* and *pJET_16S* respectively.

4.2.6 Real-Time PCR

4.2.6.1 Construction of Standard Curves

The plasmids controls were used to construct a standard curve to evaluate RT-PCR efficiency. Plasmid DNA was quantified using the Qubit HS DNA Assay (Invitrogen) and the number of molecules per μl was determined using Equation 2. A dilution series was prepared over the range of 10^8 to 10^3 for the *int1* gene primers, and 10^9 to 10^4 for the 16S rRNA primers using TE buffer (the dilution range was adapted from Hardwick *et al.*, 2008).

$$\text{Number of copies} = \frac{\text{Amount (ng)} \times 6.022 \times 10^{23}}{\text{Length (bp)} \times 1 \times 10^9 \times \text{Mass of DNA bp}}$$

Equation 2: Formula used to calculate the number of copies

4.2.6.2 Absolute Quantification of the *int1* gene and 16S rRNA reference gene

Real-Time PCR was performed using the Roche LightCycler 480 II (Roche Applied Sciences). The reactions were setup in white 96-well PCR plates (Roche Applied Sciences). All reactions were conducted using the Roche LightCycler 480 SYBR Green 1 Master as per the manufacturer's instructions.

For the quantification of the 16S rRNA gene (serving as the reference gene), each reaction contained 2X SYBR Master Mix, $0.5\mu\text{M}$ of each primer and adjusted to a final volume of $7.5\mu\text{l}$ using Molecular Grade water. $2.5\mu\text{l}$ of template DNA was added for each reaction; for the standard curve the input DNA was the control plasmid pJET_16SrRNA and for the environmental samples ~ 1 ng of metagenomic DNA. qPCR cycling conditions were as follows: initial activation step at 95°C for 2 mins, followed by 45 cycles of denaturation at 95°C for 10 seconds and a combined 15 seconds annealing/extension at 59°C for 16S rRNA gene primers. Melt curve analysis was performed from 58 to 97°C . Quantification was performed using the LC480 software and Excel.

For the quantification of the *int1* gene (serving as the target gene), each reaction contained 2X SYBR Master Mix, $0.7\mu\text{M}$ of each primer and adjusted to a final volume of $7.5\mu\text{l}$ using Molecular Grade water. $2.5\mu\text{l}$ of template DNA was added for each reaction. For the standard curve the input DNA was the control plasmid pJET_int1 and for the environmental samples ~ 1 ng of metagenomic DNA was added. qPCR cycling conditions were as follows: initial activation step at 95°C for 2 mins, followed by 45 cycles of denaturation at 95°C for 10 seconds and a combined annealing/extension for 15 seconds

at 60 °C for *int11* gene primers. Melt curve analysis was performed from 59 to 97 °C. Quantification was performed using the LC480 software and Excel.

All reactions were performed in triplicate for each sample, including the no template control (NTC), and each experiment was performed twice resulting in six quantifications of each target for each DNA extraction. Duplicates of each experiment was conducted to identify any intra- or inter run variation. The average of the two triplicate groups were used for quantitative analysis.

The gene quantities of both the *int11* and 16S rRNA genes for each environmental sample was calculated according to Hardwick *et al.* (2008). The *int11* gene quantities were normalized to the 16S ribosomal RNA gene copy number and the relative abundance values were expressed as percentages and calculated according to the following equation:

Equation 3:

$$\text{Relative Abundance (\%)} = (\text{copy number of Int11} / \text{copy number of 16S rRNA}) \times 4 \times 100$$

With four being the average number of copies of the gene encoding 16S rRNA per bacterial cell, in accordance with the ribosomal RNA database (Stalder *et al.*, 2012; Koczura *et al.*, 2014).

4.2.6.3 Statistical Analysis

Greywater and biofilm samples over 22 time points were categorized into summer, autumn, winter and spring based on the climate of the Western Cape region, South Africa.

A non-parametric Kruskal-Wallis test was applied to determine the significance of variation in abundance of the *int11* gene between collection sites and seasons, respectively. Analysis was conducted using Microsoft Excel template.

4.3 Results & Discussion

4.3.1 Comparison of Metagenomic DNA Extraction methods

The successful extraction of nucleic acids, such as DNA and RNA, from complex environmental samples allows for unparalleled insight into microbial community compositions (Simister *et al.*, 2011). The efficient extraction of high-quality, unbiased DNA from environmental samples which harbour diverse species remains a key challenge for downstream applications such as qPCR and Next generation sequencing (Bag *et al.*, 2016).

Extraction methods aim to lyse the entire microbial population within a sample, after which the nucleic acids of the lysed cells are recovered and purified for use in downstream molecular assays (Lever *et al.*, 2015). DNA extraction protocols generally address three key objectives: (1) the effective lysis of cells and extraction of intracellular nucleic acids into an aqueous solution, (2) the sufficient removal of non-nucleic acid organic and inorganic matter from the resulting extract and finally (3) the minimization of nucleic acid yield loss throughout the entire extraction process (Lever *et al.*, 2015). Previous findings have reiterated the importance of sample capture, storage, and DNA extraction methods, which ultimately influence the final detection and yield of the DNA extracted (Hinlo *et al.*, 2017).

In this study, two DNA extraction methods were evaluated to identify the most effective method to extract metagenomic DNA from greywater samples and their associated biofilm samples. A 'conventional' extraction method which made use of self-made solutions and mechanical lysis apparatus was compared to that of a commercial kit.

For optimisation, the Phosphate, SDS, Chloroform and Bead-Beater Method (PSC-B Method) by Miller *et al.* (1999), was conducted on the preliminary samples of greywater and biofilms collected from site 1 and 2. The samples were labelled GW1, GW2, BF1 and BF2, respectively.

Table 4.4: Nanodrop results for Metagenomic DNA extracted using the PSC-B Method

Sample	Concentration (ng/ul)	A260/280
BF1	0.2	0.12
BF2	0.5	0.5
GW1	2.8	1.18
GW2	1.4	2.11

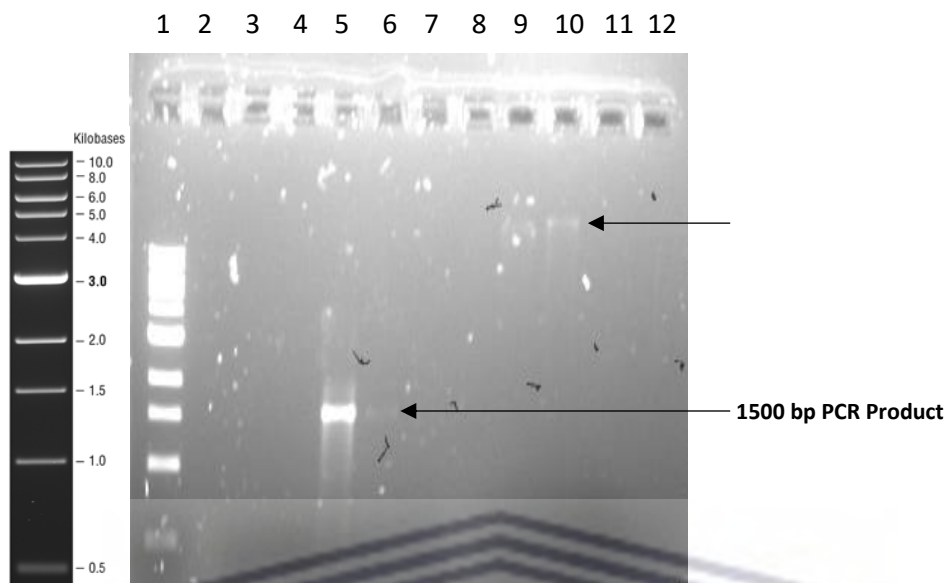


Figure 4.3: A 1% TAE agarose gel depicting the extraction of metagenomic DNA using the Phosphate, SDS, Chloroform and Bead-beater Method and the corresponding 16S rRNA gene PCR of the metagenomic DNA samples. Lane 1: 1 Kb NEB ladder; Lane 3: PCR product of the negative control (Tap water sample from Greywater Site 1); Lane 4: PCR product of Greywater Sample 1; Lane 5: PCR product of Greywater Sample 2; Lane 6: PCR product of Biofilm Sample 1; Lane 7: PCR product of Biofilm Sample 2. Lane 8: Blank; Lane 9: mDNA extracted from Greywater Sample 1; Lane 10: mDNA extracted from Greywater Sample 2; Lane 11: mDNA extracted from Biofilm Sample 1 and Lane 12: mDNA extracted from Biofilm Sample 2.

As shown in Figure 4.3, DNA was isolated from the greywater sample collected from site 1, this is indicated by the faint band present at 10.0 kb in lane 10. In terms of DNA extraction and yield, the PSC-B method was unsuccessful in extracting DNA from biofilm samples (Table 4.4). These findings are supported by the absence of a 1500 bp PCR product for the biofilm samples. Biofilms are predominantly composed of extracellular polymeric substances (EPS). As this method includes an initial physical lysis step it was expected that this would be sufficient to break up the EPS and release any bacterial cells within. Environmental biofilms have not been studied to a great extent and as such there is limited information available comparing the efficacy of DNA extraction procedures (Hwang *et al.*, 2012). Compared to many other environmental samples, biofilm samples often have limited biomass which is additional problem for DNA extraction (Hwang *et al.*, 2012). The EPS also contains an abundance of negatively charged complex polysaccharides, which have been shown to affect the isolation of DNA (Lear *et al.*, 2010). In addition, the presence of organic matter found in greywater systems may interfere with the extraction of DNA from biofilms resulting in the inhibition of downstream molecular applications, such as PCR and qPCR (Hill *et al.*, 2015; Hwang *et al.*, 2012).

The A260/A280 ratio for the greywater and biofilm samples ranged from 0.5 – 1.51, as seen in Table 4.4 indicating the presence of contaminants. The DNA concentrations were also very low indicating

that the PSC-B method was unsuccessful. While it is likely that the samples did have very low biomass, it does also appear that the physical lysis step may have been ineffective. For the biofilm samples, compounds present in the EPS may have bound to the nucleic acid during the extraction which could have resulted in further DNA loss (Corcoll *et al.*, 2017). In addition, the presence of fine materials on silica-zirconium beads often interferes with isolation procedures and hence need to be removed using an acid wash. Other studies have shown that bead beating techniques are more effective on soil samples as compared to water samples depending on the speed and duration of agitation (Fatima *et al.*, 2014).

All DNA extraction protocols were further tested by performing a 16S rRNA gene PCR. As expected, when the DNA extracted using the PSC-B method was analysed via PCR (Figure 4.3), only one greywater sample (GW2, lane 5) and one biofilm (BF1, lane 6) amplified using the universal 16S rRNA primers as indicated by the 1500 bp band in lane 5. Since the DNA extracted using the PSC-B method was of poor quality it was decided to assess other methods, such as commercial kits.

Many conventional DNA extraction methods are time consuming, the reagents (such as phenol-chloroform-*iso*-amyl alcohol) may be toxic and the methods often do not isolate good quality DNA which is required for downstream processing. The development of commercial kits has allowed for the processing of various sample types and relatively high yields can be achieved in a less time-consuming manner since standardised reagents are provided (Felczykowska *et al.*, 2015; Hinlo *et al.*, 2017). The DNEasy PowerSoil DNA Isolation kit was designed for samples with high humic acid contents, such as compost, manure, and sediments. However, as the kit has been shown to extract good quality DNA from a diverse range of sample types (Santos *et al.*, 2012), it is widely used in metagenomic studies and is in fact the recommended kit for the Human Microbiome Project. The kit makes use of a patented Inhibitor Removal Technology (IRT) and is thus effective at removing a wide range of PCR inhibitors.

For comparison, the DNEasy PowerSoil DNA Isolation kit was assessed on the same greywater and biofilm samples used to evaluate the PSC-B method.

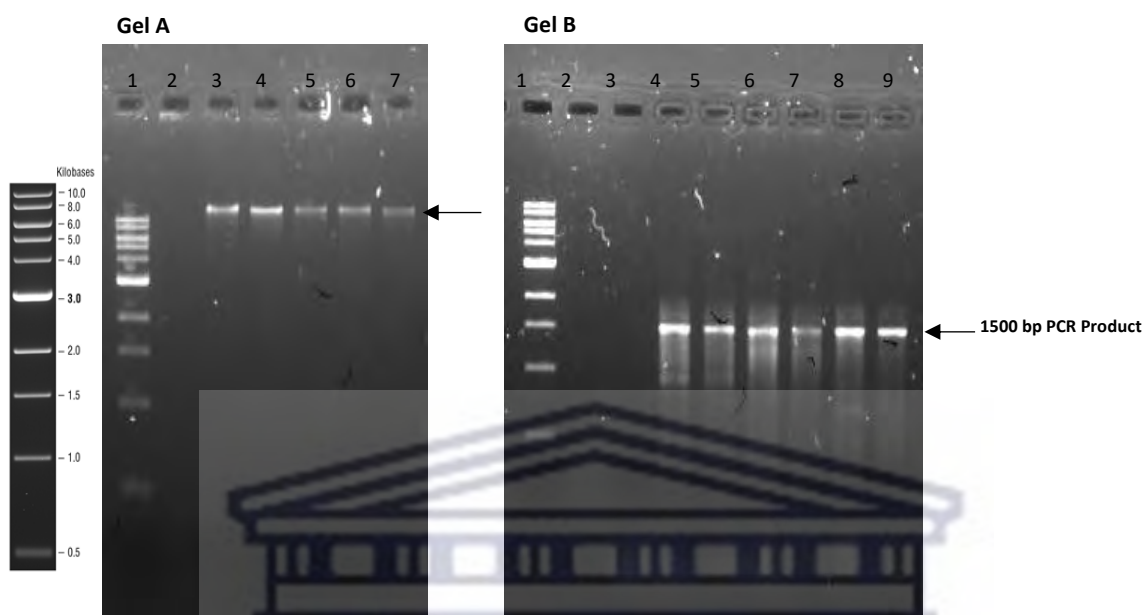


Figure 4.4: 1% TAE agarose gels confirming the quality and integrity of the metagenomic DNA extracted using the DNEasy PowerSoil DNA Isolation Kit (Gel A) and the corresponding 16S rRNA PCR products of the metagenomic DNA samples extracted. Gel A: Lane 1: 1kb NEB ladder; Lane 2: Blank; Lane 3 and 4: mDNA extracted from Greywater Sample 1; Lane 5 and 6: mDNA extracted from Greywater Sample 2; Lane 7: mDNA extracted from Biofilm Sample 1. **Gel B:** Lane 1: 1 kb NEB ladder; Lane 3: Negative control; Lane 4 and 5: PCR products for Greywater Sample 1; Lane 6 and 7: PCR products for Greywater Sample 2; Lane 8: PCR product for Biofilm Sample 1; Lane 9: PCR positive control (genomic DNA from *S. aureus*).

Table 4.5: Nanodrop results for Metagenomic DNA extracted using the PSC-B Method

Sample	Concentration (ng/ul)	A260/280	A260/A230
Greywater Sample 1A	14.5	1.69	0.75
Greywater Sample 1B	11.6	2.10	1.12
Greywater Sample 2A	8.2	2.30	1.39
Greywater Sample 2B	6.9	2.29	0.97
Biofilm Sample 1	5.4	1.97	1.60

As seen in Figure 4.4, metagenomic DNA was successfully extracted using the PowerSoil DNA Isolation Kit and a corresponding 16S rRNA PCR was detected in all metagenomic DNA samples. Greywater samples were pre-processed by centrifugation to sufficiently collect enough cell mass. Based on the A260/A280 ratios many of the samples had pure DNA extracts (Table 4.5) however, the DNA concentration of the biofilm samples was lower compared to that of the greywater samples. The A260/A230 ratio was below 2.0 indicating the presence of protein contaminants absorbing at 230nm. The smears present on the gel are indicative of PCR artefacts which is common for environmental DNA (eDNA).

Based on the results obtained, it was decided that the DNEasy PowerSoil DNA isolation kit would be used for the extraction on all environmental samples.

4.3.2 Metagenomic DNA Extraction from Greywater and Biofilm Samples

Environmental samples are composed of different microbes present in a diverse ecosystem, which often have different types of cell walls and membranes which tightly enclose and protect their cytoplasmic and genomic contents (Bag *et al.*, 2016). Therefore, the successful extraction of metagenomic DNA (mDNA) prior to high-throughput analysis such as qPCR is particularly vital.

Table 4.6 represents the samples which were screened for the presence of the *int11* gene. In total, mDNA was extracted from 22 greywater samples and 20 biofilm samples. All samples were subjected to a 16S rRNA PCR via conventional PCR for confirmation of bacterial amplification within the samples prior to qPCR analysis.

Table 4.6: Samples collected and analysed for the Int11 qPCR Assay

	Greywater Samples	mDNA	16S rRNA gene amplification	Biofilm Samples	mDNA	16S rRNA gene amplification
Site 1	GWS1S1	✓	✓	BFS1S1	✓	✓
	GWS1S2	✓	✓	BFS1S2	✓	✓
	GWS1S3	✓	✓	BFS1S3	✓	✓
	GWS1S4	✓	✓	BFS1S4	✓	✓
Site 2	GWS2S1	✓	✓	BFS2S1	✓	✓
	GWS2S2	✓	✓			
	GWS2S3	✓	✓	BFS2S3	✓	✓
	GWS2S4	✓	✓	BFS2S4	✓	✓
Site 3	GWS3S1	✓	✓	BFS3S1	✓	✓
	GWS3S2	✓	✓	BFS3S2	✓	✓
	GWS3S3	✓	✓	BFS3S3	✓	✓
	GWS3S4	✓	✓			
	GWS3S5	✓	✓	BFS3S5	✓	✓
	GWS3S6	✓	✓	BFS3S6	✓	✓
	GWS3S7	✓	✓	BFS3S7	✓	✓
Site 4	GWS4S1	✓	✓	BFS4S1	✓	✓
	GWS4S2	✓	✓	BFS4S2	✓	✓
	GWS4S3	✓	✓	BFS4S3	✓	✓
	GWS4S4	✓	✓	BFS4S4	✓	✓
	GWS4S5	✓	✓	BFS4S5	✓	✓
	GWS4S6	✓	✓	BFS4S6	✓	✓
	GWS4S7	✓	✓	BFS4S7	✓	✓

Agarose gels of the mDNA extracted using the DNEasy PowerSoil Pro Kit for some of the greywater and biofilm samples are presented in Figures C1-C3 (Appendix C – Chapter 4). mDNA was successfully extracted from both sample types, although in general less mDNA was extracted from the biofilm

samples. However, this is to be expected as the amount of cell mass used to extract mDNA from these samples was very low (cell mass was collected using 2-3 swabs compared to the greywater samples where ~8 litres of water was processed per sample).

Extracted mDNA samples were assessed initially using the NanoDrop for the assessment of quality, and then from replicates of extractions the final mDNA samples per site and collection were assessed using the Qubit dsDNA HS assay.

Table 4.7: Qubit HS DNA Assay concentrations for Metagenomic DNA samples

	GREYWATER SAMPLES			BIOFILM SAMPLES		
	GW	Extraction Method	Qubit [] ng/μl	BF	Extraction Method	Qubit [] ng/μl
Site 1	GWS1S1	DNEasy PowerSoil kit	0,22	BFS1S1	DNEasy PowerSoil kit	0,487
	GWS1S2	DNEasy PowerSoil kit	1,35	BFS1S2	DNEasy PowerSoil kit	3,36
	GWS1S3	DNEasy PowerSoil kit	0,807	BFS1S3	DNEasy PowerSoil kit	0,439
	GWS1S4	DNEasy PowerSoil kit	5,52	BFS1S4	DNEasy PowerSoil kit	0,08
Site 2	GWS2S1	DNEasy PowerSoil kit	3,78	BFS2S1	DNEasy PowerSoil kit	0,683
	GWS2S2	DNEasy PowerSoil kit	4,37			
	GWS2S3	DNEasy PowerSoil kit	5,14	BFS2S3	DNEasy PowerSoil kit	0,405
	GWS2S4	DNEasy PowerSoil kit	0,533	BFS2S4	DNEasy PowerSoil kit	5,67
Site 3	GWS3S1	DNEasy PowerSoil kit	0,641	BFS3S1	DNEasy PowerSoil kit	0,844
	GWS3S2	DNEasy PowerSoil kit	1,99	BFS3S2	DNEasy PowerSoil kit	0,489
	GWS3S3	DNEasy PowerSoil kit	4,05	BFS3S3	DNEasy PowerSoil kit	0,052
	GWS3S4	DNEasy PowerSoil kit	2,57			
	GWS3S5	DNEasy PowerSoil kit	16,4	BFS3S5	DNEasy PowerSoil kit	0,657
	GWS3S6	DNEasy PowerSoil kit	0,101	BFS3S6	DNEasy PowerSoil kit	0,295
	GWS3S7	DNEasy PowerSoil kit	7,97	BFS3S7	DNEasy PowerSoil kit	3,03
Site 4	GWS4S1	DNEasy PowerSoil kit	9,93	BFS4S1	DNEasy PowerSoil kit	1,17
	GWS4S2	DNEasy PowerSoil kit	4,51	BFS4S2	DNEasy PowerSoil kit	0,647
	GWS4S3	DNEasy PowerSoil kit	1,65	BFS4S3	DNEasy PowerSoil kit	0,21
	GWS4S4	DNEasy PowerSoil kit	1,89	BFS4S4	DNEasy PowerSoil kit	4,81
	GWS4S5	DNEasy PowerSoil kit	0,321	BFS4S5	DNEasy PowerSoil kit	2,64
	GWS4S6	DNEasy PowerSoil kit	3,43	BFS4S6	DNEasy PowerSoil kit	2,94
	GWS4S7	DNEasy PowerSoil kit	13,7	BFS4S7	DNEasy PowerSoil kit	4,20

Table 4.7 represents the concentration of the mDNA samples to be assessed using qPCR. As shown in the table, greywater samples have significantly higher concentrations to that of the biofilm samples. In terms of overall concentration, for greywater samples the concentration readings ranged between 0.22 ng/μl to 16.4 ng/μl, whereas the biofilm samples ranged between 0.08 ng/μl to 5.67 ng/μl. When comparing the mDNA yielded per site it was identified that site 3 and site 4 had significantly higher

concentrations than that of site 1 and site 2 for both greywater and biofilm samples. This may be due to differences in microbial communities present at these sites (which is ultimately linked to very diverse factors including number of occupants per site and their behaviour towards greywater use and storage, and the different input sources).

Before commencing the qPCR assays, all extracted mDNA samples were screened for the 16S rRNA gene. The PCR served as a manner of ensuring the mDNA extracted was sufficiently free of any inhibitors as well as amplifiable before conducting any qPCR assays. (Jenkins *et al.*, 2012). As PCR can be used to analyse metagenomic samples, in a culture-independent manner, it allows for the identification of bacteria which are suppressed by antibiotic treatments, have not survived sampling, viable but non culturable organism, as well as microbes with complex growth requirements (Jenkins *et al.*, 2012). Figure C4 and C5 (Appendix C – Chapter 4) represents the results obtained for the PCR for some of the mDNA extracted from biofilm and greywater samples, respectively. Intense bands were obtained for all the samples, even the biofilm samples even though the DNA concentration was very low for these samples. From these results it was decided that the extracted mDNA was of an acceptable quality for qPCR analysis.

4.3.3 PCR Optimization of Target Genes – *int11* gene and 16S rRNA gene

The use of real-time qPCR on environmental samples requires careful optimization to ensure reliable and reproducible results. As SYBR Green I detects any double-stranded DNA generated during the PCR process, including primer–dimers and nonspecific products, the PCR cycling conditions must be optimised prior to commencing real time experiments. For this reason, considerable time was spent optimising the amplification process. Primers were tested at different annealing temperatures, at a range of primer concentrations, and using genomic DNA from several bacterial test strains.

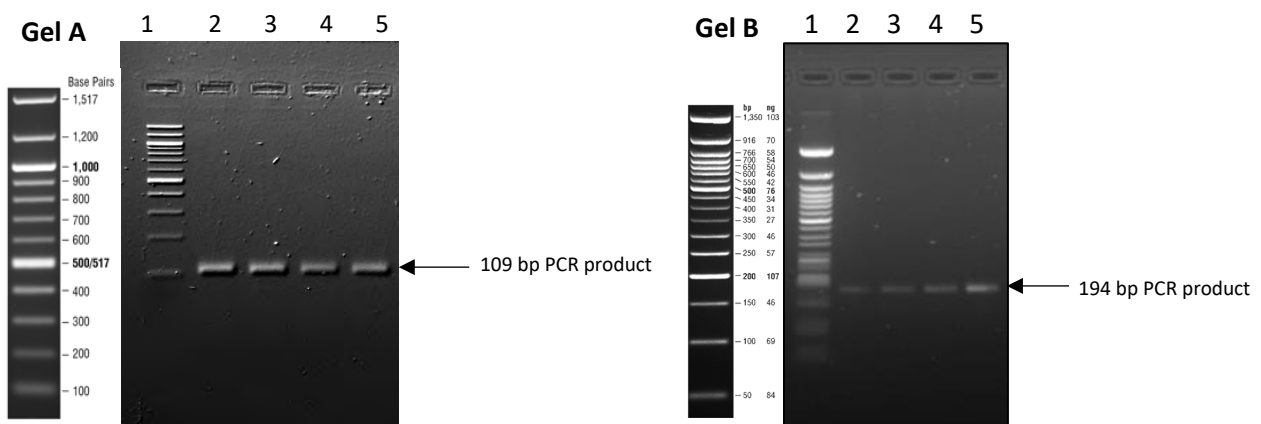


Figure 4.5. A 2% TAE gel depicting the amplicons from the optimised *int11* and 16S rRNA gene PCR, respectively.

Gel A: *int11* PCR using *K. pneumoniae* genomic DNA. Lane 1: 100 bp NEB Marker; Lane 2- 5: *int11* PCR products of 109 bp. **Gel B:** 16S rRNA gene PCR using *E. cloacae* subsp. *cloacae* ATCC BAA-1143 genomic DNA. Lane 1: 50 bp NEB Marker, Lane 2 – 5: 16S rRNA PCR products of 194 bp.

Relatively good and specific amplification was achieved as seen in Figure 4.5 for the *int11* primer set. The optimised annealing temperature of 60 °C was significantly higher than the 57 °C T_m provided on the synthesis report provided with the primers. Additionally, for the 16S rRNA gene the optimal annealing temperature was 59 °C. A single defined band was obtained for both primer sets after optimisation, as seen by the 109 bp for *int11* and 194 bp for 16S rRNA (Figure 4.5).

4.3.4 Construction of plasmid controls for RT-PCR

Based on the results in Figure 4.6, the constructed plasmids were used for the generation of standard curves for each primer set to ensure qPCR efficiency and accuracy.

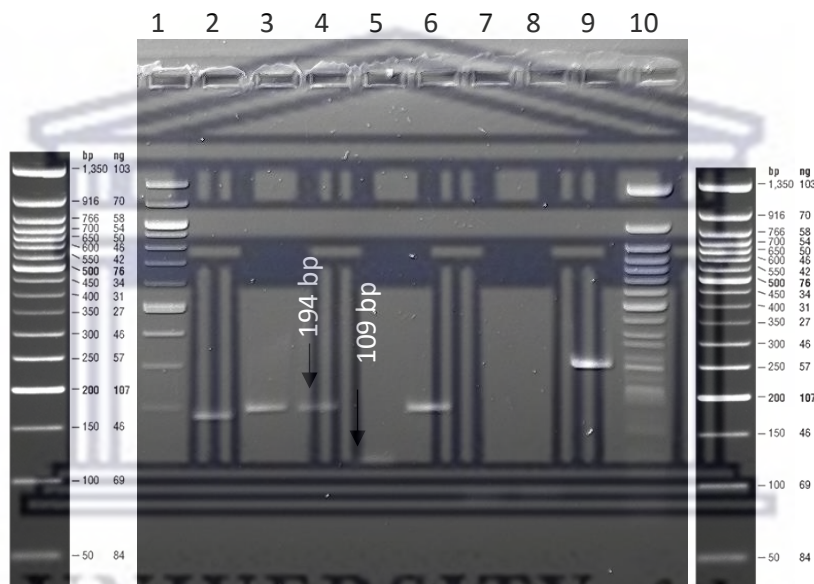


Figure 4.6: A 1% TAE agarose gel depicting the PCR confirmation of the inserts for *Int11* and 16S rRNA RT genes using gene-specific primers. Lane 1: 100 bp NEB marker; Lane 2: *gapA*; Lane 3: *mdH*; Lane 4: 16S rRNA RT; Lane 5: *Int11*; Lane 6: 16S rRNA Int; Lane 7: *vanA*; Lane 8: *ampC*; Lane 9: *aadA*; Lane 10: 100 bp NEB marker.

4.3.5 Real-time PCR

4.3.5.1 Generation of Standard Curves for the *Int11* and 16S rRNA gene for qPCR

Quantification using RT-PCR can be achieved by relative or absolute quantification (Zheng *et al.*, 2020). As absolute quantification relies on a standard plot constructed from known concentrations of standards to measure the actual number of copies of a particular target present it is considered to be the more informative and reliable method of quantification for comparisons.

In an experimental context, the subject of PCR efficiency has been critically assessed and discussed, resulting in various recommendations to account for inter-run variation, differences in instruments

and the number of replicates to be used. However, the use of a standard curve remains the most reliable approach to estimate qPCR efficiency (Bar *et al.*, 2012).

Standard curves were generated using the plasmids constructed for the *int11* and 16S rRNA gene primers, respectively. As stated in the MIQE guidelines, between 5-7 dilutions were used to generate the standard curves. Melt curve analysis revealed that the *int11* primers were highly specific as only a single sized amplicon was generated (Figure 4.7). The efficiency of the PCR was found to be within the accepted range of 90-100% (as the slope of the standard curve was -3.296) and the Pearson's correlation coefficient $R^2 = 0.9954$ (Figure 4.8). Similarly, the 16S rRNA gene primers were specific (Figure 4.9) and the efficiency (the slope) and R^2 were -3.3897 and 0.9987 (Figure 4.10), respectively.

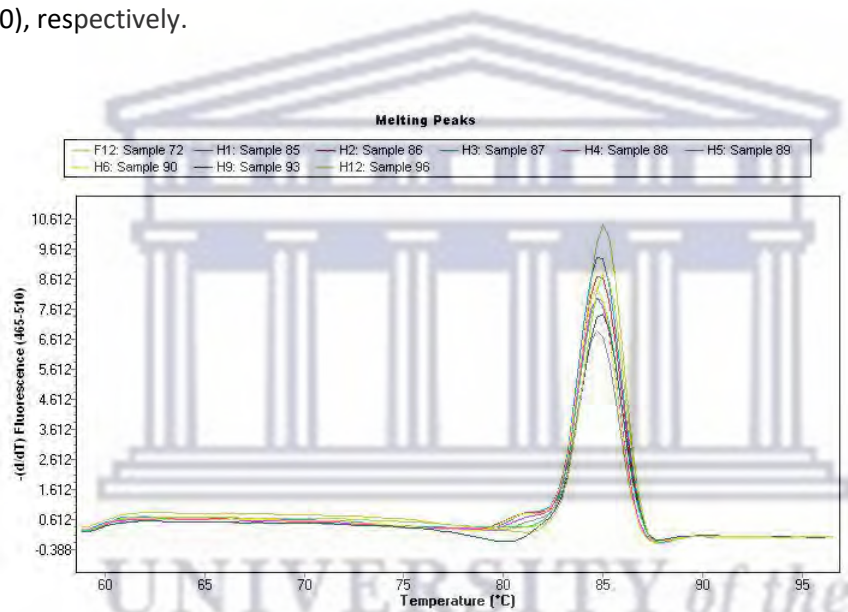


Figure 4.7. Melt Curve of *int11* gene amplicons generated using a dilution series of control plasmids. Cp values for these amplicons were used to construct the standard curve used for subsequent absolute quantification experiments.

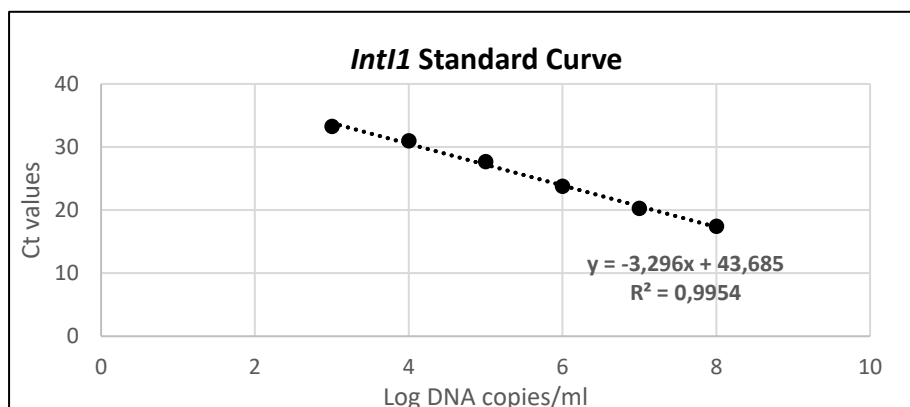


Figure 4.8. Standard curve for the *int11* primers of the log molecules/ μ l versus the Cp value.

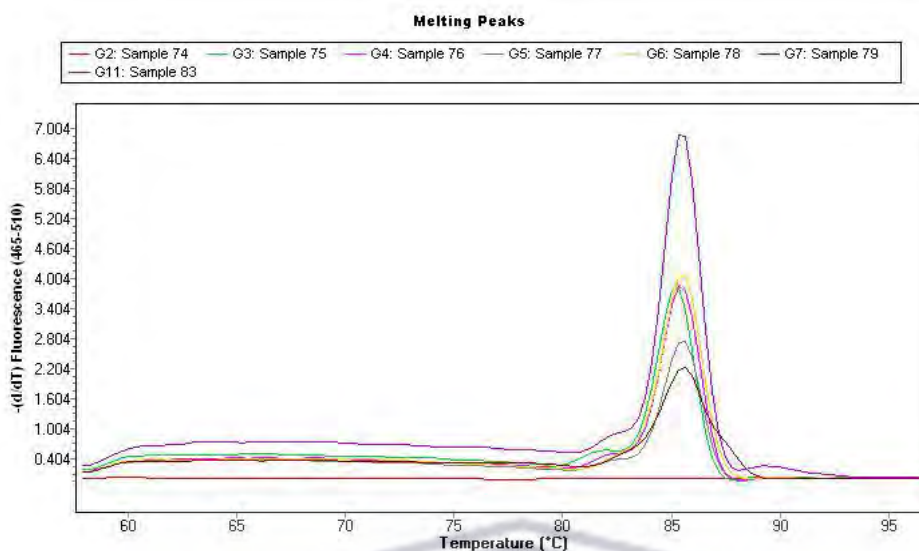


Figure 4.9. Melt Curve of 16S rRNA gene amplicons generated using a dilution series of control plasmids. Cp values for these amplicons were used to construct the standard curve used for subsequent absolute quantification experiments.

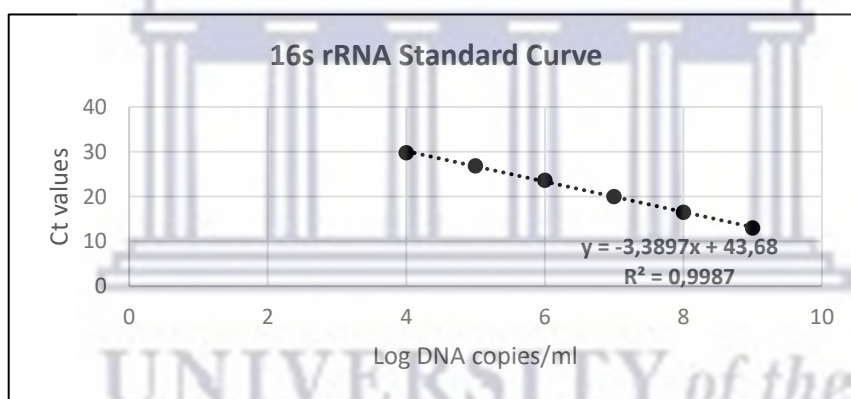


Figure 4.10. Standard curve for the 16S rRNA gene primers of the Log molecules/ μ l versus the Cp value.

4.3.5.2 Absolute Quantification of *intl1* gene and 16S rRNA RT gene in greywater and biofilm mDNA samples

The optimized qPCR conditions were used to evaluate the presence of the target genes (*intl1*, and 16S rRNA RT) in all metagenomic samples extracted.

4.3.5.2.1 Melt Curve Analysis

4.3.5.2.1.1 Melt Curve Analysis of *intl1* gene in mDNA samples

As seen in Figure 4.11, from the melting curve analysis of the *intl1* gene primers in the metagenomic DNA samples for group 1 (Figures C6 – C10 represent group 2-6, Appendix C, Chapter 4), all the samples exhibited a single peak of interest at a temperature of ~ 85 °C. Ruijter *et al.* (2019), stated that

a successful melting curve analysis assumes that the melting peak of the correct product can be identified, the efficiencies of all the amplified products are similar, the relative size of the melting peaks are reflective of the concentration of products and finally that the relative concentrations do not alter as the reaction reaches plateau. These factors were exhibited when evaluating the presence of the *intl1* gene in metagenomic samples extracted from domestic greywater. This is indicative of the efficiency of the primers used as well as the assay conditions, which were not hindered by the presence of any inhibitors. In Figure C6 (Appendix C, Chapter 4), an additional smaller peak was encountered at a temperature of approximately 90 °C. This may be indicative of mis-priming or primer-dimers, however handling and human-error should not be dismissed as this was only present in one of three replicates assayed.

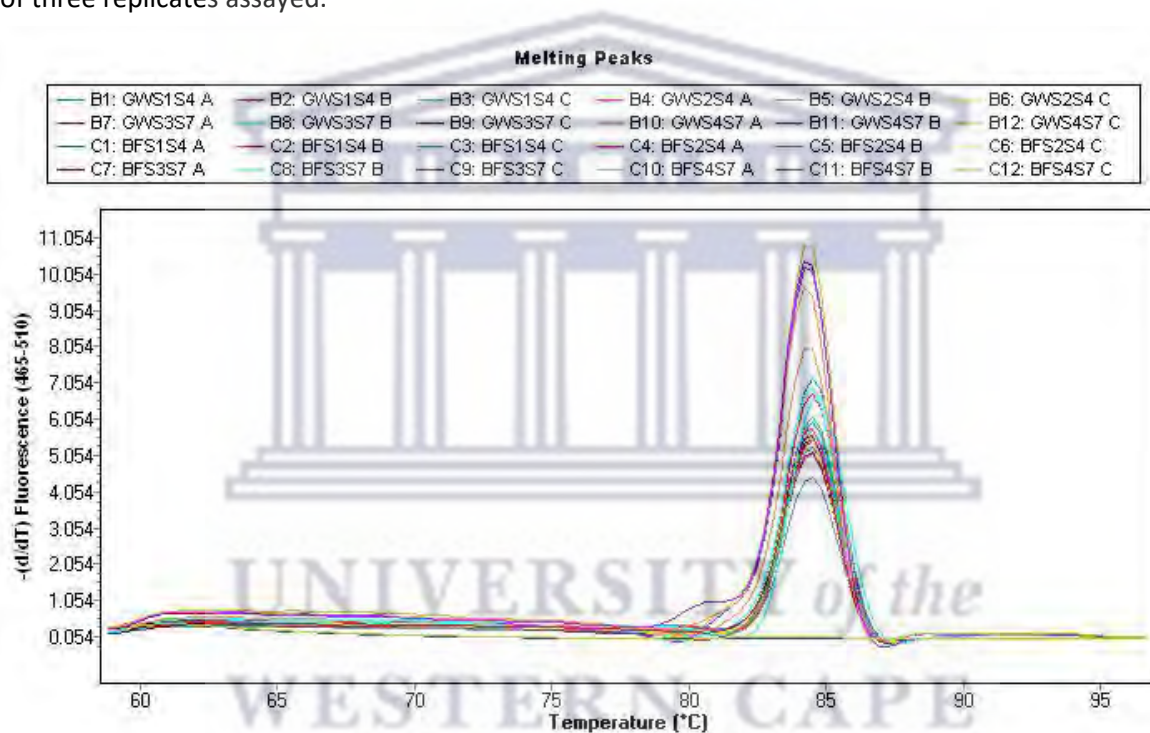


Figure 4.11: Melting Peaks for *intl1* primers in Group 1 mDNA samples.

4.3.5.2.1.2 Melt Curve Analysis of 16S rRNA gene in mDNA samples

The melt curve analysis of the 16S rRNA primer set on metagenomic samples was not as precise as that of the *intl1* primer set. Multiple peaks were detected in some samples (as seen in Figure 4.12). Based on the melting peaks produced when using the 16S rRNA standard curve, most metagenomic DNA samples produced a melting peak at ~85 °C. However, there were samples which displayed a slightly higher melting temperature between 85 °C and 90 °C, as seen in Figure 4.12. The presence of multiple melting peaks may be indicative of the variation in microbial diversity within the metagenomic samples, which would ultimately produce variation in melting temperatures. This is

supported by the fact that the primers are for the variable region of the 16S rRNA gene, which was confirmed when the primer set was subjected to a Primer-BLAST analysis.

When analysing environmental DNA, which contains the 16S rRNA gene for all the organisms present in the sample, this result is not surprising. It is expected that different species have differences in the gene sequence of their 16S rRNA genes, which ultimately result in differences in melting temperature. One would therefore expect to see more sequence differences in the variable region of the 16S rRNA gene compared to that of the *intl1* gene primer set, which targets a highly conserved region.

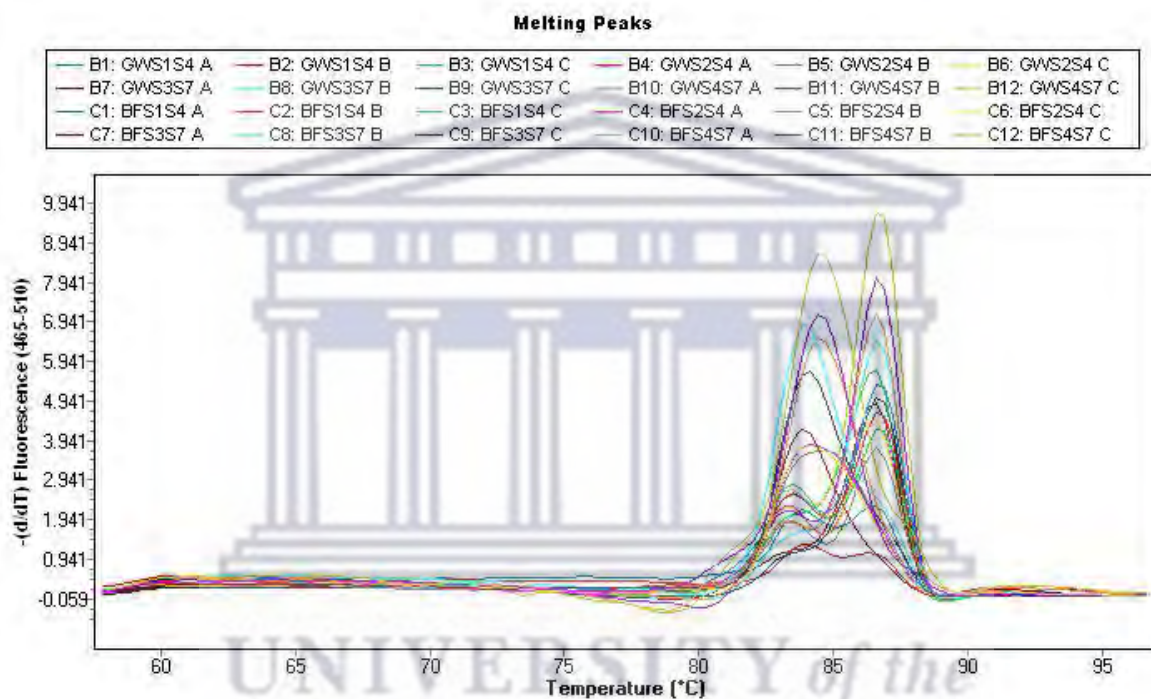


Figure 4.12: Melting peaks for 16S rRNA primers in Group 1 mDNA samples.

4.3.5.3 Comparison of *intl1* abundance at different collection sites

Absolute quantification determines the actual copy numbers of target genes by relating their respective Ct values to a standard or calibration curve (Dhanasekaran *et al.*, 2010). For the purpose of this study absolute quantification was performed using the Second derivate method, as the LightCycler 480 II software allows one to include internal controls when using the algorithm. Each sample was assessed in triplicate and the mean Ct value and copy number was derived from the standard curve. A threshold cycle (Ct/Cp) of 31 was considered the limit of detection and only samples which presented with three replicates of amplification were considered as positive and used for further analysis (Zheng *et al.*, 2020).

Quantitative analysis revealed that the class I integron-integrase *intl1* gene was detected in all 22 greywater samples as shown in Table 4.8 below, which presents the mean Ct/Cp value and mean copy

number per sample collected from its respective site. Copy numbers were calculated for each sample by plotting the Ct values on the respective standard curves, as seen in Figure 4.13. This figure furthermore confirms that each mean Ct values fell within the linear range of the *intl1* standard curve. For greywater samples, the mean copy numbers ranged from 2.71E+04 (GWS4S1, Summer sample) to 1.82E+07 (GWS3S1, Spring sample).

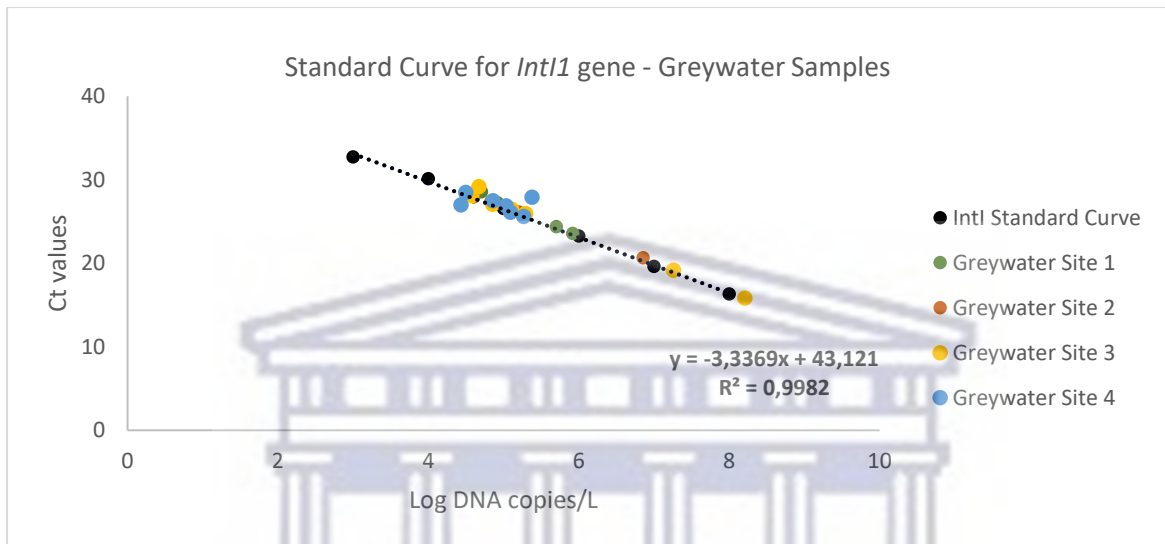


Figure 4.13: Standard curve of the Intl1 primer set with greywater samples present on the graph.

Table 4.8: Mean Ct values and Copy Numbers for the Integron qPCR Assay – Greywater Samples

Sample Name	Collection Season	Mean Ct value for <i>int11</i>	Mean Copy Number for <i>int11</i>	Mean Ct value for 16S rRNA	Mean Copy Number for 16S rRNA	Normalized Gene Copy Number	% Abundance
GWS1S1	Spring	27,23	8,38E+04	17,70	6,15E+07	2,18E-02	0,54%
GWS1S2	Winter	28,56	5,10E+04	19,33	7,73E+07	1,05E-02	0,26%
GWS1S3	Summer	23,59	8,26E+05	13,35	4,25E+09	3,11E-03	0,08%
GWS1S4	Autumn	24,39	5,06E+05	18,57	1,12E+08	7,22E-02	1,81%
		Mean copy number for Site 1	3,67E+05	Mean copy number for Site 1	1,13E+09	Mean relative abundance for Site 1	0,67%
GWS2S1	Spring	20,65	7,17E+06	14,85	4,17E+08	2,75E-01	6,87%
GWS2S2	Spring	27,94	4,03E+04	16,84	3,91E+08	1,65E-03	0,04%
GWS2S3	Summer	27,42	6,80E+04	15,78	9,57E+08	1,14E-03	0,03%
GWS2S4	Autumn	26,13	1,58E+05	13,49	1,03E+09	2,45E-03	0,06%
		Mean copy number for Site 2	1,86E+06	Mean copy number for Site 2	6,99E+08	Mean relative abundance for Site 2	1,75%
GWS3S1	Spring	19,15	1,82E+07	15,01	3,18E+08	9,16E-01	22,89%
GWS3S2	Summer	25,94	1,96E+05	15,14	3,09E+08	1,01E-02	0,25%
GWS3S3	Spring	29,15	4,71E+04	15,06	3,13E+08	2,41E-03	0,06%
GWS3S4	Summer	15,85	1,63E+08	12,64	5,33E+09	4,88E-01	12,20%
GWS3S5	Winter	27,08	7,19E+04	15,34	1,13E+09	1,02E-03	0,03%
GWS3S6	Spring	28,10	3,78E+04	15,85	8,08E+08	7,49E-04	0,02%
GWS3S7	Autumn	26,46	1,29E+05	13,52	1,02E+09	2,02E-03	0,05%
		Mean copy number for Site 3	2,59E+07	Mean copy number for Site 3	1,32E+09	Mean relative abundance for Site 3	5,07%
GWS4S1	Summer	26,98	2,71E+04	13,05	1,18E+09	3,67E-04	0,01%
GWS4S2	Autumn	27,90	2,40E+05	16,07	2,54E+08	1,51E-02	0,38%
GWS4S3	Autumn	26,87	1,08E+05	13,68	8,54E+08	2,01E-03	0,05%
GWS4S4	Spring	26,10	1,25E+05	13,01	1,41E+09	1,41E-03	0,04%
GWS4S5	Summer	25,61	1,86E+05	16,21	6,35E+08	4,67E-03	0,12%
GWS4S6	Winter	28,48	3,14E+04	16,55	4,91E+08	1,02E-03	0,03%
GWS4S7	Spring	27,50	7,23E+04	11,75	3,33E+09	3,47E-04	0,01%
		Mean copy number for Site 4	1,13E+05	Mean copy number for Site 4	1,16E+09	Mean relative abundance for Site 4	0,09%

Table 4.9: Mean Ct values and Copy Numbers for the Integron qPCR Assay – Biofilm Samples

Sample Name	Collection Season	Mean Ct value for <i>intI1</i>	Mean Copy Number for <i>intI1</i>	Mean Ct value for 16S rRNA	Mean Copy Number for 16S rRNA	Normalized Gene Copy Number	% Abundance
BFS1S1	Spring	25,36	2,58E+05	19,50	1,82E+07	2,26E-01	5,66%
BFS1S2	Winter	28,67	1,32E+05	19,74	5,85E+07	3,60E-02	0,90%
BFS1S3	Summer	27,98	8,18E+04	19,65	5,91E+07	2,21E-02	0,55%
BFS1S4	Autumn	27,27	1,63E+05	16,55	1,32E+08	1,97E-02	0,49%
		Mean copy number for Site 1	1,58E+05	Mean copy number for Site 1	6,70E+07	Mean relative abundance for Site 1	1,90%
BFS2S1	Spring	28,61	2,71E+04	23,45	5,14E+06	8,44E-02	2,11%
BFS2S3	Summer	29,07	1,87E+04	20,19	4,14E+07	7,21E-03	0,18%
BFS2S4	Autumn	25,95	1,82E+05	14,68	4,60E+08	6,33E-03	0,16%
		Mean copy number for Site 2	7,59E+04	Mean copy number for Site 2	1,69E+08	Mean relative abundance for Site 2	0,82%
BFS3S1	Spring	27,77	5,78E+04	19,58	1,51E+07	6,12E-02	1,53%
BFS3S2	Summer	30,80	9,23E+03	20,90	8,69E+06	1,70E-02	0,42%
BFS3S3	Spring	29,07	2,49E+04	22,00	3,50E+06	1,14E-01	2,85%
BFS3S5	Winter	28,86	2,41E+04	20,45	3,65E+07	1,05E-02	0,26%
BFS3S6	Spring	27,83	4,40E+04	17,53	3,04E+08	2,32E-03	0,06%
BFS3S7	Autumn	31,06	3,21E+04	21,01	6,87E+06	7,74E-02	1,87%
		Mean copy number for Site 3	3,20E+04	Mean copy number for Site 3	6,24E+07	Mean relative abundance for Site 3	1,17%
BFS4S1	Summer	32,01	2,91E+03	20,27	1,00E+07	4,65E-03	0,12%
BFS4S2	Autumn	23,82	9,28E+05	15,81	1,86E+08	7,98E-02	2,00%
BFS4S3	Autumn	29,10	2,44E+04	18,77	2,53E+07	1,54E-02	0,38%
BFS4S4	Spring	28,36	3,97E+04	17,40	7,49E+07	8,47E-03	0,21%
BFS4S5	Summer	27,63	5,24E+04	21,20	2,14E+07	3,92E-02	0,98%
BFS4S6	Winter	28,66	2,46E+04	19,91	5,11E+07	7,69E-03	0,19%
BFS4S7	Spring	28,41	3,74E+04	17,61	6,58E+07	9,09E-03	0,23%
		Mean copy number for Site 4	1,58E+05	Mean copy number for Site 4	6,21E+07	Mean relative abundance for Site 4	0,59%

Table 4.9 represents the mean Ct values and their corresponding mean copy numbers of the *intl1* gene in biofilm samples. Based on the criteria mentioned above, the *intl1* gene was detected in 18 of the 21 biofilm samples, of which the mean copy number for the *intl1* gene ranged from 9.23E+03 (BFS3S2, Summer sample) to 9.28E+05 (BFS4S2, Autumn sample). The mean copy numbers for the biofilm samples are significantly lower overall than that of the greywater samples.

Figure 4.14 represents the standard curve of the *intl1* gene with biofilm samples plotted onto the graph, by which it can be seen that all positive samples fell within the linear range of the standard curve. As stated earlier, the lower copy numbers observed for the biofilm samples reflects the amount and quality of the starting material used.

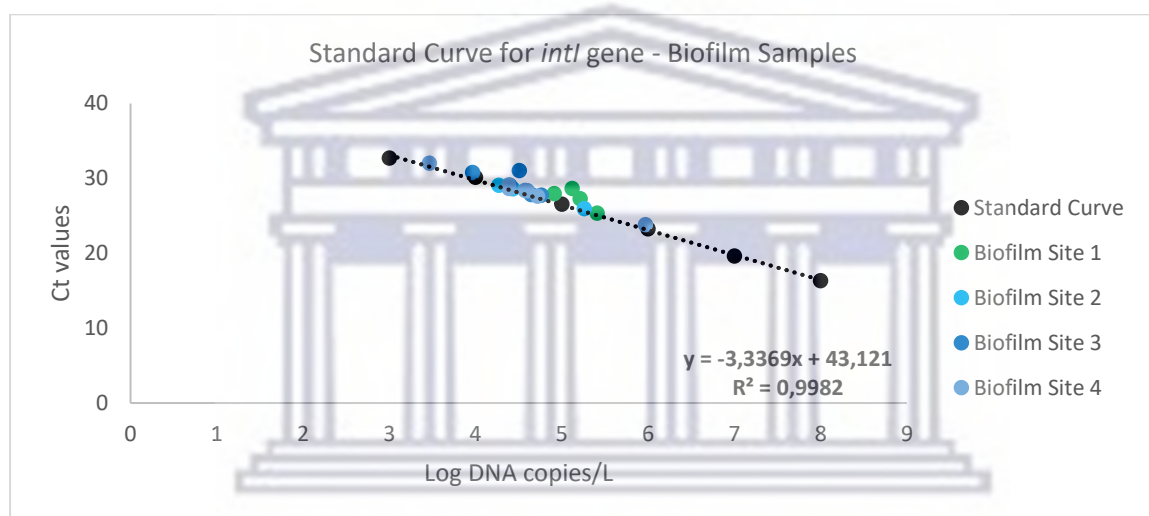


Figure 4.14: Standard curve of the *intl1* primer set with biofilm samples present on the graph.

Table 4.8 and Table 4.9 also represents the mean Ct value and their corresponding mean copy numbers for the gene 16S rRNA RT in greywater and biofilm samples respectively. For greywater samples the mean copy number ranged from 6.15E+07 (GWS1S1, Spring sample) to 5.33E+09 (GWS3S4, Summer sample). It should be noted that some greywater samples were not within the linear range of the standard curve as shown in Figure 4.15. This may be due to the high concentration of 16S rRNA genes within each sample, however even when normalized the mean copy numbers still exceeded the 10^9 range. This may be corrected for further studies by diluting the metagenomic DNA samples as well as setting up a wider dilution range to take into consideration such high copy numbers.

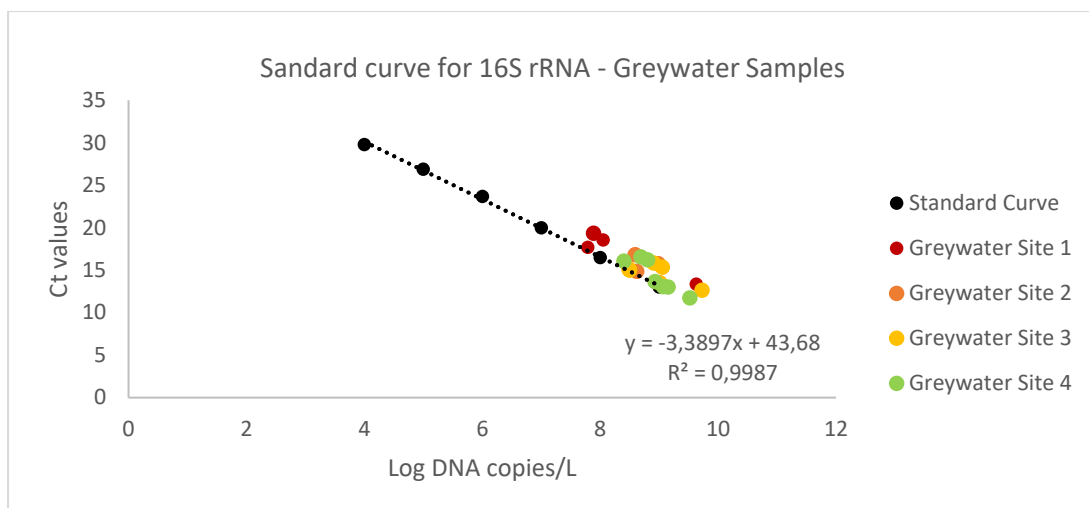


Figure 4.15: Standard curve of the 16S rRNA primer set with greywater samples present on the graph.

For biofilm samples the mean copy numbers range between $3.50E+06$ (BFS3S3, Spring sample) to $4.60E+08$ (BFS2S4, Autumn sample) for the 16S rRNA gene. Figure 4.16 represents the standard curve for the 16S rRNA gene with the biofilm samples plotted onto the graph. It was identified that all biofilm samples fell within the linear range of the standard curve.

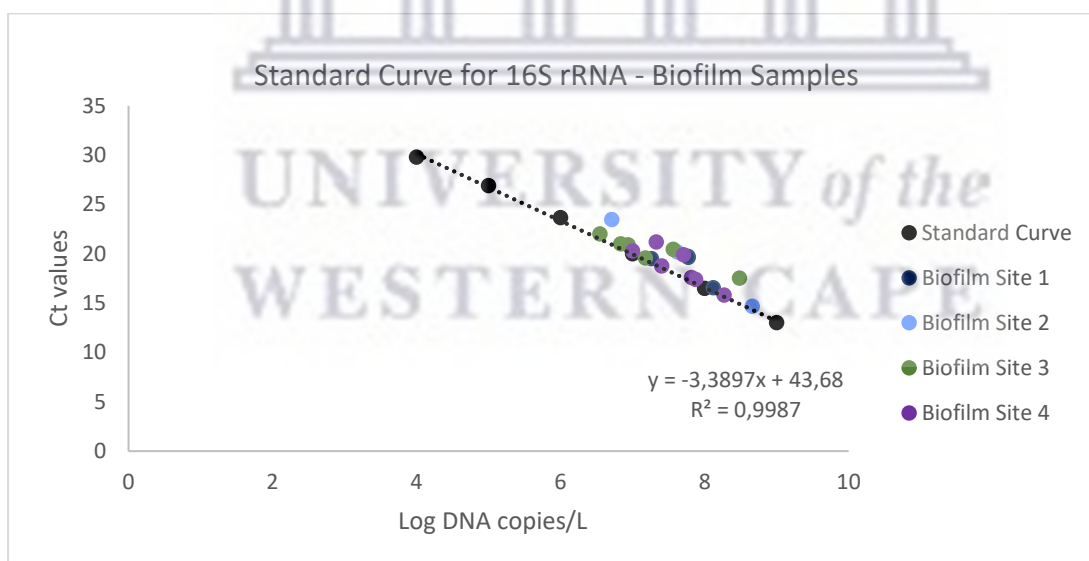


Figure 4.16: Standard curve of the 16S rRNA RT primer set with biofilm samples present on the graph.

The mean copy number and relative abundance of the *int11* gene varied across sites for both greywater and biofilm samples. Figure 4.17 (A) illustrates the mean copy number per collection site for greywater samples, of which site 3 had the highest average overall with $2.59E+07$ copies per litre greywater. This variation indicated that the proportion of bacterial cells harbouring the class 1 integron integrase gene differed between collection sites. These findings were further supported by the mean relative

abundance of the *int11* gene in greywater samples shown in Figure 4.17 (B). Site 3 had the highest percentage abundance with 5.07%; with site 4 having the lowest overall average abundance of 0.06%. The results obtained are consistent with previous findings by Rosewarne *et al.*, (2010), which identified variation in *int11* abundance in sediment samples collected from various catchment sites.

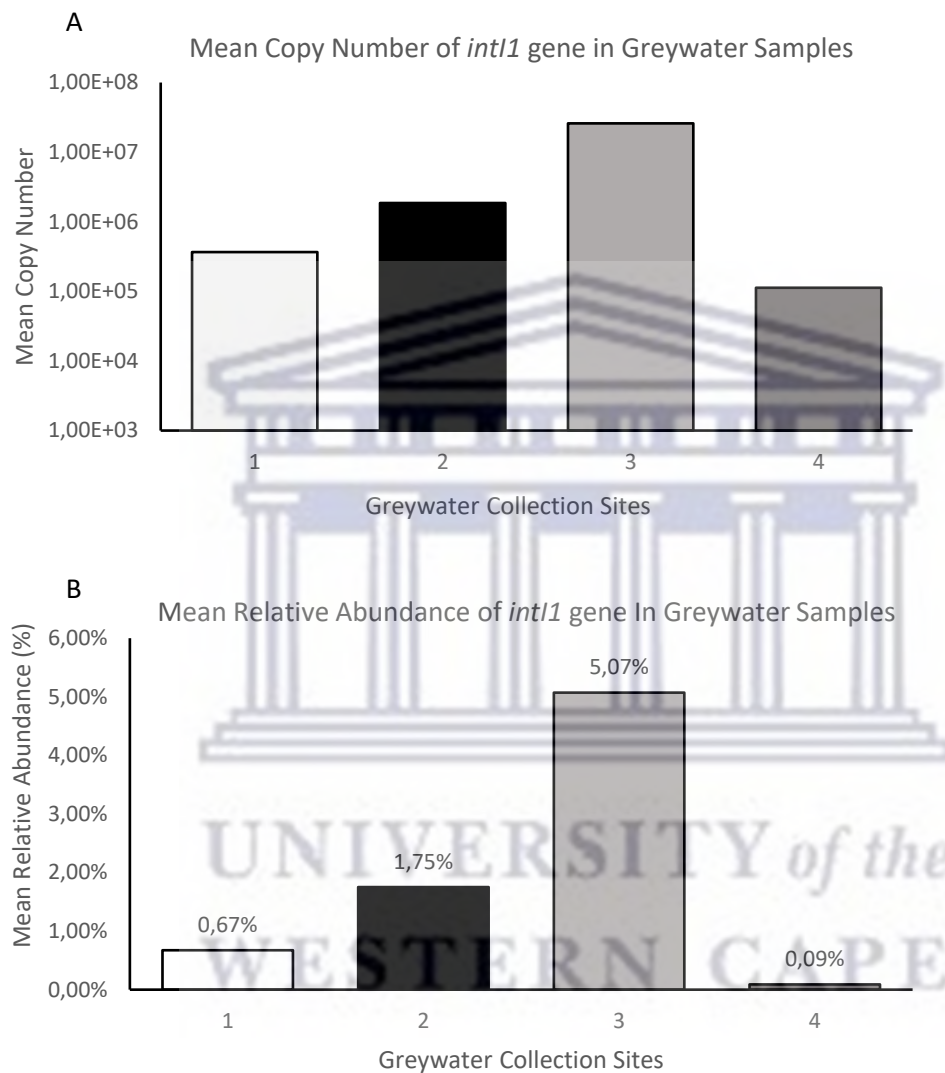


Figure 4.17: Mean copy number (a) and relative abundance (b) of *int11* gene in greywater samples collected from all four collection sites.

Figure 4.18 (A) illustrates the mean copy number for biofilm samples ranging from 3.20E+05 copies per litre at Site 3 to 1.58E+05 copies per litre at Site 1 and 4 respectively. Figure 4.18 (B) illustrates a variation in relative abundance of the *int11* gene in biofilm samples, ranging from 0.59% for Site 4 to 1.90% for Site 1. Research by Petrovich *et al.*, (2019) demonstrated that certain ARGs and integron-integrase genes were found in higher relative abundances in the upper layers of environmental biofilms, such as those found in wastewater treatment bioreactors. These findings corroborate

previous research into biofilms which found that HGT facilitated by integrons and plasmids is often enhanced in the upper layers of biofilms near the fluid-biofilm interface, an area which has oxygen more readily available (Krol *et al.*, 2011).

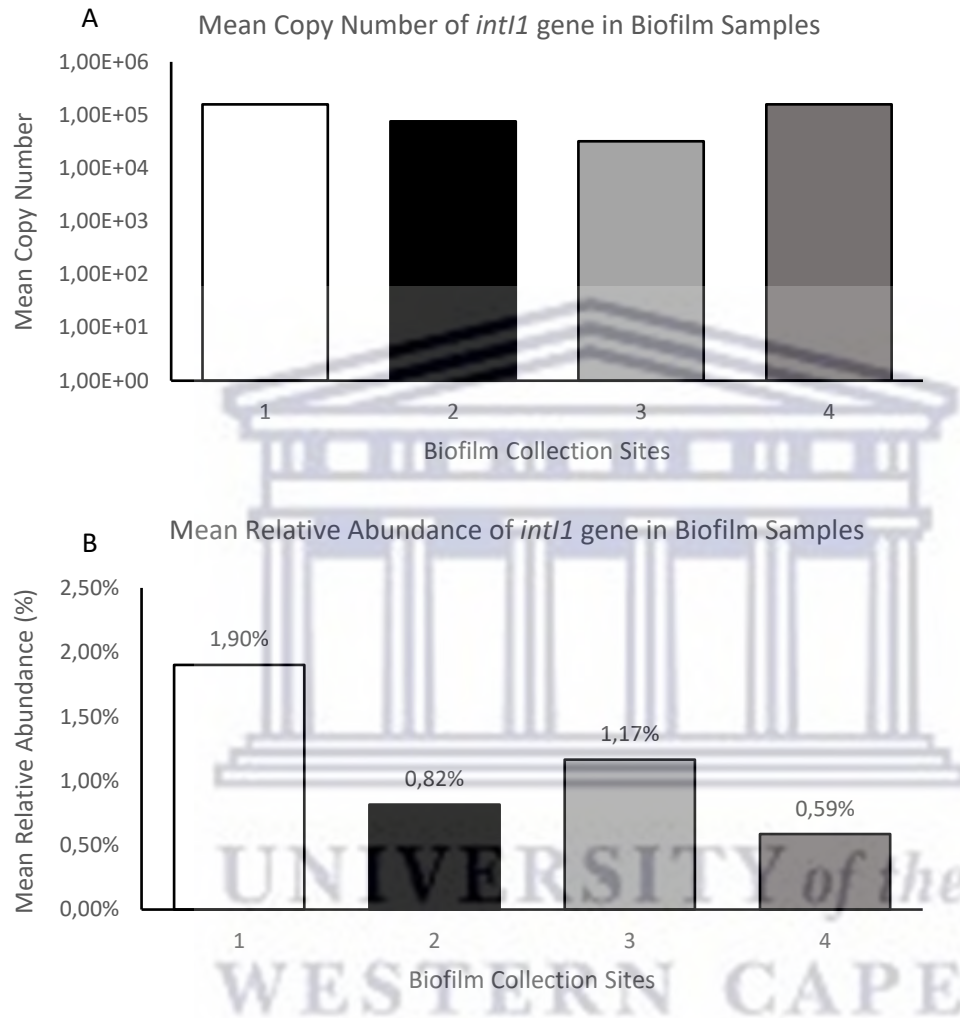


Figure 4.18: Mean copy number (a) and relative abundance (b) of *int1* gene in biofilm samples collected from all four collection sites.

In terms of variation of abundance between sites, it is evident that Site 4 had the lowest relative abundance for the *int1* gene for both greywater and biofilm samples. This may be due to the microbial composition of the collection site, as well as social and economic factors such as overall health, and exposure to opportunistic bacteria and antibiotics. Additionally, factors such as climate and tank maintenance are also to be considered influential to the outcome.

Statistical analysis was conducted using the non-parametric Kruskal-Wallis test, which allows for the comparison of more than two groups. An initial analysis confirmed that the average *int1* gene abundance at the four collection sites was not statistically significantly different from each other, as initially hypothesized ($H = 1.774$; $p = 0.61988$, $p < 0.05$).

The present study utilized qPCR to estimate the proportion of cells harbouring the class 1 Integron integrase gene in an environmental microbial population using a culture-independent approach. By comparing the copy numbers of the *int1* and 16S rRNA genes, it was deduced that on average 2.08% of bacterial cells in the greywater and 1.06% of bacterial cells in the biofilm contained the class 1 Integron integrase gene. It should be noted that the approach followed in this study made no attempt to allow for the assumption that some cells may contain more than one class 1 integron (Hardwick *et al.*, 2008). These overall findings per collection sites are supported by previous studies (including studies which made use of conventional isolation methods) which estimated that between 1 – 5% of bacterial cells contain a class 1 integron (Koczura *et al.*, 2016; Hardwick *et al.*, 2008; Stokes *et al.*, 2006).

4.3.5.4 Comparison of Seasons and *int1* gene Abundance

The relationship between collection season and relative abundance of the *int1* gene was investigated to identify the effect of seasonal changes on the microbial population within the greywater collection tanks.

Based on mean copy numbers, it was identified that microbial populations appear to be larger in the warmer months (summer and spring) than in the colder winter months. This can be seen when comparing the abundance of the *int1* gene and the sample collection seasons (Figure 4.19 and 4.20). Relative abundance was higher in the greywater samples than that of the biofilm samples in all the collection seasons. As seen in Figure 4.19, the average *int1* gene copy number in the greywater samples for summer was 2.738E+07 compared to 5.14E+04 in the winter collection months, which indicates a three-fold difference in abundance. For biofilm samples however, a similar magnitude of *int1* gene copies were present in the winter months (6.01E+04) compared to that of the summer months (3.30E+04). This may be due to the fact that seasonal fluctuations in population size is smaller in biofilm or sediments compared to the water column (Luo *et al.*, 2010). Which may be due to several factors such as more constant food supply in a biofilm matrix as well as the presence of EPS which provides protection from the external environment.

As seen in Figure 4.20, the *int1* gene levels did not fluctuate seasonally in biofilm samples when compared to greywater samples. This supports our hypothesis that biofilms are often colonized by stable microbial communities throughout the year which is less impacted by seasonal changes.

Based on the findings, it is evident that higher levels of the *int1* gene were detected in greywater samples compared to that of the biofilm samples. This could be attributed to the fact that the *int1* gene is often associated with human activity, such as bathing, washing of hands and handling of food

and as such is likely to be more dynamic which greater fluctuations in gene copy number, compared to the more stable population present in biofilms.

A Kruskal-Wallis test was conducted to identify if there was a significant difference between the *int11* abundance and the seasons the samples were collected. Based on statistical analysis it was identified that there was no significant differences between the collection seasons and the overall *int11* gene abundance in both greywater ($H(2) = 0.6131$; $p\text{-value} = 0.89$; $p < 0.05$) and biofilm ($H(2) = 0.7449$; $p\text{-value} = 0.86259$; $p < 0.05$) samples.

Variations of results found in other studies may be attributed to selected bacterial taxa, the population, and climatic conditions as well as the occurrence of events prior to sampling. Organic loading, temperature, pH and dissolved oxygen all contribute to the environment of the storage tanks during climatic seasons (Paiva *et al.*, 2015).



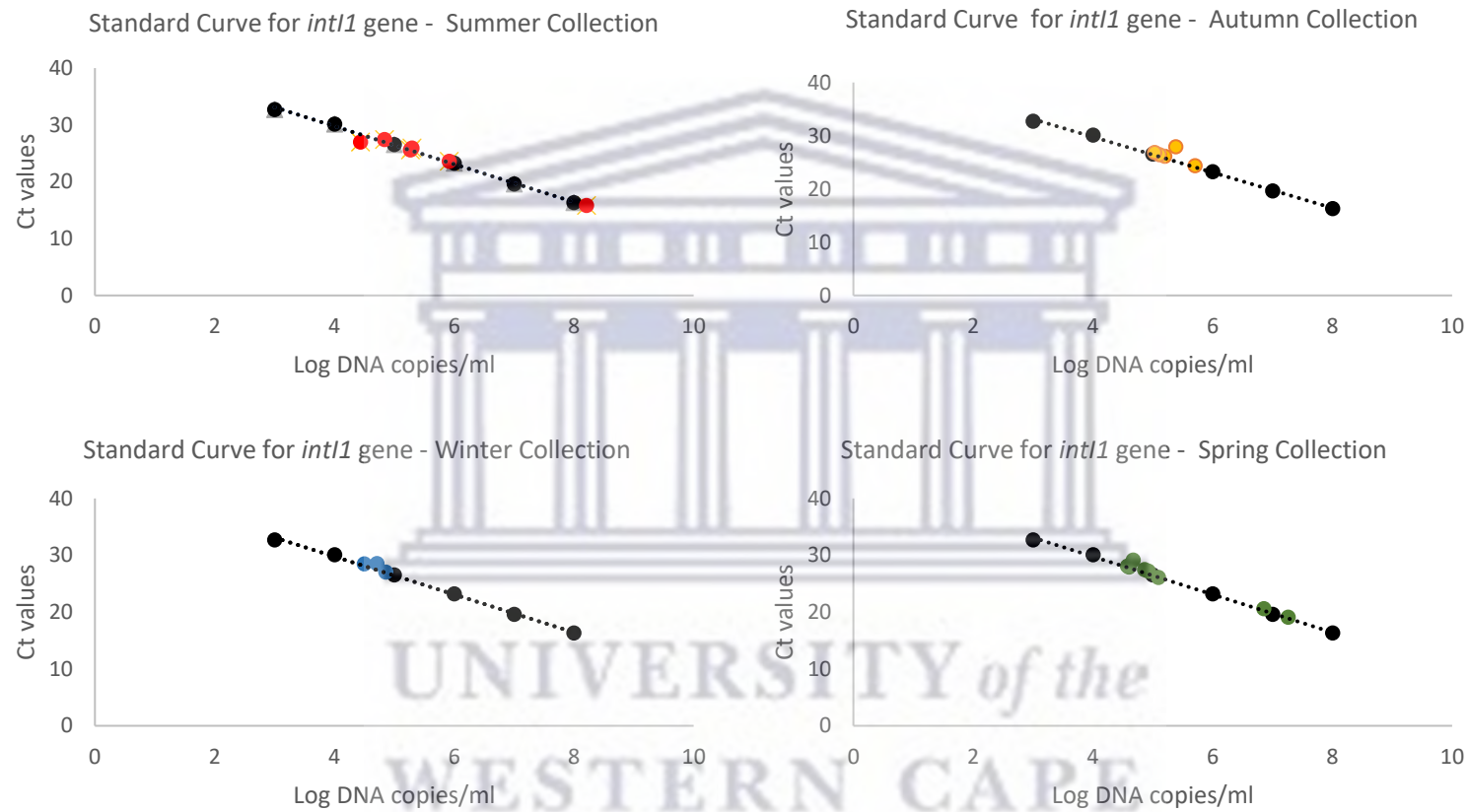


Figure 4.19: Greywater Sample Collection Seasons and the correlating *int1* gene copy numbers

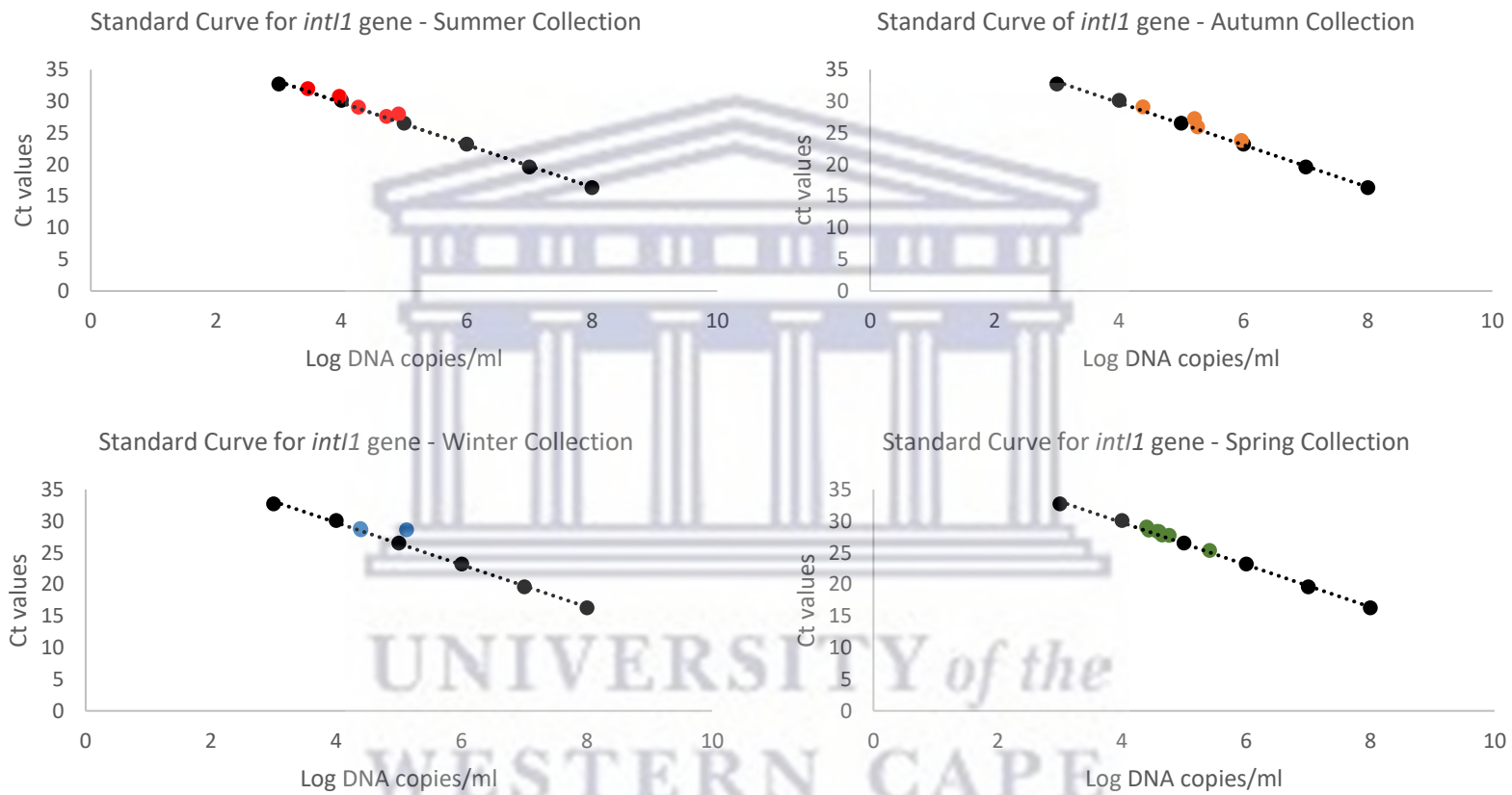


Figure 4.20: Biofilm Sample Collection Seasons and the correlating *int1* gene copy numbers

4.4 Conclusion of Chapter

Class 1 Integrons serve as key players in the global antibiotic resistance crisis as they are vehicles able to capture and express diverse resistance genes (Gillings *et al.*, 2008). Their ability to embed themselves in promiscuous plasmids and transposons, which facilitates their movement amongst a wide range of pathogens, reiterates their role as an indicator of anthropogenic pollution (Rocha *et al.*, 2019).

Recent studies have identified that the environment plays a major role in the spread of antibiotic resistance among pathogenic strains. Similarly, this has raised concern with regards to the impact it may have on human and animal health (Stalder *et al.*, 2012). With a focus on mainly human-impacted environments such as soil and aquatic environments that may have been influenced by agriculture, urbanization, and industrial waste, it has been revealed that water is one of the main vectors in the environment when it comes to integron and ARG distribution (Stalder *et al.*, 2012).

The primary focus of the study was to investigate the use of the *intI1* gene as a marker of horizontal gene transfer in domestic greywater systems using RT-PCR. Prior to RT-PCR analysis certain factors such as the efficient extraction of metagenomic DNA from greywater and biofilm samples, as well as their quality and efficiency to downstream processing was assessed. Metagenomic DNA was successfully extracted from 22 greywater and 20 biofilm samples, respectively. Overall concentrations ranged from 0.22 ng/μl to 16.4 ng/μl in greywater samples and between 0.08 ng/μl to 5.67 ng/μl in biofilm samples.

Quantitative analysis revealed that the *intI1* gene was detected in all 22 greywater samples, with the mean copy numbers ranging from 2.71E+04 (GWS4S1, Summer sample) to 1.82E+07 (GWS3S1, Spring sample). Site 3 had the highest average overall with 2.59E+07 copies per litre greywater. Sites 1, 2 and 4 had 3.67E+05; 1.86E+06 and 1.13E+05 copies per litre, respectively. The *intI1* gene was successfully detected in 18 of the 21 biofilm samples, of which the mean copy number for the *intI1* gene ranged from 9.23E+03 (BFS3S2, Summer sample) to 9.28E+05 (BFS4S2, Autumn sample). The mean copy numbers for the biofilm samples were significantly lower overall than that of the greywater samples. The mean copy number and relative abundance of *intI1* gene varied across sites for both greywater and biofilm samples, this variation indicated that the proportion of bacterial cells harbouring the class 1 integron integrase gene differed between collection sites. These findings were further supported by the mean relative abundance of the *intI1* gene in greywater samples. Site 3 had the highest percentage abundance with 5.07%; with site 4 having the lowest overall average abundance of 0.06%. The results obtained are consistent with previous findings by Rosewarne *et al.*, (2010), which identified variation in *intI1* abundance in sediment samples collected from various catchment sites. The mean copy

number for biofilm samples ranged between 3.20E+05 copies per litre at Site 3 to 1.58E+05 copies per litre at Site 1 and 4, respectively. The results revealed a variation in relative abundance of the *int11* gene in biofilm samples, ranging from 0.59% for Site 4 to 1.90% for Site 1. In terms of variation of abundance between sites, it was evident that Site 4 had the lowest relative abundance for *int11* for both greywater and biofilm samples.

The present study utilized qPCR to estimate the proportion of cells harbouring the class 1 Integron integrase gene in an environmental microbial population using a culture-independent approach (Hardwick *et al.*, 2008). By comparing the copy numbers of the *int11* and 16S rRNA genes, it was deduced that on average 2.08% of bacterial cells in greywater samples and 1.06% of bacterial cells in biofilm samples contained the class 1 Integron integrase gene. These overall findings per collection sites are supported by previous studies, of which some made use of conventional isolation methods, that have estimated between 1 – 5% of bacterial cells contain a class 1 integron (Koczura *et al.*, 2016; Hardwick *et al.*, 2008; Stokes *et al.*, 2006).

The relationship between sample collection seasons and relative abundance of the *int11* gene was investigated to identify the effect of seasonal changes on the microbial population within the greywater collection tanks. Based on mean copy numbers, it was identified that microbial populations appear to be larger in the warmer months (summer and spring) than in the colder winter months. The average *int11* gene copy number in the greywater samples for summer was 2.738E+07 compared to 5.14E+04 in the winter collection months, which indicates a three-fold difference in abundance. For biofilm samples however, a similar magnitude of *int11* gene copies were present in the winter months (6.01E+04) compared to that of the summer months (3.30E+04). This may be due to the fact that seasonal fluctuations in population size is smaller in biofilm or sediments compared to the water column (Luo *et al.*, 2010). Based on the findings, it is evident that higher levels of the *int11* gene were detected in greywater samples compared to that of the biofilm samples.

Overall, the main focus of utilizing the *int11* gene as a marker of horizontal gene transfer in greywater systems was achieved. The methodology used to assess the greywater and their associated biofilms, although complex environmental samples riddled with inhibitors, was efficient and effective furthermore confirming findings by Hardwick *et al.* (2008) which deemed a SYBR-based RT-PCR assay as effective when quantifying class 1 integrons in environmental samples. The findings support statements by Zheng *et al.* (2010) who identify that *int11* and clinical *int11* could reflect the overall abundance of ARGs in water bodies such as greywater and furthermore serve as an effective anthropogenic marker and a marker of horizontal gene transfer.

Limitations within the study were mainly attributed to preliminary factors such as metagenomic DNA quality and stability, as well as the optimization of the primer sets used to ensure accurate and efficient absolute quantification. In terms of qPCR, the dynamic range per primer set was of utmost importance. The 16S rRNA primer set was the hardest to optimize based mainly on the fact that metagenomic samples often have a wide range of microbial diversity. An additional limitation within the study was the sampling schedule in terms of sites and seasons, as the summer and spring samples were disproportionately more sampled to that of the winter and autumn samples. In terms of sites sampled, the issue of availability of the residences for sampling greatly affected the progression of the project. Future work proposed for the current study include the use of next generation sequencing to identify the microbial community diversity present within each sample set, as well as provide a greater insight into the pathogens, if any, harbouring *int1* genes. Therefore, potentially allowing for the discovery of unique integron-integrase gene cassette.



Chapter 5: Conclusion and Future work

Climate change has greatly impacted countries all around the world and as the global population increases, water scarcity remains an ever-looming issue. The 2016-2019 Western Cape Drought provided residents with first-hand experience to the effects of climate change.

The use of alternative water sources where applicable was encouraged, thus the use of greywater systems remains prominent within Western Cape communities still today. Greywater generated from non-toilet activities, greatly alleviated the pressure on freshwater usage per household for irrigation and other uses. However, little consideration was taken into the potential health risks associated with its use.

Like wastewater, greywater harbours bacteria, including pathogens, and without careful consideration for handling, storage and treatment, the bacteria present can be released directly into the environment. Numerous studies have investigated wastewater, reclaimed water, and greywater to identify their potential to harbour pathogenic bacteria. However, many do not address whether these water environments act as a reservoir for Antibiotic Resistance Genes (ARGs). The conditions within greywater systems support the growth of microorganisms, especially long periods of stagnant water. In addition, the presence of antibiotics and chemical pollutants can serve as a driving force for the proliferation and exchange of ARGs.

Therefore, the main hypothesis of this study was that domestic greywater systems are a source of antibiotic resistant bacteria and furthermore may serve as a hotspot for ARG exchange amongst susceptible bacteria.

This study was successful in utilizing a combination of culture-based assays with molecular analysis as a mode of antimicrobial susceptibility testing. The Kirby-Bauer method served as a phenotypic confirmation of antibiotic resistance in greywater and biofilm samples, therefore serving as an effective preliminary evaluation of the samples. The LIVE/DEAD BacLight Bacterial Viability assay coupled with flow cytometry revealed that many samples had a larger proportion of dead or injured cells than live cells.

qPCR analysis confirmed the presence of two clinically relevant ARGs, *vanA* and *ampC*, in domestic greywater samples. Furthermore, confirming the effectiveness of qPCR in AMR monitoring. Additionally, it is proposed that the Hot Phenol SDS method by Ares *et al.*, (2018) for total RNA extraction has been successfully and effectively optimised for extraction from greywater samples for downstream applications.

Finally, in this study the presence of Class 1 Integrons as a marker of HGT was evaluated. Findings revealed the *int1* gene was detected in all samples. These findings support the hypothesis that greywater may serve as a reservoir for the exchange and proliferation of ARGs and ARBs.

In conclusion, this study confirms that domestic greywater systems are a source of ARGs and ARBs, which could ultimately be a source of environmental contamination.

Future work should evaluate a wider selection of antibiotics and ARGs as a potential environmental pollutant of water sources, in combination with metagenomic analysis using Next Generation Sequencing (NGS). The incorporation of NGS will allow for insight into the microbial composition of greywater systems and more specifically how these populations may fluctuate in response to seasonal changes.



Reference List

- Adefisoye, M.A. and Okoh, A.I. (2016) 'Identification and antimicrobial resistance prevalence of pathogenic *Escherichia coli* strains from treated wastewater effluents in Eastern Cape, South Africa,' *Microbiology Open*, 5(1), pp. 143–151. <https://doi.org/10.1002/mbo3.319>.
- Agersø, Y. and Petersen, A. (2006) 'The tetracycline resistance determinant Tet 39 and the sulphonamide resistance gene *sulIII* are common among resistant *Acinetobacter* spp. isolated from integrated fish farms in Thailand,' *Journal of Antimicrobial Chemotherapy*, 59(1), pp. 23–27. <https://doi.org/10.1093/jac/dkl419>.
- Agersø, Y. and Sandvang, D. (2005) 'Class 1 Integrons and Tetracycline Resistance Genes in *Alcaligenes*, *Arthrobacter*, and *Pseudomonas* spp. Isolated from Pigsties and Manured Soil,' *Applied and Environmental Microbiology*, 71(12), pp. 7941–7947. <https://doi.org/10.1128/aem.71.12.7941-7947.2005>.
- Alygizakis, N. *et al.* (2021) 'Change in the chemical content of untreated wastewater of Athens, Greece under COVID-19 pandemic,' *Science of the Total Environment*, 799, p. 149230. <https://doi.org/10.1016/j.scitotenv.2021.149230>.
- Aminov, R. (2011) 'Horizontal gene exchange in environmental microbiota,' *DOAJ (DOAJ: Directory of Open Access Journals)* [Preprint]. <https://doi.org/10.3389/fmicb.2011.00158>.
- Aminov, R., Garrigues-Jeanjean, N. and Mackie, R.I. (2001) 'Molecular ecology of tetracycline resistance: Development and validation of primers for detection of tetracycline resistance genes encoding ribosomal protection proteins,' *Applied and Environmental Microbiology*, 67(1), pp. 22–32. <https://doi.org/10.1128/aem.67.1.22-32.2001>.
- Ares, M. (2012) 'Bacterial RNA isolation,' *CSH Protocols*, 2012(9), p. pdb.prot071068. <https://doi.org/10.1101/pdb.prot071068>.
- Artika, I.M. *et al.* (2022) 'Real-Time polymerase chain Reaction: Current techniques, applications, and role in COVID-19 diagnosis,' *Genes*, 13(12), p. 2387. <https://doi.org/10.3390/genes13122387>.
- Auerbach, E., Seyfried, E.E. and McMahon, K.D. (2007) 'Tetracycline resistance genes in activated sludge wastewater treatment plants,' *Water Research*, 41(5), pp. 1143–1151. <https://doi.org/10.1016/j.watres.2006.11.045>.
- Bag, S. *et al.* (2016) 'An Improved Method for High Quality Metagenomics DNA Extraction from Human and Environmental Samples,' *Scientific Reports*, 6(1). <https://doi.org/10.1038/srep26775>.
- Batt, A.L., Bruce, I.B. and Aga, D.S. (2006) 'Evaluating the vulnerability of surface waters to antibiotic contamination from varying wastewater treatment plant discharges,' *Environmental Pollution*, 142(2), pp. 295–302. <https://doi.org/10.1016/j.envpol.2005.10.010>.

- Bauer, A.W. *et al.* (1966) 'Antibiotic susceptibility testing by a standardized single disk method,' *American Journal of Clinical Pathology*, 45(4), pp. 493–496. https://doi.org/10.1093/ajcp/45.4_ts.493.
- Beinhauerová, M. *et al.* (2020) 'Utilization of digital PCR in quantity verification of plasmid standards used in quantitative PCR,' *Frontiers in Molecular Biosciences*, 7. <https://doi.org/10.3389/fmolb.2020.00155>.
- Bello–López, J.M. *et al.* (2019) 'Horizontal Gene Transfer and Its Association with Antibiotic Resistance in the Genus *Aeromonas* spp.,' *Microorganisms*, 7(9), p. 363. <https://doi.org/10.3390/microorganisms7090363>.
- Berglund, B. (2015) 'Environmental dissemination of antibiotic resistance genes and correlation to anthropogenic contamination with antibiotics,' *Infection Ecology & Epidemiology*, 5(1), p. 28564. <https://doi.org/10.3402/iee.v5.28564>.
- Berney, M. *et al.* (2007) 'Assessment and Interpretation of Bacterial Viability by Using the LIVE/DEAD BacLight Kit in Combination with Flow Cytometry,' *Applied and Environmental Microbiology*, 73(10), pp. 3283–3290. <https://doi.org/10.1128/aem.02750-06>.
- Bonacorsi, S. *et al.* (2021) 'Systematic review on the correlation of quantitative PCR cycle threshold values of gastrointestinal pathogens with patient clinical presentation and outcomes,' *Frontiers in Medicine*, 8. <https://doi.org/10.3389/fmed.2021.711809>.
- Botai, C.M. *et al.* (2017) 'Drought Characteristics over the Western Cape Province, South Africa,' *Water*, 9(11), p. 876. <https://doi.org/10.3390/w9110876>.
- Boulter, N.R. *et al.* (2016) 'A simple, accurate and universal method for quantification of PCR,' *BMC Biotechnology*, 16(1). <https://doi.org/10.1186/s12896-016-0256-y>.
- Brankatschk, R. *et al.* (2012) 'Simple absolute quantification method correcting for quantitative PCR efficiency variations for microbial community samples,' *Applied and Environmental Microbiology*, 78(12), pp. 4481–4489. <https://doi.org/10.1128/aem.07878-11>.
- Brankatschk, R. *et al.* (2012) 'Simple absolute quantification method correcting for quantitative PCR efficiency variations for microbial community samples,' *Applied and Environmental Microbiology*, 78(12), pp. 4481–4489. <https://doi.org/10.1128/aem.07878-11>.
- Brito, I.L. (2021) 'Examining horizontal gene transfer in microbial communities,' *Nature Reviews Microbiology*, 19(7), pp. 442–453. <https://doi.org/10.1038/s41579-021-00534-7>.
- Brühl, J. *et al.* (2020) 'Decision-Making in a Water Crisis: Lessons from the Cape Town drought for urban water policy,' *Oxford Research Encyclopedia of Environmental Science* [Preprint]. <https://doi.org/10.1093/acrefore/9780199389414.013.706>.

- Bustin, S.A. *et al.* (2005) 'Quantitative real-time RT-PCR – a perspective,' *Journal of Molecular Endocrinology*, 34(3), pp. 597–601. <https://doi.org/10.1677/jme.1.01755>.
- Bustin, S.A. *et al.* (2009) 'The MIQE Guidelines: Minimum information for publication of Quantitative Real-Time PCR experiments,' *Clinical Chemistry*, 55(4), pp. 611–622. <https://doi.org/10.1373/clinchem.2008.112797>.
- Calverley, C.M. and Walther, S.C. (2022) 'Drought, water management, and social equity: Analyzing Cape Town, South Africa's water crisis,' *Frontiers in Water*, 4. <https://doi.org/10.3389/frwa.2022.910149>.
- Caplin, J., Hanlon, G.W. and Taylor, H. (2008) 'Presence of vancomycin and ampicillin-resistant *Enterococcus faecium* of epidemic clonal complex-17 in wastewaters from the south coast of England,' *Environmental Microbiology*, 10(4), pp. 885–892. <https://doi.org/10.1111/j.1462-2920.2007.01507.x>.
- Caraguel, C. *et al.* (2011) 'Selection of a cutoff value for Real-Time Polymerase chain reaction results to fit a diagnostic purpose: analytical and epidemiologic approaches,' *Journal of Veterinary Diagnostic Investigation*, 23(1), pp. 2–15. <https://doi.org/10.1177/104063871102300102>.
- Chang, S., Puryear, J. and Cairney, J. (1993) 'A simple and efficient method for isolating RNA from pine trees,' *Plant Molecular Biology Reporter*, 11(2), pp. 113–116. <https://doi.org/10.1007/bf02670468>.
- Cheng, C.Y. *et al.* (2021) 'Evolutionarily informed machine learning enhances the power of predictive gene-to-phenotype relationships,' *Nature Communications*, 12(1). <https://doi.org/10.1038/s41467-021-25893-w>.
- Cheng, X. *et al.* (2021) 'Analysis of antibiotic resistance genes, environmental factors, and microbial community from aquaculture farms in five provinces, China,' *Frontiers in Microbiology*, 12. <https://doi.org/10.3389/fmicb.2021.679805>.
- Chetty, S. (2021) 'South Africa's capacity to conduct antimicrobial stewardship,' *Southern African Journal of Infectious Diseases*, 36(1). <https://doi.org/10.4102/sajid.v36i1.297>.
- Chomczynski P. A reagent for the single-step simultaneous isolation of RNA, DNA and proteins from cell and tissue samples. *Biotechniques*. 1993 Sep;15(3):532-4, 536-7. PMID: 7692896.
- Cichocki, N. *et al.* (2020) 'Bacterial mock communities as standards for reproducible cytometric microbiome analysis,' *Nature Protocols*, 15(9), pp. 2788–2812. <https://doi.org/10.1038/s41596-020-0362-0>.
- Coertze, R.D. and Bezuidenhout, C.C. (2019) 'Global distribution and current research of *AmpC* beta-lactamase genes in aquatic environments: A systematic review,' *Environmental Pollution*, 252, pp. 1633–1642. <https://doi.org/10.1016/j.envpol.2019.06.106>.

- Coertze, R.D. and Bezuidenhout, C.C. (2020) 'Detection and quantification of clinically relevant plasmid-mediated *AmpC* beta-lactamase genes in aquatic systems,' *Water Science & Technology: Water Supply*, 20(5), pp. 1745–1756. <https://doi.org/10.2166/ws.2020.085>.
- Cohen, K.A. *et al.* (2020) 'Evidence for Expanding the Role of Streptomycin in the Management of Drug-Resistant *Mycobacterium tuberculosis*,' *Antimicrobial Agents and Chemotherapy*, 64(9). <https://doi.org/10.1128/aac.00860-20>.
- Corcoll, N. *et al.* (2017) 'Comparison of four DNA extraction methods for comprehensive assessment of 16S rRNA bacterial diversity in marine biofilms using high-throughput sequencing,' *FEMS Microbiology Letters*, 364(14). <https://doi.org/10.1093/femsle/fnx139>.
- Crouse, J. and Amorese, D., 1987. Ethanol precipitation: ammonium acetate as an alternative to sodium acetate. *Focus*, 9(2), pp.3-5.
- Czekalski, N. *et al.* (2012) 'Increased Levels of Multiresistant Bacteria and Resistance Genes after Wastewater Treatment and Their Dissemination into Lake Geneva, Switzerland,' *Frontiers in Microbiology*, 3. <https://doi.org/10.3389/fmicb.2012.00106>.
- Dalsgaard, A. *et al.* (2000) 'Distribution and Content of Class 1 Integrons in Different *Vibrio cholerae* O-Serotype Strains Isolated in Thailand,' *Antimicrobial Agents and Chemotherapy*, 44(5), pp. 1315–1321. <https://doi.org/10.1128/aac.44.5.1315-1321.2000>.
- Davies, J. and Davies, D. (2010) 'Origins and evolution of antibiotic resistance,' *Microbiology and Molecular Biology Reviews*, 74(3), pp. 417–433. <https://doi.org/10.1128/mnbr.00016-10>.
- Davis, M.B., Shaw, R.G. and Etterson, J.R. (2005) 'Evolutionary Responses To Changing Climate,' *Ecology*, 86(7), pp. 1704–1714. <https://doi.org/10.1890/03-0788>.
- De Paiva, M.C. *et al.* (2015) 'The microbiota and abundance of the Class 1 Integron-Integrase gene in tropical sewage treatment plant influent and activated sludge,' *PLOS ONE*, 10(6), p. e0131532. <https://doi.org/10.1371/journal.pone.0131532>.
- De Silva, S.S., Abery, N.W. and Nguyen, T.T.T. (2007) 'Endemic freshwater finfish of Asia: distribution and conservation status,' *Diversity and Distributions*, 13(2), pp. 172–184. <https://doi.org/10.1111/j.1472-4642.2006.00311.x>.
- Deng, Y. *et al.* (2015) 'Resistance integrons: class 1, 2 and 3 integrons,' *Annals of Clinical Microbiology and Antimicrobials*, 14(1). <https://doi.org/10.1186/s12941-015-0100-6>.
- Dhanasekaran, S., Doherty, T.M. and Kenneth, J. (2010) 'Comparison of different standards for real-time PCR-based absolute quantification,' *Journal of Immunological Methods*, 354(1–2), pp. 34–39. <https://doi.org/10.1016/j.jim.2010.01.004>.

- Die, J.V. *et al.* (2016) 'Design and Sampling Plan optimization for RT-QPCR experiments in plants: A case study in Blueberry,' *Frontiers in Plant Science*, 7. <https://doi.org/10.3389/fpls.2016.00271>.
- Domingues, S., Silva, G. and Nielsen, K.M. (2012) 'Integrans,' *Mobile Genetic Elements*, 2(5), pp. 211–223. <https://doi.org/10.4161/mge.22967>.
- Dube, K., Nhamo, G. and Chikodzi, D. (2022) 'Climate change-induced droughts and tourism: Impacts and responses of Western Cape province, South Africa,' *Journal of Outdoor Recreation and Tourism*, 39, p. 100319. <https://doi.org/10.1016/j.jort.2020.100319>.
- Ekwanzala, M.D. *et al.* (2018) 'Systematic review in South Africa reveals antibiotic resistance genes shared between clinical and environmental settings,' *Infection and Drug Resistance*, Volume 11, pp. 1907–1920. <https://doi.org/10.2147/idr.s170715>.
- El-Ashram, S., Nasr, I.A. and Suo, X. (2016) 'Nucleic acid protocols: Extraction and optimization,' *Biotechnology Reports*, 12, pp. 33–39. <https://doi.org/10.1016/j.btre.2016.10.001>.
- Eramo, A., Medina, W.R.M. and Fahrenfeld, N. (2019) 'Viability-based quantification of antibiotic resistance genes and human fecal markers in wastewater effluent and receiving waters,' *Science of the Total Environment*, 656, pp. 495–502. <https://doi.org/10.1016/j.scitotenv.2018.11.325>.
- Fahrenfeld, N. *et al.* (2013) 'Reclaimed water as a reservoir of antibiotic resistance genes: distribution system and irrigation implications,' *Frontiers in Microbiology*, 4. <https://doi.org/10.3389/fmicb.2013.00130>.
- Fatima, F., Pathak, N. and Verma, S.R. (2014) 'An Improved Method for Soil DNA Extraction to Study the Microbial Assortment within Rhizospheric Region,' *Molecular Biology International*, 2014, pp. 1–6. <https://doi.org/10.1155/2014/518960>.
- Felczykowska, A. *et al.* (2015) 'Sampling, metadata and DNA extraction - important steps in metagenomic studies,' *Acta Biochimica Polonica*, 62(1), pp. 151–160. https://doi.org/10.18388/abp.2014_916.
- Fernando, D.M. *et al.* (2016) 'Detection of Antibiotic Resistance Genes in Source and Drinking Water Samples from a First Nations Community in Canada,' *Applied and Environmental Microbiology*, 82(15), pp. 4767–4775. <https://doi.org/10.1128/aem.00798-16>.
- Fierer, N. *et al.* (2005) 'Assessment of soil microbial community structure by use of Taxon-Specific Quantitative PCR assays,' *Applied and Environmental Microbiology*, 71(7), pp. 4117–4120. <https://doi.org/10.1128/aem.71.7.4117-4120.2005>.

- Fleige, S. and Pfaffl, M.W. (2006) 'RNA integrity and the effect on the real-time qRT-PCR performance,' *Molecular Aspects of Medicine*, 27(2–3), pp. 126–139. <https://doi.org/10.1016/j.mam.2005.12.003>.
- Foka, F.E.T., Kumar, A. and Ateba, C.N. (2018) 'Emergence of vancomycin-resistant enterococci in South Africa: Implications for public health,' *South African Journal of Science*, 114(9/10). <https://doi.org/10.17159/sajs.2018/4508>.
- Gambino, G., Perrone, I. and Gribaudo, I. (2008) 'A Rapid and effective method for RNA extraction from different tissues of grapevine and other woody plants,' *Phytochemical Analysis*, 19(6), pp. 520–525. <https://doi.org/10.1002/pca.1078>.
- Garibyan, L. and Avashia, N. (2013) 'Polymerase chain reaction,' *Journal of Investigative Dermatology*, 133(3), pp. 1–4. <https://doi.org/10.1038/jid.2013.1>.
- Ghaitidak, D.M. and Yadav, K.D. (2013) 'Characteristics and treatment of greywater—a review,' *Environmental Science and Pollution Research*, 20(5), pp. 2795–2809. <https://doi.org/10.1007/s11356-013-1533-0>.
- Ghaly, T.M. et al. (2020) 'The Peril and Promise of integrons: Beyond antibiotic resistance,' *Trends in Microbiology*, 28(6), pp. 455–464. <https://doi.org/10.1016/j.tim.2019.12.002>.
- Gillings, M.R. (2014) 'Integrons: past, present, and future,' *Microbiology and Molecular Biology Reviews*, 78(2), pp. 257–277. <https://doi.org/10.1128/mubr.00056-13>.
- Gillings, M.R., Holley, M. and Stokes, H.W. (2009) 'Evidence for dynamic exchange of *qac* gene cassettes between class 1 integrons and other integrons in freshwater biofilms,' *FEMS Microbiology Letters*, 296(2), pp. 282–288. <https://doi.org/10.1111/j.1574-6968.2009.01646.x>.
- Gomes, A.É.I. et al. (2018) 'Selection and validation of reference genes for gene expression studies in *Klebsiella pneumoniae* using Reverse Transcription Quantitative real-time PCR,' *Scientific Reports*, 8(1). <https://doi.org/10.1038/s41598-018-27420-2>.
- Guerra, M.E.S. et al. (2022) '*Klebsiella pneumoniae* Biofilms and Their Role in Disease Pathogenesis,' *Frontiers in Cellular and Infection Microbiology*, 12. <https://doi.org/10.3389/fcimb.2022.877995>.
- Hall, M. a. L. et al. (2003) 'Multidrug Resistance among Enterobacteriaceae Is Strongly Associated with the Presence of Integrons and Is Independent of Species or Isolate Origin,' *The Journal of Infectious Diseases*, 187(2), pp. 251–259. <https://doi.org/10.1086/345880>.
- Hall, R.M. and Collis, C.M. (1995) 'Mobile gene cassettes and integrons: capture and spread of genes by site-specific recombination,' *Molecular Microbiology*, 15(4), pp. 593–600. <https://doi.org/10.1111/j.1365-2958.1995.tb02368.x>.

- Hardwick, S.A. *et al.* (2008) 'Quantification of class 1 integron abundance in natural environments using real-time quantitative PCR,' *FEMS Microbiology Letters*, 278(2), pp. 207–212. <https://doi.org/10.1111/j.1574-6968.2007.00992.x>.
- Hatt, J.K. and Löffler, F.E. (2012) 'Quantitative real-time PCR (qPCR) detection chemistries affect enumeration of the *Dehalococcoides* 16S rRNA gene in groundwater,' *Journal of Microbiological Methods*, 88(2), pp. 263–270. <https://doi.org/10.1016/j.mimet.2011.12.005>.
- Hazra, M. *et al.* (2022) 'Antibiotics and antibiotic resistant bacteria/genes in urban wastewater: A comparison of their fate in conventional treatment systems and constructed wetlands,' *Chemosphere*, 303, p. 135148. <https://doi.org/10.1016/j.chemosphere.2022.135148>.
- Henderson, M. *et al.* (2022) 'Occurrence of Antibiotic-Resistant genes and bacteria in household greywater treated in constructed wetlands,' *Water*, 14(5), p. 758. <https://doi.org/10.3390/w14050758>.
- Henriques, I. *et al.* (2006) 'Occurrence and diversity of integrons and β -lactamase genes among ampicillin-resistant isolates from estuarine waters,' *Research in Microbiology*, 157(10), pp. 938–947. <https://doi.org/10.1016/j.resmic.2006.09.003>.
- Hill, V.R. *et al.* (2015) 'Development of a Nucleic Acid Extraction Procedure for Simultaneous Recovery of DNA and RNA from Diverse Microbes in Water,' *Pathogens*, 4(2), pp. 335–354. <https://doi.org/10.3390/pathogens4020335>.
- Hinlo, R. *et al.* (2017) 'Methods to maximise recovery of environmental DNA from water samples,' *PLOS ONE*, 12(6), p. e0179251. <https://doi.org/10.1371/journal.pone.0179251>.
- Hwang, C. *et al.* (2012) 'Evaluation of Methods for the Extraction of DNA from Drinking Water Distribution System Biofilms,' *Microbes and Environments*, 27(1), pp. 9–18. <https://doi.org/10.1264/jsme2.me11132>.
- Itzhari, D. and Ronen, Z. (2023) 'The emergence of antibiotics resistance genes, bacteria, and micropollutants in grey wastewater,' *Applied Sciences*, 13(4), p. 2322. <https://doi.org/10.3390/app13042322>.
- Iweriebor, B.C., Chikwelu, L. and Okoh, A.I. (2015) 'Virulence and antimicrobial resistance factors of *Enterococcus* spp. isolated from fecal samples from piggery farms in Eastern Cape, South Africa,' *BMC Microbiology*, 15(1). <https://doi.org/10.1186/s12866-015-0468-7>.
- Jacobs, L. and Chenia, H.Y. (2007) 'Characterization of integrons and tetracycline resistance determinants in *Aeromonas* spp. isolated from South African aquaculture systems,' *International Journal of Food Microbiology*, 114(3), pp. 295–306. <https://doi.org/10.1016/j.ijfoodmicro.2006.09.030>.

- Jahn, C.E., Charkowski, A.O. and Willis, D.K. (2008) 'Evaluation of isolation methods and RNA integrity for bacterial RNA quantitation,' *Journal of Microbiological Methods*, 75(2), pp. 318–324. <https://doi.org/10.1016/j.mimet.2008.07.004>.
- Jaja, I.F. *et al.* (2020) 'Prevalence and distribution of antimicrobial resistance determinants of *Escherichia coli* isolates obtained from meat in South Africa,' *PLOS ONE*, 15(5), p. e0216914. <https://doi.org/10.1371/journal.pone.0216914>.
- Jansson, J.K. and Leser, T.D. (1996) 'Quantitative PCR of environmental samples,' in *Springer eBooks*, pp. 43–61. https://doi.org/10.1007/978-94-009-0215-2_5.
- Jiang, M. *et al.* (2023) 'Ampicillin-controlled glucose metabolism manipulates the transition from tolerance to resistance in bacteria,' *Science Advances*, 9(10). <https://doi.org/10.1126/sciadv.ade8582>.
- Jones-Dias, D. *et al.* (2016) 'Architecture of Class 1, 2, and 3 Integrons from Gram Negative Bacteria Recovered among Fruits and Vegetables,' *Frontiers in Microbiology*, 7. <https://doi.org/10.3389/fmicb.2016.01400>.
- Kállai, A. *et al.* (2021) 'MICy: a Novel Flow Cytometric Method for Rapid Determination of Minimal Inhibitory Concentration,' *Microbiology Spectrum*, 9(3). <https://doi.org/10.1128/spectrum.00901-21>.
- Karaoğlu, Ş.A. *et al.* (2007) 'Investigation of antibiotic resistance profile and TEM-type β -lactamase gene carriage of ampicillin-resistant *Escherichia coli* strains isolated from drinking water,' *Annals of Microbiology*, 57(2), pp. 281–288. <https://doi.org/10.1007/bf03175221>.
- Khan, F.A., Söderquist, B. and Jaß, J. (2019) 'Prevalence and diversity of antibiotic resistance genes in Swedish aquatic environments impacted by household and hospital wastewater,' *Frontiers in Microbiology*, 10. <https://doi.org/10.3389/fmicb.2019.00688>.
- Khan, S. *et al.* (2016) 'Role of recombinant DNA technology to improve life,' *International Journal of Genomics*, 2016, pp. 1–14. <https://doi.org/10.1155/2016/2405954>.
- Khan, Z.A., Siddiqui, M.F. and Park, S. (2019) 'Current and emerging methods of antibiotic susceptibility testing,' *Diagnostics*, 9(2), p. 49. <https://doi.org/10.3390/diagnostics9020049>.
- King, D.T., Sobhanifar, S. and Strynadka, N.C.J. (2016) 'One ring to rule them all: Current trends in combating bacterial resistance to the β -lactams,' *Protein Science*, 25(4), pp. 787–803. <https://doi.org/10.1002/pro.2889>.
- Koch, N. *et al.* (2021) 'Environmental antibiotics and resistance genes as emerging contaminants: Methods of detection and bioremediation,' *Current Research in Microbial Sciences*, 2, p. 100027. <https://doi.org/10.1016/j.crmicr.2021.100027>.

- Koczura, R. *et al.* (2016) 'Abundance of Class 1 Integron-Integrase and sulfonamide resistance genes in river water and sediment is affected by anthropogenic pressure and environmental factors,' *Microbial Ecology*, 72(4), pp. 909–916. <https://doi.org/10.1007/s00248-016-0843-4>.
- Koenig, J.E. *et al.* (2008) 'Integron-associated gene cassettes in Halifax Harbour: assessment of a mobile gene pool in marine sediments,' *Environmental Microbiology*, 10(4), pp. 1024–1038. <https://doi.org/10.1111/j.1462-2920.2007.01524.x>.
- Król, J. *et al.* (2011) 'Increased Transfer of a Multidrug Resistance Plasmid in *Escherichia coli* Biofilms at the Air-Liquid Interface,' *Applied and Environmental Microbiology*, 77(15), pp. 5079–5088. <https://doi.org/10.1128/aem.00090-11>.
- Lee, C. *et al.* (2006) 'Absolute and relative QPCR quantification of plasmid copy number in *Escherichia coli*,' *Journal of Biotechnology*, 123(3), pp. 273–280. <https://doi.org/10.1016/j.jbiotec.2005.11.014>.
- Lee, J. *et al.* (2017) 'Quantitative and qualitative changes in antibiotic resistance genes after passing through treatment processes in municipal wastewater treatment plants,' *Science of the Total Environment*, 605–606, pp. 906–914. <https://doi.org/10.1016/j.scitotenv.2017.06.250>.
- Leonard, M.M. *et al.* (2016) 'Field study of the composition of greywater and comparison of microbiological indicators of water quality in on-site systems,' *Environmental Monitoring and Assessment*, 188(8). <https://doi.org/10.1007/s10661-016-5442-9>.
- Lerminiaux, N.A. and Cameron, A.D.S. (2019) 'Horizontal transfer of antibiotic resistance genes in clinical environments,' *Canadian Journal of Microbiology*, 65(1), pp. 34–44. <https://doi.org/10.1139/cjm-2018-0275>.
- Lever, M.A. *et al.* (2015) 'A modular method for the extraction of DNA and RNA, and the separation of DNA pools from diverse environmental sample types,' *Frontiers in Microbiology*, 6. <https://doi.org/10.3389/fmicb.2015.00476>.
- Li, W. *et al.* (2012) 'Transposable elements in TDP-43-Mediated Neurodegenerative Disorders,' *PLOS ONE*, 7(9), p. e44099. <https://doi.org/10.1371/journal.pone.0044099>.
- Lim, N.Y.N., Roco, C.A. and Frostegård, Å. (2016) 'Transparent DNA/RNA co-extraction workflow protocol suitable for Inhibitor-Rich environmental samples that focuses on complete DNA removal for transcriptomic analyses,' *Frontiers in Microbiology*, 7. <https://doi.org/10.3389/fmicb.2016.01588>.
- Liu, Z. *et al.* (2018) 'Neutral mechanisms and niche differentiation in steady-state insular microbial communities revealed by single cell analysis,' *Environmental Microbiology*, 21(1), pp. 164–181. <https://doi.org/10.1111/1462-2920.14437>.
- Lochan, H. *et al.* (2016) 'Emergence of vancomycin-resistant *Enterococcus* at a tertiary paediatric hospital in South Africa,' *South African Medical Journal*, 106(6), p. 562. <https://doi.org/10.7196/samj.2016.v106i6.10858>.

- Luby, E.M. *et al.* (2016) 'Molecular Methods for Assessment of Antibiotic Resistance in Agricultural ecosystems: Prospects and challenges,' *Journal of Environmental Quality*, 45(2), pp. 441–453. <https://doi.org/10.2134/jeq2015.07.0367>.
- Lucassen, R. *et al.* (2019) 'Strong correlation of total phenotypic resistance of samples from household environments and the prevalence of class 1 integrons suggests for the use of the relative prevalence of *intI1* as a screening tool for multi-resistance,' *PLOS ONE*, 14(6), p. e0218277. <https://doi.org/10.1371/journal.pone.0218277>.
- Luo, Y. *et al.* (2010) 'Trends in antibiotic resistance genes occurrence in the Haihe River, China,' *Environmental Science & Technology*, 44(19), pp. 7220–7225. <https://doi.org/10.1021/es100233w>.
- Luo, Y. *et al.* (2010) 'Trends in antibiotic resistance genes occurrence in the Haihe River, China,' *Environmental Science & Technology*, 44(19), pp. 7220–7225. <https://doi.org/10.1021/es100233w>.
- Lupo, A., Coyne, S. and Berendonk, T.U. (2012) 'Origin and evolution of antibiotic resistance: the common mechanisms of emergence and spread in water bodies,' *Frontiers in Microbiology*, 3. <https://doi.org/10.3389/fmicb.2012.00018>.
- Ma, Z. *et al.* (2015) 'Isolation of High-Quality Total RNA from Chinese Fir (*Cunninghamia lanceolata* (Lamb.) Hook),' *PLOS ONE*, 10(6), p. e0130234. <https://doi.org/10.1371/journal.pone.0130234>.
- Mackie, R.I. *et al.* (2006) 'Tetracycline residues and tetracycline resistance genes in groundwater impacted by swine production facilities,' *Animal Biotechnology*, 17(2), pp. 157–176. <https://doi.org/10.1080/10495390600956953>.
- Madsen, J.S. *et al.* (2012) 'The interconnection between biofilm formation and horizontal gene transfer,' *Fems Immunology and Medical Microbiology*, 65(2), pp. 183–195. <https://doi.org/10.1111/j.1574-695x.2012.00960.x>.
- Mahlalela, P. *et al.* (2020) 'Drought in the Eastern Cape region of South Africa and trends in rainfall characteristics,' *Climate Dynamics*, 55(9–10), pp. 2743–2759. <https://doi.org/10.1007/s00382-020-05413-0>.
- Maimon, A. *et al.* (2010) 'Safe On-Site reuse of greywater for irrigation - A critical review of current guidelines,' *Environmental Science & Technology*, 44(9), pp. 3213–3220. <https://doi.org/10.1021/es902646g>.
- Maimon, A., Friedler, E. and Gross, A. (2014) 'Parameters affecting greywater quality and its safety for reuse,' *Science of the Total Environment*, 487, pp. 20–25. <https://doi.org/10.1016/j.scitotenv.2014.03.133>.

- Malek, M.M. *et al.* (2015) 'Occurrence of classes I and II integrons in *Enterobacteriaceae* collected from Zagazig University Hospitals, Egypt,' *Frontiers in Microbiology*, 6. <https://doi.org/10.3389/fmicb.2015.00601>.
- Măruțescu, L. (2023) 'Current and future flow cytometry applications contributing to antimicrobial resistance control,' *Microorganisms*, 11(5), p. 1300. <https://doi.org/10.3390/microorganisms11051300>.
- Mazel, Didier. (2004). Integrons and the origin of antibiotic resistance gene cassettes. *ASM news*. 70. 520-525.
- McKenney, P.T. *et al.* (2016) 'Complete Genome Sequence of *Enterococcus faecium* ATCC 700221,' *Genome Announcements*, 4(3). <https://doi.org/10.1128/genomea.00386-16>.
- McLain, J.E. *et al.* (2016) 'Culture-based methods for detection of antibiotic resistance in agroecosystems: Advantages, challenges, and gaps in knowledge,' *Journal of Environmental Quality*, 45(2), pp. 432–440. <https://doi.org/10.2134/jeq2015.06.0317>.
- McMillan, M. and Pereg, L. (2014) 'Evaluation of Reference Genes for Gene Expression Analysis Using Quantitative RT-PCR in *Azospirillum brasilense*,' *PLOS ONE*, 9(5), p. e98162. <https://doi.org/10.1371/journal.pone.0098162>.
- Meissner, Richard & Jacobs-Mata, Inga & Nohayi, Ngowenani. (2017). South Africa's Drought and the Role of Public Engagement in Water Saving in the City of Tshwane. 10.13140/RG.2.2.23623.60329.
- Messi, P. *et al.* (2006) 'Vancomycin-resistant enterococci (VRE) in meat and environmental samples,' *International Journal of Food Microbiology*, 107(2), pp. 218–222. <https://doi.org/10.1016/j.ijfoodmicro.2005.08.026>.
- Meza, I. *et al.* (2021) 'Drought risk for agricultural systems in South Africa: Drivers, spatial patterns, and implications for drought risk management,' *Science of the Total Environment*, 799, p. 149505. <https://doi.org/10.1016/j.scitotenv.2021.149505>.
- Mohapatra, H. *et al.* (2008) 'Vibrio cholerae non-O1, non-O139 strains isolated before 1992 from Varanasi, India are multiple drug resistant, contain intSXT, dfr18 and aadA5 genes,' *Environmental Microbiology*, 10(4), pp. 866–873. <https://doi.org/10.1111/j.1462-2920.2007.01502.x>.
- Mtsetwa, H.N. *et al.* (2021) 'Wastewater-Based Surveillance of Antibiotic Resistance Genes Associated with Tuberculosis Treatment Regimen in KwaZulu Natal, South Africa,' *Antibiotics*, 10(11), p. 1362. <https://doi.org/10.3390/antibiotics10111362>.
- Mukherjee, S. and Chakraborty, R. (2006) 'Incidence of class 1 integrons in multiple antibiotic-resistant Gram-negative copiotrophic bacteria from the River Torsa in India,' *Research in Microbiology*, 157(3), pp. 220–226. <https://doi.org/10.1016/j.resmic.2005.08.003>.

- Mulroney, K.T. *et al.* (2022) 'Same-day confirmation of infection and antimicrobial susceptibility profiling using flow cytometry,' *EBioMedicine*, 82, p. 104145. <https://doi.org/10.1016/j.ebiom.2022.104145>.
- Nappier, S.P. *et al.* (2020) 'Antibiotic Resistance in Recreational Waters: State of the science,' *International Journal of Environmental Research and Public Health*, 17(21), p. 8034. <https://doi.org/10.3390/ijerph17218034>.
- Navarro, E. *et al.* (2015) 'Real-time PCR detection chemistry,' *Clinica Chimica Acta*, 439, pp. 231–250. <https://doi.org/10.1016/j.cca.2014.10.017>.
- Nilsen, T.W. (2013) 'The fundamentals of RNA purification,' *CSH Protocols*, 2013(7), p. pdb.top075838. <https://doi.org/10.1101/pdb.top075838>.
- Noman, E.A. *et al.* (2022) 'Antibiotics and antibiotic-resistant bacteria in greywater: Challenges of the current treatment situation and predictions of future scenario,' *Environmental Research*, 212, p. 113380. <https://doi.org/10.1016/j.envres.2022.113380>.
- O'Toole, J.E. *et al.* (2012) 'Microbial quality assessment of household greywater,' *Water Research*, 46(13), pp. 4301–4313. <https://doi.org/10.1016/j.watres.2012.05.001>.
- Odoulami, R.C., Wolski, P. and New, M. (2020) 'A SOM-based analysis of the drivers of the 2015–2017 Western Cape drought in South Africa,' *International Journal of Climatology*, 41(S1). <https://doi.org/10.1002/joc.6785>.
- Park, J.C. *et al.* (2003) 'Antibiotic selective pressure for the maintenance of antibiotic resistant genes in coliform bacteria isolated from the aquatic environment,' *Water Science and Technology*, 47(3), pp. 249–253. <https://doi.org/10.2166/wst.2003.0203>.
- Pascale, S. *et al.* (2020) 'Increasing risk of another Cape Town “Day Zero” drought in the 21st century,' *Proceedings of the National Academy of Sciences of the United States of America*, 117(47), pp. 29495–29503. <https://doi.org/10.1073/pnas.2009144117>.
- Pei, R. *et al.* (2006) 'Effect of River Landscape on the sediment concentrations of antibiotics and corresponding antibiotic resistance genes (ARG),' *Water Research*, 40(12), pp. 2427–2435. <https://doi.org/10.1016/j.watres.2006.04.017>.
- Petrovich, M. *et al.* (2018) 'Antibiotic resistance genes show enhanced mobilization through suspended growth and biofilm-based wastewater treatment processes,' *FEMS Microbiology Ecology*, 94(5). <https://doi.org/10.1093/femsec/fiy041>.
- Pinto, F. *et al.* (2012) 'Selection of suitable reference genes for RT-QPCR analyses in cyanobacteria,' *PLOS ONE*, 7(4), p. e34983. <https://doi.org/10.1371/journal.pone.0034983>.
- Ploy, M.-C. *et al.* (2000) 'Integrins: an Antibiotic Resistance Gene Capture and Expression System,' *Clinical Chemistry and Laboratory Medicine*, 38(6), pp. 483–487. <https://doi.org/10.1515/cclm.2000.070>.

- Ponchel, F. *et al.* (2003) 'Real-time PCR based on SYBR-Green I Fluorescence: an alternative to the TAQMan assay for a relative quantification of gene rearrangements, gene amplifications and micro gene deletions,' *BMC Biotechnology*, 3(1), p. 18. <https://doi.org/10.1186/1472-6750-3-18>.
- Poppe, C. *et al.* (2006) 'Characterization of antimicrobial resistance of Salmonella Newport isolated from animals, the environment, and animal food products in Canada.,' *PubMed* [Preprint]. <https://pubmed.ncbi.nlm.nih.gov/16639942>.
- Porob, S. *et al.* (2020) 'Quantification and characterization of antimicrobial resistance in greywater discharged to the environment,' *Water*, 12(5), p. 1460. <https://doi.org/10.3390/w12051460>.
- Rahman, Md.H. *et al.* (2008) 'Occurrence of Two Genotypes of Tetracycline (TC) Resistance Gene tet(M) in the TC-Resistant Bacteria in Marine Sediments of Japan,' *Environmental Science & Technology*, 42(14), pp. 5055–5061. <https://doi.org/10.1021/es702986y>.
- Rawlins, J. (2019) 'Political economy of water reallocation in South Africa: Insights from the Western Cape water crisis,' *Water Security*, 6, p. 100029. <https://doi.org/10.1016/j.wasec.2019.100029>.
- Rio, D.C. *et al.* (2010a) 'Determining the yield and quality of purified RNA,' *CSH Protocols*, 2010(6), p. pdb.top82. <https://doi.org/10.1101/pdb.top82>.
- Rio, D.C. *et al.* (2010b) 'Ethanol precipitation of RNA and the use of carriers,' *CSH Protocols*, 2010(6), p. pdb.prot5440. <https://doi.org/10.1101/pdb.prot5440>.
- Rio, D.C. *et al.* (2010c) 'Nondenaturing Agarose gel electrophoresis of RNA,' *CSH Protocols*, 2010(6), p. pdb.prot5445. <https://doi.org/10.1101/pdb.prot5445>.
- Robertson, J. *et al.* (2019) 'Optimisation of the protocol for the LIVE/DEAD® BacLight™ Bacterial Viability Kit for rapid determination of bacterial load,' *Frontiers in Microbiology*, 10. <https://doi.org/10.3389/fmicb.2019.00801>.
- Robertson, J. *et al.* (2021) 'Rapid Detection of Escherichia coli Antibiotic Susceptibility Using Live/Dead Spectrometry for Lytic Agents,' *Microorganisms*, 9(5), p. 924. <https://doi.org/10.3390/microorganisms9050924>.
- Rocha, D.J.P.G., Santos, C.S.A.B. and Pacheco, L.G.C. (2015) 'Bacterial reference genes for gene expression studies by RT-qPCR: survey and analysis,' *Antonie Van Leeuwenhoek*, 108(3), pp. 685–693. <https://doi.org/10.1007/s10482-015-0524-1>.
- Rocha, J. *et al.* (2019) 'Comparison of culture- and quantitative PCR-Based indicators of antibiotic resistance in wastewater, recycled water, and tap water,' *International Journal of Environmental Research and Public Health*, 16(21), p. 4217. <https://doi.org/10.3390/ijerph16214217>.

- Rosewarne, C.P. *et al.* (2010) 'Class 1 integrons in benthic bacterial communities: abundance, association with Tn402-like transposition modules and evidence for coselection with heavy-metal resistance,' *FEMS Microbiology Ecology*, 72(1), pp. 35–46. <https://doi.org/10.1111/j.1574-6941.2009.00823.x>.
- Rubinstein, E. and Keynan, Y. (2014) 'Vancomycin Revisited: 60 Years Later,' *Frontiers in Public Health*, 2. <https://doi.org/10.3389/fpubh.2014.00217>.
- Safford, H. and Bischel, H.N. (2019) 'Flow cytometry applications in water treatment, distribution, and reuse: A review,' *Water Research*, 151, pp. 110–133. <https://doi.org/10.1016/j.watres.2018.12.016>.
- Salam, Md.A. *et al.* (2023) 'Conventional methods and future trends in antimicrobial susceptibility testing,' *Saudi Journal of Biological Sciences*, 30(3), p. 103582. <https://doi.org/10.1016/j.sjbs.2023.103582>.
- Santajit, S. and Indrawattana, N. (2016) 'Mechanisms of antimicrobial resistance in ESKAPE pathogens,' *BioMed Research International*, 2016, pp. 1–8. <https://doi.org/10.1155/2016/2475067>.
- Schlüter, A. *et al.* (2005) 'Plasmid pB8 is closely related to the prototype IncP-1 β plasmid R751 but transfers poorly to *Escherichia coli* and carries a new transposon encoding a small multidrug resistance efflux protein,' *Plasmid*, 54(2), pp. 135–148. <https://doi.org/10.1016/j.plasmid.2005.03.001>.
- Schwartz, T. *et al.* (2003) 'Detection of antibiotic-resistant bacteria and their resistance genes in wastewater, surface water, and drinking water biofilms,' *FEMS Microbiology Ecology*, 43(3), pp. 325–335. <https://doi.org/10.1111/j.1574-6941.2003.tb01073.x>.
- Scott, L., Lee, N. and Aw, T.G. (2020) 'Antibiotic resistance in minimally Human-Impacted environments,' *International Journal of Environmental Research and Public Health*, 17(11), p. 3939. <https://doi.org/10.3390/ijerph17113939>.
- Sekyere, J.O. (2016) 'Current State of Resistance to Antibiotics of Last-Resort in South Africa: A Review from a Public Health Perspective,' *Frontiers in Public Health*, 4. <https://doi.org/10.3389/fpubh.2016.00209>.
- Shannon, K. *et al.* (2007) 'Application of real-time quantitative PCR for the detection of selected bacterial pathogens during municipal wastewater treatment,' *Science of the Total Environment*, 382(1), pp. 121–129. <https://doi.org/10.1016/j.scitotenv.2007.02.039>.
- Shin, H. *et al.* (2022) 'Resistome study in aquatic environments,' *Journal of Microbiology and Biotechnology*, 33(3), pp. 277–287. <https://doi.org/10.4014/jmb.2210.10044>.
- Simister, R.L., Schmitt, S. and Taylor, M.W. (2011) 'Evaluating methods for the preservation and extraction of DNA and RNA for analysis of microbial communities in marine sponges,' *Journal*

- of *Experimental Marine Biology and Ecology*, 397(1), pp. 38–43.
<https://doi.org/10.1016/j.jembe.2010.11.004>.
- Singh, A.K. *et al.* (2022) 'Antimicrobials and antibiotic resistance genes in water bodies: Pollution, risk, and control,' *Frontiers in Environmental Science*, 10.
<https://doi.org/10.3389/fenvs.2022.830861>.
- Sorensen, P. (2017) 'The chronic water shortage in Cape Town and survival strategies,' *International Journal of Environmental Studies*, 74(4), pp. 515–527.
<https://doi.org/10.1080/00207233.2017.1335019>.
- Stafford, L. *et al.* (2019). The Greater Cape Town Water Fund: Assessing The Return On Investment For Ecological Infrastructure Restoration. 10.13140/RG.2.2.23814.11844.
- Stalder, T. *et al.* (2012) 'Integron involvement in environmental spread of antibiotic resistance,' *Frontiers in Microbiology*, 3. <https://doi.org/10.3389/fmicb.2012.00119>.
- Stokes, H.W. *et al.* (2006) 'Class 1 Integrons Potentially Predating the Association with Tn 402 -Like Transposition Genes Are Present in a Sediment Microbial Community,' *Journal of Bacteriology*, 188(16), pp. 5722–5730. <https://doi.org/10.1128/jb.01950-05>.
- Sunde, M. and Norström, M. (2005) 'The genetic background for streptomycin resistance in *Escherichia coli* influences the distribution of MICs,' *Journal of Antimicrobial Chemotherapy*, 56(1), pp. 87–90. <https://doi.org/10.1093/jac/dki150>.
- Švec, D. *et al.* (2015) 'How good is a PCR efficiency estimate: Recommendations for precise and robust qPCR efficiency assessments,' *Biomolecular Detection and Quantification*, 3, pp. 9–16.
<https://doi.org/10.1016/j.bdq.2015.01.005>.
- Takle, G.W., Toth, I.K. and Brurberg, M.B. (2007) 'Evaluation of reference genes for real-time RT-PCR expression studies in the plant pathogen *Pectobacterium atrosepticum*,' *BMC Plant Biology*, 7(1). <https://doi.org/10.1186/1471-2229-7-50>.
- Tamma, P.D. *et al.* (2019) 'A primer on AMPC B-Lactamases: Necessary knowledge for an increasingly multidrug-resistant world,' *Clinical Infectious Diseases*, 69(8), pp. 1446–1455.
<https://doi.org/10.1093/cid/ciz173>.
- Tan, S.C. and Yiap, B.C. (2009) 'DNA, RNA, and protein extraction: The past and the present,' *Journal of Biomedicine and Biotechnology*, 2009, pp. 1–10. <https://doi.org/10.1155/2009/574398>.
- Tanaka, Y., Yamaguchi, N. and Nasu, M. (2000) 'Viability of *Escherichia coli* O157:H7 in natural river water determined by the use of flow cytometry,' *Journal of Applied Microbiology*, 88(2), pp. 228–236. <https://doi.org/10.1046/j.1365-2672.2000.00960.x>.

- Taviani, E. *et al.* (2008) 'Environmental *Vibrio* spp., isolated in Mozambique, contain a polymorphic group of integrative conjugative elements and class 1 integrons,' *FEMS Microbiology Ecology*, 64(1), pp. 45–54. <https://doi.org/10.1111/j.1574-6941.2008.00455.x>.
- Tennstedt, T. *et al.* (2003) 'Occurrence of integron-associated resistance gene cassettes located on antibiotic resistance plasmids isolated from a wastewater treatment plant,' *FEMS Microbiology Ecology*, 45(3), pp. 239–252. [https://doi.org/10.1016/s0168-6496\(03\)00164-8](https://doi.org/10.1016/s0168-6496(03)00164-8).
- Toni, L.S. *et al.* (2018) 'Optimization of phenol-chloroform RNA extraction,' *MethodsX*, 5, pp. 599–608. <https://doi.org/10.1016/j.mex.2018.05.011>.
- Troiano, E. *et al.* (2018) 'Antibiotic-Resistant bacteria in greywater and Greywater-Irrigated soils,' *Frontiers in Microbiology*, 9. <https://doi.org/10.3389/fmicb.2018.02666>.
- Trujillo, C.A. *et al.* (2021) 'Reintroduction of the archaic variant of NOVA1 in cortical organoids alters neurodevelopment,' *Science*, 371(6530). <https://doi.org/10.1126/science.aax2537>.
- Van Boeckel, T.P. *et al.* (2014) 'Global antibiotic consumption 2000 to 2010: an analysis of national pharmaceutical sales data,' *The Lancet Infectious Diseases*, 14(8), pp. 742–750. [https://doi.org/10.1016/s1473-3099\(14\)70780-7](https://doi.org/10.1016/s1473-3099(14)70780-7).
- Vaz-Moreira, I., Nunes, O.C. and Manaia, C.M. (2017) 'Ubiquitous and persistent Proteobacteria and other Gram-negative bacteria in drinking water,' *Science of the Total Environment*, 586, pp. 1141–1149. <https://doi.org/10.1016/j.scitotenv.2017.02.104>.
- Ventola CL. The antibiotic resistance crisis: part 1: causes and threats. P T. 2015 Apr;40(4):277-83. PMID: 25859123; PMCID: PMC4378521.
- Vineetha, G. *et al.* (2015) 'Seasonal dynamics of the copepod community in a tropical monsoonal estuary and the role of sex ratio in their abundance pattern,' *Zoological Studies*, 54(1). <https://doi.org/10.1186/s40555-015-0131-x>.
- Volkman, H. *et al.* (2004) 'Detection of clinically relevant antibiotic-resistance genes in municipal wastewater using real-time PCR (TaqMan),' *Journal of Microbiological Methods*, 56(2), pp. 277–286. <https://doi.org/10.1016/j.mimet.2003.10.014>.
- Wang, X. *et al.* (2018) 'Abundances of clinically relevant antibiotic resistance genes and bacterial community diversity in the Weihe River, China,' *International Journal of Environmental Research and Public Health*, 15(4), p. 708. <https://doi.org/10.3390/ijerph15040708>.
- Webber, D., Wallace, M.A. and Burnham, C.D. (2022) 'Stop Waiting for Tomorrow: Disk Diffusion Performed on Early Growth Is an Accurate Method for Antimicrobial Susceptibility Testing with Reduced Turnaround Time,' *Journal of Clinical Microbiology*, 60(5). <https://doi.org/10.1128/jcm.03007-20>.

- Weingarten, R.A. *et al.* (2018) 'Genomic analysis of hospital plumbing reveals diverse reservoir of bacterial plasmids conferring carbapenem resistance,' *MBio*, 9(1). <https://doi.org/10.1128/mbio.02011-17>.
- Wilde, F.D. and Radtke, D.B. (1998) *Handbooks for water-resources investigations: National field manual for the collection of water-quality data. Field measurements.*
- Winder, L.M. *et al.* (2010) 'Evaluation of DNA melting analysis as a tool for species identification,' *Methods in Ecology and Evolution*, 2(3), pp. 312–320. <https://doi.org/10.1111/j.2041-210x.2010.00079.x>.
- Winward, G.P. *et al.* (2008) 'A study of the microbial quality of grey water and an evaluation of treatment technologies for reuse,' *Ecological Engineering*, 32(2), pp. 187–197. <https://doi.org/10.1016/j.ecoleng.2007.11.001>.
- Woolhouse, M. *et al.* (2016) 'Global disease burden due to antibiotic resistance – state of the evidence,' *Journal of Global Health*, 6(1). <https://doi.org/10.7189/jogh.06.010306>.
- Yang, S. and Carlson, K. (2003) 'Evolution of antibiotic occurrence in a river through pristine, urban and agricultural landscapes,' *Water Research*, 37(19), pp. 4645–4656. [https://doi.org/10.1016/s0043-1354\(03\)00399-3](https://doi.org/10.1016/s0043-1354(03)00399-3).
- Zhang, H. *et al.* (2020) 'PCR multiplexing based on a single fluorescent channel using dynamic melting curve analysis,' *ACS Omega*, 5(46), pp. 30267–30273. <https://doi.org/10.1021/acsomega.0c04766>.
- Zhang, K. *et al.* (2022) 'Characterization of antibiotic resistance genes in drinking water sources of the Douhe Reservoir, Tangshan, northern China: the correlation with bacterial communities and environmental factors,' *Environmental Sciences Europe*, 34(1). <https://doi.org/10.1186/s12302-022-00635-x>.
- Zhang, S. *et al.* (2020) 'Dissemination of antibiotic resistance genes (ARGs) via integrons in *Escherichia coli*: A risk to human health,' *Environmental Pollution*, 266, p. 115260. <https://doi.org/10.1016/j.envpol.2020.115260>.
- Zhang, S., Lin, W. and Yu, X. (2016) 'Effects of full-scale advanced water treatment on antibiotic resistance genes in the Yangtze Delta area in China,' *FEMS Microbiology Ecology*, 92(5), p. fiw065. <https://doi.org/10.1093/femsec/fiw065>.
- Zhang, X. *et al.* (2009) 'Class 1 integronase gene and tetracycline resistance genes *tetA* and *tetC* in different water environments of Jiangsu Province, China,' *Ecotoxicology*, 18(6), pp. 652–660. <https://doi.org/10.1007/s10646-009-0332-3>.
- Zheng, W. *et al.* (2020) 'Clinical class 1 integron-integrase gene – A promising indicator to monitor the abundance and elimination of antibiotic resistance genes in an urban wastewater treatment

plant,' *Environment International*, 135, p. 105372.
<https://doi.org/10.1016/j.envint.2019.105372>.

Zhu, B. (2007). Abundance dynamics and sequence variation of neomycin phosphotransferase gene (*nptII*) homologs in river water. *Aquatic Microbial Ecology*, 48, 131-140.



Appendix A – Chapter 2

Table A: Zone of Inhibition Criteria used to evaluate greywater and biofilm samples

Species	<i>Enterobacteriales</i>			<i>Enterococcus</i>			<i>Staphylococcus</i>		
	<i>Susceptible (S)</i>	<i>Intermediate (I)</i>	<i>Resistant (R)</i>	<i>Susceptible (S)</i>	<i>Intermediate (I)</i>	<i>Resistant (R)</i>	<i>Susceptible (S)</i>	<i>Intermediate (I)</i>	<i>Resistant (R)</i>
Streptomycin	≥ 15mm	12-14 mm	≤ 11mm	≥ 10 mm	7-9mm	6mm			
Vancomycin	≥ 17 mm	15-16 mm	≤ 17mm						
Ampicillin	≥ 17 mm	14 - 16 mm	≤ 13mm	≥ 17 mm		≤ 16 mm			
Kanamycin	≥ 18 mm	14 - 17 mm	≤ 13mm						
Chloramphenicol	≥ 18 mm	13 - 17 mm	≤ 12mm	≥ 18 mm	13 - 17 mm	≤ 12mm	≥ 18 mm	13 - 17 mm	≤ 12mm
Gentamicin	≥ 15mm	13-14 mm	≤ 12mm				≥ 15mm	13-14 mm	≤ 12mm
Teicoplanin	≥ 14mm	11-13 mm	≤ 10mm						
Cefpodoxime	≥ 21mm	18 - 20mm	≤ 17mm						
Cephalothin									

UNIVERSITY of the
WESTERN CAPE

Appendix B – Chapter 3

DNA and RNA Quantification Tables

Table B1: Quantitation and analysis of RNA extracted from experimental trial greywater samples using the CTAB RNA Extraction method

Sample	Concentration	A260/A280	A260/A230
GW 1A	11,5	2,91	1,87
GW 1B	30,7	2,1	0,18
GW 2A	16,2	2,18	0,18
GW 2B	14,8	2,33	0,2
BF 1	6,4	2,91	0,08
BF 2	10,5	3,73	0,06
TW 1	7	4,45	0,07
TW 2	4,1	4,26	0,07
E.coli 1	19,8	2,76	0,27
E.coli 2	17,4	2,31	0,23
Pooled Sample (PS)	123,2	2,08	0,64

Table B2: Quantitation and analysis of RNA extracted from experimental trial greywater samples using the Hot Phenol RNA extraction method

Sample	Concentration	A260/A280	A260/A230
GW 1A	3,5	1,92	0,5
GW 1B	4,6	4,73	0,2
GW 2A	22,6	2,26	0,71
GW 2B	30	1,37	0,51
<i>E. coli</i> 1	30,6	2,22	0,8
<i>E. coli</i> 2	63,6	2,18	1,51

Table B3: Quantitation and analysis of RNA extracted from a pellet of centrifuged greywater sample using the RNEasy PowerWater Kit.

Sample	Concentration	A260/A280	A260/230
GW 1	65,2	1,92	1,13
GW 2	39,6	2,22	1,68
Tap-water (negative control)	66,8	1,5	0,65

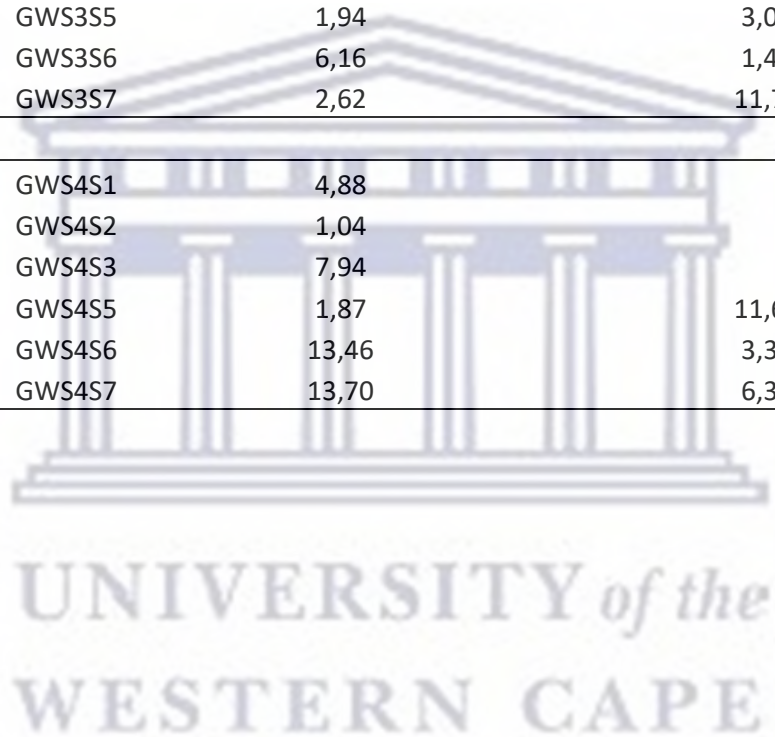
Table B4: The effect of precipitation times on RNA concentration

Sample Name	Concentration (ng/ul)	A260/280	A260/230
<i>Precipitation time of one hour at -80</i>			
1 GWS4S1	222,1	1,98	1,61
2 GWS4S1 (+)	220	1,95	2,1
3 GWS2S2	287	2,07	2,1
4 GWS2S2 (+)	304	2,09	2,24
<i>Precipitation overnight at -80</i>			
5 GWS4S1	600,9	2,14	2,7
6 GWS4S1 (+)	501,5	2,07	1,96
7 GWS2S2	395,1	2,15	2,83
8 GWS2S2 (+)	434,8	2,01	1,29

UNIVERSITY of the
WESTERN CAPE

Table B5: Qubit HS DNA Assay of synthesized cDNA using total RNA extracted from greywater samples

SITE	SAMPLE	NAME	Replicate 1 (ng/μl)	Replicate 2 (ng/μl)
1	2	GWS1S2	0,52	
	3	GWS1S3	7,22	3,94
	4	GWS1S4	2,88	0,23
2	2	GWS2S2	5,64	
	4	GWS2S4	1,54	3,34
3	2	GWS3S2	3,04	
	4	GWS3S4	4,02	4,52
	5	GWS3S5	1,94	3,00
	6	GWS3S6	6,16	1,47
	7	GWS3S7	2,62	11,72
4	1	GWS4S1	4,88	
	2	GWS4S2	1,04	
	3	GWS4S3	7,94	
	5	GWS4S5	1,87	11,62
	6	GWS4S6	13,46	3,30
	7	GWS4S7	13,70	6,32



Gel Electrophoresis Figures – Total RNA Extractions

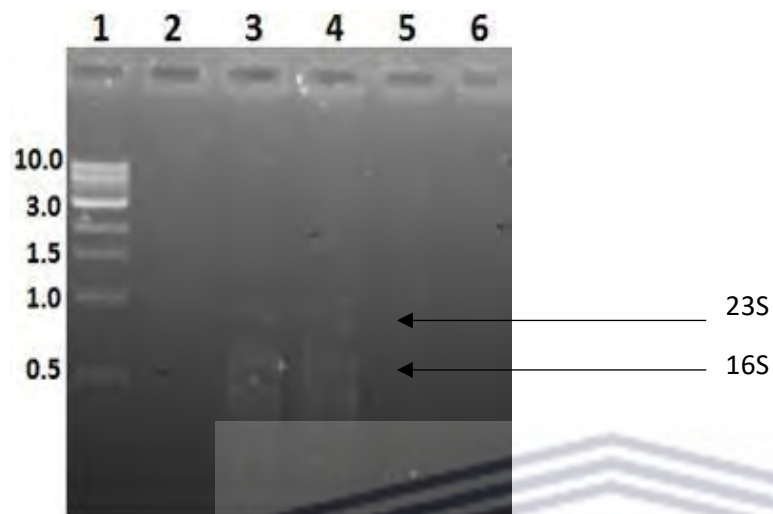
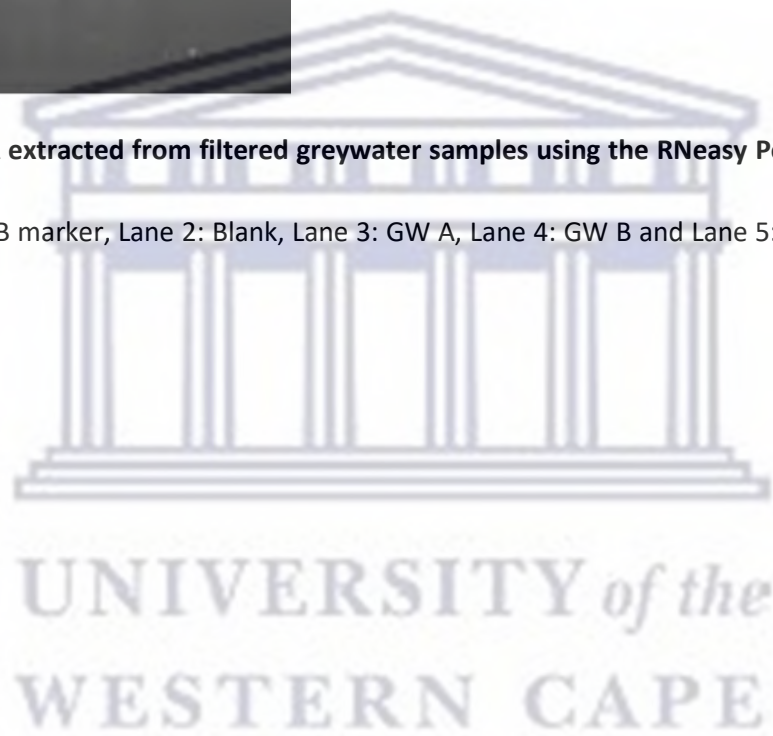


Figure B1: RNA extracted from filtered greywater samples using the RNeasy PowerWater kit.

Lane 1: 1 kb NEB marker, Lane 2: Blank, Lane 3: GW A, Lane 4: GW B and Lane 5: Tap water (-) control.



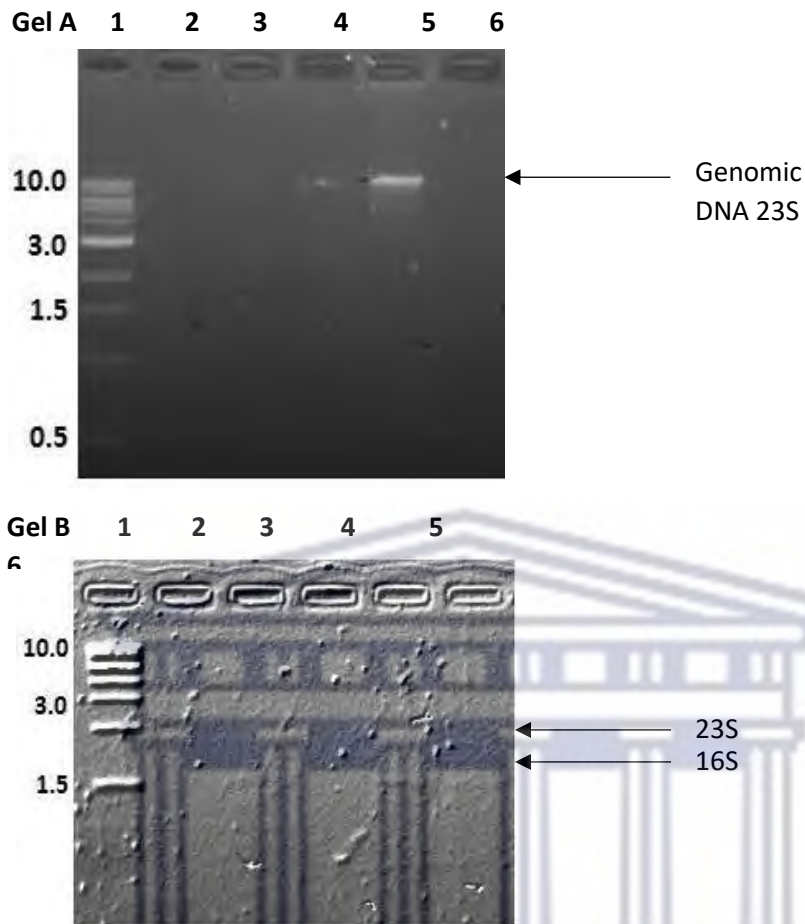


Figure B2: A comparison of the DNA and RNA extracted from filtered greywater samples using the commercial kits.

Gel A - DNA extracted using the PowerSoil DNA Isolation Kit

Lane 1: 1kb NEB marker, Lane 2: Blank, Lane 3: 20 μ m filter, Lane 4: 10 μ m filter, Lane 5: 0.45 μ m filter, and Lane 6: 0.45 μ m filter.

Gel B - RNA extracted using the RNeasy PowerWater Kit.

Lane 1: 1kb NEB marker, Lane 2: Blank, Lane 3: 20 μ m filter, Lane 4: 10 μ m filter, Lane 5: 0.45 μ m filter, and Lane 6: 0.45 μ m filter.

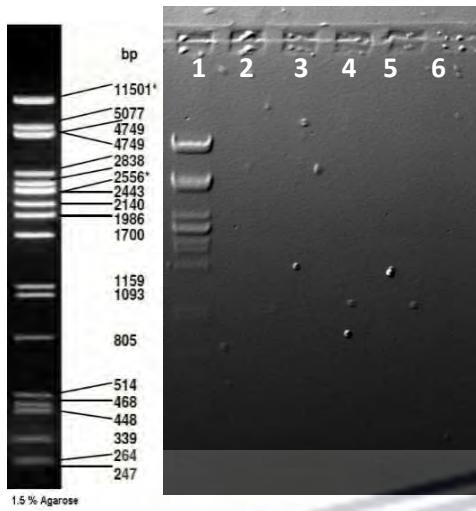
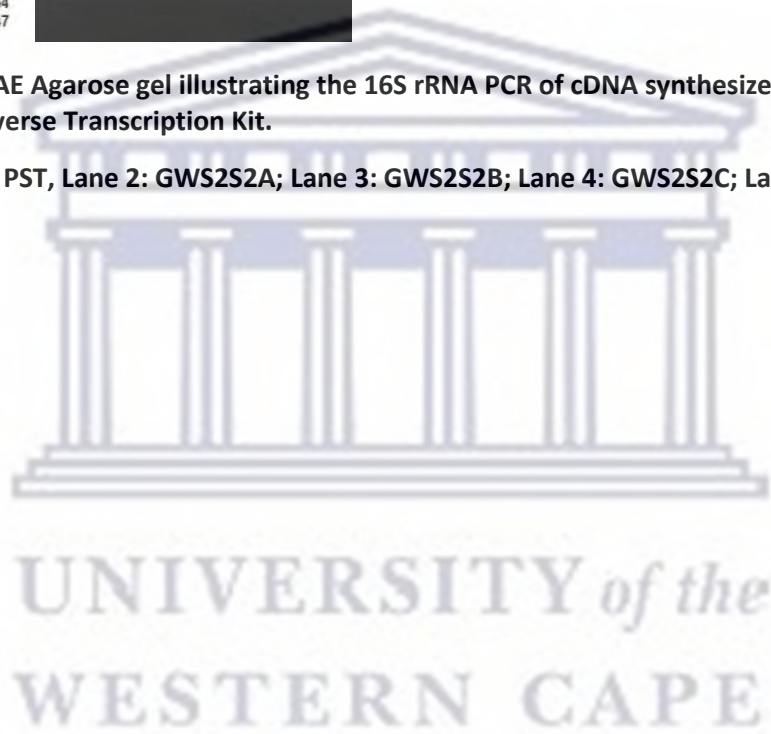


Figure B3: 1% TAE Agarose gel illustrating the 16S rRNA PCR of cDNA synthesized using the QuantiNova Reverse Transcription Kit.

Lane 1: Lambda PST, Lane 2: GWS2S2A; Lane 3: GWS2S2B; Lane 4: GWS2S2C; Lane 5: GWS2S2D; Lane 6: NTC.



Standard Curves and Melt Curves analysis for qPCR Target Genes

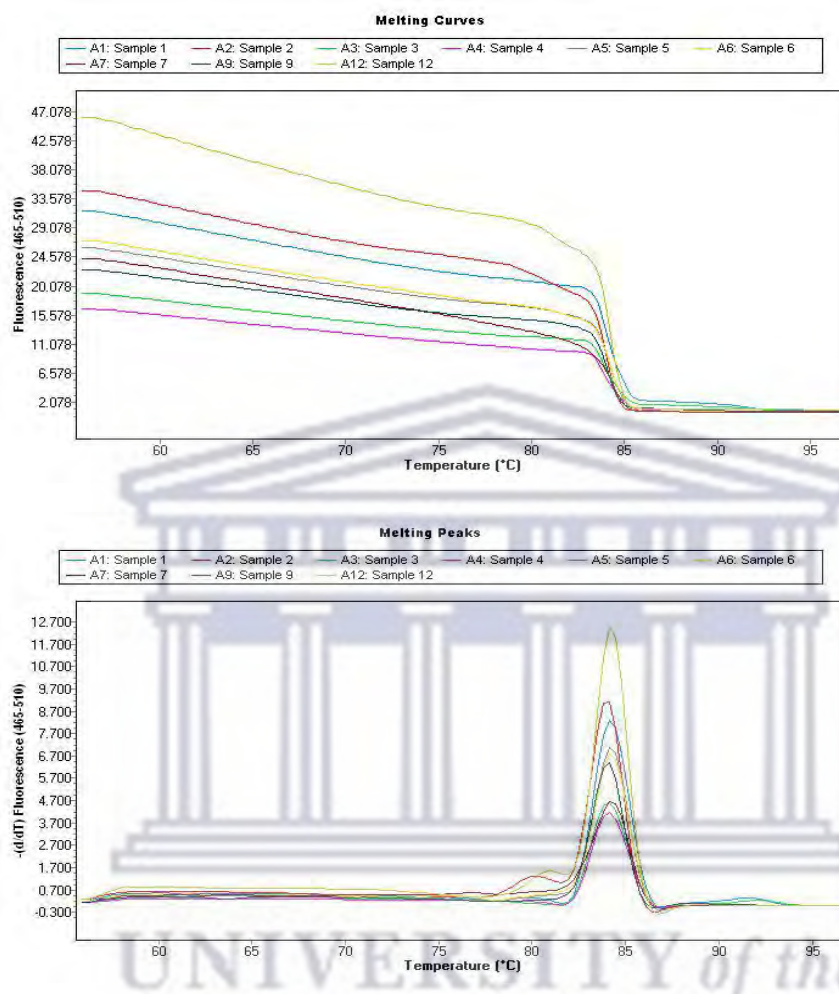


Figure B4: Melt Curve analysis of *gapA* gene amplicons generated using a dilution series of control plasmids. Cp values for these amplicons were used to construct the standard curve used for subsequent absolute quantification experiments.

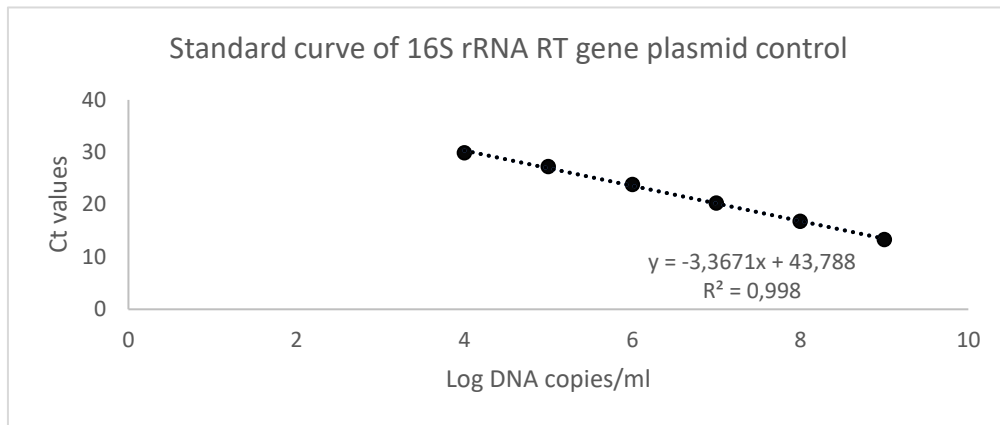


Figure B5: Standard curve generated using the 16S rRNA RT reference gene primers.

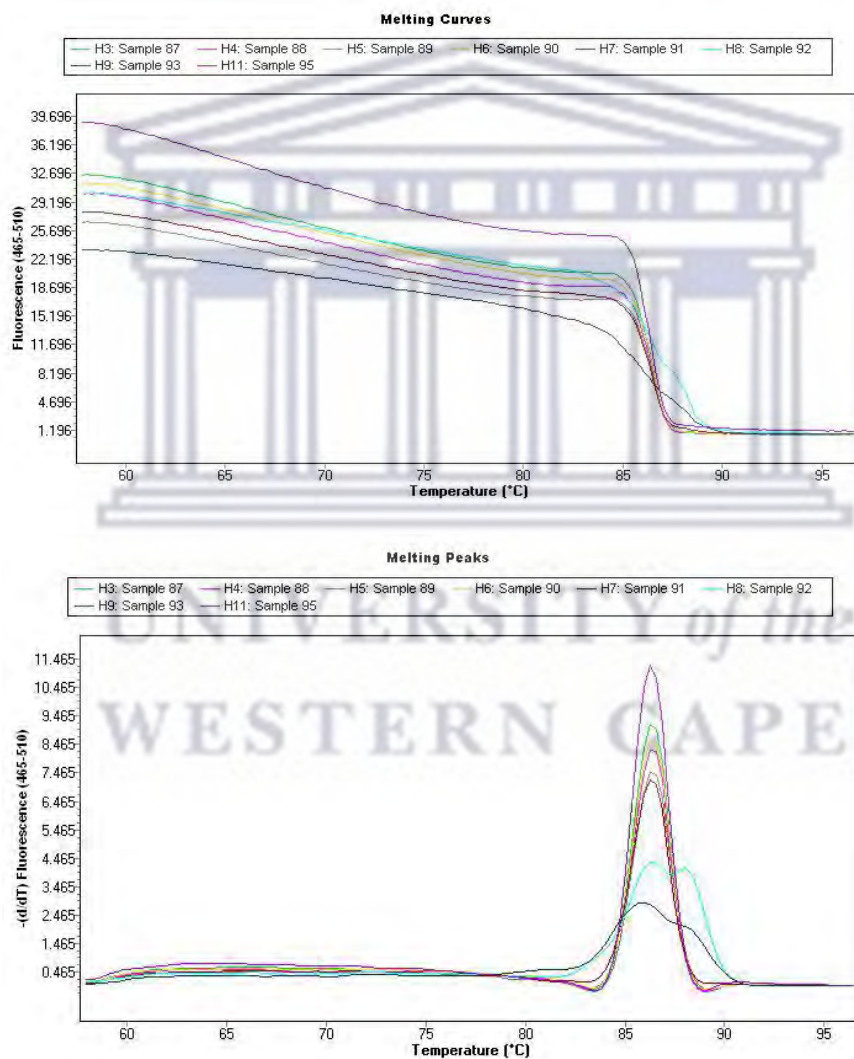


Figure B6: Melt Curve of 16S rRNA RT gene amplicons generated using a dilution series of control plasmids. Cp values for these amplicons were used to construct the standard curve used for subsequent absolute quantification experiments.

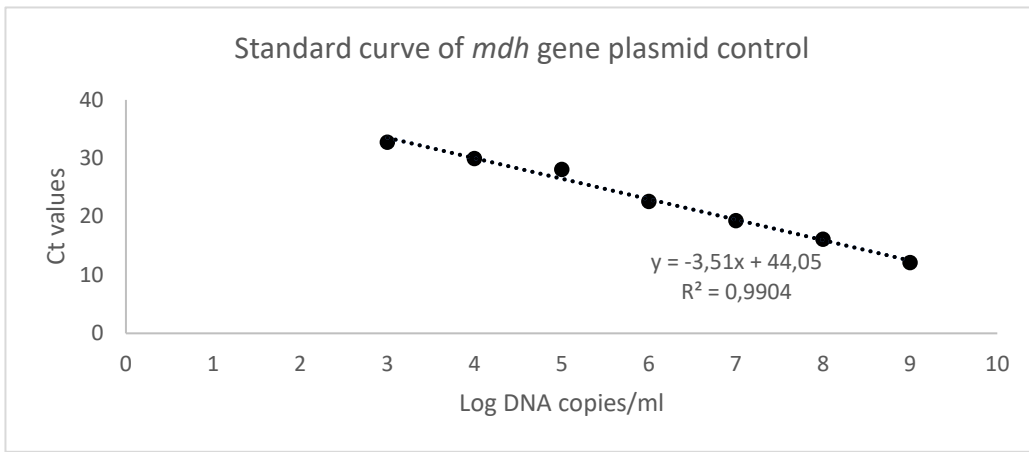


Figure B7: Standard curve generated using the *mdh* reference gene primers.

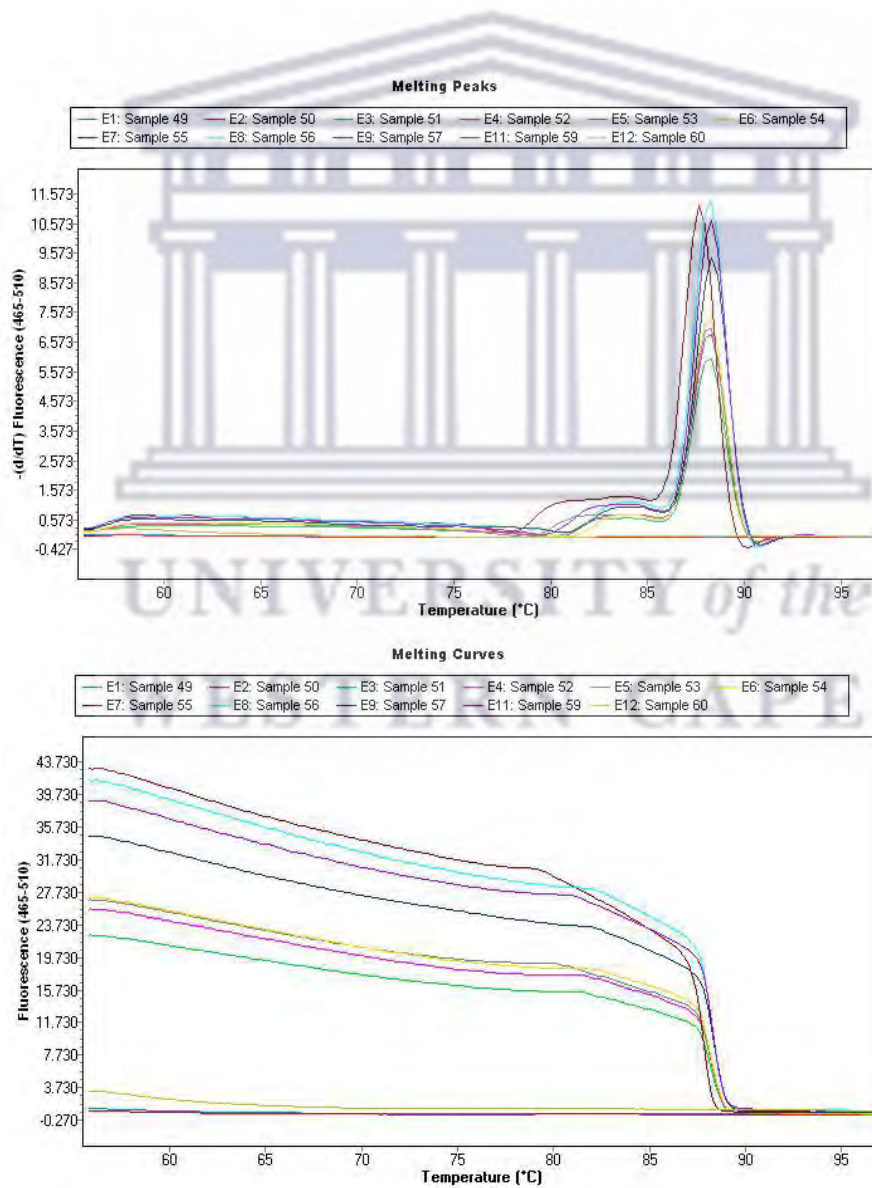


Figure B8: Melt Curve of *mdh* gene amplicons generated using a dilution series of control plasmids. Cp values for these amplicons were used to construct the standard curve used for subsequent absolute quantification experiments.

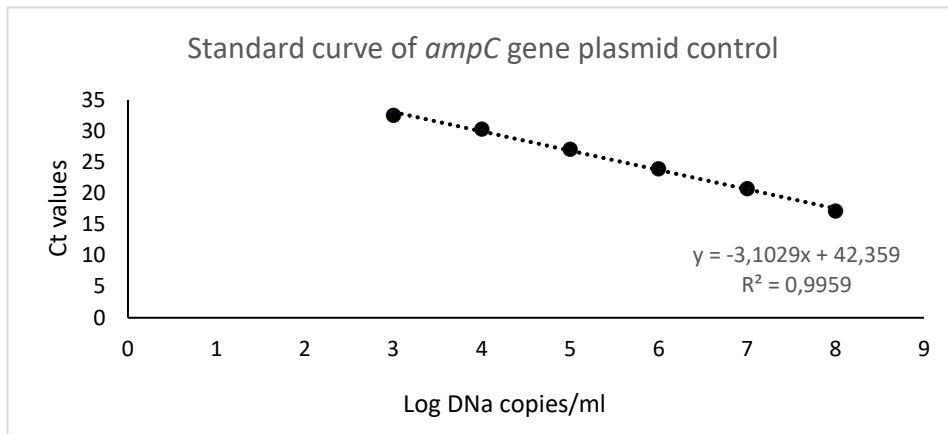


Figure B9: Standard curve generated using the *ampC* reference gene primers.

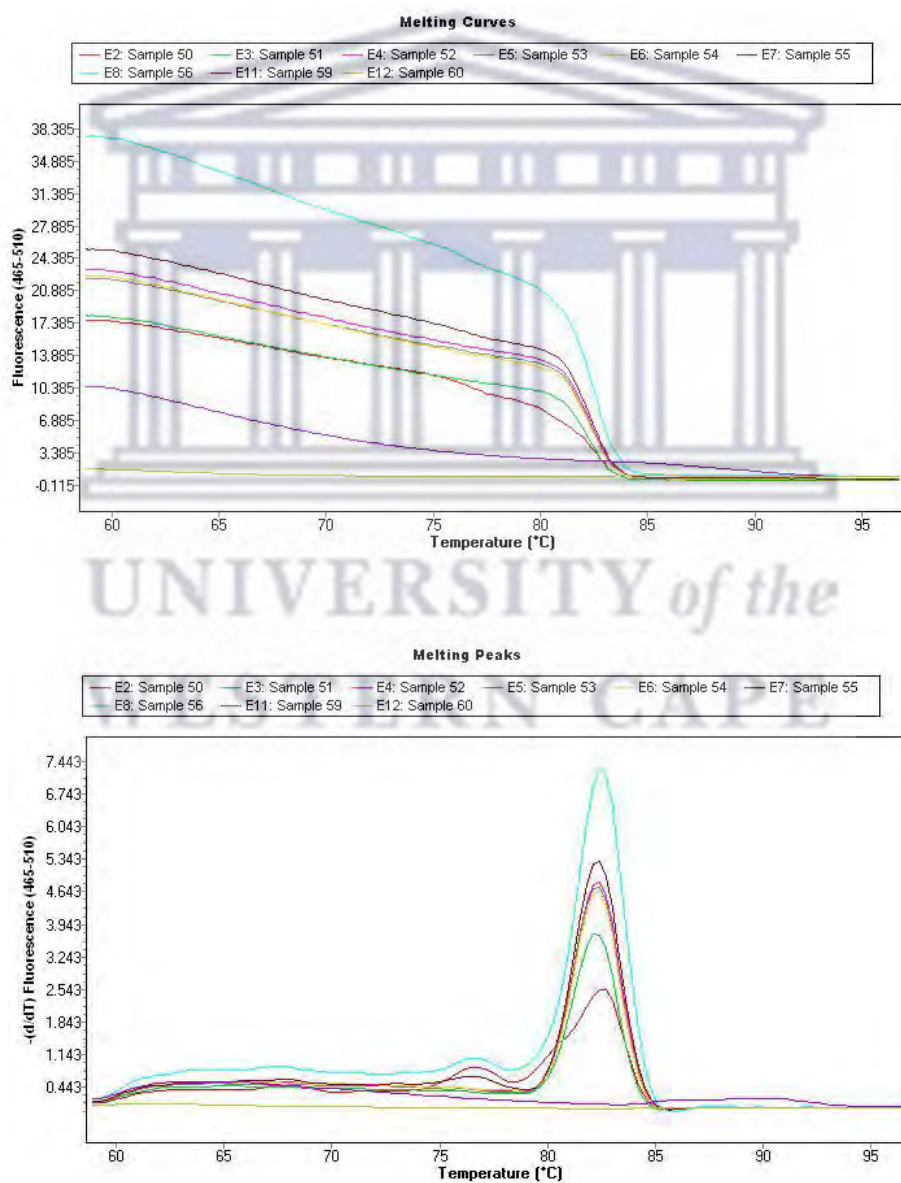


Figure B10: Melt Curve of *ampC* gene amplicons generated using a dilution series of control plasmids. Cp values for these amplicons were used to construct the standard curve used for subsequent absolute quantification experiments.

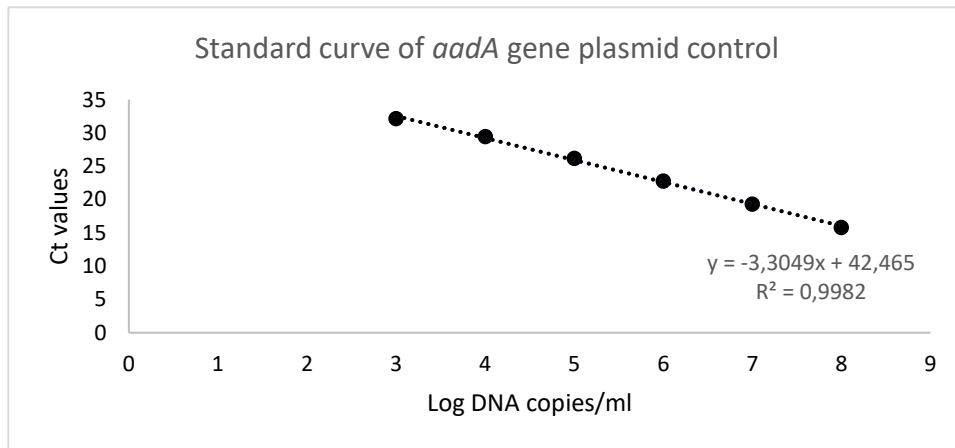


Figure B11: Standard curve generated using the *aadA* reference gene primers.

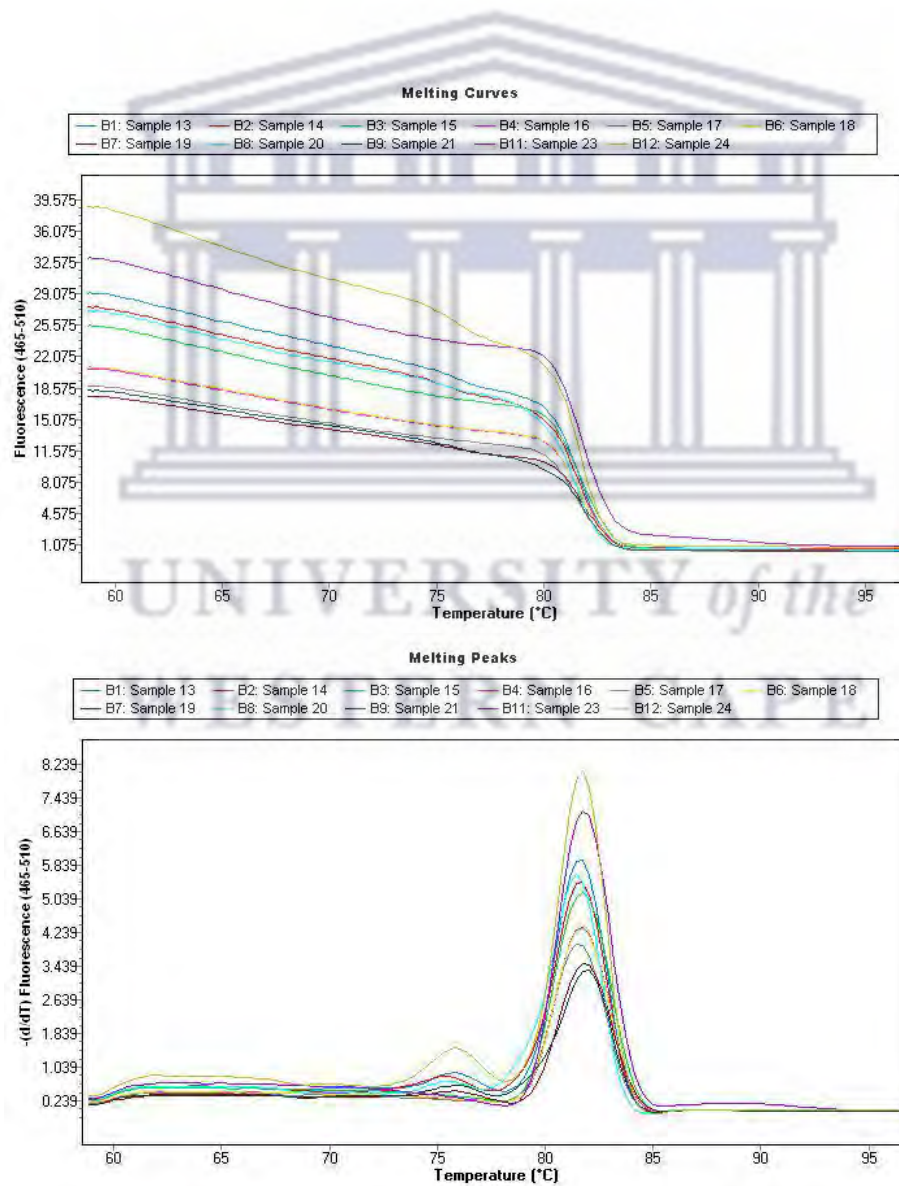


Figure B12: Melt Curve of *aadA* gene amplicons generated using a dilution series of control plasmids. Cp values for these amplicons were used to construct the standard curve used for subsequent absolute quantification experiments.

Appendix C – Chapter 4

Gel Electrophoresis Figures – mDNA Extractions

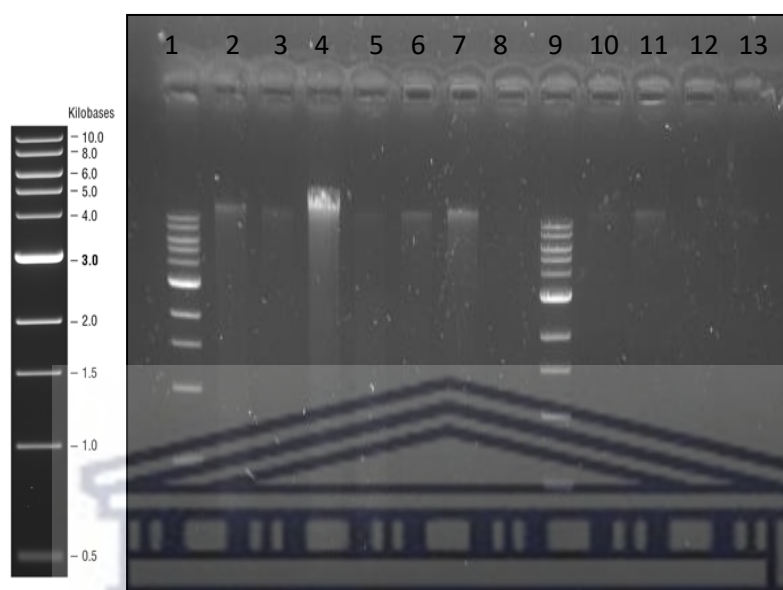


Figure C1: A 1% TAE gel representing metagenomic DNA extracted from greywater and biofilm samples using the DNEasy PowerSoil Pro kit. Lane 1: 1 Kb NEB Marker; Lane 2: GWS1S3; Lane 3: GWS2S3; Lane 4: GWS3S4; Lane 5: GWS4S5; Lane 6: GWS3S6; Lane 7: GWS3S5. Lane 9: 1 kb NBE Marker; Lane 10: BFS1S4, Lane 11: BFS2S4; Lane 12: BFS3S7; Lane 13: BFS4S7.

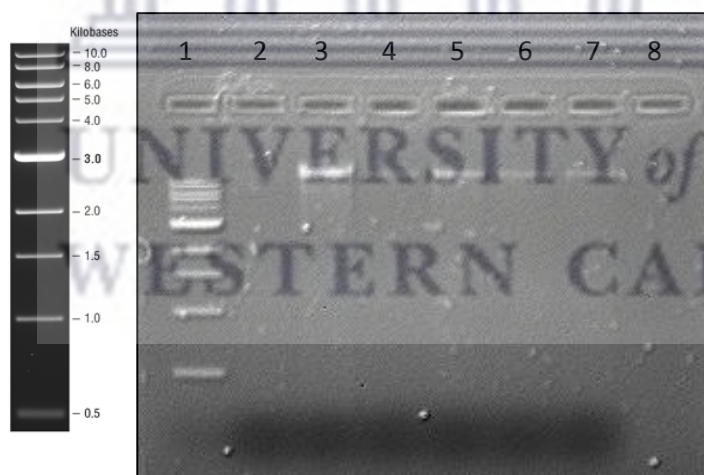


Figure C2: A 1% TAE gel representing environmental DNA extracted from greywater samples using the DNEasy PowerSoil Pro Kit. Lane 1: 1 Kb NEB Marker; Lane 2: GWS4S6; Lane 3: GWS4S7; Lane 4: GWS1S4; Lane 5: GWS2S4; Lane 6: GWS2S3; Lane 7: GWS3S7.

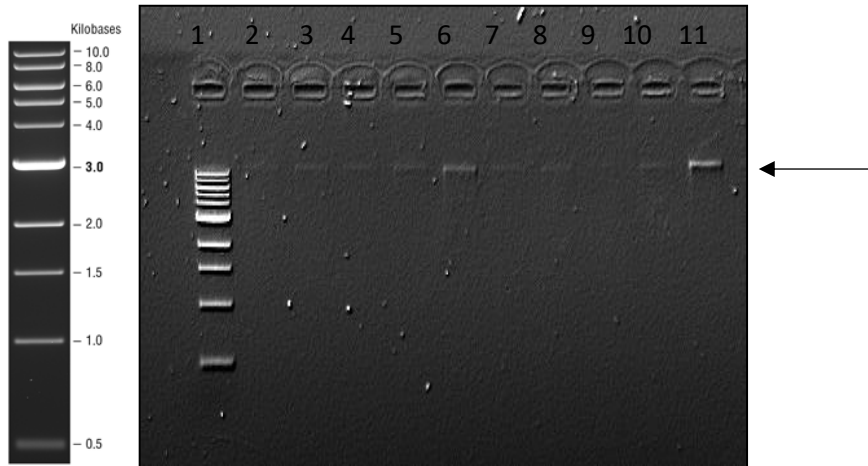


Figure C3: A 1% TAE gel representing Metagenomic DNA extracted from biofilm samples using the DNEasy PowerSoil Pro Kit. Lane 1: 1 Kb NEB Marker; Lane 2: BFS1S2; Lane 3: BFS2S3; Lane 4: BFS3S3; Lane 5: BFS3S5; Lane 6: BFS3S6; Lane 7: BFS4S3; Lane 9: BFS4S4; Lane 10: BFS4S5, Lane 11: BFS4S6



Figure C4: A 1% TAE gel depicting a 16S rRNA PCR of environmental DNA extracted from biofilm samples. Lane 1: 1 Kb NEB Marker; Lane 2: BFS1S2; Lane 3: BFS2S3; Lane 4: BFS3S3; Lane 5: BFS3S5; Lane 6: BFS3S6; Lane 7: BFS4S3; Lane 8: BFS4S; Lane 9: BFS4S5; Lane 10: BFS4S6; Lane 11: BFS2S4; Lane 12: BFS4S7; Lane 13; *S. aureus* genomic DNA control.

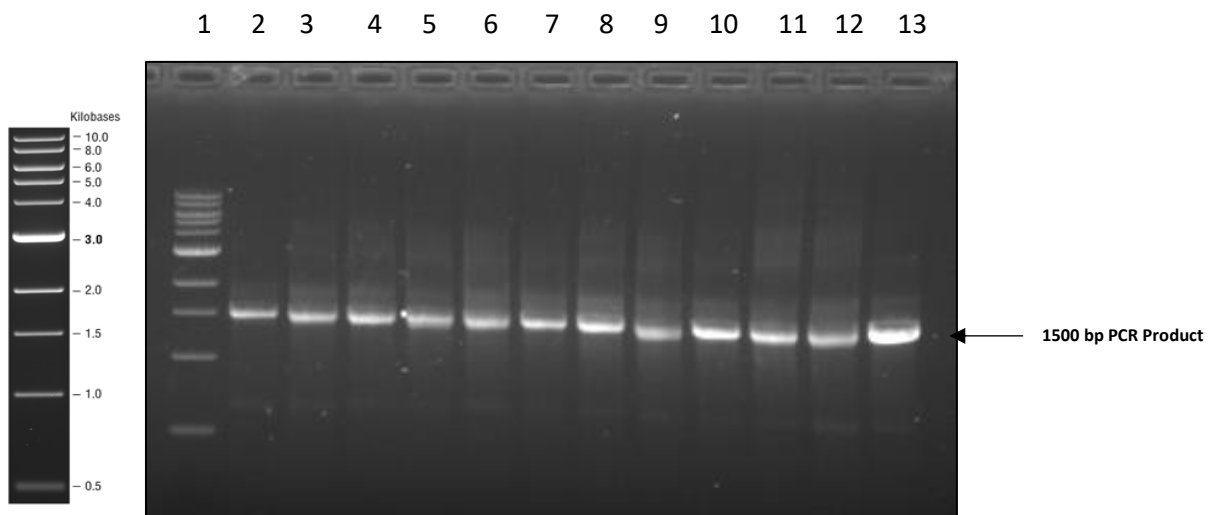


Figure C5: 1% TAE gel depicting a 16S rRNA PCR of environmental DNA extracted from greywater samples. Lane 1: 1 Kb NEB Marker; Lane 2: GWS1S1; Lane 3: GWS1S2; Lane 4: GWS2S2; Lane 5: GWS3S1; Lane 6: GWS3S2; Lane 7: GWS3S3, Lane 8: GWS4S1; Lane 9: GWS4S2; Lane 10: GWS4S3; Lane 11: GWS4S4; Lane 12: GWS1S3; Lane 13: *S. aureus* genomic DNA control.

Melt curve Analysis

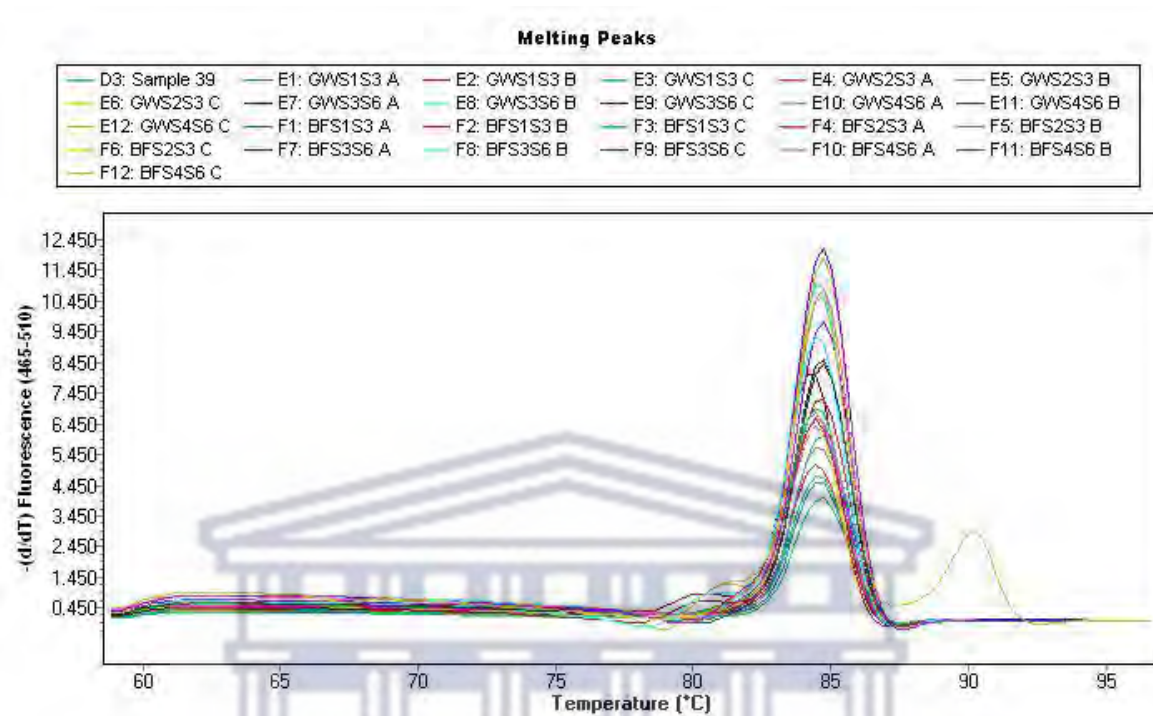


Figure C6: Melting peaks for *int11* primers in Group 2 mDNA samples.

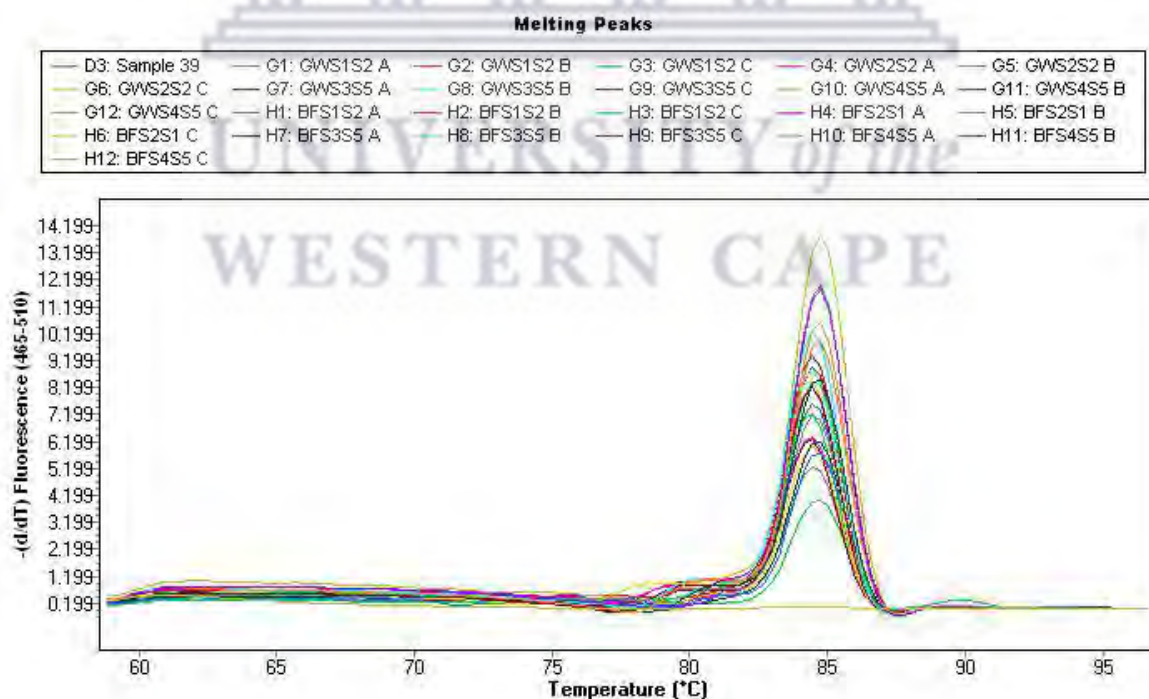


Figure C7: Melting peaks for *int11* primers in Group 3 mDNA samples.

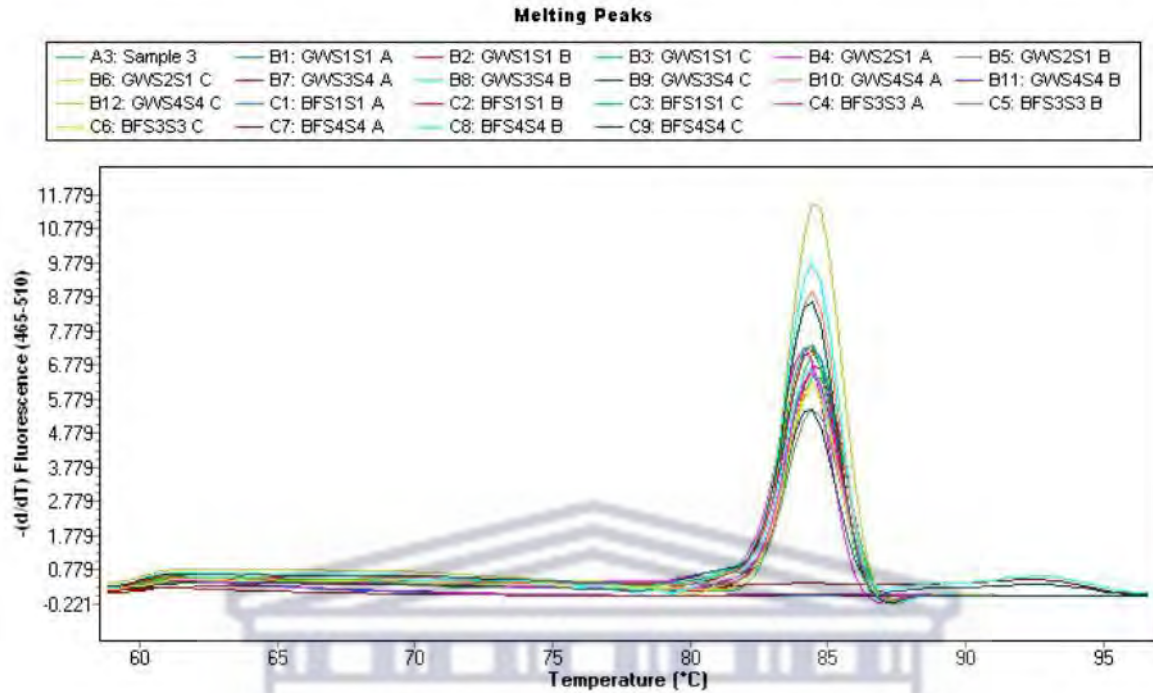


Figure C8: Melting peaks for *int1* primers in Group 4 mDNA samples.

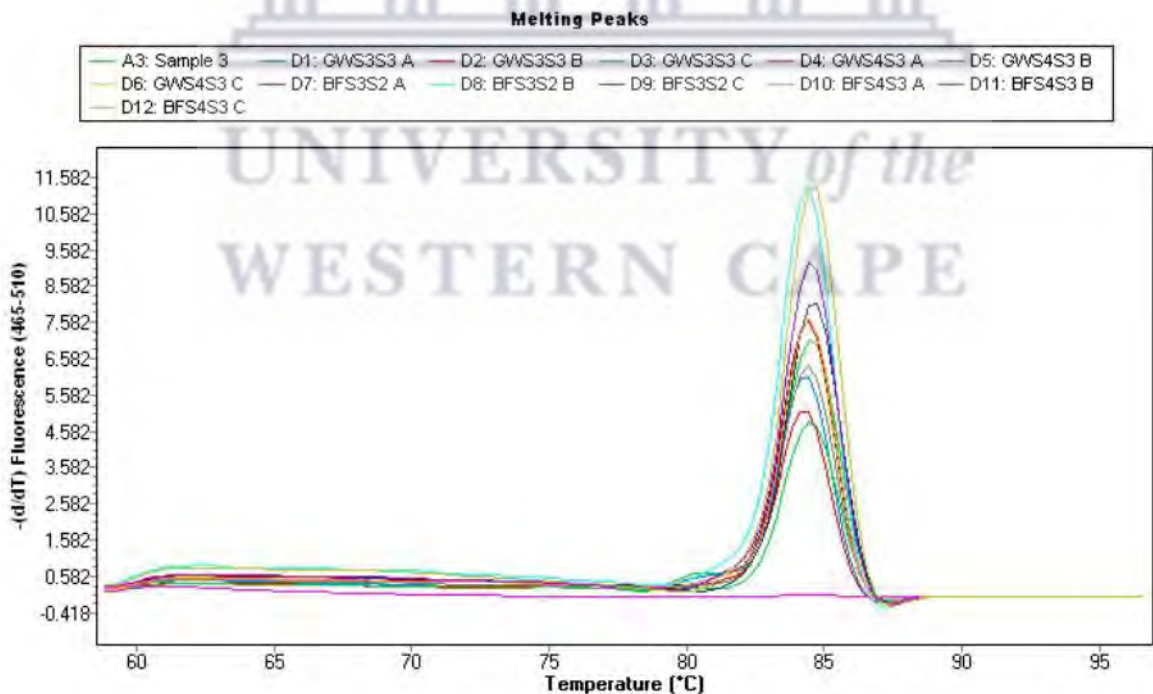


Figure C9: Melting peaks for *int1* primers in Group 5 mDNA samples.

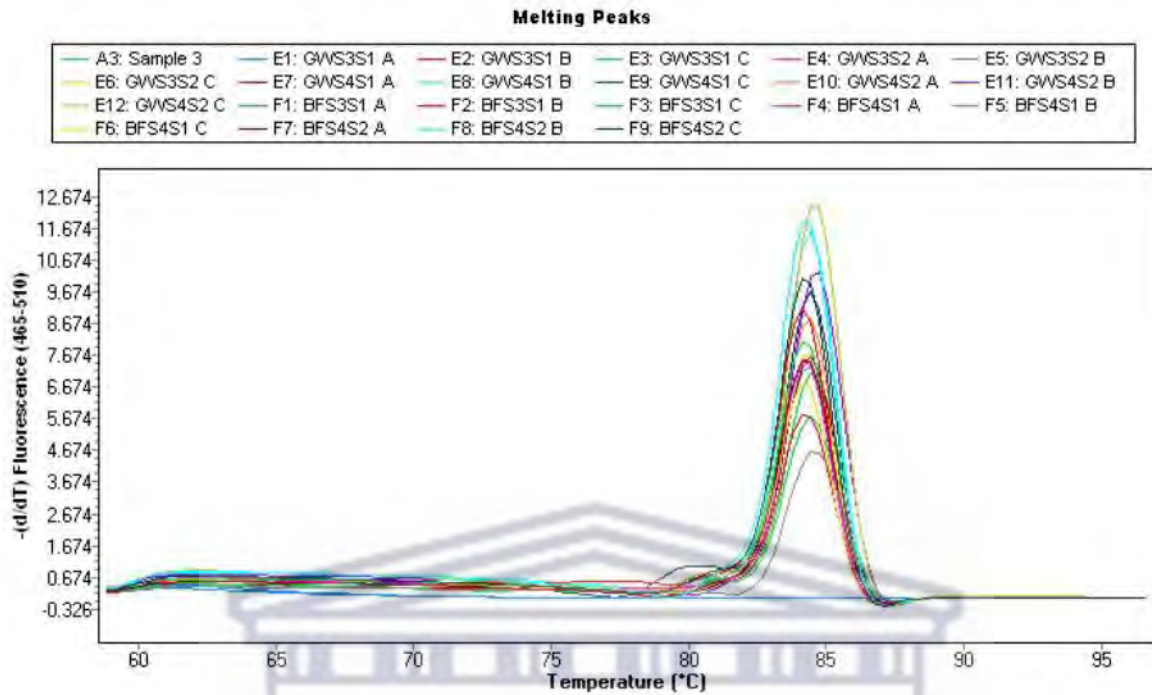


Figure C10: Melting peaks for *int1* primers in Group 6 mDNA samples.

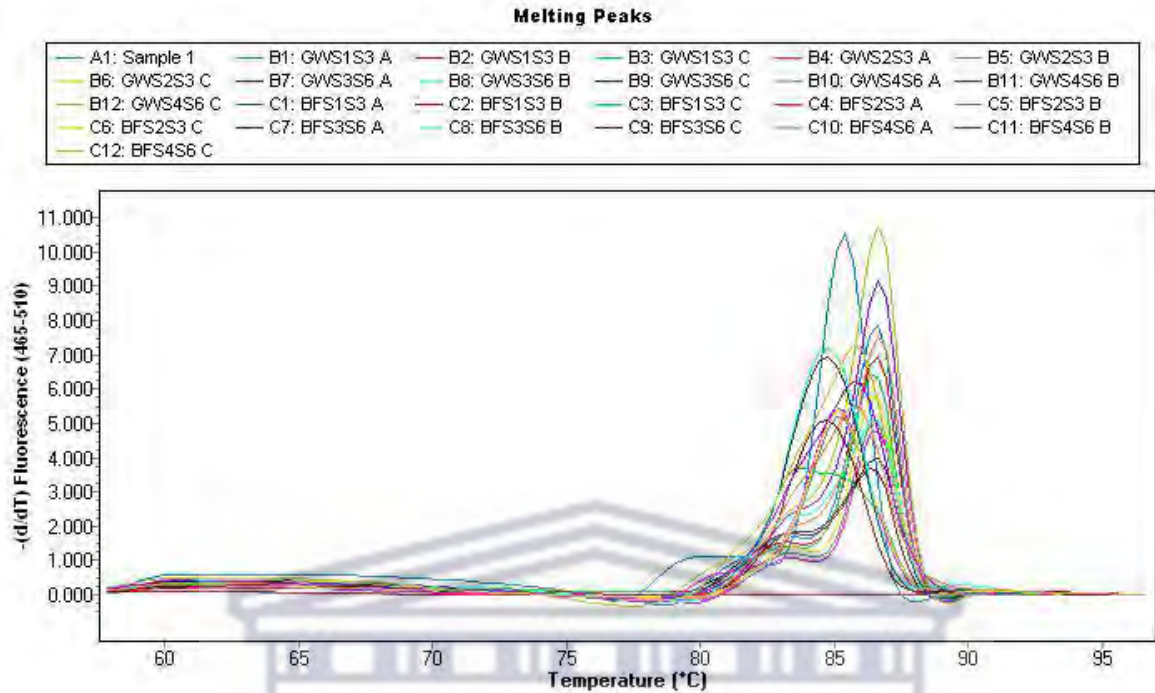


Figure C11: Melting peaks for 16S rRNA primers in Group 2 mDNA samples.

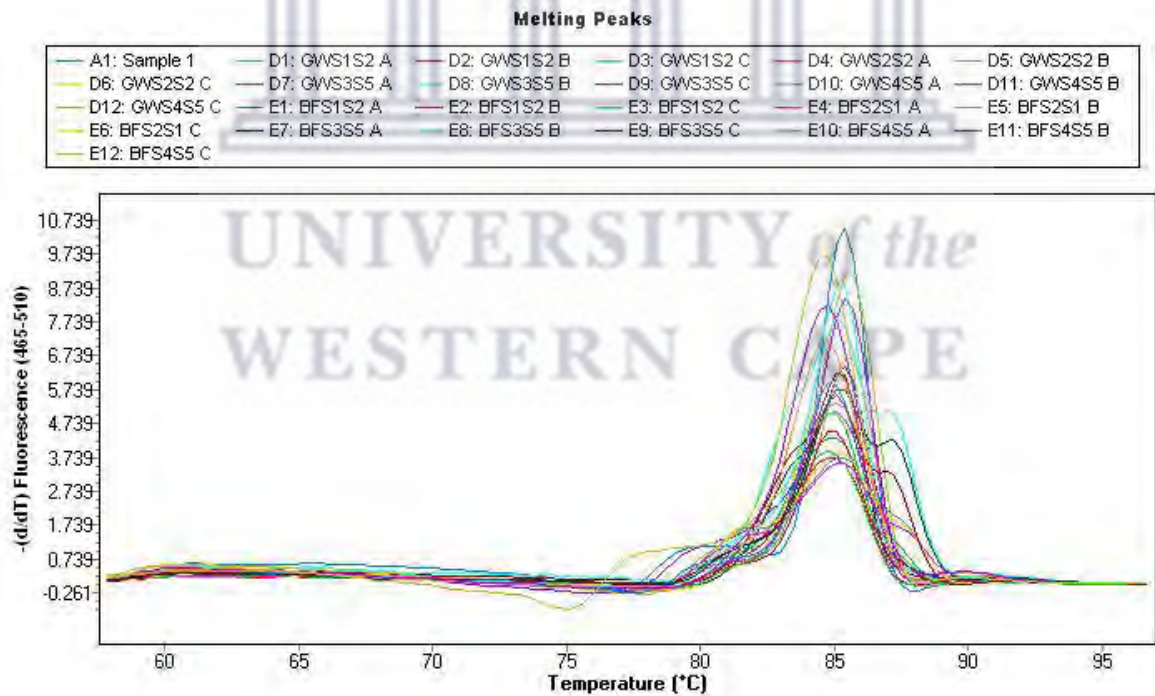


Figure C12: Melting curves for 16S rRNA primers in Group 3 mDNA samples.

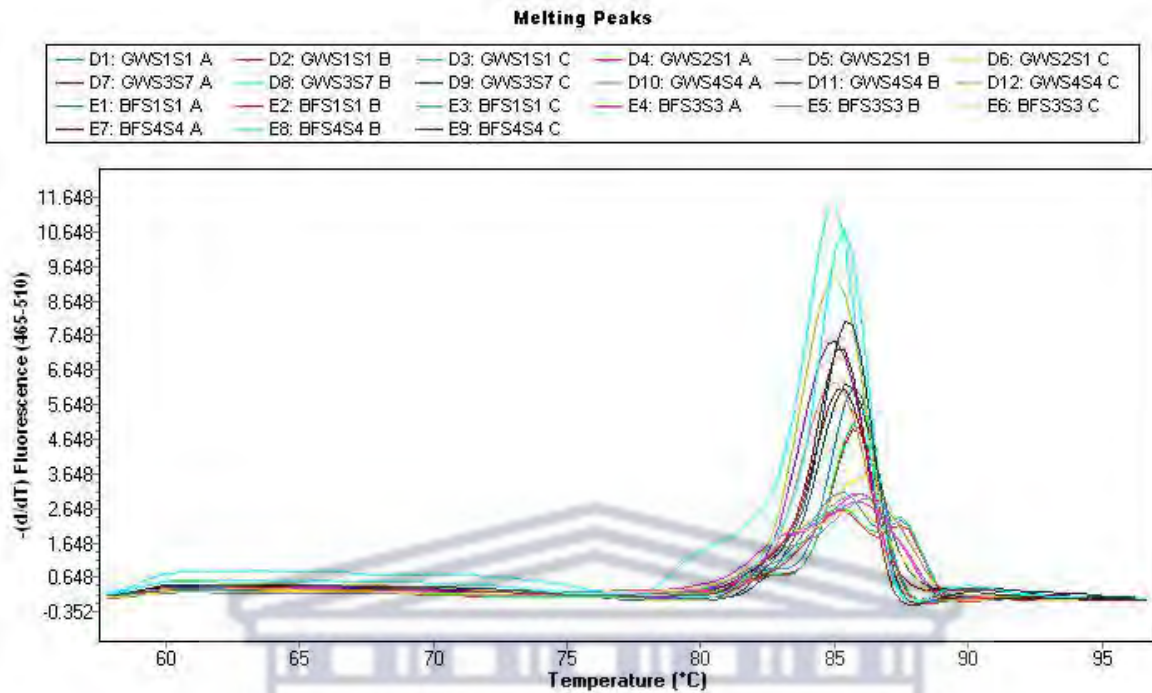


Figure C13: Melting peaks for 16S rRNA primers in Group 4 mDNA samples.

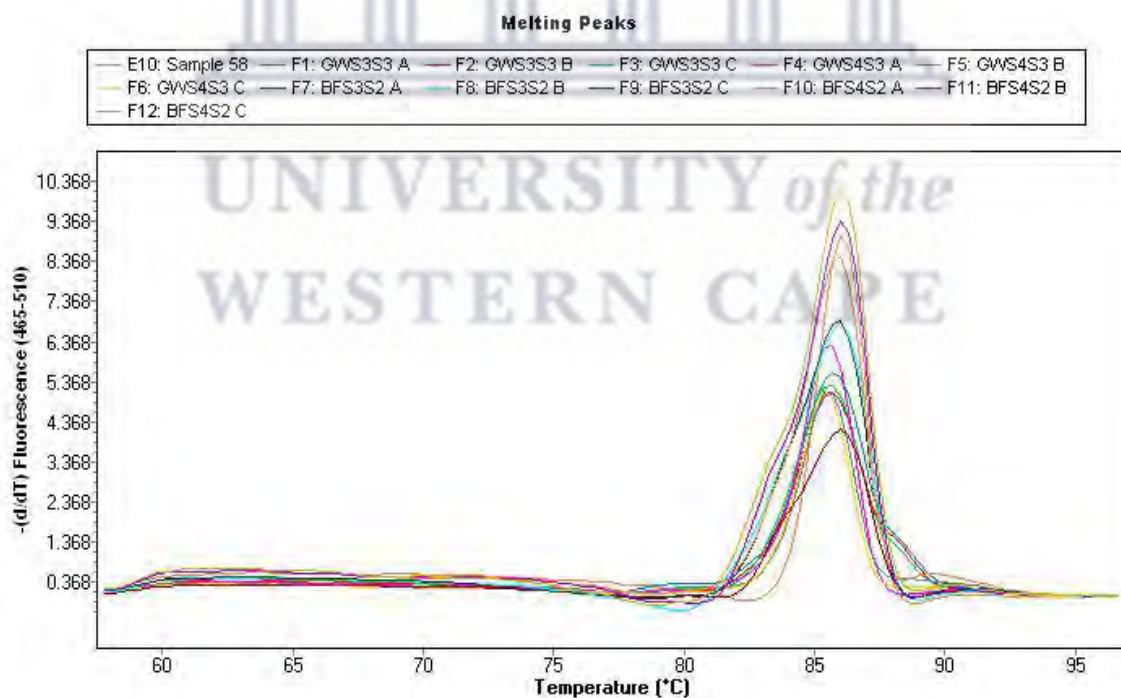


Figure C14: Melting peaks for 16S rRNA primers in Group 5 mDNA samples.

Melting Peaks

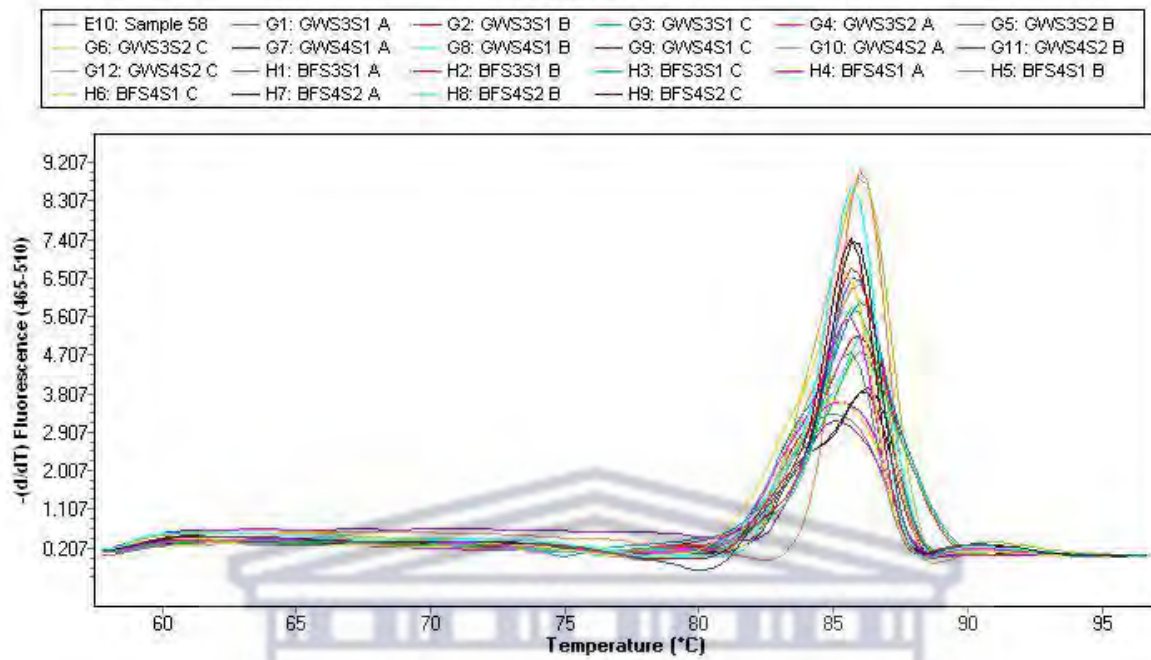


Figure C15: Melting peaks for 16S rRNA primers in Group 6 mDNA samples.